UNIVERSIDAD COMPLUTENSE DE MADRID

FACULTAD DE FARMACIA
DEPARTAMENTO DE QUÍMICA ORGÁNICA Y FARMACEUTICA

TESIS DOCTORAL

Exploring the N-Benzylpiperidine and N, N-Dibenzyl(N-Methyl)amine fragments as privileged structures in the search of new multitarget directed drugs for Alzheimer's disease

MEMORIA PARA OPTAR AL GRADO DE DOCTOR

PRESENTADA POR

Martín H. Estrada Valencia

DIRECTORA

María Isabel Rodríguez Franco

Madrid, 2017

UNIVERSIDAD
COMPLUTENSE
MADRID

EXPLORING THE *N*-BENZYLPIPERIDINE AND *N*, *N*-DIBENZYL(N-METHYL)AMINE FRAGMENTS AS PRIVILEGED STRUCTURES IN THE SEARCH OF NEW MULTITARGET DIRECTED DRUGS FOR ALZHEIMER'S DISEASE

Doctoral Thesis

Martín H. Estrada Valencia

IQM-CSIC

Madrid 2016

Universidad Complutense de Madrid

Facultad de Farmacia

Departamento de Química Orgánica y Farmacéutica

Evaluación de Fragmentos de *N*-Bencilpiperidina y *N*, *N*-Dibencil(N-metil)amina Como Estructuras Privilegiadas en la Búsqueda de Nuevos Fármacos Multifuncionales Para el Tratamiento de la Enfermedad de Alzheimer

Martín H. Estrada Valencia

Supervisora

María Isabel Rodríguez Franco PhD.

Instituto de Química Médica

Consejo Superior de Investigaciones Científicas (IQM-CSIC)

Madrid 2016

A mi Madre…

Agradecimientos

En primer lugar, todo mi agradecimiento a la Doctora María Isabel Rodríguez Franco por su confianza, su trabajo, y por todos los recursos puestos a mi disposición para desarrollar en las mejores condiciones y con toda libertad las ideas reflejadas en esta Tesis Doctoral.

Gracias a COLCIENCIAS, Departamento Administrativo de Ciencia Tecnología en Innovación de Colombia, por la concesión de la beca que ha permitido el desarrollo de mi doctorado. Así mismo a los proyectos del Ministerio de Economía y Competitividad (SAF2012-31035), Fundación de Investigación Médica de la Mutua Madrileña Automovilística (AP103952012) y Consejo Superior de Investigaciones Científicas (PIE-201280E074) por su financiación.

Al Instituto de Química Médica a través de su directora actual la Doctora Ana Castro Morera y anterior, la Doctora María Jesús Pérez Pérez por abrirme las puertas y brindarme todo su apoyo durante este provechoso tiempo. Igualmente a todo el personal del Instituto, especialmente al equipo administrativo y a los equipos de RMN y HPLC que siempre han tenido la disposición de ayudar con su valioso trabajo, en especial a Guadalupe Romero y Felipe Pérez.

A los colaboradores que han permitido el desarrollo de muchos de los experimentos llevados a cabo en este trabajo: Doctor Mario Guerrero de la Universidad Nacional de Colombia; Doctoras Matilde Yáñez y Dolores Viña de la Universidad de Santiago de Compostela; Doctora Elena Soriano del Instituto de Química Orgánica General, Doctores Erik Laurini, Maurizio Romano y Sabrina Pricl de la Universidad de Trieste; Doctores José A. Morales-García y Ana Pérez Castillo del Instituto de

Investigaciones Biomédicas “Alberto Sols” y del Centro de Investigación Biomédica en Red sobre Enfermedades Neurodegenerativas y al Dr. Alejandro Romero del Departamento de Toxicología y Farmacología de Universidad Complutense de Madrid.

A la Sociedad Española de Química Terapéutica (SEQT), por haber patrocinado mediante sus becas la divulgación de los resultados de este trabajo en diferentes eventos científicos.

A los Doctores Santiago Conde, Ana Martínez, Carmen Gil, Daniel Pérez, Concepción Pérez y Vicente Arán por su amistad y colaboración, igualmente a las personas que han sido parte del grupo de investigación, a Mario de la Fuente por estos años compartiendo el camino, a Lucía de Andrés por su participación en la síntesis de algunos compuestos durante su trabajo de máster, a Leticia Monjas, Nerea Fernández, Ángela Soriano, Joana Reis, Plácido Ceballos, Valle Palomo, Irene García, Myriam Redondo, Mónica Duarte, con quienes tuve menos tiempo para compartir, sin embargo, su compañía lo ha hecho valioso. A las personas que actualmente conforman el grupo; a Gracia Baquero, Olaia Martí y a la mejor compi, Clara Herrera, gracias por tus revisiones y todo el tiempo que has dedicado a leer esta tesis y hacer tus valiosas aportaciones, así como por este valioso tiempo compartido.

A todos los amigos y compañeros que han contribuido en este proceso: Oskía Bueno, Pilar Cercós, Paula Morales, Beatriz Balsera, Jonathan Nue, Belén Martínez, Marta Ruiz, Asier Gómez, Sergio Quesada, Carlos Ríos, Ana Gamo, y especialmente por los buenos momentos a Guadalupe Romero, Alejandra Riesco, Andrea Taladriz, Ana Torres, Sylvain Petit, Alba Gigante y Francisco Sánchez.

A todos, gracias.

Index

Abbreviations

AChE	Acetylcholinesterase
AChEi	Acetylcholinesterase Inhibitor
ACN	Acetonitrile
ARE	Antioxidant Response Element
BACE1	Beta-Site Amyloid Precursor Protein-Cleaving Enzyme 1
BBr_3	Boron Tribromide
BiP	Binding immunoglobulin protein
BOP	(Benzotriazol-1-Yloxy)Tris(Dimethylamino)Phosphonium Hexafluorophosphate
bs	Broad Singlet
$CDCl_3$	Deuterated Chloroform
CDI	*N,N*-Carbonyldiimidazole
CoA	Coenzyme A
CSF	Cerebrospinal Fluid
DAPI	4 ',6-Diamino-2-Fenilindol
DBMA	N,N-Dibenzyl(N-Methyl)Amine
DCM	Dichloromethane
DHLA	Dihydrolipoic Acid
DMSO-d_6	Deuterated DMSO
dt	Doublet of Triplets
DTG	N,N'-Di(O-tolyl)guanidine
ER	Endoplasmic Reticulum
Et_2O	Ethyl Ether
EtOAc	Ethyl Acetate
EtOH	Ethanol
FRET	Fluorescence Resonance Energy Transfer
g.t.	Gradient time
GSK-3β	Glycogen Synthase-3β
HNE	4-Hydroxy-2-Nonenal
IP_3	Inositol triphosphate
KA	Kynurenic acid
Ki	Affinity constant
LA	Lipoic acid
LDH	Lactate dehydrogenase

MAM	Mithocondria associated membrane
MAO	Monoamino Oxidase
MD	Molecular Dinamics
MeOD	Deuterated Methanol
mp	Melting Point
MTDL	Multi-Target Directed Ligands
MTT	3-(4,5-Dimethylthiazol-2-Yl)-2,5-Diphenyltetrazolium Bromide
NBP	*N*-Benzylpiperidine
nM	Nanomolar
NS	Neurospheres
NSC	Neural Stem Cells
ORAC	Oxigen Radical Absorbance Capacity
PBS	Phosphate-Buffered Saline
PCP	Phencyclidine
Pd-C	Paldium over charcoal
Ph	Phenyl
PKB, Akt	Protein Kinase B
SEM	Standard Error Media
σ1R	Sigma-1 Receptor
sAPPβ	Soluble Amyloid Precursor Protein Alpha
SD	Standard Deviation
SOD	Superoxide Dismutase
UPR	Unfolded protein response
VMAT	Vesicular Monoamine Transporter

Throughout this manuscript, abbreviations and acronyms recommended by the American Chemical Society in the Medicinal Chemistry area (revised in the *Journal of Medicinal Chemistry* on January **2016.**

http://pubs.acs.org/paragonplus/submission/jmcmar/jmcmar_authguide.pdf

Abstract

Introduction

Alzheimer's disease (AD) is a neurodegenerative illness characterized by a progressive loss of neurons in specific areas, such as forebrain, neocortex and subcortical cholinergic projections from nucleus basalis of Meynert. Loss of cholinergic neurons entails low levels of acetylcholine (ACh); this diminished amount of neurotransmitter is responsible for the disruption in the neuronal transmission between the cells involved in learning and memory processes. This interruption in neuronal communication is the origin of the cognitive symptoms of AD such as memory loss, incapacity to learn, to reason, to make judgments and failure to communicate.

Understanding of disruption in cholinergic system led to acetylcholinesterase (AChE) as the first target in the search of therapeutic agents to treat AD. Acetylcholinesterase inhibitors (AChEi) were the first class of drugs successfully used in the symptomatic treatment of this disease. However, despite the improvement in cognitive and behavioral impairments in patients treated with AChEi's, this kind of drugs is not able to stop the neurodegeneration.

Explaining the origin of cognitive symptoms is not enough to understand the real cause of neurodegeneration in AD. Nowadays, beta-amyloid peptide (Aβ) is considered the initiating substance in the process leading to neuronal death. Insoluble Aβ fibrils are the main constituent of the senile plaques, which are considered the toxic element triggering the cascade of cellular responses that finally produce degeneration and death of neurons. Some of these events are neuro-inflammation, production of reactive oxygen species (ROS) and *tau* protein hyper phosphorylation.

An important strategy in the search for new drugs able to avoid the production of Aβ and subsequent senile plaques deposition, has been the

synthesis of inhibitors of the beta-site amyloid precursor protein cleavage enzyme (BACE1); one of the three secretases involved in processing amyloid precursor protein (APP).

Along with the decrease in ACh, there is a decline in brain levels of other neurotransmitters such as dopamine, serotonin and norepinephrine compared to healthy aging brain. At the same time, it has been demonstrated that levels of MAO-B increase with age in healthy humans, as well as in degenerative processes. These increased levels of MAO-B, correlate with the exacerbated production of ROS, which are responsible for the toxic environment characteristic of neurodegeneration. MAO inhibitors have been explored as a complementary alternative in the search of new drugs to treat AD, both to reduce ROS in the case of MAO-B, as to treat concomitant depression of AD patients, in the case of MAO-A.

This brief introduction highlights the complexity of the network of factors influencing AD. In the rest of this report the role of these enzymes and some other factors will be discussed in a deeper manner. Taking into account this complexity, we proposed to develop the next general objective

Objective

In this work, we aimed to explore the usefulness of the *N*-benzyl piperidine (NBP) and the *N, N*-dibenzyl-*N*-methylamine (DBMA) in the design, synthesis and evaluation of new multitarget compounds with affinity for relevant enzymes related to AD. To achieve this goal, several naturally occurring structures, (chromone, 4-quinolinone, lipoic acid (LA) and cinnamic acid) which could give to the resulting products a multitarget profile, were hybridized with NBP and DBMA into simple small molecules. Synthetic ease and accessibility to the biological experiments was always considered to develop in the most rapid and

efficient way this research. The newly obtained products were evaluated in biological assays (*in vitro* and *in vivo*) and *in silico* experiments in order to establish a relationship between the structure and their biological activity.

Results

Along this work we have demonstrated that NBP and DBMA fragments are able to give to the new hybrids affinity for the cholinesterases, as we expected from the very beginning according to the initial bibliographic review. Depending on the complementary scaffold, newly obtained hybrids exhibited affinity for the several enzymes related to AD.

We have found that the combination of these two fragments with LA give molecules with affinity for the σ1R, and consequently, with the potential to preserve the health of the neurons affected in AD. Through this property, they may help to avoid or at least delay the neurodegenerative process. Simultaneously, these compounds are BACE1 inhibitors and neurogenic agents.

In the second and fourth chapter we successfully combined the fragments of interest with the chromone scaffold and the cinnamic structure, respectively. Once more, naturally occurring scaffolds were the inspiration to obtain the desired multitarget products. These new hybrids exhibited the wanted AChE and MAO inhibitory activity and radical scavenger capacity. The cinnamic based compounds were more effective than the chromone-based hybrids in providing antioxidant properties, at the same time they were able to stimulate neurogenesis.

The compounds obtained in the third chapter, combining the kynurenic acid (KA) scaffold with the NBP and DBMA fragments were utterly unable to antagonize the NMDA receptor, which they were designed for. However, they exhibited a good potency as MAO and AChEi's.

The neurogenic properties exhibited by compounds of chapter one and four were a nice discovery. Although these results are qualitative, it is clear that a neurogenic effect was observed. Even though, the role of neurogenesis in adults is not yet fully understood and the usefulness of the neurogenic agents is still a topic of discussion; it is worth to continue the study of this kind of compounds. Maybe their ability to influence this process could be a valuable tool that may help us to increase our understanding in this field.

Conclusions

The NBP and DBMA fragments have proven to behave as privileged structures providing eight series of new bioactive compounds.

The hybridization strategy applied along this research effectively provided new compounds with a multitarget profile. All compounds were designed on the basis this strategy, taking together two privileged structures into a single small molecule. The resulting compounds from this combination, exhibited in most of cases the expected biological activity.

The new molecules presented in this work intend to be a small contribution in the quest for the urgently needed disease modifying drug to treat Alzheimer's disease.

General Introduction

Alzheimer's disease (AD) is a neurodegenerative illness characterized by a progressive loss of neurons in specific areas, such as forebrain, neocortex and subcortical cholinergic projections from nucleus basalis of Meynert.[1-4] Loss of cholinergic neurons entails low levels of acetylcholine (ACh); this diminished amount of neurotransmitter is responsible for the disruption in the neuronal transmission between the cells involved in learning and memory processes. This interruption in neuronal communication is the origin of the cognitive symptoms of AD such as memory loss, incapacity to learn, to reason, to make judgments and failure to communicate.

Understanding of disruption in cholinergic system led to acetylcholinesterase (AChE) as the first target in the search for therapeutic agents to treat AD. Acetylcholinesterase inhibitors (AChEi) were the first class of drugs successfully used in the symptomatic treatment of this disease. However, despite the improvement in cognitive and behavioral impairments in patients treated with AChEi's, this kind of drugs is not able to stop the neurodegeneration.

Explaining the origin of cognitive symptoms is not enough to understand the real cause of neurodegeneration in AD. Nowadays, amyloid-beta peptide (Aβ) is considered the initiating substance in the process leading to neuronal death.[5] Insoluble Aβ fibrils are the main constituent of the senile plaques, which are considered the toxic element triggering the cascade of cellular responses that finally produce degeneration and death of neurons.[6] Some of these events are neuro-inflammation,[7,8] production of reactive oxygen species (ROS)[9-11] and *tau* protein hyper phosphorylation.[12] An important strategy in the search of new drugs able to avoid the production of Aβ and subsequent senile plaques deposition, has been the synthesis of inhibitors of the beta-site amyloid precursor

protein cleavage enzyme (BACE1); one of the three secretases involved in processing amyloid precursor protein (APP).

Along with the decrease in ACh, there is a decline in brain levels of other neurotransmitters such as dopamine, serotonin and norepinephrine compared to healthy aging brain.[13] At the same time, it has been demonstrated that levels of MAO-B increase with age in healthy humans,[14,15] as well as in degenerative processes.[16] These increased levels of MAO-B, correlate with the exacerbated production of ROS, which are responsible for the toxic environment characteristic of neurodegeneration.[11] MAO inhibitors have been explored as a complementary alternative in the search of new drugs to treat AD, both to reduce ROS in the case of MAO-B, as to treat concomitant depression of AD patients, in the case of MAO-A.[17-19]

In this work, we have focused on the design, synthesis and biological evaluation of new molecules able to interact simultaneously with some of the most important enzymes related to AD, possessing at the same time, antioxidant properties. To achieve this goal, we have synthesized several compounds resulting from the hybridization of a variety of privileged structures.

We have selected as targets of these new compounds AChE and butyrylcholinesterase (BuChE) given that the cholinergic hypothesis is still a valid approach as discussed earlier, BACE1 because which is considered the starting point in the amyloid hypothesis, the oxidative stress, common to all neurodegenerative processes, MAO-A and MAO-B as complementary targets related to AD symptoms, and the sigma 1 receptor (σ1R) as an emerging alternative that seems to be involved in some processes related to memory and cognition. The next section explains the role of BACE1 in AD because almost all compounds have been evaluated as inhibitors of this enzyme. On the other hand, the introduction of the following chapters will discuss separately the

importance of rest of the targeted enzymes, as well as the strategy applied to design and synthesize each compound.

Beta-site Amyloid Precursor Protein Cleavage Enzyme

Nowadays, Aβ is considered the initiating substance leading to neuronal death in neurodegenerative processes.[5] Insoluble βA fibrils are the main component of the senile plaques, the pathological element triggering the cascade of events that finally produces degeneration and death of neurons.[6] Some of these events are neuro-inflammation,[7,8] production of ROS[9-11] and neurofibrillary tangles deposition produced by hyper-phosphorylated *tau*-protein.[12] The most important strategy in the search for new drugs able to avoid the production of βA and subsequent senile plaques deposition, has been the synthesis of inhibitors of the BACE1; one of the three secretases involved in processing APP, namely: α, β and γ-secretases. BACE1 is considered the initiating enzyme of the amyloidogenic pathway; it cleaves APP to produce the carboxy-terminal fragment (C99) and the soluble β-secretase metabolite sAPPβ. Subsequently, C99 is cleaved by the non-precise γ-secretase to produce mainly two forms of toxic βA peptide, differing by two amino acids βA_{1-40} and βA_{1-42}, being the latter the most toxic. Given the paramount role of β and γ-secretase in the production of toxic βA, inhibition of these two enzymes has been considered a valid approach to seek new disease modifying drugs for AD; specially BACE1 for participating in the very beginning of the amyloid cascade.

Consequences and Benefits of BACE1 inhibition in AD

Two aspects must be taken into account when discussing about BACE1 inhibition as a strategy against AD. It has been demonstrated that the levels of this protein are augmented in AD patients.[20] Consequently, inhibition of BACE1 in the right proportion might help to recover the normal levels of enzyme activity and reduction of Aβ synthesis. This proof of concept has been validated in several preclinical and clinical studies, where BACE1 inhibitors effectively reduced the production of Aβ species. However, given the complexity of AD pathogenesis, not always, the reduction of Aβ correlates with a rescue of cognitive abilities as demonstrated in studies using different molecules targeting Aβ production.[21] It is worth to mention the cases of tarenflurbil and semagacestat (γ-secretase inhibitors) and AN1792 (anti-Aβ vaccine) which effectively reduced plasma and CSF levels of Aβ and clear senile plaques but were not able to improve the cognitive abilities of AD patients in phase 3 clinical trials.[22-25] On the other hand, an excessive inhibition of BACE1 may produce strong side effects due to the diversity of substrates, the lack of specificity of some inhibitors and the distribution of the enzyme through different nervous and peripheral organs. Some of secondary effects of BACE1 inhibition are inferred from gene suppression studies which have demonstrated that complete suppression of BACE1 may produce perinatal mortality, smaller size, hyper activity, hypomyelination in CNS and peripheral nervous system (PNS), increased susceptibility to seizures and schizophrenia-like behavior, retinal toxicity, among others.[26-29]

BACE1 Inhibitors

The first class of BACE1 inhibitors was developed as transition state analogues. These compounds, usually show a non-hydrolysable peptide-based structure, large enough to fill the active site of the enzyme.[30] Due to their structural features, these inhibitors present high potencies but

poor pharmacological properties, such as low BBB penetration and bioavailability. Some non peptidic BACE1 inhibitors mimicking the transition state include derivatives of hydroxyethylene, hydroxylamine, carbineamine and reduced amides.[27,31] The poor drug-like properties of this kind of compounds led to the search of new small molecule inhibitors with high potencies and improved drug-like properties. Non-peptidic small molecule inhibitors include compounds based on acyl guanidine, 2-aminopyridine, amino imidazole, amino hydantoins, amino thiazoline, amino oxazoline, dihydroquinazoline, aminoquinoline, pyrrolidine and some natural derivatives containing the chromone, flavonoid and stilbenoid scaffolds.[27,32-35]

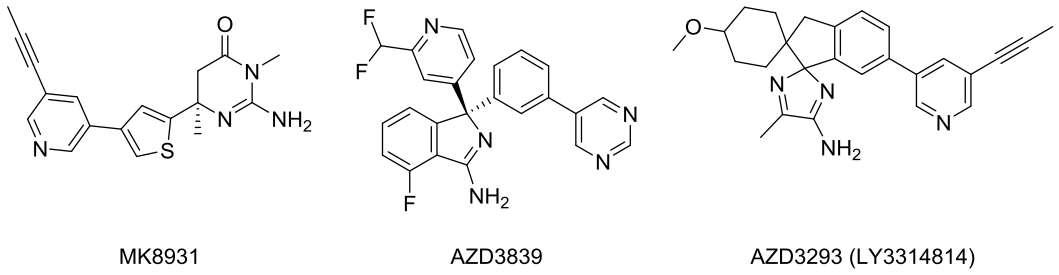

Figure 1. BACE1 inhibitors in clinical trials

In spite of the wide variety of compounds able to inhibit potently BACE1, only a few molecules have reached clinical phases. BACE1 inhibitor E2609[36] developed by Eisai Company is being currently evaluated in a phase 2 clinical study (NCT02322021) aimed to evaluate safety and efficacy in AD patients. Most advanced candidates are verubecestat, also known as MK8931 developed by Merck and AZD3293 (figure 1) from AstraZeneca; these drugs have demonstrated to be able to reduce Aβ levels in plasma and cerebrospinal fluid (CSF) by inhibition of BACE1, exhibiting safety and tolerability. Currently they have advanced to phase 3 clinical trials (NCT01739348 and NCT02245737 respectively).[26-28,37]

General Approach

During the last years, research in drug development for neurodegeneration has been driven for the paradigm of one target-one drug,[38] based on the idea that targeting specifically a single enzyme, receptor or gen could stop or reverse a pathological process. This approach has failed in putting into the clinic a disease-modifying drug or treatment, defined as any intervention able to affect the pathogenesis of disease and consequently able to prevent, to stop, or at least to delay neuronal loss.[39]

The reason of this failure lies on the complexity of the network of pathophysiological processes underlying the origin of neurodegeneration, and our lack of knowledge about the primordial event, which triggers the others; if it does exist. So far, we understand that genetic, epigenetic and environmental factors are involved in neurodegenerative processes; moreover, today is accepted that multifactorial processes such neurodegenerative diseases cannot be stopped or prevented by a drug or treatment based on a single mechanism of action.

Regarding to AD, we must tell the same story; current drugs used in AD therapy are based on the same paradigm and are included into two categories, AChEi's and antagonists of *N*-methyl-D-aspartic acid (NMDA) receptor. These drugs are aimed to treat the symptoms of the disease but are not able to affect the progression of neuronal loss. Research in drug discovery for AD, has been conducted in a similar manner, on the basis of the main accepted hypotheses. It has led to the synthesis of hundreds of new inhibitors of the enzymes involved in its onset and progression; (i.e. AChE, BuChE, BACE1, glycogen synthase-3β (GSK-3β), phosphodiesterases (PDE's), and MAO's). However, in spite of their potency and pharmacological properties, none

of them has been able to act as a disease modifying drug, or at least to show better results than those of the currently used drugs. These disappointing outcomes have led to researchers to envision new strategies in the quest for a pharmacological cure for AD.

Multitarget Strategy

One of these new approaches is based on the idea that a single molecule acting at different targets and different levels of the pathophysiology of a disease would exert synergic effects, which in turn could affect in a more effective way the progress of the disease; this kind of drug are denominated, among other names, multi-target directed ligands (MTDL).[40] This new approach could be considered an evolution of two older concepts, multi-medication therapy (MMT) and the multi-compound medication (MCM). The former consists of administering separately several medications with different mechanisms of action (cocktail) and the latter comprises the combination of several drugs in an unique formulation (single pill).[41]

One example of MCM related to AD is the administration of rivastigmine and memantine in a single transdermal patch. The study of Han and coworkers (2012),[42] evaluated the effects of this combination in patients with mild and moderate AD. They observed that results of this treatment vary depending on the apolipoprotein E genotype. According to the authors, patients carrying ε4 allele responded in a more favorable manner. However, whether or not, combined treatment of these drugs is better than individual administration remains controversial, since this putative improvement is small regard to the effects of individual administration of AChEi's.[43]

Disadvantages of these strategies may include different and accumulative side effects, different ADME properties or different regimens of administration. Theoretically, MDTL strategy may avoid these

disadvantages, since one single drug would require a unique administration via, showing a unique pharmacological profile and acting on different interconnected targets in a synergic manner and with a reduced pattern of side effects.

Two Ways to MTDL's

Two general strategies exist to design MTDL's; construction of molecules with merged or overlapping pharmacophores with in-built ability to interact with the desired targets, and the combination of independent moieties through a linker with the hope to maintain the individual activities in the resulting "hybrid" molecule.

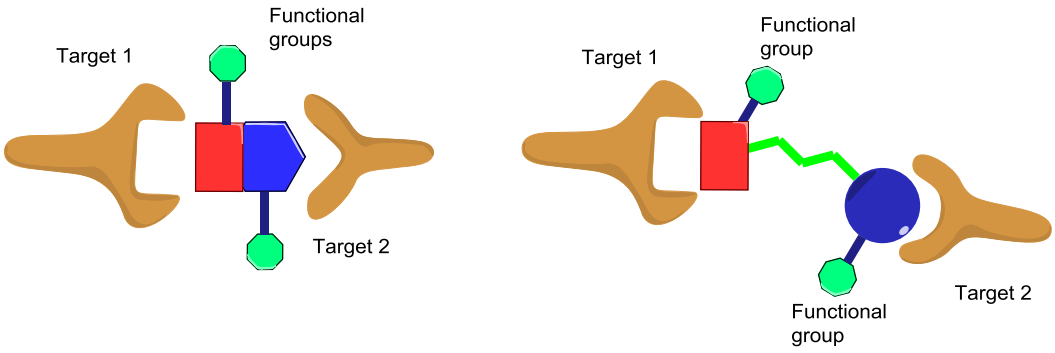

Figure 2. Description of the strategies used to build MTDL's

In both cases it is possible to apply the traditional functionalization strategy in order to increase the affinity or modulate the selectivity profile of a given ligand.[40,44,45]

Traditionally, the resulting hybrid molecules are defined as the combination of different independently acting compounds into a single covalently bonded compound, able to provide a greater potency than the sum of each individual moiety.[46] However, today it is accepted that MTDL's, must not necessarily own high affinity towards each one of the targets which they are aimed to. Generally, it is considered unlikely that a single small molecule binds equally to its different targets with the

same high affinity. Speaking about MTDL's, low affinity does not necessarily means low efficacy; a multitarget-ligand might be enough to produce a disease modifying effect, since would be able to affect the network of pathophysiological factors involved in a disease.[47]

Privileged Structure Concept

One of the most important aspects in the design of new MTDL's, is the selection of the structures to be hybridized. It is possible to combine whole molecules or fragments believed to be involved in the interactions with the active site of the targets to be aimed. One important idea to be considered is the privileged structure concept.

There are two ways to understand this general concept. The first one refers to the definition of Evans et al.[48] as those structures able to provide ligands for more than one receptor. The second one refers to the concept of a privileged scaffold, defined as a molecular framework present in several molecules with biological activity.[49,50]

Along this work, we planned to use this general concept in the design of new MTDL's with potential use in AD therapy. We have selected the NBP fragment to be hybridized with other privileged scaffolds important to AD in order to obtain several families with different combinations of biological activities. In the next section, some studies demonstrating the ability of NBP to participate in molecular interaction with some enzymes related to AD are explained.

NBP Fragment as a Privileged Structure with potential use in AD.

NBP fragment accomplishes the classical concept of privileged structure; it is part of numerous molecules with affinity for different targets related to central nervous system (CNS). Benzetimide, (muscarinic antagonist), and donepezil (AChEi) bear an NBP fragment in their structure.[49,51]

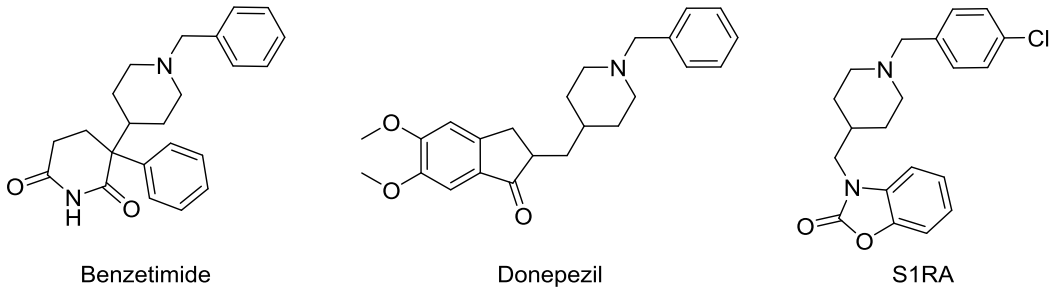

Figure 3. Active molecules containing the NBP fragment

Since we have selected BACE1, the sigma-1 receptor (σ1R), AChE and BuChE as our targets of interest, we describe here some examples demonstrating the importance of NBP fragment in the interactions of some selected ligands with these proteins.

In donepezil-hAChE complex, the benzylic ring forms a π-π stacking interaction with tryptophan 86, while the nitrogen atom of donepezil interacts through a water molecule with tyrosine 341 and tyrosine 337.[52] (Figure 4)

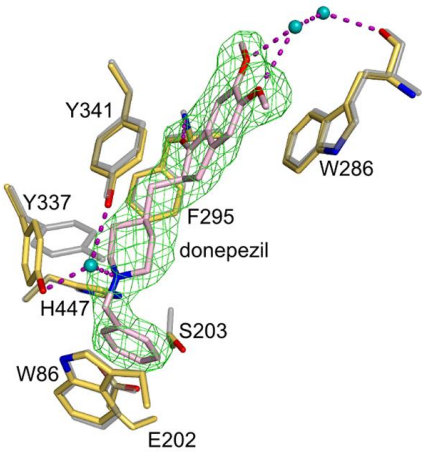

Figure 4. Molecular interactions between donepezil and AChE; taken from reference 31.

Regarding to σ1R, it has been demonstrated that analgesic compound S1RA, synthesized by Zampieri and coworkers, (K_i = 0.1 nM),[53] bearing an NBP fragment in its structure, may interacts with the putative active

site of the receptor through a T-stacking π-π interaction between the benzylic ring and tryptophan 121, a salt bridge between the protonated nitrogen of the piperidine and aspartic 126 and finally Van de Walls interactions between arginine 119 and *p*-Cl-phenyl ring according to the homology model of Laurini et al.[54,55] (Figure 5)

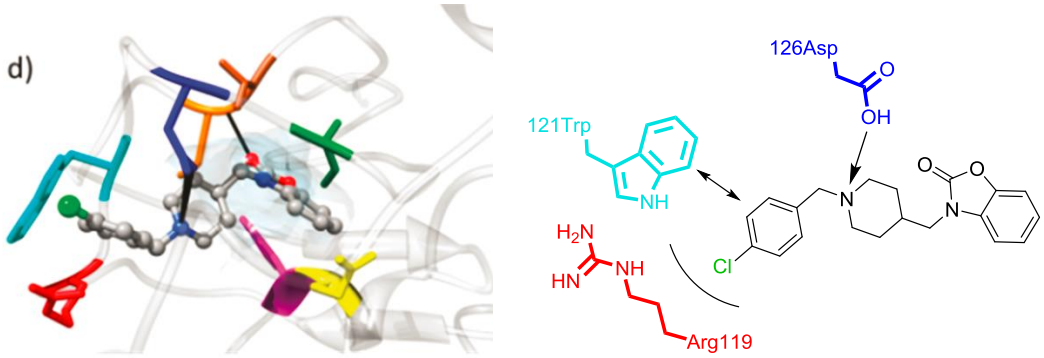

Figure 5. Molecular interactions between S1RA and σ1R homology model, taken from reference 33

Concerning to BACE1, Yang and coworkers (2009),[56] demonstrated the utility of *N*-(1-benzyl-piperidin-4-yl)-4-mercapto-butyramide as a probe to be covalently bonded to a cysteine residue in the protein in order to study its ability to occupy the catalytic site of the enzyme (figure 6). They observed that the tertiary amine of the NBP fragment is able to interact with Asp32, while the amide nitrogen interacts with Asp228 in the open conformation of the catalytic site. On the basis of these observations, authors developed a new series of reversible BACE inhibitors with IC_{50} values in the low micromolar range.

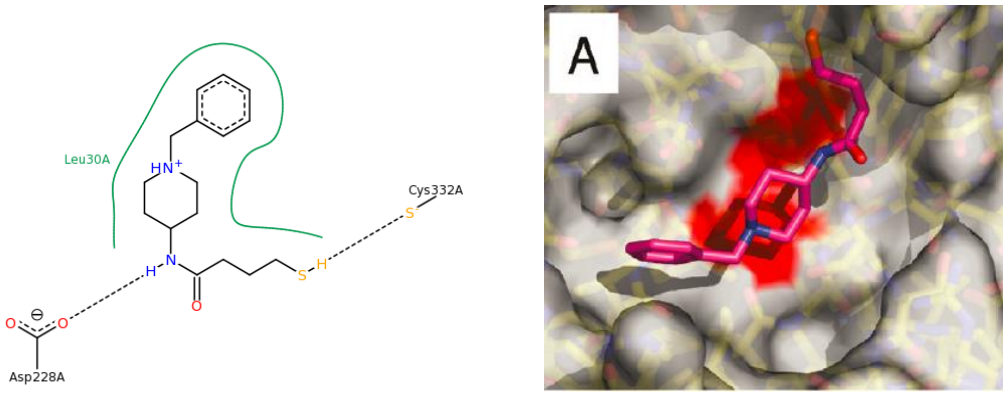

Figure 6. Molecular interactions between *N*-(1-benzyl-piperidin-4-yl)-4-mercapto-butyramide and human BACE1; taken from Protein Data Bank, entry 2ZJH and reference 35

These examples make evident the potential of a privileged structure such as the NBP fragment to obtain new compounds with affinity for three crucial enzymes involved in AD.

We propose to use this structure to be hybridized with different privileged scaffolds with complementary affinity for other important targets such as MAO-A, MAO-B, NMDA receptors, and oxidative stress. On the other hand, given the similarity between the NBP and the DBMA fragments, and taking into account that DBMA has been successfully used in the synthesis of some potent AChE inhibitors such as APP2238.[57] We have aimed to use it along this work as an isosteric replacement which could improve the potency or modulate the selectivity for each target. All of above, aiming to obtain new MTDL's with potential use in the therapy of AD.

The chapters coming next are written in a full paper style, containing their own introduction explaining the corresponding main target, the description and discussion of results and the corresponding conclusions. In the last part of this document, a section of concluding remarks has been included to give an overview of the results and some perspectives about future studies that could be derived from this work.

Chapter 1

Design Synthesis and Evaluation of New Sigma-1 Agonists with AChE-BACE1 Inhibitory Activity and Antioxidant Properties

Introduction

Sigma Receptor

The history of sigma receptor is closely related to the opioid receptors family; before its isolation and pharmacological characterization,[58-60] it was mistakenly classified as a subclass of opioid receptor. The opioid-like effects of morphine, ketocyclazocine and alazocine (SKF10047 or SKF) (figure 1.1), led to Martin and co-workers in 1976, to presume the existence of three opioid receptors, since these three structurally related substances exerted three different syndromes in dogs.[61] Morphine induced the μ syndrome, characterized by miosis, bradycardia, hypothermia, depression of the nociceptive responses, indifference to environmental stimuli and euphoria. According to the authors, this syndrome was attributable to the interaction between morphine and its putative receptor (μ receptor). On the other hand, ketocyclazocine symptoms including dysphoria, miosis, sedation, depression of the flexor reflex and low effects in nociception and pulse rate were attributed to the interaction of ketocyclazocine with its receptor (κ receptor). The third compound exerted different symptoms including mydriasis, tachypnea, tachycardia, and surprisingly, dog delirium and hallucinations. Since the symptoms exerted by this opiate compound were different to those exerted by morphine and ketocyclazocine, Martin and coworkers proposed the target of alazocine as a new opioid receptor, supported by

the fact that this protein interacts with an opiate molecule which effects are antagonized by naltrexone, a classical opioid antagonist used as a control to determine whether or not a receptor is opioid in character (Figure 1.2).

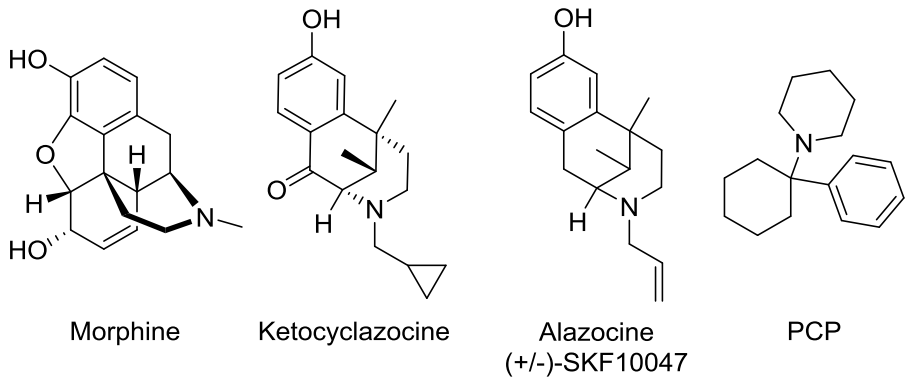

Figure 1.1 Compounds used by Martin and coworkers to propose μ, κ and σ syndromes

Controversially, in 1983 Vaupel reported that naltrexone was not able to antagonize the effects of phencyclidine (PCP) and SKF.[62] This study observed that a dose of 0.8 mg/Kg of naltrexone, required to produce abstinence in SKF dependent dogs, was 40 times higher than the dose used for morphine dependent dogs; this finding pointed out a low affinity of naltrexone for the sigma receptor. Indeed, according to the authors, withdrawal abstinence in SKF-dependent dogs was stronger than naltrexone triggered abstinence, ratifying the weak affinity for the sigma receptor. Abstinence syndrome precipitated by naltrexone included antagonism on the flexor reflex paradigm.

The observations of Vaupel, added to the study of Herling and Shannon (1982) in which was demonstrated that κ opioid-like effects of racemic SKF are attributable exclusively to the isomer (-)-SKF10047, since they are antagonized by naloxone (figure 1.2),[63] led to conclude that the σ syndrome observed by Martin is produced by the interaction between isomer (+)-SKF10047 and the putative sigma receptor; however,

considering that these effects are not antagonized by naloxone or naltrexone, which is a requirement for a receptor to be considered opioid, it was decided to avoid the terms opioid or opiate when referring to sigma receptor proteins.[64]

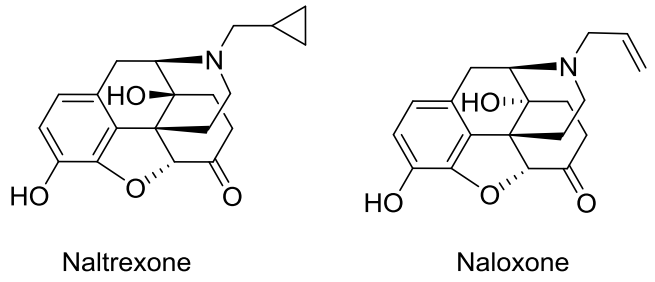

Naltrexone Naloxone

Figure 1.2 Typical opioid antagonists

Nowadays, it is accepted that sigma receptor is a unique kind of protein, different to opioid receptors and phencyclidine (PCP) binding site, an ionophore of the NMDA receptor which shares affinity for (+)-SKF.[65] There are two subtypes of sigma receptors, designated as σ1 and σ2 on the basis of their different pharmacological profiles.[66,67] σ1R structure consists of a 223 amino acid chain with two transmembrane domains, different to G-protein coupled receptors (GPCR) and with no homology with any other mammalian protein. σ2R structure still remains to be elucidated. [68-70]

The work of Hayashi and Su (2007) is considered one of the most important studies on σ1R.[71] They proposed that σ1 is a ligand activated "receptor chaperone" located on the mitochondria-associated endoplasmic reticulum membrane (MAM), complexed with other chaperon known as binding immunoglobulin protein (BiP, Grp78 or HSPA5). Activation of σ1 leads to the dissociation of σ1/BiP complex and subsequent redistribution of σ1 to form a new complex with type 3 inositol triphosphate receptors (3IP3R). This new association stabilizes 3IP3R prolonging their action and maintaining the influx of calcium from

endoplasmic reticulum (ER) to mitochondria. Cytosolic calcium levels are not affected by activation of σ1, since it does not form any complex with type 1 IP3 receptors.

ER-stress conditions, such as glucose deprivation, ER Ca^{+2} depletion and unfolded proteins accumulation, produce σ1R redistribution and transcriptional up-regulation which suppress ER-stress induced activation of PERK (protein kinase RNA–like endoplasmic reticulum kinase) and ATF6 (activating transcription factor 6), two proteins involved in unfolded protein response (UPR). This upregulation has no effects on ER-stress induced IRE1 (inositol-requiring transmembrane kinase/endonuclease 1) expression and basal activity of the three UPR proteins. This is considered a proof of the involvement of σ1R in cell survival. Indeed, in the same work it was established that knocking down of σ1R enhances apoptosis induced by ER-calcium depletion and glucose deprivation.[71,72]

σ1R is currently considered a new promising target in several neurodegenerative diseases such as amyotrophic lateral sclerosis (ALS)[73,74], Parkinson's disease (PD),[75] Huntington's disease,[76] and numerous neurodegenerative diseases.[77,78]

Sigma-1 Receptor in Alzheimer's Disease

Presence of σ1R has been demonstrated in different animal and human brain regions: hippocampus, neocortex, substantia nigra, dentate gyrus of hippocampus and cerebellum;[79-82] areas involved in motor function, emotions and memory. Besides neurons, such as Purkinje cells, σ1R has been detected in astrocytes, oligodendrocytes and Schwann cells.[83-85] Given its presence in neural tissue, the role of σ1R has been evaluated in several processes related to CNS diseases. Although the whole biological role of these receptors remains unknown, today we know they regulate

the function of a variety of processes trough opioid, NMDA, dopaminergic and cholinergic receptors.[86,87]

Regarding to AD, numerous studies have demonstrated the effects of σ1R agonists in various models of amnesia, learning and neuroprotection, among others. For example, enhancement of acetylcholine release from rat prefrontal cortex and hippocampus has been observed after administration of (+)SKF10047.[88] These observations led to study the effects of other σ1 agonists in learning and memory. For instance SA4503 (figure 1.3), a selective σ1 agonist, counteracts the amnesic effects of scopolamine, a potent cholinergic muscarinic antagonist known for producing memory impairment by blockade of ACh transmission.

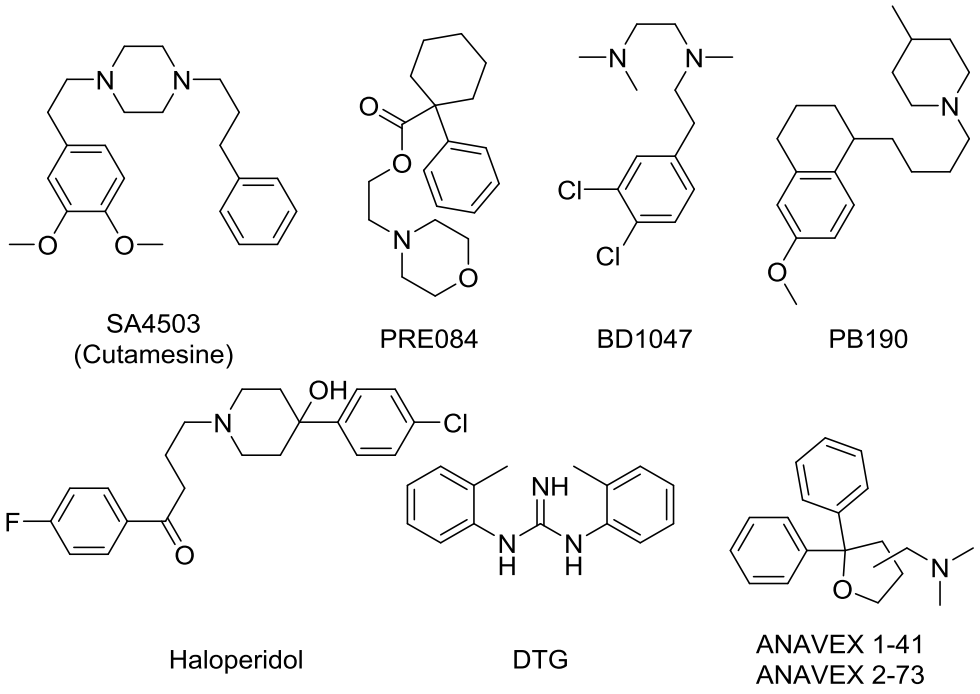

Figure 1.3 Some of the most studied σ1 receptor ligands

On the other hand, SA4503 alleviates amnesic effects of basal forebrain lesion induced by ibotenic acid; this brain region is rich in cholinergic neurons and corresponds to nucleus basalis of Meynert in humans. Ibotenic acid destroys selectively these neurons, damaging the central

cholinergic system and simulating AD conditions. Interestingly, effects of SA4503 in memory impairment induced by scopolamine and basal fore brain lesion, are reversed by haloperidol, a typical σ1 antagonist, confirming the involvement of this receptor in the mechanism of action of SA4503 and the potential of σ1 agonists in AD treatment.[89,90]

In regard to cognition, the σ1 agonist PRE-084 (figure 1.3) was evaluated in aged rats by Maurice (2001) using the water-maze model.[91] Aged but not adult animals presented learning deficits which were alleviated by pretreatment with PRE-084. Age matched animals treated with saline, did not show any significant improvement of learning abilities; however, this work did not provide any information about using a σ1 antagonist to counteract beneficial effects of PRE-084 in order to confirm the involvement of this receptor in the mechanism of action. A later study reported the protective effects of PRE-084 in a model of Aβ-induced toxicity. Learning and memory deficits exerted by $A\beta_{25-35}$ administration, were reverted in the spontaneous alternation test (Y maze) and passive avoidance test. Beneficial effects of PRE-084 were reverted in a dose-dependent manner by administration of the σ1 antagonist BD1047.[92]

Apart from the effects against learning and memory deficits, several studies have evaluated the potential neuroprotective properties of σ1R agonists against the oxidative stress induced by Aβ administration.[92-94] ANAVEX1-41 and ANAVEX2-73, two mixed muscarinic and σ1 agonists, have demonstrated to protect against the cell loss induced by Aβ toxicity in areas of hippocampus involved in memory and cognition, and sensitive to senile plaques deposition. In addition to cell death rescue, ANAVEX compounds proved to protect neurons against oxidative stress and apoptosis induced by toxic Aβ fragments, as demonstrated by diminution of levels of some oxidative stress markers, such as protein nitration, lipid peroxidation and caspase-3 production. Authors proposed a synergic mechanism of action involving muscarinic and σ1R; since protective

effects are antagonized by scopolamine and BD1047.[93,94] Another study reported that ANAVEX2-73 was able to reduce $A\beta_{25-35}$ induced *tau* hyper phosphorylation by two ways: restoration of levels of the active form of Akt (protein kinase B), which regulates the activity of GSK-3β and by diminution of the active form GSK-3β which was increased by $A\beta_{25-35}$ administration and is considered to be upregulated in AD patients.[95] ANAVEX 2-73 has successfully completed a phase 1 clinical trial and is currently being evaluated in a phase 2a clinical study (NCT02244541).

Another important finding connecting σ1R and AD is the decrease of σ1 binding sites in human AD brain. The postmortem study carried out by Jansen and coworkers (1993) demonstrated that loss of neurons from hippocampus in AD diagnosed brains, correlates with the diminished amount of σ1 binding sites in the same regions.[96] Similar findings were observed *in vivo* by Mishina et al. (2008) with positron emission tomography (PET), using σ1 agonist [^{11}C]-SA4503; authors reported a reduced cortical and cerebellar distribution of σ1 in early AD patients compared with healthy controls.[97] However, in this study, the fact that some of the participating patients were treated with donepezil before experiments was not taken into account. Donepezil is known to possess high affinity for σ1R and might affect its levels and distribution.

σ1R activation exerts protection against oxidative stress by activation of the antioxidant response element (ARE) and subsequent transcription of the proteins involved in the cellular response to oxidative damage. According to the results of Pal et al. (2012) in σ1 transfected COS-7 cells, these effects can be potentiated by σ1 agonists and reduced by antagonists.[98] Moreover, σ1 knocked-out mice showed higher levels of oxidative markers and some antioxidant proteins compared to naive animals; this may point out a protective role of σ1R against oxidative offense, additional to the chaperone activity discussed earlier.

Additional properties of σ1 agonists may include protection against excitotoxicity. It has been demonstrated that σ1 agonists are able to suppress the response to NMDA in rat ganglion retinal cells,[99] as discussed earlier, σ1 chaperone activity may be involved in these effects. However, regardless to the mechanism, reducing response to NMDA could prevent excitotoxicity induced apoptosis.[100,101] Lobner et al. (1990) demonstrated that glutamate release induced by *in vitro* ischemic conditions (anoxia and glucose deprivation) was attenuated in rat brain slices by addition of σ1 agonist *N,N'*-di(o-tolyl)guanidine (DTG).[102] Moreover, inhibition of glutamate release combined with NMDA receptors blockade exerted neuroprotective effects in rat brain slices, noteworthy, NMDA blockade alone was not neuroprotective by itself. A plausible mechanism which explains these observations remains unknown.

Recently, it was discovered that the σ1 agonist PB190 is able to block the microglial response to neuronal injuries. Such response consists on moving toward the damaged region, engulfing apoptotic neurons and releasing important cytokines, chemokines and ROS. Exacerbated microglial response is believed to be in part, responsible for neurodegeneration; consequently, modulation of this response could be paramount in slowing down neuronal loss. It was proved that σ1 agonists administration to zebra fish larvae, blocks the microglial response to neural injury, without affecting microglial motility and ability to engulf apoptotic neurons, allowing microglial cells to move away from injured areas and permitting subsequent repair. Based on these outcomes, and in the fact that the effect of PB190 in microglial activation were abolished by knocking-down of σ1R, authors proposed that the role of σ1 *in vivo* is to switch-off microglial reaction, reinforcing the potential of σ1R as a therapeutic target in neurodegenerative diseases.[103]

Taken together, these findings put clear the importance of σ1R as a plausible target in the quest for finding new disease-modifying drugs for AD.

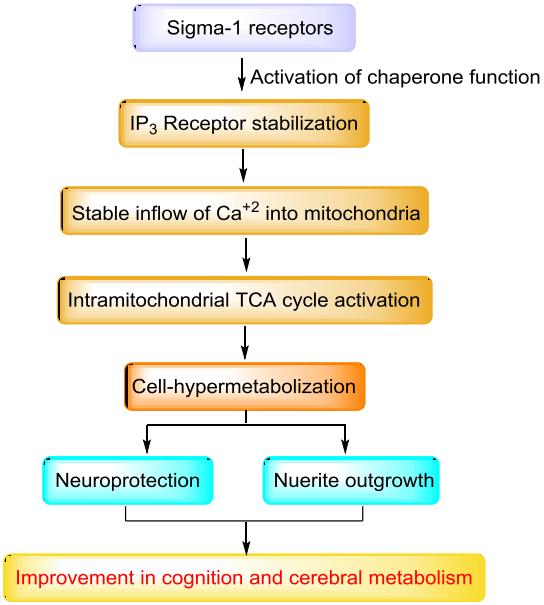

Figure 1.4 Protective effects of σ1 agonists, adapted from Ishikawa and Hashimoto (2010)[104]

Lipoic Acid

Lipoic acid is a naturally occurring antioxidant substance, isolated for the first time by Reed et al. in 1951.[105,106] Only *R*-LA occurs in nature, both in animals[107] and humans.[108] It has been identified as a cofactor for several enzymes, important in energetics and mitochondrial metabolism.[109]

Biochemical and pharmacological features of LA make it an interesting tool in the search for new molecular entities with the potential to become anti-AD drugs. Most renowned of these features is its antioxidant capacity. LA is rapidly absorbed from diet and easily reaches the blood stream and tissues where is likely converted to its reduced form, dihydrolipoic acid (DHLA)[110]

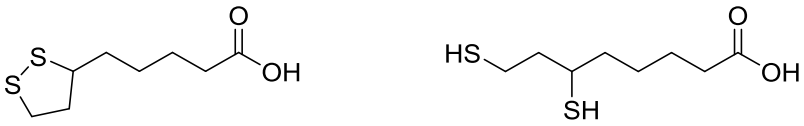

Lipoic acid Dihydrolipoic acid

Figure 1.5 Lipoic acid and its reduce form, dihydrolipoic acid

LA and DHLA achieve some of the most important requirements to be considered as good antioxidants. They are able to quench free radicals in aqueous and lipid phases, possess chelating properties and are able to regenerate other biogenic antioxidants.[111]

A great number of studies have confirmed the beneficial properties of LA in several models of oxidative stress and neuroprotection.[112-117] Indeed, positive effects of LA on cognitive parameters and disease progression of AD patients has been reported, despite postmortem confirmation of diagnosis remains needed in some of these studies.[118-120] These effects could be explained by the ability of DHLA to increase the activity of acetylcholine transferase, and therefore, the production of acetylcholine, as demonstrated by Haugaard and Levin in 2000 and 2002,[121,122] to protect against toxicity induced by Aβ, as confirmed in cultured rat cerebral neurons by Zhang et al. in 2001[123] and Lovell et al. in 2003,[124] to stimulate glucose uptake, according to Seaton et al.,[125] who proved the ability of LA to promote the incorporation of ^{14}C-deoxyglucose in rat basal ganglia. These results were attributed to the ability of LA to act as an insulinomimetic agent and to stimulate the utilization of glucose *in vivo* and therefore, the synthesis of the neurotransmitter acetyl choline which is dependent on acetyl-CoA, a substrate in the glycolytic pathway. Since it has been hypothesized that AD could be considered a type of diabetes confined to CNS,[126,127] a compound with the ability to regulate the homeostasis of glucose and insulin brain levels could be relevant to treat not only AD but different neurodegenerative diseases.

Besides their antioxidant properties, BACE-1 inhibitory properties have been reported for hybrid compounds containing LA. One example is lipocrine, a hybrid between the AChE inhibitor tacrine and LA, which possesses the ability to inhibit simultaneously AChE, BACE-1 and self-induced and AChE-catalyzed Aβ aggregation.[128-131] Other examples demonstrating the value of LA as part of bioactive molecules include derivatives showing cytoprotective properties,[132] neuro-protectants[133] and σ1R agonists.[114]

In this section we aim to hybridize the LA structure with the NBP and DBMA fragments present in the well-known AChE inhibitors donepezil and AP2238,[134] in order to take advantage of their privileged properties described earlier. We propose that a combination of LA and a moiety containing a tertiary amine bearing a benzyl group could interact with the active sites of AChE, BACE-1 and/or σ1R.

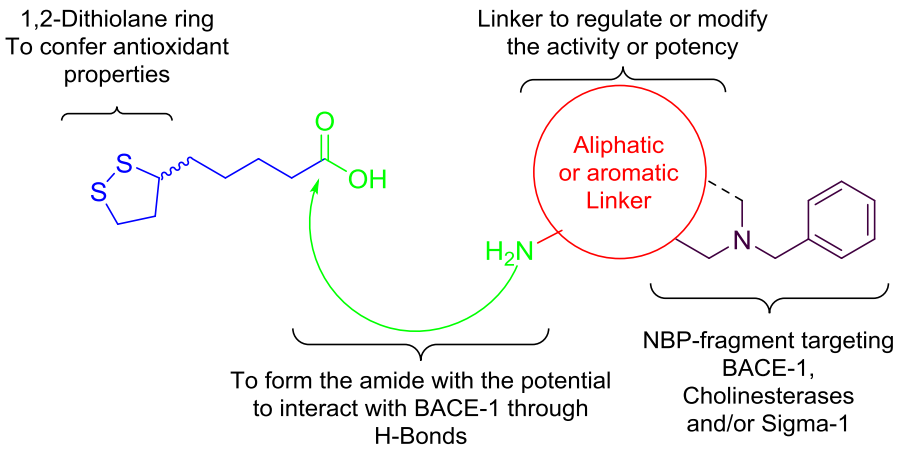

Figure 1.6 Description of the proposed LA-hybrids and their potential interactions

Recently, Prezzavento and coworkers, obtained similar esters containing the NBP fragment which effectively binds to the σ1R.[114] However, here we intend to obtain new amide derivatives modifying the distance and geometry between the amide group and the tertiary amine, keeping intact the benzyl fragment which is crucial for interaction with the proposed targets as explained in the general approach section.

Results and Discussion

Synthesis of LA-NBP and LA-DMBA hybrids.

In the NBP series, the required intermediates 1-benzylpiperidin-4-amine (n = 0) and 2-(1-benzylpiperidin-4-yl)ethanamine (n = 2) are commercially available whereas NBP amines with n = 1 and 3, were synthesized by two different methods depending on the length of the hydrocarbon chain.

Compound **1.1** was obtained in excellent yield (92%) reacting benzyl bromide and piperidine-4-carbonitrile in refluxing toluene for 3 h. Subsequent reduction of nitrile **1.1** gave amine **1.2** (85%) by overnight treatment with $LiAlH_4$ in ethyl ether at room temperature (rt) (Scheme 1.1).

On the other hand, compound **1.3** was synthesized by a Knoevenagel-Doebner reaction from 1-benzylpiperidine-4-carbaldehyde and cyanoacetic acid in refluxing pyridine for 3 hours. The unsaturated intermediates were not isolated and were reduced with $LiAlH_4$ to obtain **1.4** as a sole product in 87% yield.

In the DBMA series, compounds **1.5** and **1.6** were synthesized in high yields (95-97%) by reaction between *N*-methyl benzylamine and the corresponding nitro benzyl bromide in refluxing toluene during 3 h. Their reduction by catalytic hydrogenation provided amines **1.7** and **1.8** in almost quantitative yields (97-98%).

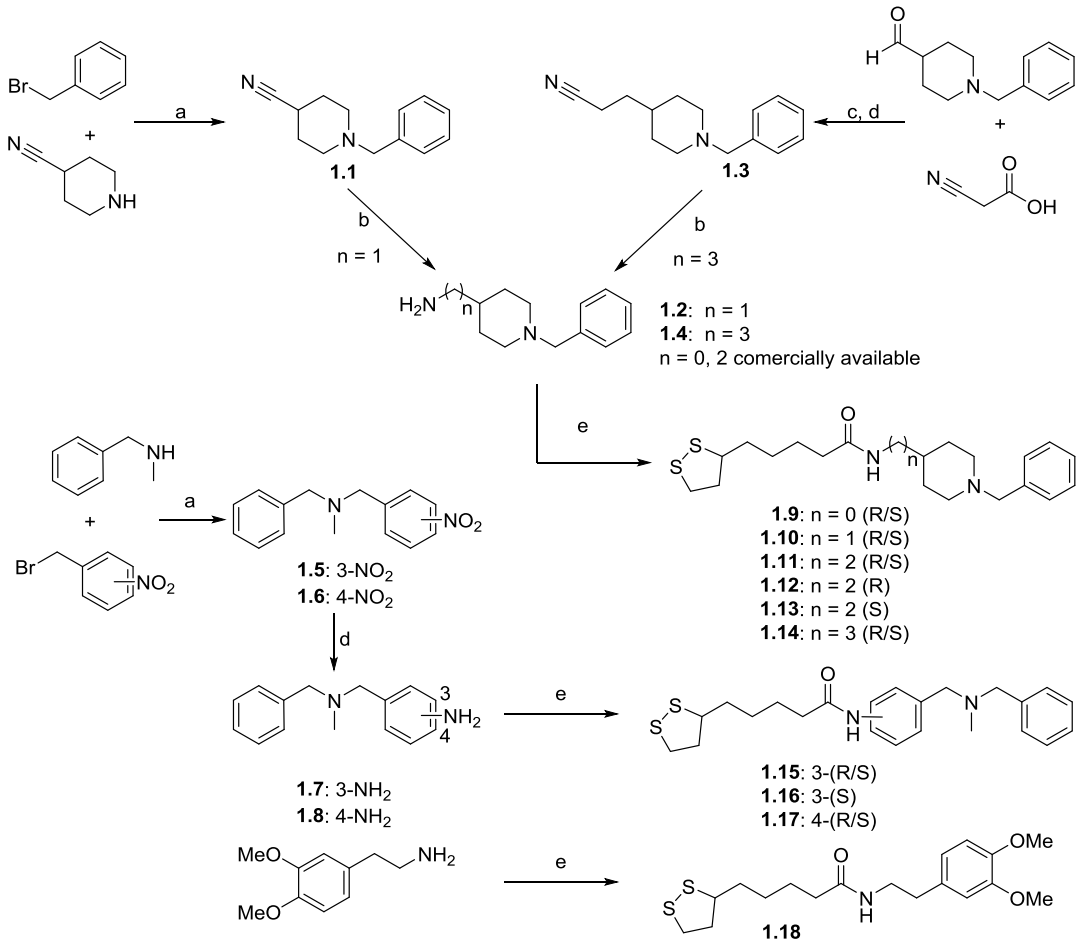

Scheme 1.1 Reagents and conditions. (a) Toluene/Triethyl amine (Et_3N)/reflux/3h; (b) $LiAlH_4/Et_2O$/rt.; (c) Pyridine/reflux/3h/-CO_2; (d) H_2/Pd-C(5%)/EtOH/rt./overnight; (e). LA/CDI/THF/mw/120°C

Finally, LA-based hybrids **1.9**-**1.17** were obtained by a coupling reaction between the corresponding amine derivative and LA into a microwave reactor at 120 ºC for 3 min. Carbonyl diimidazol (CDI) was used as activating agent and THF as solvent. In general, hybrids were isolated in high yields (80-93%), although in the case of **1.10** an unexpected low 25% was obtained despite several attempts to improve the reaction work-up (Scheme 1.1).

For comparison purposes, previously reported compound **1.18** was also obtained from 2-(3,4-dimethoxyphenyl)ethan-1-amine and racemic LA.[133]

Biological Evaluation

Human Cholinesterases Inhibition and Oxygen Radical Absorbance Capacity (ORAC). Initially, all LA-based hybrids were evaluated as inhibitors of human AChE and BuChE (h-AChE and h-BuChE), following the Ellman method[135] (Table 1.1). For the NBP series and in relation to h-AChE inhibition, the chain length connecting the LA and NBP fragments was found to be a critical parameter, the best activity results being obtained for n=2 (i.e., -$(CH_2)_2$-). Interestingly, racemic (*R*,*S*)-**1.11** and its enantiomers (*R*)-**1.12** and (*S*)-**1.13** showed IC_{50} values for h-AChE in the sub-micromolar range, without any noticeable difference between racemic mixture and pure enantiomers. However, in the case of h-BuChE, both pure enantiomers (*R*)-**1.12** and (*S*)-**1.13** displayed better inhibition (around one order of magnitude) than the corresponding racemic mixture (*R*,*S*)-**1.11**. Replacement of the NBP fragment with DBA did not improve the inhibitory potency of the relevant compounds but shifted the selectivity between the two cholinesterases. Hybrids **1.15** and **1.16**, bearing a *meta*-substituted intermediate ring, maintained their sub-micromolar inhibition for h-BuChE, unlike their para-substituted counterpart **1.17**. These results evidenced that NBP and DBA fragments are important for the affinity towards both cholinesterases.

Radical scavenging properties were evaluated with the ORAC assay.[136] Trolox, the scavenging part of vitamin E, was used as internal standard with the arbitrary value of ORAC = 1.0. Results are expressed as trolox equivalents (trolox mmol / tested compd mmol) in a comparative scale. All tested LA-based hybrids showed radical scavenging properties close to vitamin E and thus, they could be considered as good antioxidant agents (table 1.1).

Table 1.1 Inhibition of h-AChE, h-BuChE, and h-BACE1 (IC_{50}, μM), evaluation of the Oxygen Radical Absorbance Capacity (ORAC, trolox equivalents.), and Prediction of the CNS-Permeation by the PAMPA-BBB Assay.[a]

	IC_{50} (μM)			ORAC	PAMPA-BBB
Compd	**h-AChE**	**h-BuChE**	**h-BACE1**	(Trolox equiv.)	P_e (10^{-6} cm s^{-1})
1.9	6.81±0.25	7.99±0.35	27%[b]	0.94±0.07	nd
1.10	31%[b]	<20%[b]	6.33±0.21	nd	nd
1.11	0.39±0.03	2.13±0.14	5.65±0.26	0.96±0.02	nd
1.12	0.43±0.11	0.79±0.20	8.11±0.26	1.04±0.09	33.0±3.1[e]
1.13	0.21±0.09	0.63±0.09	9.92±0.39	0.80±0.08	26.6±0.7 [e]
1.14	3.75±0.91	0.93±0.3	7.91±0.77	0.63±0.01	nd
1.15	46%[b]	0.53±0.21	28%[b]	1.00±0.08	nd
1.16	48%[b]	0.33±0.12	25%[b]	0.79±0.09	nd
1.17	2.43±0.12	4.87±0.23	38%[b]	0.73±0.11	37.6±0.3[e]
Donepezil	0.01±0.002	2.5±0.07	0.17[c]	nd	nd
AP2238	0.044[d]	48.9[d]	nd	nd	nd

[a] Results are expressed as mean ± SEM. (n =3); [b] Inhibition percentage at 10 μM; [c] Taken from ref[137]. [d] Taken from ref[138]. [e] CNS permeation positive. nd: Not determined.

Evaluation at Human BACE1 and Sigma-1 Receptor. LA-based hybrids were evaluated as inhibitors of the human recombinant BACE1 protein in a fluorescence resonance energy transfer (FRET)-based assay.[139,140] Initially, compounds were tested at a single concentration (10 μM) and those displaying an inhibition percentage above 50% were re-evaluated in a concentration range comprised between 0.1 μM and 100 μM. The corresponding calculated IC_{50} values are listed in table 1.1

Compared to the inhibition against the cholinesterases, the activity over h-BACE1 was more tolerant to the modifications over the aliphatic chain linker, but more sensitive to the substitution of NBP by DBMA. Whereas

compounds **1.9** and **1.15**-**1.17** showed low percentage of h-BACE1 inhibition at 10 μM, hybrids **1.10**-**1.14** (n=1-3) were found to be good h-BACE1 inhibitors, with IC_{50} values in the low micromolar range. Thus, compounds containing the NBP moiety were more potent than DBMA derivatives. In the NBP series, hybrids **1.10**-**1.14** showed little variations in their IC_{50} values (5.7 – 9.9 μM, table 1.1).

Taking into account the results reported above, we selected racemic mixture **1.11**, pure enantiomers (*R*)-**1.12** and (*S*)-**1.13**, which showed the best dual h-AChE – h-BACE1 inhibition, as well as the DBA derivatives (*R*,*S*)-**1.15** (substitution at position 3) and (*R*,*S*)-**1.17** (substitution at position 4) to evaluate their ability to displace the agonists [^{3}H]pentazocine and [^{3}H]-DTG from the σ_1 and σ_2 receptors of animal origin obtained from guinea pig brain (σ_1) and rat liver (σ_2), respectively.

Table 1.2 Affinities and selectivities towards σ_1R and σ_2R of compounds **1.11**-**1.13**, **1.15** and **1.17**. The affinity of pentazocine and DTG is reported as reference compounds.

	K_i (nM)[a]		Selectivity *vs.* σ_1R[b]
Compd	σ_1R	σ_2R	($K_i\sigma_2$R/ $K_i\sigma_1$R)
11	8.90 ± 0.45	232 ± 27	26
12	7.56 ± 0.98	205 ± 42	27
13	15.1 ± 1.4	289 ± 51	19
15	25.3 ± 1.9	1200 ± 170	48
17	21.0 ± 2.6	1400 ± 230	67
Pentazocine	15.0 ± 3.0	-	-
DTG	-	54 ± 8	-

[a]Results are expressed as K_i (nM) and are the mean ± SEM of the experiments repeated in triplicates. [b]Selectivity *vs.* σ_1R was calculated as $K_i\sigma_2$R/ $K_i\sigma_1$R

Two well-known sigma binding site ligands, (+)-pentazocine and DTG, were also tested for comparative purposes (Table 1.2).

As shown in table 1.2, tested compounds showed good affinities for sigma receptors, with K_i's comprised between the low-micromolar and the

low-nanomolar scale. In all cases, LA-based hybrids exhibited a remarkable preference for the σ_1R subtype since their experimental affinities are in the range of low-nanomolar concentration with a selectivity ratio against the σ_2R greater than at least 19 times.

New compounds were then functionally characterized at σ_1R. The general consensus is that σ_1R antagonists provoke a high cytotoxic effect leading to cell death, whereas σ_1R agonists promote cell survival.[141] For defining the agonist/antagonist profile of the new derivatives we tested their cytotoxicity on the SH-SY5Y neuroblastoma cell line by adapting the approach originally proposed by Zeng et al. based on the MTT assay.[142] To this aim, the cytotoxicity of the novel σ_1R ligands was tested in SH-SY5Y cells and compared to that measured for NE-100 and pentazocine, two commonly accepted σ_1R antagonist and agonist, respectively.

Figure 1.7 shows cytotoxicity data of σ_1R ligands at 50 μM, expressed as a percent relative to the cytotoxicity of NE-100 at the same concentration, as obtained from the cell viability assay. Conversely, at the same concentration, pentazocine showed only limited toxicity (2%) to the SH-SY5Y cells. As inferred from figure 3, the moderate or low cytotoxicity of all lipoic-based hybrids is more consistent with a σ_1R-agonist, rather than with a σ_1R-antagonist activity. Both DBMA derivatives (*R*,*S*)-**15** and (*R*,*S*)-**17** could be define as full agonists, as demonstrated by a cytotoxic level under 10%, comparable to the prototypical agonist pentazocine. Instead, the NBP derivative (*R*,*S*)-**11** and its pure enantiomers (*R*)-**12** and (*S*)-**13** behaved as partial agonists with a cytotoxicity comprised between 40-60%, in any case lower compared to the antagonist NE-100. This fact could be ascribed to their smaller selectivity against the σ_1R subtype as illustrated in table 1.2.

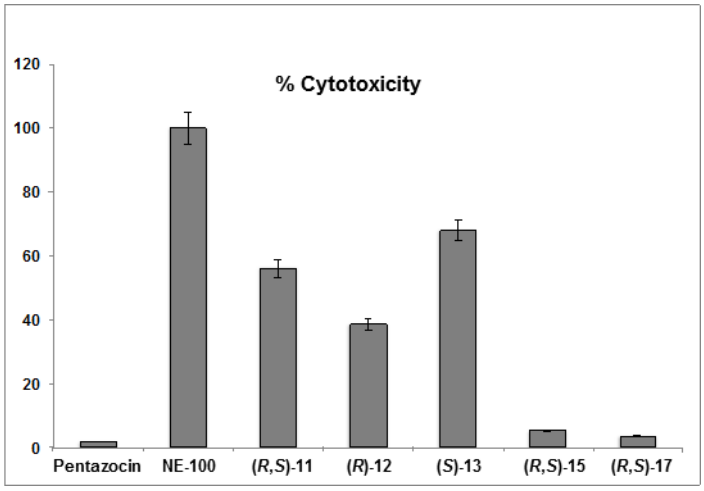

Figure 3. Cytotoxicity of σ_1R ligands as obtained from the MTT assay. SH-SY5Y cells were treated with different σ_1R ligands (50 μM) for 48h. MTT assay was then performed, cytotoxicity of compounds was determined, and data were reported as % of NE-100 cytotoxicity at 50 μM (100%). The bars represent the mean ± SD from three independent experiments performed in triplicate

Neurogenic Studies. These studies were performed to assess the potential ability of new LA-based compounds to promote differentiation of brain stem-cells into a neuronal phenotype. Derivatives **1.12** and **1.17** were selected for these studies, covering different structural features and biological activities. The LA-NBP compound **1.12** showed inhibition of h-ChEs and h-BACE1, an ORAC value similar to vitamin E, and was found to be the most potent σ_1R agonist of this work. In contrast, the LA-DBA hybrid **1.17** showed worse inhibition of h-ChEs, no activity at h-BACE1, an ORAC value under the trolox value, but displayed the most selective σ_1R agonism compared to σ_2R. Adult mice neural stem-cells were isolated from the SGZ of the dentate gyrus of the hippocampus, and cultured as neurospheres (NS) following described protocols.[143-145] NS were incubated in the presence of **1.12** and **1.17** during 7 days and then adhered on a substrate to allow differentiation for 3 days. Immunocytochemical analysis using β-III-tubulin (clone TuJ1) and MAP-2 (microtubule-associated protein 2) antibodies were used to visualize early proliferation and neuronal maturation, respectively.

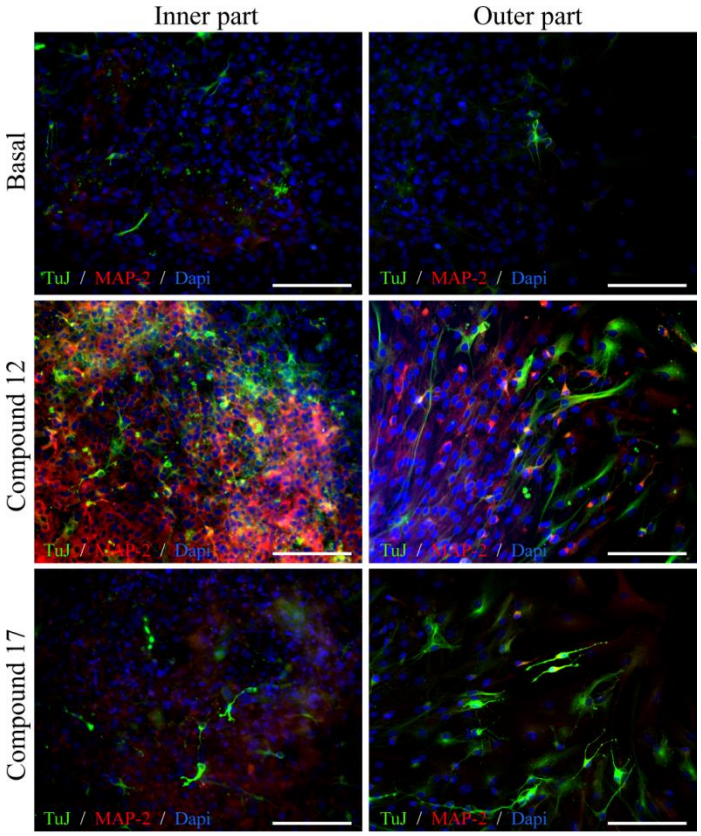

Figure 1.8 *In vitro* neurogenic effect of compounds **1.12** and **1.17** on murine hippocampal SGZ-derived spheres. Neural stem-cells enriched spheres (NS) were grown for 7 days in culture in the presence of compounds **1.12** and **1.17** (10 μM). Later on, NS were adhered on a substrate to allow differentiation for 3 days in the presence of compounds. Representative images show the expression of β-III-tubulin (TuJ clone; green) and MAP-2 (red) inside the NS (inner part) and in the distal area (outer part). DAPI was used for nuclear staining. Scale bar, 200μm.

As shown in figure 1.8, treatment with **12** and **17** clearly enhanced neurogenic activity on cultured NS. Both compounds were able to induce the expression of early neurogenesis markers like β-III-tubulin and also promoted neuronal maturation, increasing the number of MAP-2 expressing cells. Interestingly, compound **12** appeared to be more effective not only promoting early neurogenesis but also stimulating neuronal maturation, showing a great neurogenic effect.

Parallel Artificial Membrane Assay (PAMPA). Derivatives **11**, **12** and **17** were next selected as representative compounds of the two families to evaluate their ability to cross the blood-brain barrier in the PAMPA assay

Table 1.3 Permeability (P_e 10^{-6} cm s^{-1}) in the PAMPA-BBB Assay of 10 Commercial Drugs Used in the Experiment Validation

Compd	Bibl.[a]	Exp.[b]
Testosterone	17.0	30.97 ± 3.78
Verapamil	16.0	31.56 ± 3.89
Imipramine	13.0	21.55 ± 3.03
Desipramine	12.0	23.74 ± 3.17
Promazine	8.8	22.31 ± 1.69
Corticosterone	5.1	12.65 ± 0.14
Piroxicam	2.5	9.12 ± 0.04
Hydrocortisone	1.9	10.47 ± 0.03
Caffeine	1.3	7.56 ± 0.15
Ofloxacin	0.8	6.17 ± 0.31

[a]Taken from Ref. [145]. [b]Data are the mean ± SD of three independent experiments

The values of permeability were validated by comparison with previously reported values for several commercial drugs. All evaluated compounds were predicted to reach the CNS according to this *in vitro* model (Table 3).

Figure 1.9 describes the relation between bibliographic and experimental values of permeability summarized in table 3; as well as the calculated range of permeability values to determine whether or not any given compound is able to reach CNS. Compounds with values greater than 11.9 are interpreted as positive to cross the BBB.

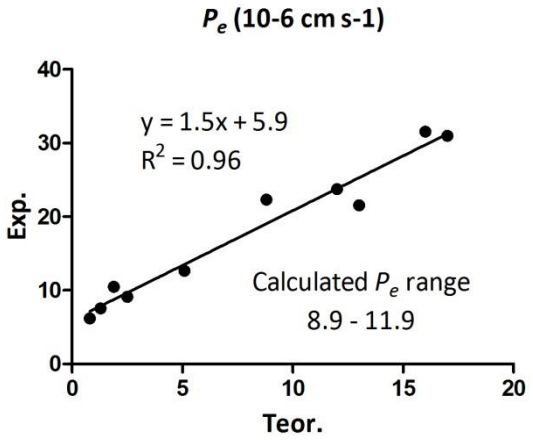

Figure 1.9 Correlation of permeability values of the standard compounds used in PAMPA

Modeling Studies

Modeling Studies in h-BACE1.

BACE1 is an aspartic protease, which functions in the first step of the pathway leading to the production and deposition of Aβs. It is a structurally challenging protein target, which displays a pronounced induced-fit conformational adjustment upon ligand interaction. Indeed, a detailed comparison of the available X-ray structures suggests that both the flap open region of the enzyme (residues 68–74 forming a β hairpin loop) and the 10s-loop (residues 9–14) located near the S3 site undergo a substantial rearrangement upon ligand binding.[146,147] Accordingly, BACE1 adopts a bilobal structure with the inhibitor binding in the

substrate binding pocket between the *N*-terminal and C-terminal lobes of the enzyme. Catalytic aspartates D32 and D228 are located at the center of this pocket, and form part of an extensive hydrogen bonding network within the protein active site.[27]

A challenge in the design and discovery of BACE1 inhibitors is posed by the large size of its substrate pocket. However, the development of large inhibitors is of poor practical use, given the known pharmacokinetics and pharmacodynamics problems such drugs may encounter *in vivo*. Concomitantly, small-molecule inhibitors would hardly fill the binding pocket adequately and, as such, are not endowed with great inhibitory potency. A way to overcome this issue can consist of increasing the affinity of a given inhibitor for the BACE1 active site by potentiating its interactions with the residues lining the enzyme binding cavity. In this context, we have carried out a molecular modeling study aimed at providing insights into the binding mode of the new LA-NBP and LA-DBMA hybrids onto BACE1.

Table 1.4 Binding Free Energies ΔG_{bind} and its Components for **1.12**, **1.13**, (*R*)-**1.17** and (*S*)-**1.17** in Complex with the BACE1[a]

Compd.	ΔH (kcal/mol)	TΔS (kcal/mol)	ΔG_{bind} (kcal/mol)
(*R*)-**1.12**	-47.50 (0.21)	-29.16 (0.27)	-18.34 (0.35)
(*S*)-**1.13**	-47.26 (0.23)	-29.10 (0.26)	-18.16 (0.33)
(*R*)-**1.17**	-32.11 (0.21)	-23.42 (0.29)	-8.69 (0.37)
(*S*)-**1.17**	-32.09 (0.19)	-23.28 (0.28)	-8.81 (0.44)

[a]Values are expressed in kcal/mol and errors are given in parenthesis as standard errors of the mean.

A three-step computational procedure was followed. In the first stage, we performed docking studies on the whole target protein surface. In a second stage, the best determined binding mode was further refined by molecular dynamics (MD) simulations. Finally, binding free energy

(ΔG_{bind}) calculations in the MM-PBSA framework of theory[148] were carried out to gain insight into thermodynamics and the nature of the stabilizing interactions for each drug/protein complex (table 4).

Analysis of the binding mode of (*R*)-**1.12** and (*S*)-**1.13** into the BACE1 enzyme revealed that the NBP scaffold locates below the flap region, allowing the protonated nitrogen of the piperidine to interact with both catalytic aspartic acids D32 and D228,[27,149,150] and with T231 via electrostatic and H-bond interactions (figure. 1.10).

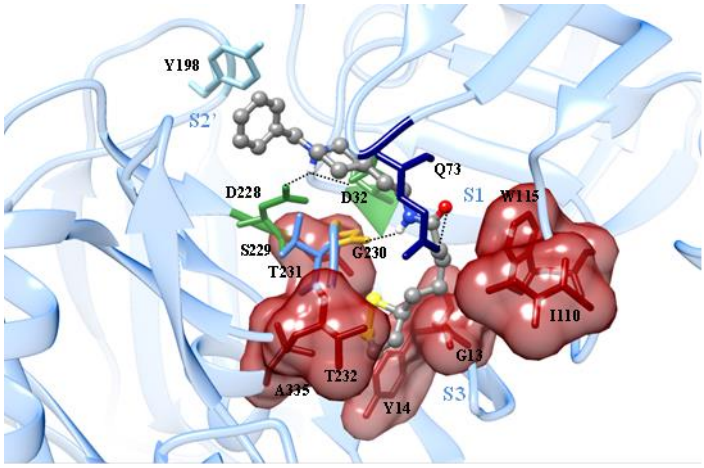

Figure 1.10 Details of compound (*S*)-**1.13** (in atom-colored sticks-and-balls: gray, C; blue, N; red, O; yellow, S) in the binding pocket of BACE1. The secondary structure of the protein is portrayed as a light-blue ribbon. Hydrogen bonds are highlighted as black dotted lines. Hydrogen atoms, water molecules, ions and counterions are omitted for clarity.

The benzylic group establishes favorable π-π stacking contacts with the side chain of Y198 (S2' pocket) and hydrophobic interactions with V332, I226, and T329 in the entry region of the binding pocket. The piperidine ring sits in the S1' subsite, defined by residues D32, D228, G34, S35 and T231.

The hydrophobic side chains of L30, Y71, F108, W115, and L118 in the S1 site nicely accommodate the linker portion of the compounds, with a

hydrogen bond formed between the amide carbonyl and the flap backbone NH of Q73. This is an important finding since hydrogen bonds to the backbone NH of the flap are essential to exhibit activity.[151-155] Additionally, the amide proton is hydrogen bonded to the backbone nitrogen of G230. Also in this case, the presence of an amide moiety that occupies the S1/S3 pockets of BACE1 and engages G230 proved to be a successful strategy to significantly increase BACE1 potency.[156] The chain of the LA fragment extends deep into the S3 pocket, thereby establishing hydrophobic contacts with I110, W115, G11, G13, and Q12 side chains, while the dithiolane ring docks in the hydrophobic subpocket formed by the side chains of Y14, S229, T232, and A335. All together, these interactions may account for the micromolar inhibitory potency of (*R*)-**1.12** and (*S*)-**1.13**. Traditionally, appropriate substituents in S3 contribute significantly to potency;[157-160] moreover, the S3 pocket can accommodate large hydrophobic ligands.[161,162] Thus, the chirality on the LA fragment is expected to have a minor impact. In fact, and in line with the experimentally determined IC_{50} values, we did not detect any significant difference in the binding mode of the two enantiomers (*R*)-**1.12** and (*S*)-**1.13**.

In all complexes analyzed, BACE1 assumes a closed conformation; the flap adopts a conformation complementary to the shape and nature of the ligand bound in the active site, while Y71 is hydrogen bonded to W76 side chain, which physically separates the S1 and S2′ sites. However, some differences have been found regarding the DBMA derivative **1.17** (figure 1.11). The protonated nitrogen of the ligand is able to reach the acid environment formed by the catalytic dyad D32 and D228, but less efficiently (larger and, hence, weaker H-bonds, see figure 1.11, right panel) than **1.12**/**1.13**, whereas the *N*-benzyl ring establishes π interaction with Y198, its position inside the active site resembling that of **1.12**/**1.13**. Nevertheless, the presence of the rigid aromatic core induces a severe clash with the flap: indeed, the flap residue Y71 breaks the hydrogen bond with W76 that is not counterbalanced in energy by

the formation of π interactions with the aromatic ring of the ligand. Moreover, as a consequence of this flap conformational change, the H-bond between the amide and Q73 is weaker than for **1.12**/**1.13**, as revealed by the corresponding per residue binding enthalpy deconvolution (figure 1.11, right panel). Overall, the complex is less stable and, accordingly, shows a higher ΔG_{bind} value than the NBP derivatives. Thus, even if the ligand somehow interacts with both key catalytic aspartic acids and the LA is also well accommodated in the hydrophobic cavity S3, the opening and destabilization of the flap due to the aromatic core could account for the lower potency of the DBMA derivatives.

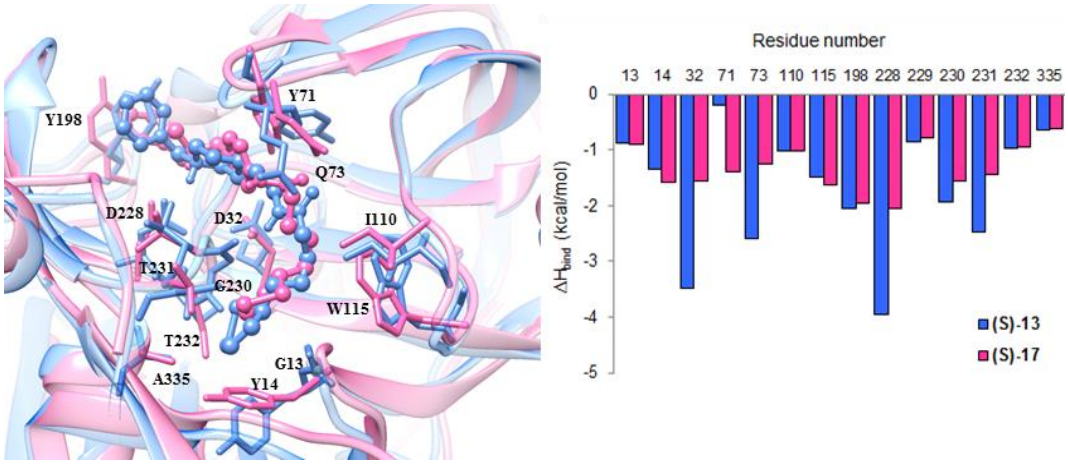

Figure 1.11 (Left) Comparison between the optimized MD binding conformations within the BACE1 receptor putative binding site of compounds (*S*)-**1.13** (blue) and (*S*)-**1.17** (pink). (Right) Per residue enthalpy decomposition for the same system.

Finally, we noted that the presence of a basic amine group ($pK_a \geq 6$) as in NBP or DBMA, seems crucial for BACE1 inhibition since the replacement by a 1,2-dimethoxybenzene group (Compound **1.18**) results in a drop of activity. Indeed, our calculations were unable to isolate a stable complex along the pertinent MD simulation trajectory.

Modeling Studies in Sigma-1 Receptor

During the past years several three-dimensional (3D) pharmacophore models for σ_1R ligands have been published,[163-167] and all these models propose a basic amino group and at least two hydrophobic substituents at the N-atom. However, the last-generation of σ_1R pharmacophore models[165,166] are characterized by an additional requirement: a heteroatom, such as O or S, in the scaffold of the molecule that can form hydrogen bond interactions with a counterpart in the receptor binding cavity. From a qualitative point of view, both NBP and DBMA scaffolds match the pharmacophore requirements to efficiently bind the σ_1R. Actually, all tested derivatives demonstrated low nanomolar affinities for the σ_1R (table 2). As for the BACE1 receptor, to describe at molecular level the binding mechanism of these new derivatives, compounds (*R*)-**1.12** and (*S*)-**1.13** as well as both enantiomers of compounds **1.15** and **1.17** were docked in the putative binding site of our well validated 3D-model of σ_1R.[54,168] Consequently, the corresponding ligand/receptor free energies of binding (ΔG_{bind}) were calculated by applying a validated MD procedure[168,169] based on MM/PBSA calculations[148] (table 4). Lastly, to investigate in detail the binding mode of the inhibitors to the target, a deconvolution of the enthalpic component (ΔH_{bind}) of ΔG_{bind} into contributions from each protein residue was carried out.[168]

Table 1.5 ΔG_{bind} and its Components for (*R*)-**1.12**, (*S*)-**1.13**, (*R*)-**1.15**, (*S*)-**1.15**, (*R*)-**1.17** and (*S*)-**1.17** in Complex with the σ_1R[a]

Compd.	ΔH (kcal/mol)	TΔS (kcal/mol)	ΔG_{bind} (kcal/mol)
(*R*)-**1.12**	-39.07 (0.19)	-28.62 (0.26)	-10.45 (0.32)
(*S*)-**1.13**	-39.42 (0.21)	-28.76 (0.28)	-10.66 (0.35)
(*R*)-**1.15**	-37.95 (0.21)	-27.68 (0.26)	-10.27 (0.34)
(*S*)-**1.15**	-38.41 (0.17)	-27.98 (0.25)	-10.43 (0.33)
(*R*)-**1.17**	-38.23 (0.20)	-27.84 (0.27)	-10.39 (0.34)
(*S*)-**1.17**	-38.39 (0.18)	-27.88 (0.29)	-10.51 (0.34)

[a]Values are expressed in kcal/mol and errors are given in parenthesis as standard errors of the mean.

The results of our computational methodology confirmed the experimental data about the binding capability of the new LA-based hybrids. As shown in Table 4, NBP and DBMA derivatives established a stable complex with σ_1R and this is translated in a favorable ΔG_{bind} values, less than -10 kcal/mol for each complex.

Taking compound (*S*)-**1.13** as a proof of concept, the analysis of the binding mode revealed the classical main interactions involved in the stabilization of the ligand/receptor complexes, in line with our previous findings on other similar σ_1R ligands.[141,166,168-170] As we can see from figure 1.12A, during the MD simulation (*S*)-**1.13** performed stable salt bridge and H-bond interaction with the side chain group of residue D126 and T151 respectively. Additionally, the *N*-benzyl ring established π interactions with R119 and W121 while the bulky dithiolanpentanamide moiety is perfectly encased in the typical hydrophobic pocket of σ_1R surrounding residues I128, F133 Y173 and L186 in which also the aliphatic portion of the piperidine group plays a role in the stabilization of the complex.

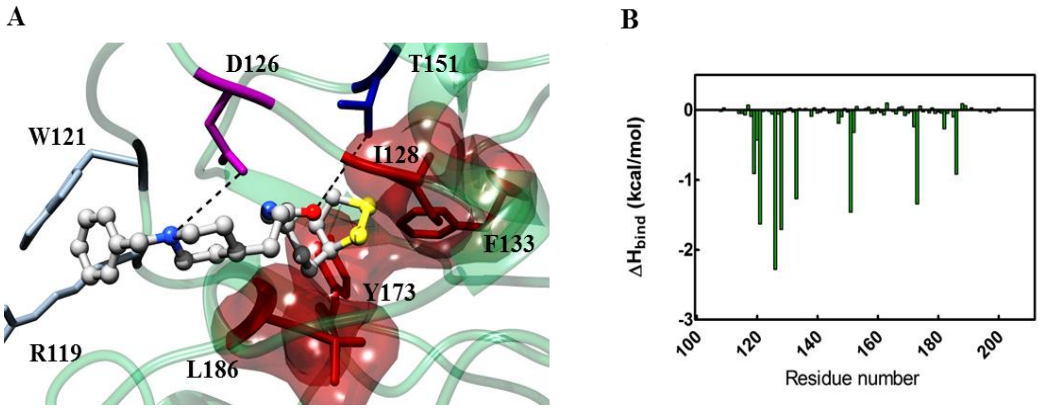

Figure 1.12. (A) Details of compound (*S*)-**1.13** (in stick-and-ball representation) in the binding pocket. Salt bridge and hydrogen bond are highlighted as black broken lines. (B) Per residue binding free energy decomposition for the σ_1R in complex with (*S*)-**1.13**. Only σ_1R amino acids from position 100 to 200 are shown, as for all the remaining protein residues the contribution to ligand binding is irrelevant.

Even the deconvolution of the free energy of binding (figure 1.12B) supported the binding mode of (*S*)-**1.13**: the interaction spectra, in fact, shows that the major contributions to the binding are afforded by the aforementioned σ_1R ligands.

For the purpose to compare the results obtained for (*S*)-**1.13** with the remaining compounds, we assessed the role of the chirality and the effect of the substitution of the NBP group with the DBMA moiety on the interactions in the σ_1R binding site. Concerning the first point, as expected from previous evidences on this topic,[171,172] we did not detect any significant difference in the binding mode of the two enantiomers (figure 1.13A). In fact, the flexible nature of the σ_1R binding site enables the receptor to easily and efficiently accommodate the (*R*)-configuration of compound **1.12** that is able to perform similar interactions with the same σ_1R residues (figure 1.13C).

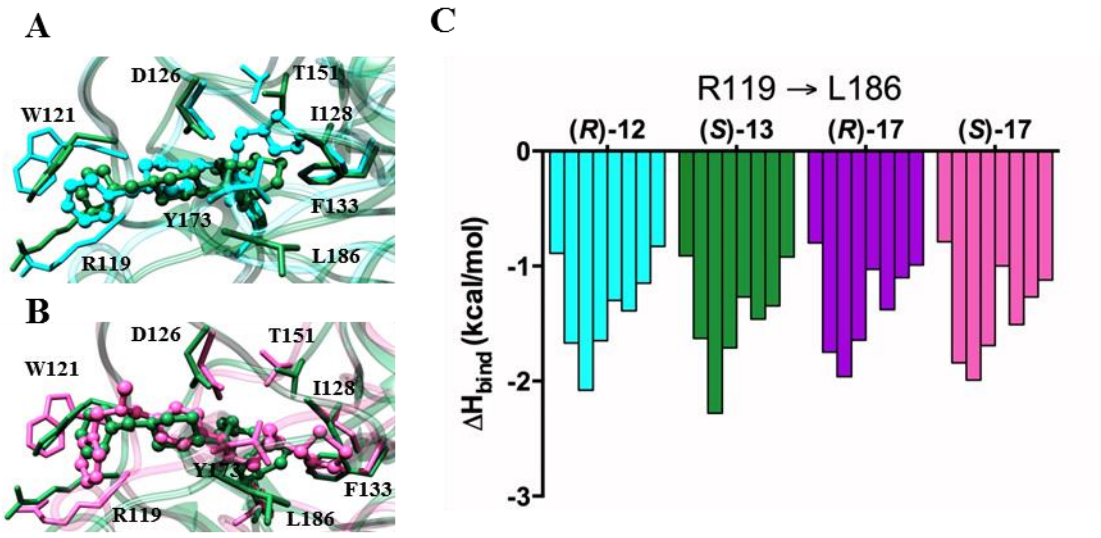

Figure 1.13 (A) Comparison between the optimized MD binding conformations within the σ_1R putative binding site between compounds (*R*)-**1.12** (cyan) and (*S*)-**1.13** (green). (B) Comparison between the optimized MD binding conformations within the σ_1R putative binding site between compounds (*S*)-**1.13** (green) and (*S*)-**17** (hot pink). (C) Per residue enthalpic contribution to binding for the σ_1R in complex with (*R*)-**1.12**, (*S*)-**1.13**, (*R*)-**1.17** and (*S*)-**1.17**. Only σ_1R amino acids critical for receptor binding are shown.

Even in the comparison between the NBP and DBMA derivatives our computational approach confirmed the experimental results, the *N*,*N*-dibenzyl(*N*-methyl)amine group of compounds **1.15** and **1.17** can interact with the external part of the binding site in the same way as the *N*-benzylpiperidine scaffold without affecting the correct arrangement of the dithiolanpentanamide part of the molecule in the hydrophobic cavity of σ_1R (figures 1.13B and 1.13C).

Conclusions

In this section we have synthesized a new series of LA-based multitarget directed compounds with proved affinity for AChE, BACE1 and σ1R, three important enzymes involved in the pathogenesis of AD. If these compounds acted *in vivo* as we have observed in our *in vitro* and *in sílico* studies, they could be able to affect the onset and progression of AD.

By their ability to inhibit BACE1, these LA-based hybrids could prevent the formation of the toxic beta-amyloid species, which are considered the molecular structure which unchains the cascade of events leading to neuronal death. At the same time, these compounds could alleviate the learning and memory symptoms, in a similar manner than the drugs currently used in AD treatment. Alternatively, since oxidative stress is accepted as an important factor in the neurodegenerative processes, these compounds could preserve neurons health through their antioxidant properties, as demonstrated in the ORAC model.

In light of this, our compounds could be able to influence the development of AD acting on the basis of three of the most accepted hypothesis explaining AD pathogenesis.

Given the importance of the communication between endoplasmic reticulum and mitochondria, and the homeostasis of the calcium levels to avoid excitotoxicity, processes mediated by σ1R. The ability of these new hybrids to agonize this kind of receptors could help to preserve the health of neurons in CNS and contribute to slow the progress of several neurodegenerative diseases including AD.

An important issue to be considered to evaluate the potential of these new LA-MTDl's is the difference of affinities for each target; compound **1.11** exhibit values ranging from low nanomolar to low micromolar ($K_{i\text{-}\sigma1}$ = 8,9 nM, $IC_{50\text{-AChE}}$ = 390 nM, $IC_{50\text{-BACE1}}$ = 5.6 μM); regarding to σ receptors, some studies have demonstrated that dose-response interaction describes a bell-shaped curve,[173-175] according to the hormetic model,[176] it means that at high concentrations of the ligand, the pharmacological effect could be significantly reduced or even disappear. Considering these differences of affinities, we must assume that a low concentration will be required to inhibit σ1R and a higher concentration might be needed to inhibit BACE1; therefore, the question of what level of dose should be considered to use in AD patients arises. In this regard,

even though, more experiments are required to determine how our compounds behave, we believe they have a great potential for several reasons; despite the relationship between level of BACE1 inhibition, amyloid burden and cognitive impairments is not fully understood, some genetic studies have demonstrated that a modest reduction of Aβ production may exert protective effects against AD;[177] on the other hand, BACE1 inhibition might be important in early stages of AD, when Aβ burden is not significant; in late stages, when senile plaques are largely distributed, inhibiting BACE1 might be useless or at least high percentages of inhibition may be required to avoid the progress of plaques deposition, although dead neurons will never be recovered. In this way, we consider these new hybrids could combine neuroprotective effects by agonizing σ1R and by preventing amyloid production in mild to moderate AD patients.

On the other hand, it has been demonstrated that targeting simultaneously cholinergic system and σ1R could be a successful strategy, for example, ANAVEX 2-73 combining σ1 and muscarinic agonist effects (0.86 μM and 5.2 μM respectively)[95], has successfully completed phase 1 studies and have demonstrated to be effective improving the cognitive markers in electrophysiological studies in a phase 2a clinical trial with AD patients. Additionally, according to ANAVEX Company, ANAVEX PLUS, a combination of ANAVEX 2-73 and a low dose of donepezil has been tested in some AD models and is planned to be evaluated in the same phase 2a study.[178] The compounds obtained in this work, combine advantageously the same abilities in a single small molecule.

As demonstrated in our predictive permeability studies, these compounds are able to cross the blood brain barrier and reach the CNS, which is necessary to act over their targets and exert their protective effects.

Through our molecular modeling studies at BACE1 and σ_1R, we have obtained a sensible molecular rationale for the interactions of our hybrids with these fundamental proteins and interesting clues for improving the potency and affinity of these new multifunctional compounds and possibly their ability to reduce Aβ species and increase neuroprotective effects.

Experimental Section

Chemical Synthesis

General Procedure 1.1. Synthesis of *N*-Benzylpiperidine-lipoic acid hybrids: 100 mg of (±)-LA (0.49 mmol) and 86 mg (0.53 mmol) of *N,N*-carbonyldiimidazole (CDI) were mixed into a microwave tube under nitrogen (N_2) atmosphere. Once the tube was sealed, 5 mL of anhydrous THF were added using a syringe to dissolve the mixture (CO_2 evolution was observed). This solution of activated LA was heated into a microwave reactor at 120 °C during 1.5 min to complete the activation. Afterward, a solution of 0.56 mmol of the corresponding amine in 2 mL of THF was added with a syringe into the sealed tube; this final solution was heated during 3 min at 120 °C to obtain the desired amide. After completion of the reaction, the THF was evaporated under reduced pressure; the crude obtained was resolved in 25 mL of EtOAc and washed five times with water, dried over magnesium sulfate ($MgSO_4$) and concentrated. The crude was purified by column chromatography using EtOAc/MeOH (9:1) as eluent.

1-Benzylpiperidine-4-carbonitrile. (1.1)

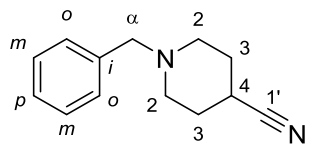

Piperidine-4-carbonitrile (5.1 mL, 45.4 mmol) was dissolved in 5 mL of toluene and 4 mL of pyridine; afterward, benzyl bromide (6.5 mL, 54. 5 mmol) was added to reflux for 3 h. After completion of reaction, toluene and pyridine were eliminated under reduced pressure and the crude dissolved in 100 mL of ethyl acetate (EtOAc) and washed with NaOH 0.5M (5x10 mL), water (3x10 mL) and brine (2x10 mL); the organic phase was dried over $MgSO_4$ and concentrated to obtain **1** pure enough to characterize and use in the subsequent reaction. Brown oil, 8.3 g (92%). ^{1}H NMR (300 MHz, MeOD) δ 7.39 – 7.24 (m, 5H, Ph), 3.55 (s, 2H, H_α), 2.87 – 2.75 (m,

1H, H_4), 2.73 – 2.62 (m, 2H, H_{2eq}), 2.45 – 2.31 (m, 2H, H_{2ax}), 2.03 – 1.91 (m, 2H, H_{3eq}), 1.90 – 1.72 (m, 2H, H_{3ax}). ^{13}C NMR (75 MHz, MeOD) δ 138.47 (C_i), 130.55 (C_o), 129.34 (C_m), 128.43 (C_p), 122.96 ($C_{1'}$), 64.07 (C_α), 52.32 (C_2), 29.67 (C_3), 26.93 (C_4). LC-MS *m/z* = 201.3 $[M + H]^+$, calcd for $[C_{13}H_{16}N_2 + H]^+$ 201.2 HPLC (94%).

(1-Benzylpiperidin-4-yl)methanamine. (1.2)

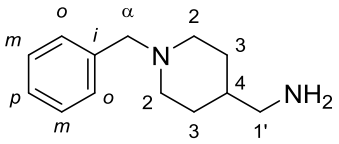

Over an ice bath, 7 mL of dissolution of $LiAlH_4$ 1 M in Et_2O (7.0 mmol) were added to 1.0 g (5.0 mmol) of **1** dissolved in 1 mL of ether under N_2 athmosphere. The mixture was allowed to reach rt and was stirred overnight. After completion of reaction, excess of $LiAlH_4$ was eliminated adding water dropwise until end of effervescence; ether was eliminated under reduced pressure and the crude dissolved in 50 mL of dichloromethane (DCM) washed with $NaHCO_3$ (5x5 mL), water (3x10 mL) and brine (2x10 mL); the organic phase was dried over $MgSO_4$ and concentrated to obtain **2** as a mixture of a light yellow oil and a solid; this mixture was washed several times with cold hexane to obtain the product as white amorphous solid, 0.86 g (85%) mp. 106-109 °C. ^{1}H NMR (300 MHz, MeOD) δ 7.41 – 7.19 (m, 5H, Ph), 3.51 (s, 2H, H_α), 2.97 – 2.84 (m, 2H, H_2), 2.52 (d, *J* = 6.4 Hz, 2H, $H_{1'}$), 2.08 – 1.94 (m, 2H, $H_{2'}$), 1.83 – 1.64 (m, 2H, H_3), 1.45 – 1.14 (m, 3H, $H_{3',4}$). ^{13}C NMR (75 MHz, MeOD) δ 138.41 (C_i), 130.83 (C_o), 129.25 (C_m), 128.37 (C_p), 64.33 (C_α), 54.44 (C_2), 48.26 ($C_{1'}$), 39.47 (C_4), 30.56 (C_3). LC-MS *m/z* = 205.2 $[M + H]^+$, calcd for $[C_{13}H_{20}N_2 + H]^+$ 205.2 HPLC (97%).

3-(1-Benzylpiperidin-4-yl)propanenitrile. (1.3)

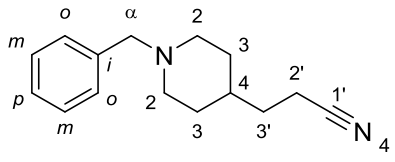

1-Benzylpiperidine-4-carbaldehyde 200 mg (0.98 mmol) and cyanoacetic acid 100 mg (0.12 mmol) were refluxed during 3 hours in 2 mL of pyridine under N_2 atmosphere. After completion of reaction, 20 mL of EtOAc were added and the remaining acid washed out with NaOH 0.5M (5x5 mL), water (3x5 mL) and brine (2x5 mL); the organic phase was dried over $MgSO_4$ and concentrated. The crude was dissolved in 20 mL of EtOH and a catalytic amount of Pd over charcoal (Pd-C) 5% was added; the air was replaced by hydrogen (H_2), the flask sealed with a septum and the mixture stirred overnight at 30 °C under H_2 balloon. Finally, the catalyst was eliminated by filtration and the solvent evaporated. Purification was developed by column chromatography using EtOAc/MeOH 9:1 as eluent. Yellow oil (87%). ^{1}H NMR (300 MHz, MeOD) δ 7.45 – 7.17 (m, 5H, Ph), 3.53 (s, 2H, H_α), 2.93 (dt, *J* = 11.8, 3.4 Hz, 2H, H_{2eq}), 2.47 (td, *J* = 7.3, 3.3 Hz, 2H, $H_{2'}$), 2.09 – 1.96 (m, 2H, H_{2ax}), 1.79 – 1.68 (m, 2H, H_{3eq}), 1.60 (q, *J* = 7.3 Hz, 2H, $H_{3'}$), 1.48 – 1.36 (m, 1H, H_4), 1.35 – 1.20 (m, 2H, H_{3ax}). ^{13}C NMR (75 MHz, MeOD) δ 138.35 (C_i), 130.85 (C_o), 129.27 (C_m), 128.41 (C_p), 121.20 ($C_{1'}$), 64.29 (C_α), 54.45 (C_2), 36.04 (C_4), 32.86 ($C_{3'}$), 32.18 (C_3), 14.83 ($C_{2'}$). HRMS [ESI+] *m/z* =229.1703 $[M]^+$, calcd for $[C_{15}H_{20}N_2]^+$ 229.1699. HPLC purity 100%.

3-(1-Benzylpiperidin-4-yl)propan-1-amine. (1.4)

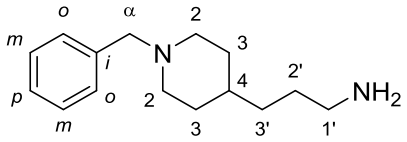

1-Benzylpiperidine-4-carbaldehyde 2 g (9.84 mmol) and cyanoacetic acid 1.17 g (13.75 mmol) were refluxed for 4 h in 100 mL of pyridine under N_2 atmosphere. After completion of reaction, pyridine was evaporated until half of the initial volume and 200 mL of EtOAc were added. This mixture was washed with NaOH 0.5M (5x50 mL), water (3x50 mL) and brine (2x50 mL); the organic

phase was dried over $MgSO_4$ and concentrated. The crude obtained was dissolved in 200 mL of EtOH, a catalytic amount of Pd-C (5%) was added and the mixture stirred overnight at 30 °C under H_2 40 psi, afterward, the catalyst was eliminated by filtration and the solvent evaporated; subsequently, 200 mL of DCM were added, air was replaced by N_2 and the mixture cooled to 0 °C to add 13.5 mL of $LiAlH_4$ 1M and stirred overnight at rt. The final mixture was washed with water (5x25 mL), brine (2x25 mL), dried over $MgSO_4$ and concentrated under reduced pressure. Purification was developed by column chromatography using EtOAc/MeOH 9:1 as eluent. Yellow oil (75%). ^{1}H NMR (500 MHz, MeOD) δ 7.35 – 7.23 (m, 5H, Ph), 3.52 (s, 2H, H_α), 2.95 – 2.85 (m, 2H, H_{2eq}), 2.75 (t, *J* = 7.6 Hz, 2H, $H_{1'}$), 2.08 – 1.97 (m, 2H, H_{2ax}), 1.74 – 1.66 (m, 2H, H_{3eq}), 1.57 (p, *J* = 7.6 Hz, 2H, $H_{2'}$), 1.36 – 1.18 (m, 5H, $H_{3'}$, $H_{4,}$, H_{3ax}). ^{13}C NMR (126 MHz, MeOD) δ 138.25 (C_i), 130.93 (C_o), 129.26 (C_m), 128.43 (C_p), 64.39 (C_α), 54.72 (C_2), 41.86 ($C_{1'}$), 36.59 ($C_{3'}$), 34.50 (C_4), 32.82 (C_3), 28.47 ($C_{2'}$). HRMS [ESI+] *m/z* =232.1946 $[M]^+$, calcd for $[C_{15}H_{24}N_2]^+$ 232.1939. HPLC purity 96%.

_N_-Benzyl-_N_-methyl-1-(3-nitrophenyl)methanamine. (1.5)

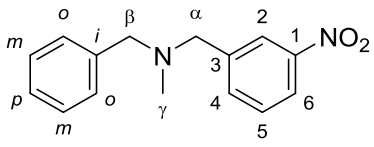

Equimolar quantities of *N*-benzylmethylamine and 3-nitrobenzyl bromide (23.1 mmol) dissolved in 50 mL of toluene and 8.1 mL (57.9 mmol) of triethylamine were refluxed during 3h. After completion of reaction, the solvent was eliminated under reduced pressure; afterward, 20 mL of a saturated solution on $NaHCO_3$ were added, subsequently, NaOH 2M dropwise until basic pH. The organic phase was extracted with EtOAc (3x15 mL), dried over $MgSO_4$ and concentrated under reduced pressure; brown oil, 5.6g (95%). ^{1}H NMR (300 MHz, MeOD) δ 8.33 (t, *J* = 2.2 Hz, 1H, H_2), 8.20 (dd, *J* = 7.8, 2.2 Hz, 1H, H_6), 7.84 (d, *J* = 7.8 Hz, 1H, H_4), 7.65 (t, *J* = 7.8 Hz, 1H, H_5),

7.50 – 7.20 (m, 5H, Ph), 3.72 (s, 2H, H_α), 3.65 (s, 2H, H_β), 2.29 (s, 3H, H_γ). ^{13}C NMR (75 MHz, MeOD) δ 149.76 (C_1), 142.95 (C_3), 139.81 (C_i), 136.23 (C_4), 130.47 (C_5), 130.17 (C_o), 129.35 (C_m), 128.29 (C_p), 124.52 (C_2), 123.05 (C_6), 62.89 (C_β), 61.62 (C_α), 42.45 (C_γ).The crude was analyzed by LC-MS and was used for the subsequent reactions without any further purification. HPLC-MS (Water-ACN 15→95%, g.t. 5 min), retention time 1.55 min, *m/z* = 257.3 $[M + H]^+$, calcd for $[C_{15}H_{16}N_2O_2 + H]^+$ 257.3.

_N_-Benzyl-_N_-methyl-1-(4-nitrophenyl)methanamine. (1.6)

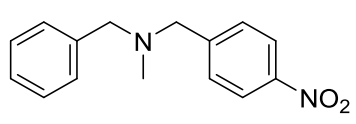

A mixture of equimolar quantities of *N*-benzylmethylamine and 4-nitrobenzylbromide (23.1 mmol) in 50 mL of toluene and 8.1 mL (58.5 mmol) of triethylamine was refluxed during 3h. After completion of reaction, the solvent was eliminated under reduced pressure, 20 mL of a saturated solution on $NaHCO_3$ were added and subsequently, NaOH 2M dropwise until basic pH. The organic phase was extracted with EtOAc (3x15 mL), dried over $MgSO_4$ and concentrated under reduced pressure; brown oil, 5.6g (97%). ^1H NMR (300 MHz, $CDCl_3$) δ 8.18 (d, *J* = 8.4 Hz, 2H), 7.55 (d, *J* = 8.4 Hz, 2H), 7.45 – 7.21 (m, 5H), 3.61 (s, 2H), 3.57 (s, 2H), 2.22 (s, 3H). ^{13}C NMR (75 MHz, $CDCl_3$) δ 147.53, 147.18, 138.75, 129.39, 128.93, 128.46, 127.33, 123.60, 62.19, 60.98, 42.46. LC-MS *m/z* = 257.3 $[M + H]^+$, calcd for $[C_{15}H_{16}N_2O_2 + H]^+$ 257.3.

3-((Benzyl(methyl)amino)methyl)aniline. (1.7)

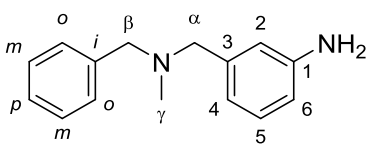

Into a round-bottom flask containing **5** (5.6 g 24.19 mmol) in 50 mL of MeOH, was added a catalytic amount of Pd-C (5%). Air was replaced by hydrogen (H_2), the flask was sealed with a rubber septum

and the reaction mixture was stirred overnight at rt under H_2. The catalyst was eliminated by filtration and the solvent evaporated, obtaining **7** pure enough to be characterized and used in the next reactions; yellow oil 4.8 g (98%). ^{1}H NMR (300 MHz, MeOD) δ 7.31 – 7.21 (m, 4H, $H_{o, m}$), 7.21 – 7.14 (m, 1H, H_p), 7.01 (t, *J* = 7.7 Hz, 1H, H_5), 6.73 – 6.67 (m, 1H, H_4), 6.65 – 6.56 (m, 2H, $H_{2,6}$), 3.41 (s, 2H, H_β), 3.33 (s, 2H, H_α), 2.08 (s, 3H, H_γ). ^{13}C NMR (75 MHz, MeOD) δ 148.56 (C_1), 140.36 (C_3), 139.59 (C_i), 130.37 (C_o), 129.92 (C_5), 129.21 (C_m), 128.15 (C_p), 120.30 (C_2), 117.42 (C_4), 115.50 (C_6), 62.84 (C_α), 62.57 (C_β), 42.43 (C_{10}). HRMS [ESI+] *m/z* =226.1474 $[M]^+$, calcd for $[C_{15}H_{18}N_2]^+$ 226.1470. HPLC purity 96%.

4-((Benzyl(methyl)amino)methyl)aniline. (1.8)

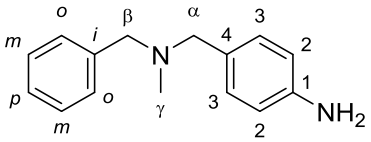

Into a round-bottom flask containing **1.6** (6.2 g 24.19 mmol) in 50 mL of MeOH, was added a catalytic amount of Pd-C (5%). Air was replaced by H_2, the flask was sealed with a rubber septum and the reaction mixture was stirred overnight at rt under H_2 (2 balloons). The catalyst was eliminated by filtration and the solvent evaporated, obtaining **1.8** pure enough to be characterized and used in the next reactions. Light brown oil 97%. ^{1}H NMR (300 MHz, $CDCl_3$) δ 7.42 – 7.23 (m, 5H, Ph), 7. 16 (d, *J* = 8.2 Hz, 2H, H_2), 6.67 (d, *J* = 8.2 Hz, 2H, H_3), 3.52 (s, 2H, H_β), 3.46 (s, 2H, H_α), 2.19 (s, 3H, H_γ). ^{13}C NMR (75 MHz, $CDCl_3$) δ 145.45 (C_1), 139.35 (C_i), 130.27 (C_2), 129.15 (C_o), 129.00 (C_4), 128.31 (C_m), 127.02 (C_p), 115.09 (C_3), 61.64 (C_β), 61.48 (C_α), 42.07 (C_γ). LC-MS *m/z* = 227.2 $[M + H]^+$, calcd for $[C_{15}H_{18}N_2 + H]^+$ 227.2 HPLC (98%)

***N*-(1-Benzylpiperidin-4-yl)-5-(1,2-dithiolan-3-yl)pentanamide. (1.9)**

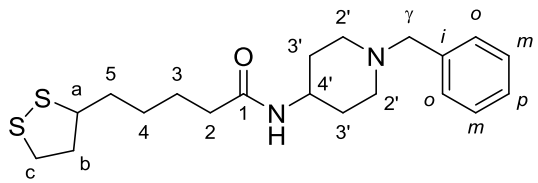

According to the general procedure 1.1, **1.9** was obtained from 100 mg of (±)-LA (0.49 mmol), 86 mg (0.52 mmol) of CDI and 106 mg (0.57 mmol) of 1-benzylpiperidin-4-amine as a light yellow oil, 145 mg (80%). ^{1}H NMR (300 MHz, MeOD) δ 7.35 - 7.22 (m, 5H, Ph), 3.72 - 3.55 (m, 2H, $H_{a,\ 4'}$), 3.54 (s, 2H, H_{γ}), 3.22 - 3.02 (m, 2H, H_{c}), 2.88 (dt, *J* = 12.5, 3.6 Hz, 2H, $H_{2'eq}$), 2.45 (dtd, *J* = 13.2, 6.6, 5.4 Hz, 1H, H_{b}), 2.27 - 2.08 (m, 4H, $H_{2,\ 2'ax}$), 1.94 – 1.78 (m, 3H, $H_{b',\ 3'eq}$), 1.77 – 1.37 (m, 8H, $H_{3,\ 4,\ 5,\ 3'ax}$). ^{13}C NMR (75 MHz, MeOD) δ 175.38(C_1), 138.22(C_i), 130.82(C_o), 129.34(C_m), 128.52(C_p), 63.94(C_γ), 57.57(C_a), 53.31($C_{2'}$), 47.78($C_{4'}$), 41.30(C_b), 39.35(C_c), 36.85(C_2), 35.73(C_5), 32.30($C_{3'}$), 29.81(C_4), 26.77(C_3). HRMS [ESI+] *m/z* =378.1816 $[M]^+$, calcd for $[C_{20}H_{30}N_2SO_2]^+$ 378.1800. HPLC purity 100%

***N*-((1-Benzylpiperidin-4-yl)methyl)-5-(1,2-dithiolan-3-yl)pentanamide. (1.10)**

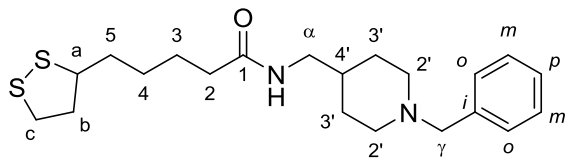

1.10 was synthesized from 55 mg (±)-LA (0.27 mmol), 48 mg (0.29 mmol) CDI and 63 mg (0.31 mmol) of (1-benzylpiperidin-4-yl) methanamine (General procedure 1.1). The crude was purified by column chromatography using EtOAc/MeOH (9:1) as eluent, obtaining **1.10** as a yellow oil; however a poor yield of 10% was achieved. In a second assay, the crude obtained after evaporation of the THF was purified with no further treatment; EtOAc/MeOH (9:1), improving the yield up to 25% (26 mg). ^{1}H NMR (500 MHz, $CDCl_3$) δ 7.32 – 7.28 (m, 4H, $H_{o,\ m}$), 7.25 – 7.21 (m, 1H, H_p), 5.47 (t, *J* = 6.5 Hz, 1H, NH),

3.56 (dq, *J* = 8.6, 6.5 Hz, 1H, H_a), 3.49 (s, 2H, H_γ), 3.20 – 3.06 (m, 4H, $H_{\alpha, c}$), 2.94 – 2.81 (m, 2H, $H_{2'eq}$), 2.45 (dtd, *J* = 13.0, 6.5, 5.4 Hz, 1H, H_b), 2.21 – 2.15 (m, 2H, H_2), 1.98 – 1.86 (m, 3H, $H_{b', 2'ax}$), 1.70 – 1.58 (m, 6H, $H_{4, 5, 3'eq}$), 1.53 – 1.41 (m, 3H, $H_{3, 4'}$), 1.26 (m, 2H, $H_{3'ax}$). ^{13}C NMR (126 MHz, $CDCl_3$) δ 172.84 (C_1), 138.43 (C_i), 129.34 (C_o), 128.31 (C_m), 127.12 (C_p), 63.47 (C_γ), 56.57 (C_a), 53.44 ($C_{2'}$), 45.15 (C_α), 40.39 (C_b), 38.63 (C_c), 36.73 (C_2), 36.15 ($C_{4'}$), 34.77 (C_5), 30.03 ($C_{3'}$), 29.06 (C_3), 25.60 (C_4). HRMS [ESI+] *m/z* =392.1956 $[M]^+$, calcd for $[C_{21}H_{32}N_2SO_2]^+$ 392.1961. HPLC purity 100%

_N_-(2-(1-Benzylpiperidin-4-yl)ethyl)-5-(1,2-dithiolan-3-yl)pentanamide. (1.11)

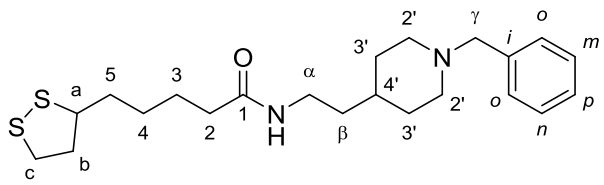

According to the general procedure 1.1, **1.11** was obtained from 100 mg of (±)-LA (0.49 mmol), 86 mg (0.53 mmol) of CDI and 121 mg (0.56 mmol) of 2-(1-benzylpiperidin-4-yl)ethan-1-amine as a light yellow oil 183 mg (93%). ^{1}H NMR (300 MHz, $CDCl_3$) δ 7.36 – 7.21 (m, 5H, Ph), 5.46 (t, *J* = 5.7 Hz, 1H, NH), 3.63 – 3.49 (m, 3H, H_γ, H_a), 3.26 (dt, *J* = 7.6, 5.7 Hz, 2H, H_α), 3.22 – 3.06 (m, 2H, H_c), 2.92 (dt, *J* = 12.7, 3.1 Hz, 2H, $H_{2'eq}$), 2.45 (dtd, *J* = 12.9, 6.8, 5.4 Hz, 1H, H_b), 2.15 (t, *J* = 7.1Hz, 2H, H_2), 2.00 (t, *J* = 11.1 Hz, 2H, $1H_{2'ax}$), 1.90 (dq, *J* = 12.8, 6.8 Hz, 1H, $H_{b'}$), 1.74 – 1.59 (m, 6H, $H_{3, 5, 3'eq}$), 1.50 – 1.31 (m, 7H, $H_{4, \beta, 3'ax, 4'}$). ^{13}C NMR (75 MHz, $CDCl_3$) δ 172.71 (C_1), 137.20 (C_i), 129.62 (C_o), 128.39 (C_m), 127.44 (C_p), 63.21 (C_γ), 56.59 (C_a), 53.62 ($C_{2'}$), 40.37 (C_b), 38.58 (C_c), 37.25 (C_α), 36.62 (C_2), 36.39 (C_β), 34.73 (C_5), 33.39 ($C_{4'}$), 31.81 ($C_{3'}$), 20.00 (C_4), 25.53 (C_3). HRMS [ESI+] *m/z* =406.2114 $[M]^+$, calcd for $[C_{22}H_{34}N_2OS_2]^+$ 406.2112. HPLC purity 100%

(*R*)-*N*-(2-(1-Benzylpiperidin-4-yl)ethyl)-5-(1,2-dithiolan-3-yl)pentanamide. (1.12)

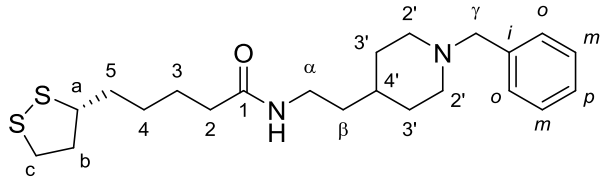

1.12 was synthesized as described in the general procedure1.1 from 100 mg of (*R*)-LA (0.49 mmol), 86 mg (0.53 mmol) of CDI and 121 mg (0.56 mmol) of 2-(1-benzylpiperidin-4-yl)ethan-1-amine. Yellow oil, 179 mg (91%). ^{1}H NMR (500 MHz, $CDCl_3$) δ 7.31 – 7.27 (m, 4H, $H_{o,\ m}$), 7.26 – 7.20 (m, 1H, H_p), 5.36 (bs, 1H, NH), 3.56 (dq, J = 8.6, 6.5 Hz, 1H, H_a), 3.48 (s, 2H, H_γ), 3.25 (ddd, J = 8.6, 7.4, 5.9 Hz, H_α), 3.20 – 3.08 (m, 2H, H_c), 2.90 – 2.81 (m, 2H, $H_{2'eq}$), 2.45 (dtd, J = 12.9, 6.5, 5.4 Hz, 1H, H_b), 2.22 – 2.10 (m, 2H, H_2), 2.06 – 1.85 (m, 3H, $H_{2'ax}$, $H_{b'}$), 1.75 – 1.55 (m, 6H, $H_{3,\ 5,\ 3'eq}$), 1.53 – 1.37 (m, 4H, $H_{4,}$ H_β), 1.33 – 1.19 (m, 3H, $H_{4',\ 3'ax}$). ^{13}C NMR (126 MHz, $CDCl_3$) δ 172.66 (C_1), 138.49 (C_i), 129.37(C_o), 128.27 (C_m), 127.06 (C_p), 63.59(C_γ), 56.59 (C_a), 53.85 ($C_{2'}$), 40.39 (C_b), 38.61 (C_c), 37.36 (C_α), 36.69 (C_2), 36.55 (C_β), 34.76 (C_5), 33.65 ($C_{4'}$), 32.32 ($C_{3'}$), 29.04 (C_4), 25.56 (C_3). HRMS [ESI+] *m/z* =406.2114 $[M]^+$, calcd for $[C_{22}H_{34}N_2OS_2]^+$ 406.2112. HPLC purity 99%

(*S*)-*N*-(2-(1-Benzylpiperidin-4-yl)ethyl)-5-(1,2-dithiolan-3-yl)pentanamide. (1.13)

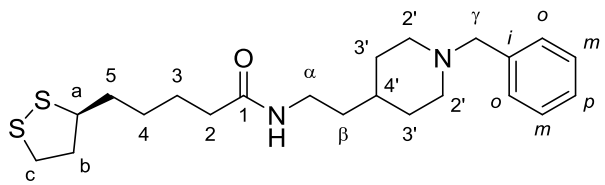

1.13 was synthesized as described in the general procedure 1.1 from 100 mg of (*S*)-LA (0.49 mmol), 86 mg (0.53 mmol) of CDI and 121 mg (0.56 mmol) of 2-(1-benzylpiperidin-4-yl)ethan-1-amine. Yellow oil, 180 mg (92%). ^{1}H NMR (400 MHz, $CDCl_3$) δ 7.36 – 7.28 (m, 4H, $H_{o,\ m}$), 7.27 – 7.21 (m, 1H, H_p), 5.39 (t, J = 5.6 Hz,

1H, NH), 3.56 (dq, *J* = 8.5, 6.5 Hz, 1H, H_a), 3.48 (s, 2H, H_γ), 3.26 (ddd, *J* = 8.6, 7.3, 5.9 Hz, H_α), 3.21 – 3.07 (m, 2H, H_c), 2.91 – 2.84 (m, 2H, $H_{2'eq}$), 2.45 (dtd, *J* = 13.0, 6.5, 5.4 Hz, 1H, H_b), 2.15 (td, *J* = 7.4, 1.5 Hz, 2H, H_2), 1.98 – 1.85 (m, 3H, $H_{2'ax}$, $H_{b'}$), 1.79 – 1.59 (m, 6H, $H_{3,\ 5,\ 3'eq}$), 1.52 – 1.38 (m, 4H, $H_{4,}$ H_β), 1.32 – 1.23 (m, 3H, $H_{4',\ 3'ax}$). ^{13}C NMR (126 MHz, $CDCl_3$) δ 172.69 (C_1), 138.35 (C_i), 129.41(C_o), 128.27 (C_m), 127.08 (C_p), 63.54(C_γ), 56.57 (C_a), 53.80 ($C_{2'}$), 40.38 (C_b), 38.59 (C_c), 37.33 (C_α), 36.67 (C_2), 36.51 (C_β), 34.75 (C_5), 33.60 ($C_{4'}$), 32.24 ($C_{3'}$), 29.03 (C_4), 25.54 (C_3). HRMS [ESI+] *m/z* =406.2135 $[M]^+$, calcd for $[C_{22}H_{34}N_2OS_2]^+$ 406.2112. HPLC purity 100%.

***(R, S)-N*-(3-(1-Benzylpiperidin-4-yl)propyl)-5-(1,2-dithiolan-3-yl)pentanamide. (1.14)**

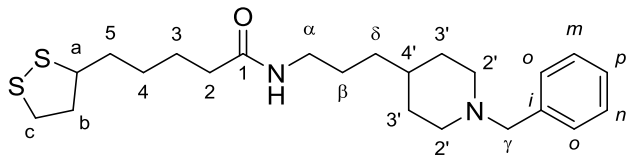

According to the general procedure 1.1, **1.14** was obtained from 100 mg of (±)-LA (0.49 mmol), 86 mg (0.53 mmol) of carbonyldiimidazol and 129 mg (0.56 mmol) of **1.4** as a light yellow oil 189 mg (93%). ^{1}H NMR (500 MHz, MeOD) δ 7.34 – 7.30 (m, 4H, $H_{o,\ m}$), 7.29 – 7.25 (m, 1H, H_p), 3.60 – 3.54 (m, 1H, H_a), 3.53 (s, 2H, H_γ), 3.21 – 3.05 (m, 4H, $H_{\alpha,\ c}$), 2.94 – 2.87 (m, 2H, $H_{2'eq}$), 2.49 – 2.42 (m, 1H, H_b), 2.18 (t, *J* = 7.3 Hz, 2H, H_2), 2.07 – 2.01 (m, 2H, $H_{2'ax}$), 1.91 – 1.84 (m, 1H, $H_{b'}$), 1.74 – 1.59 (m, 6H, $H_{3,\ 3'eq,\ 5}$), 1.54 – 1.38 (m, 4H, $H_{\beta,\ 4}$), 1.31 – 1.19 (m, 5H, $H_{4',\delta,\ 3'ax}$). ^{13}C NMR (126 MHz, MeOD) δ 175.91 (C_1), 137.96 (C_i), 130.99 (C_o), 129.29 (C_m), 128.52 (C_p), 64.29 (C_γ), 57.61 (C_a), 54.71 ($C_{2'}$), 41.31 (C_b), 40.49 (C_α), 39.34 (C_c), 36.90 (C_2), 36.46 ($C_{4'}$), 35.74 (C_5), 34.75 (C_δ), 32.82 ($C_{3'}$), 29.86 (C_4), 27.66 (C_β), 26.81 (C_3). HRMS [ESI+] *m/z* =420.2264 $[M]^+$, calcd for $[C_{23}H_{36}N_2OS_2]^+$ 420.2269. HPLC purity 99%

***(R, S)-N*-(3-((Benzyl(methyl)amino)methyl)phenyl)-5-(1,2-dithiolan-3-yl)pentanamide. (1.15)**

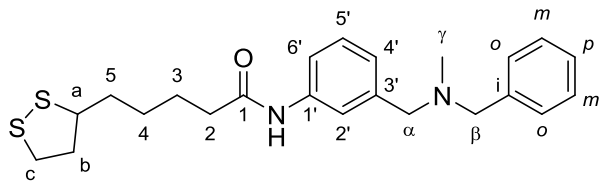

The general procedure 1.1, 100 mg of (±)-LA (0.48 mmol), was followed until the addition of 126 mg (0.56 mmol) of 3-((benzyl(methyl)amino)methyl)aniline; the final mixture was heated during 10 min at 120 °C to yield the desired amide. After completion of the reaction the THF was evaporated under reduced pressure; the crude obtained was purified with directly by column chromatography using EtOAc/MeOH (9:1) as eluent, obtaining **1.15** as a yellow oil, 185 mg (92%). ^{1}H NMR (400 MHz, $CDCl_3$) δ 7.48 (d, *J* = 7.6 Hz, 1H, $H_{5'}$), 7.46 (s, 1H, $H_{2'}$), 7.38 – 7.22 (m, 6H, $H_{6', o, m, p}$), 7.11 (d, *J* = 7.6 Hz, 1H, $H_{4'}$), 3.57 (dq, *J* = 8.7, 6.6 Hz, 1H, H_a), 3.52 (s, 2H, H_β), 3.49 (s, 2H, H_α), 3.21 – 3.06 (m, 2H, H_c), 2.45 (dtd, *J* = 12.9, 6.6, 5.4 Hz, 1H, H_b), 2.36 (td, *J* = 7.4, 1.6 Hz, 2H, H_2), 2.17 (s, 3H, H_γ), 1.91 (dq, *J* = 12.9, 6.6 Hz, 1H, $H_{b'}$), 1.82 – 1.67 (m, 4H, $H_{3, 5}$), 1.52 (ddt, *J* = 16.0, 8.6, 6.2 Hz, 2H, H_4). ^{13}C NMR (101 MHz, $CDCl_3$) δ 171.07 (C_1), 140.54 ($C_{3'}$), 139.26 (C_i), 137.97 ($C_{1'}$), 129.05 (C_o), 129.00 ($C_{6'}$), 128.34 (C_m), 127.07 (C_p), 124.89 ($C_{4'}$), 120.18 ($C_{2'}$), 118.59 ($C_{5'}$), 62.07 (C_β), 61.77 (C_α), 56.51 (C_a), 42.34 (C_γ), 40.37 (C_b), 38.60 (C_c), 37.59 (C_2), 34.78 (C_5), 29.00 (C_4), 25.37 (C_3). HRMS [ESI+] *m/z* =414.1802 $[M]^+$, calcd for $[C_{23}H_{30}N_2SO_2]^+$ 414.1799. HPLC purity 100%

***(S)-N*-(3-((Benzyl(methyl)amino)methyl)phenyl)-5-(1,2-dithiolan-3-yl)pentanamide. (1.16)**

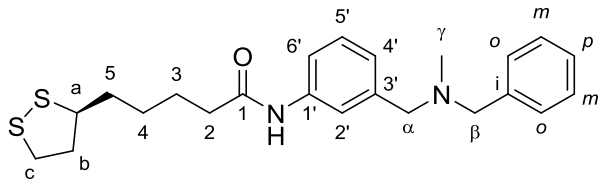

The general procedure 1.1, 100 mg of (S)-LA (0.48 mmol), was followed until the addition of 126 mg (0.56 mmol) of 3-((benzyl(methyl)amino)methyl)aniline; the final mixture was heated during 10 min at 120 °C to yield the desired amide. After completion of the reaction the THF was evaporated under reduced pressure; the crude obtained was purified directly by column chromatography using EtOAc:MeOH (9:1) as eluent, obtaining **1.16** as a yellow oil, 180 mg (90%). ^{1}H NMR (400 MHz, $CDCl_3$) δ 7.48 (d, *J* = 7.6 Hz, 1H, $H_{5'}$), 7.45 (s, 1H, $H_{2'}$), 7.39 – 7.18 (m, 6H, $H_{6', o, m, p}$), 7.11 (d, *J* = 7.6 Hz, 1H, $H_{4'}$), 3.58 (dq, *J* = 8.7, 6.7 Hz, 1H, H_a), 3.52 (s, 2H, H_β), 3.49 (s, 2H, H_α), 3.23 – 3.07 (m, 2H, H_c), 2.46 (dtd, *J* = 13.4, 6.6, 5.4 Hz, 1H, H_b), 2.37 (td, *J* = 7.4, 1.7 Hz, 2H, H_2), 2.17 (s, 3H, H_γ), 1.92 (dq, *J* = 13.4, 6.6 Hz, 1H, $H_{b'}$), 1.84 – 1.66 (m, 4H, $H_{3, 5}$), 1.52 (ddt, *J* = 16.0, 8.9, 6.2 Hz, 2H, H_4). ^{13}C NMR (101 MHz, $CDCl_3$) δ 171.03 (C_1), 140.55 ($C_{3'}$), 139.26 (C_i), 137.96 ($C_{1'}$), 129.05 (C_o), 129.02 ($C_{6'}$), 128.35 (C_m), 127.08 (C_p), 124.91 ($C_{4'}$), 120.16 ($C_{2'}$), 118.58 ($C_{5'}$), 62.08 (C_β), 61.76 (C_α), 56.51 (C_a), 42.35 (C_γ), 40.38 (C_b), 38.61 (C_c), 37.61 (C_2), 34.79 (C_5), 29.00 (C_4), 25.36 (C_3). HRMS [ESI+] *m/z* =414.1795 $[M]^+$, calcd for $[C_{23}H_{30}N_2SO_2]^+$ 414.1799. HPLC purity 100%

***(R, S)-N*-(4-((Benzyl(methyl)amino)methyl)phenyl)-5-(1,2-dithiolan-3-yl)pentanamide. (1.17)**

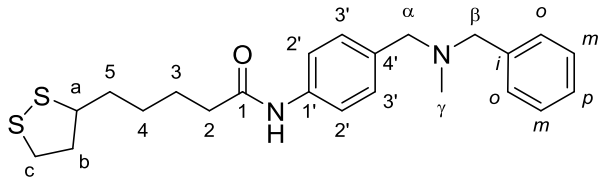

The general procedure 1.1, 100 mg of (±)-LA (0.49 mmol), was followed until the addition of 126 mg (0.56 mmol) of 4-((benzyl(methyl)amino)methyl)aniline; this mixture was heated during 40 min at 120 °C into a microwave reactor to yield the desired amide. After completion of the reaction the THF was evaporated under reduced pressure; the crude obtained was purified directly by column chromatography using EtOAc:MeOH (9:1) as eluent, obtaining **1.17** as a yellow oil, 167 mg (83%). ^{1}H NMR (300 MHz, $CDCl_3$) δ 7.48 (d, *J* = 8.4 Hz, 2H, $H_{3'}$), 7.36 – 7.29 (m, 6H, $H_{2', o, m}$), 7.27 – 7.18 (m, 1H, H_p), 3.57 (dt, *J* = 8.6, 6.6 Hz, 1H, H_a), 3.51 (s, 2H, H_β), 3.49 (s, 2H, H_α), 3.24 – 3.03 (m, 2H, H_c), 2.46 (td, *J* = 12.6, 6.6 Hz, 1H, H_b), 2.37 (t, *J* = 7.4 Hz, 2H, H_2), 2.17 (s, 3H, H_γ), 1.91 (dq, *J* = 13.8, 6.6 Hz, 1H, $H_{b'}$), 1.82 – 1.65 (m, 4H, $H_{3, 5}$), 1.59 – 1.45 (m, 2H, H_4). ^{13}C NMR (75 MHz, $CDCl_3$) δ 171.06 (C_1), 139.15 (C_i), 136.87 ($C_{1'}$), 135.15 ($C_{4'}$), 129.68 ($C_{2'}$), 129.07 (C_m), 128.35 (C_o), 127.11 (C_p), 119.81 ($C_{3'}$), 61.80 (C_β), 61.36 (C_α), 56.51 (C_a), 42.22 (C_γ), 40.37 (C_b), 38.61 (C_c), 37.55 (C_2), 34.78 (C_5), 28.99 (C_4), 25.39 (C_3). HRMS [ESI+] *m/z* =414.1812 $[M]^+$, calcd for $[C_{23}H_{30}N_2SO_2]^+$ 414.1799. HPLC purity 100%

Biochemical Studies.

Inhibition of Human AChE and BuChE. The method of Ellman et al. was followed [135]. The assay solution consisted of 0.1 M phosphate buffer pH 8.0, 400 μM 5,5´-dithiobis(2-nitrobenzoic acid) (DTNB, Ellman's reagent), 0.05 U/mL h-AChE (human recombinant acetylcholinesterase,

Sigma Chemical Co.) or 0.024 U/mL h-BuChE (butyrylcholinesterase from human serum, Sigma Chemical Co.), and 800 μM acetylthiocholine iodide, or 500 μM butyrylthiocholine as the substrate of the enzymatic reaction, respectively. The compounds tested were added to the assay solution and preincubated with the enzyme for 5 min at 30 ºC. After that period, the substrate was added. The absorbance changes at 412 nm were recorded for 5 min with a UV/Vis microplate spectrophotometer, Multiskan Spectrum, Thermo-Electron Co. The reaction rates were compared and the inhibition percentage due to the presence of test compound was calculated. The IC_{50} is defined as the concentration of each compound that reduces at 50% the enzymatic activity without any inhibitor.

Human BACE1 Inhibition Assay. This experiment was carried out using fluorescence resonance energy transfer (FRET), according to the protocol described by the manufacturer (Invitrogen).[11] Briefly, an APP-based peptide substrate (rhodamine-EVNLDAEFK-quencher, *K*m of 20 μM) carrying the Swedish mutation and containing a rhodamine as a fluorescence donor and a quencher acceptor at each end was used. The intact substrate is weakly fluorescent and becomes highly fluorescent upon enzymatic cleavage. The assays were conducted in 50 mM sodium acetate buffer, pH 4.5, in a final enzyme concentration (1 U/mL). The mixture was incubated for 60 min at 25 °C under dark conditions and then stopped with 2.5 M sodium acetate. Fluorescence was measured with a FLUOstar Optima (BMG Labtechnologies GmbH, Offenburg, Germany) microplate reader at 545 nm excitation and 585 nm emission.

In Vitro Blood–Brain Barrier Permeation Assay. Prediction of the brain penetration was evaluated using the PAMPA assay, in a similar manner as previously described.[145,179-181] Pipetting was performed with a semi-automatic robot (CyBi®-SELMA) and UV reading with a microplate spectrophotometer (Multiskan Spectrum, Thermo Electron Co.).

Commercial drugs, phosphate buffered saline solution at pH 7.4 (PBS), and dodecane were purchased from Sigma, Aldrich, Acros, and Fluka. Millex filter units (PVDF membrane, diameter 25 mm, pore size 0.45 μm) were acquired from Millipore. The porcine brain lipid (PBL) was obtained from Avanti Polar Lipids. The donor microplate was a 96-well filter plate (PVDF membrane, pore size 0.45 μm) and the acceptor microplate was an indented 96-well plate, both from Millipore. The acceptor 96-well microplate was filled with 200 μL of PBS : ethanol (70:30) and the filter surface of the donor microplate was impregnated with 4 μL of porcine brain lipid (PBL) in dodecane (20 mg mL^{-1}). Compounds were dissolved in PBS: ethanol (70:30) at 100 μg mL^{-1}, filtered through a Millex filter, and then added to the donor wells (200 μL). The donor filter plate was carefully put on the acceptor plate to form a sandwich, which was left undisturbed for 240 min at 25 °C. After incubation, the donor plate is carefully removed and the concentration of compounds in the acceptor wells was determined by UV-Vis spectroscopy. Every sample is analyzed at five wavelengths, in four wells and at least in three independent runs, and the results are given as the mean ± standard deviation. In each experiment, 11 quality control standards of known BBB permeability were included to validate the analysis set.

Oxygen Radical Absorbance Capacity Assay. The ORAC method was followed, using a Polarstar Galaxy plate reader (BMG Labtechnologies GmbH, Offenburg, Germany) with 485-P excitation and 520-P emission filters.[136,182] The equipment was controlled by the Fluorostar Galaxy software (version 4.11-0) for fluorescence measurement. 2,2'-Azobis-(amidinopropane) dihydrochloride (AAPH), (±)-6-hydroxy-2,5,7,8-tetramethylchromane-2-carboxylic acid (trolox) and fluorescein (FL) were purchased from Sigma-Aldrich. The reaction was carried out in 75 mM phosphate buffer (pH 7.4) and the final reaction mixture was 200 μL. Antioxidant (20 μL) and FL (120 μL; 70 mM, final concentration) solutions

were placed in a black 96-well microplate (96F untreat, Nunc). The mixture was pre-incubated for 15 min at 37 ºC and then, AAPH solution (60 μL, 12 mM, final concentration) was added rapidly using a multichannel pipette. The microplate was immediately placed in the reader and the fluorescence recorded every minute for 80 min. The microplate was automatically shaken prior each reading. Samples were measured at eight different concentrations (0.1-1μM). A blank (FL + AAPH in phosphate buffer) instead of the sample solution and eight calibration solutions using trolox (1-8 μM) were also carried out in each assay. All the reaction mixtures were prepared in duplicate, and at least three independent assays were performed for each sample. Raw data were exported from the Fluostar Galaxy Software to an Excel sheet for further calculations. Antioxidant curves (fluorescence *vs.* time) were first normalized to the curve of the blank corresponding to the same assay, and the area under the fluorescence decay curve (AUC) was calculated. The net AUC corresponding to a sample was calculated by subtracting the AUC corresponding to the blank. Regression equations between net AUC and antioxidant concentration were calculated for all the samples. ORAC-FL values were expressed as trolox equivalents by using the standard curve calculated for each assay, where the ORAC-FL value of trolox was taken as 1.0.

Binding Assays at σ1 and σ2 Receptor.[168,169,171,183-185] For σ_1R assay, the thawed membrane preparation of guinea pig brain cortex (about 100 ug of protein) were incubated for 120 min at 37°C with 2 nM [^{3}H]-(+)-pentazocine (PerkinElmer, specific activity 34.9 C_i/mmol) in 50 mM Tris-HCl, pH 7.4, 0.5 mL final volume. Nonspecific binding was defined in the presence of 10 μM of unlabeled (+)-pentazocine. The reaction was stopped by vacuum filtration through GF/B glass-fiber filters presoacked with 0.5% polyethylenimine, followed by rapid washing with 2 ml ice-cold buffer. Filters were placed in 3 ml scintillation cocktail and the radioactivity determined by liquid scintillation counting.

For σ_2R assay, 150 µg of rat liver homogenate were incubated for 120 min at rt with 3 nM [^{3}H]-DTG (PerkinElmer, specific activity 58.1 C_i/mmol) in 50 mM Tris-HCl, pH 8.0, 0.5 mL final volume. (+)-Pentazocine (500 nM) was used to mask σ_1R and to define nonspecific binding, respectively.

Competition studies were done using at least 11 different concentrations of the ligand under investigation. As internal control, three increasing concentrations of unlabelled (+)-pentazocine (σ_1R) or DTG (σ_2R) were always included. The compounds were prepared as 10 mM stock solutions in 100% DMSO and diluted with Tris-HCl buffer on the day of the experiment. The final DMSO concentration in the incubation tubes was maintained at 0.1%.

IC_{50} values and Hill's coefficients n_H were calculated by nonlinear regression using a four parameters curve-fitting algorithm of the GraphPad Prism software (v.6, La Jolla California USA), and are reported as the mean ± SE of three separate determinations performed in duplicate. The corresponding K_i values were obtained by means of the Cheng-Prusoff equation, using the K_d values obtained in saturation experiments.

Functional Characterization at σ1 Receptor. SH-SY5Y (human neuroblastoma) cells were maintained in Dulbecco's modified Eagle's medium (DMEM) Glutamax (Life Technologies) supplemented with 10% (v/v) fetal bovine serum and 1x Antibiotic Antimycotic Solution (Sigma-Aldrich, 100 U penicillin, 100µg/ml streptomycin and 0.25µg/ml amphotericin B) at 37 °C in a humidified incubator with a 5% CO_2/95% air atmosphere. The cytotoxicity of the σ_1R ligands was evaluated by MTT test on SH-SY5Y cell cultures. Cells were plated in 96-well plates ($1x10^3$ cells/well) for 24 h prior to compounds addition. σ_1R ligands were dissolved in DMSO and serially diluted in culture medium to achieve the desired final concentrations. All compounds were assayed in triplicates,

and the results were derived from three independent experiments. Statistical analysis was done using one-way ANOVA Test (GraphPad Prism; GraphPad Software, La Jolla, CA). Cell viability was determined by calculating the mean absorbance of treated samples (A595 subtracted by A655) divided by the mean absorbance of respective control (DMSO), and expressed as percentage of the reference compound. Cell cytotoxicity was determined by the simple formula % Cytotoxicity = 100 - cell viability (%), and expressed as σ_1R ligand cytotoxicity with respect to that obtained for the reference compound NE-100 at 100μM (=100%).

Neurogenic Assays. Adult (3 months old) male C57BL/6 mice were used for neurogenesis determination. All animal experimental procedures were previously approved by the Ethics Committee for Animal Experimentation of the CSIC following national (normative 1201/2005) and international recommendations (Directive 2010/63 from the European Communities Council). Special care was taken to minimize animal suffering. Neural stem cells were isolated from the SGZ of the dentate gyrus of the hippocampus of adult mice and cultured as NS as previously described.[144,186] After treatment of NS with compounds **12** and **17** at 10 μM, the expression of neuronal markers was analyzed by immunocytochemistry according to published protocols,[144] using two well-known neurogenesis-associated markers: β-III-tubulin linked to early stages of neurogenesis and microtubule-associated protein type 2 (MAP-2), a classical marker of late neuronal maturation. A rabbit anti-β-III-tubulin (TuJ clone; Abcam) polyclonal antibody coupled to an Alexa-488-fluor-labeled secondary antibody (Molecular Probes) and a mouse anti-MAP-2 (Sigma) monoclonal antibody coupled to an Alexa-546-fluor-labeled secondary antibody (Molecular Probes) were used. DAPI staining was used as a nuclear marker. Fluorescent representative images were acquired with a Nikon fluorescence microscope 90i coupled to a digital

camera Qi. The microscope configuration was adjusted to produce the optimum signal-to-noise ratio.

Computational Binding Studies. The ligands were optimized using the Gaussian09 software (Gaussian, Inc. Wallingford, CT) at the B3LYP/6-31G* level of theory and partial atomic charges were assigned using a standard restricted electrostatic potential fit (RESP) method[187] with the tertiary nitrogen considered in a protonated state. The molecular structure of BACE1 was obtained from the Protein Data Bank (pdb code: 2b8l).[188] The protein target was converted to AutoDock 4.2[189] format files using AutoDockTools 1.5.6 generating automatically all other atom values. The docking area has been centred on the catalytic residue D228 and grids points of 60 x 60 x 60 with 0.375 Å spacing were calculated around the docking area for all the ligand atom types using AutoGrid4. 100 separate docking calculations were performed for each binder. Each docking calculation consisted of 25 x 10^6 energy evaluations using the Lamarckian genetic algorithm local search (GALS) method. A low-frequency local search according to the method of Solis and Wets was applied to docking trials to ensure that the final solution represents a local minimum. The docking results from each of the 100 calculations were clustered and ranked on the basis of the free energy of binding.

For the σ_1R, the optimized structure of selected compounds was docked into the putative binding pockets by applying a consolidated procedure[168,169,171,183-185,190] with AutoDock. The resulting docked conformations for each complex were clustered and visualized; then, for each compound, only the molecular conformation satisfying the combined criteria of having the lowest (i.e., more favourable) Autodock energy and belonging to a highly populated cluster was selected to carry for further modeling.

The ligand/receptor complexes obtained from the docking procedure for both protein targets, BACE1 and σ_1R, were further refined in Amber 12[191]

and 14[192] using the quenched molecular dynamics (QMD) method as previously described.[168,169,183] According to QMD, the best energy configuration of each complex resulting from this step was subsequently solvated by a cubic box of TIP3P[193] water molecules extending at least 10 Å in each direction from the solute. The system was neutralized and the solution ionic strength was adjusted to the physiological value of 0.15 M by adding the required amounts of Na^+ and Cl^- ions. Each solvated system was relaxed by 500 steps of steepest descent followed by 500 other conjugate-gradient minimization steps and then gradually heated to a target temperature of 300 K in intervals of 50 ps of NVT MD, using a Verlet integration time step of 1.0 fs. The Langevin thermostat was used to control temperature, with a collision frequency of 2.0 ps^{-1} The protein was restrained with a force constant of 2.0 kcal/(mol Å), and all simulations were carried out with periodic boundary conditions. Subsequently, the density of the system was equilibrated via MD runs in the isothermal-isobaric (NPT) ensemble (with isotropic position scaling and a pressure relaxation time of 1.0 ps), for 50 ps with a time step of 1 fs. All restraints on the protein atoms were then removed, and each system was further equilibrated using NPT MD runs at 300 K, with a pressure relaxation time of 2.0 ps. Three equilibration steps were performed, each 2 ns long and with a time step of 2.0 fs. To check the system stability, the fluctuations of the root-mean-square-deviation (rmsd) of the simulated position of the backbone atoms of the receptor with respect to those of the initial protein were monitored. All chemophysical parameters and rmsd values showed very low fluctuations at the end of the equilibration process, indicating that the systems reached a true equilibrium condition. The equilibration phase was followed by a data production run consisting of 40 ns of MD simulations in the canonical (NVT) ensemble. Only the last 20 ns of each equilibrated MD trajectory were considered for statistical data collections. A total of 1000 trajectory snapshots were analyzed the each ligand/receptor complex. The binding free energy, ΔG_{bind}, between the two ligands and the

σ1R was estimated by resorting to the MM/PBSA approach implemented in Amber 14. According to this well validated methodology,[148] the free energy was calculated for each molecular species (complex, receptor, and ligand), and the binding free energy was computed as the difference:

$$\Delta G_{bind} = G_{complex} - (G_{receptor} + G_{ligand}) = \Delta E_{MM} + \Delta G_{sol} - T\Delta S$$

in which ΔE_{MM} represents the molecular mechanics energy, ΔG_{sol} includes the solvation free energy and $T\Delta S$ is the conformational entropy upon ligand binding. The per residue binding free energy decomposition was performed exploiting the MD trajectory of each given compound/complex, with the aim of identifying the key residues involved in the ligand/receptor interaction. This analysis was carried out using the MM/GBSA approach,[194,195] and was based on the same snapshots used in the binding free energy calculation. All simulations with σ_1R were carried out using the Pmemd modules of Amber 14, running on the EURORA-CPU/GPU calculation cluster of the CINECA (Bologna, Italy). The entire MD simulation and data analysis procedure was optimized by integrating Amber 14 in modeFRONTIER, a multidisciplinary and multiobjective optimization and design environment.[196]

Studies of Cell viability and Neuroprotection. Culture of SH-SY5Y Cells. SH-SY5Y cells, at passages between 3 and 16 after de-freezing, were maintained in a Dulbecco's modified Eagle's medium (DMEM) containing 15 non-essential amino acids and supplemented with 10% fetal calf serum (FCS), 1 mM glutamine, 50 units/mL penicillin, and 50 µg/mL streptomycin (reagents from GIBCO, Madrid, Spain). Cultures were seeded into flasks containing supplemented medium and maintained at 37 °C in 5% CO_2/humidified air. Stock cultures were passaged 1:4 twice weekly. For assays, SH-SY5Y cells were sub-cultured in 48-well plates at a seeding density of 10^5 cells per well. For the cytotoxicity experiments, cells were treated with drugs before confluence in DMEM free of serum.

Cell Viability Experiments. To study the cytotoxic effects of compounds alone, cells were plated at a density of 10^5 cells per well at least 48 h before the toxicity measurements. Cells were exposed for 24 h to the compound at 1 µM, and the quantitative assessment of cell death was made by measurement of the percent of the intracellular enzyme lactate dehydrogenase (LDH) released to the extracellular medium (cytotoxicity detection kit, Roche). The quantity of LDH was evaluated in a microplate reader (Anthos 2010 or Labsystems iMES Reader MS) at 492 nm (λ excitation) and 620 nm (λ emission).

Neuroprotection Studies. To study the cytoprotective action of the compounds against cell death induced by the mixture of rotenone (30 µM) and oligomycin A (10 µM), drugs were given at time zero and maintained for 24 h. Then, the media were replaced by fresh media still containing the drug plus the cytotoxic insult, which was left for an additional 24 h period. Thereafter, cell survival was assessed measuring MTT activity.

Measurement of Cell Viability by MTT Assay. Cell viability was also measured by quantitative colorimetric assay with 3-[4,5-dimethylthiazol-2-yl]-2,5-diphenyl-tetrazolium bromide (MTT) (Sigma Aldrich), as described previously.[197] Briefly, 50 µL of the MTT labeling reagent, at a final concentration of 0.5 mg/mL, was added to each well at the end of the incubation period and the plate was placed in a humidified incubator at 37 ºC with 5 % CO_2 and 95 % air (v/v) for an additional 2 h period. Then, the insoluble formazan was dissolved with dimethylsulfoxide; colorimetric determination of MTT reduction was measured at 540 nm. Control cells treated with 0.1% DMSO were taken as 100 % viability.

Chapter 2

New Antioxidant AChE-MAO Dual Inhibitors Based on the Chromone Scaffold

Introduction

Monoamine Oxidase (MAO)

Monoamine oxidase (MAO) catalyzes the oxidative deamination of dietary amines such as tyramine or phenethylamine and biogenic amines, including neurotransmitters dopamine (DA), epinephrine, norepinephrine (NE) and serotonin (5-HT). Almost all mammalian tissues express two isoforms of MAO (MAO-A and MAO-B), they were initially distinguished by their susceptibility to different inhibitors as well as by their affinity for different substrates, MAO-A catalyzes deamination of 5-HT and NE and is potently inhibited by clorgiline. On the other hand, MAO-B is inhibited by deprenyl or selegiline and shows affinity for phenylethyl amine and benzyl amine.[198] Distribution of each isoenzyme varies depending on the organ; in peripheral nervous system (PNS) and CNS, neuronal MAO protects against exogenous amines and regulates the levels of amine neurotransmitters.

In human brain, 75% of MAO activity corresponds to MAO-B; it has been detected in serotonergic neurons where contributes to the purity of 5-HT degrading other biogenic or exogenous amines, and in micro-vessels of the BBB[199] as part of the protecting system against foreign substances.

MAO-A has been detected in catecholaminergic neurons (locus coeruleus, substantia nigra or paraventricular nucleus of hypothalamus, among others) involved in different processes such as stress response, attention, emotions or movement. In astrocytes and glial cells, both isoforms are

present and participate in degradation of neurotransmitters released into the synaptic cleft.

MAO and Alzheimer's disease

Oxidative deamination catalyzed by MAO produces hydrogen peroxide (H_2O_2), the corresponding aldehyde and ammonia in the case of primary amines or a substituted amine in the case of secondary amines. H_2O_2 is considered a source of hydroxyl radicals which in turn contributes to generate an oxidative environment. In agreement with this mechanism, it is expectable that augmented levels of MAO-B observed AD brain,[16,200] mainly in glial cells associated to senile plaques,[201] potentiate the oxidative stress typical of neurodegenerative processes, by production of radical species.

On the other hand, changes in MAO-A levels in AD patients seem to be more intricate. While elevated activity of MAO-A has been reported in several regions of AD brain such as neocortex and locus coeruleus,[202,203] other studies have determined a decreased amount of intra-neuronal MAO-A in nucleus basalis of Meynert. Additionally, it has been proposed that some metabolites of catecholamines catabolized preferentially by MAO-A are potentially neurotoxic, one example is the aldehyde and alcohol resulting from dopamine oxidation, which have been demonstrated to be apoptotic agents, and oxidative stressors.[204]

MAO inhibitors as therapeutic agents for AD

Commonly, AD patients exhibit neuropsychiatric symptoms such as depression, psychosis and aggressive behavior.[205,206] Depression is associated with low levels of 5-HT and could be considered a risk factor to develop AD,[207] on the other hand, aggressive behavior in AD has been related to low levels of NE in some brain regions.[18,208] Assuming that NE and 5-HT are both substrates of MAO-A, inhibiting this isozyme could be beneficial in some cases of AD.

Additionally, as stated above, MAO-B activity is exacerbated in AD; mainly in glial cells associated to senile plaques, this increased activity contributes to the neuronal death through the production of oxidative stress and toxic metabolites.[209,210]

Benefits of MAO isoforms inhibition in AD could include increase of 5-HT levels, reduction of oxidative stress caused by radical species[17] and restoration of the unbalanced amounts of amine neurotransmitters.[13,211] In agreement with these facts, MAO inhibitors might be an interesting and complementary tool for the treatment of neurodegenerative diseases including PD and AD.

In spite of all stated above, the use of drugs which exclusively act over MAO enzymes in AD remains controversial; one example is selegiline, there are some studies which have demonstrated that this MAO-B inhibitor affects positively learning and memory in animal models,[212] however, it has not demonstrated any beneficial effect in AD patients,[213] in light of this, a different strategy must be envisioned to take advantage of MAO inhibition in AD treatment, the design of multifunctional molecules with the potential of acting in different processes related to the disease.[214]

Chromones

The chromone ring is the central core of several naturally occurring substances, such as flavonoids, responsible for the antioxidant properties of red wine and numerous fruits.[215] The interesting biological properties of natural chromones have led to the synthesis of hundreds of new derivatives with a wide variety of activities, proving the chromone framework as a privileged scaffold useful in the search for new bioactive compounds.[216,217] Drugs based on the chromone scaffold (Blue in figure 2.1) currently used in humans, include sodium cromoglicate and nedocromil which act as mast cell stabilizer drugs, iguratimode, an anti-

inflammatory agent, diosmin an anti-hemorroidal drug, and flavoxate, a muscle relaxant. (Figure 2.1)

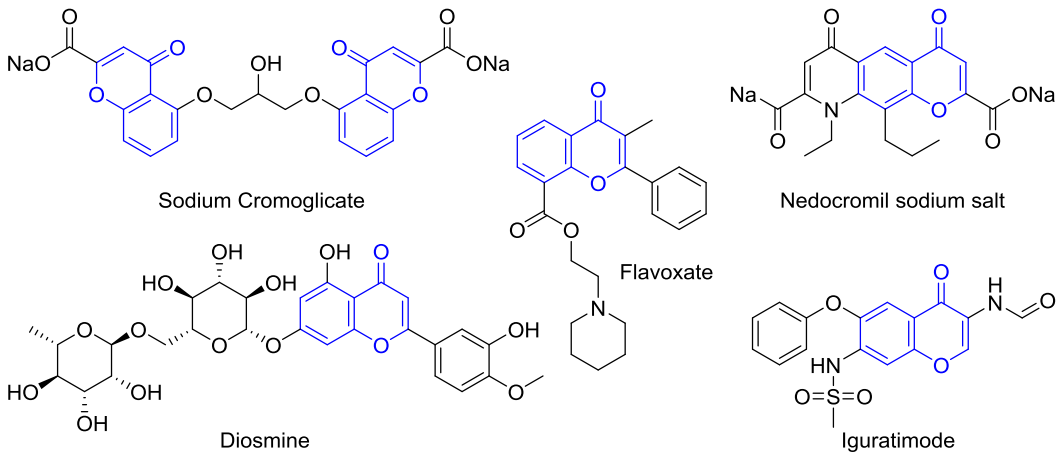

Figure 2.1 Chromone scaffold containing drugs

The use of the chromone ring as part of new potential drugs for neurodegenerative diseases is based on the diversity of biological effects reported for synthetic and natural chromone derivatives, such as antioxidant, anti-inflammatory, AChE inhibition and MAO inhibition, among others.[216-220]

In this chapter we intend to take advantage of the affinity demonstrated by different chromone derivatives towards MAO enzymes, as well as their antioxidant properties to combine this scaffold with the NBP and DBMA fragments in order to obtain potential multifunctional molecules acting as dual AChE-MAO inhibitors with antioxidant properties.

In order to generate a diverse set of target compounds and evaluate the structure-activity relationship, we decided to carry out modifications in the nature and place of the substituents in the aromatic ring of the chromone scaffold (H, OMe, OH, NO_2 and NH_2), being preferred those able which potentiate the antioxidant properties; changes in the nature of the bond linking the chromone system to the moiety bearing the

tertiary amine, (amide or ester); changes in the aliphatic chain in the case NBP (n=1-3) and changes in the position of the amine group in the case of DBMA derivatives.

Results and Discussion

Synthesis of Chromone-NBP and Chromone-DMBA hybrids

The synthesis of the methoxylated chromone-2-carboxlic acids (**2.1-2.6**) was achieved from the corresponding phenols and dimethyl acetylenedicarboxylate, according to the method of Stoermer et al.[221] However, since this methodology is widely known and the intermediate diesters and dicarboxylic acids have been previously reported, we did not isolate them and carried out the synthesis in a continuous process until the desired acids as described in the experimental section.

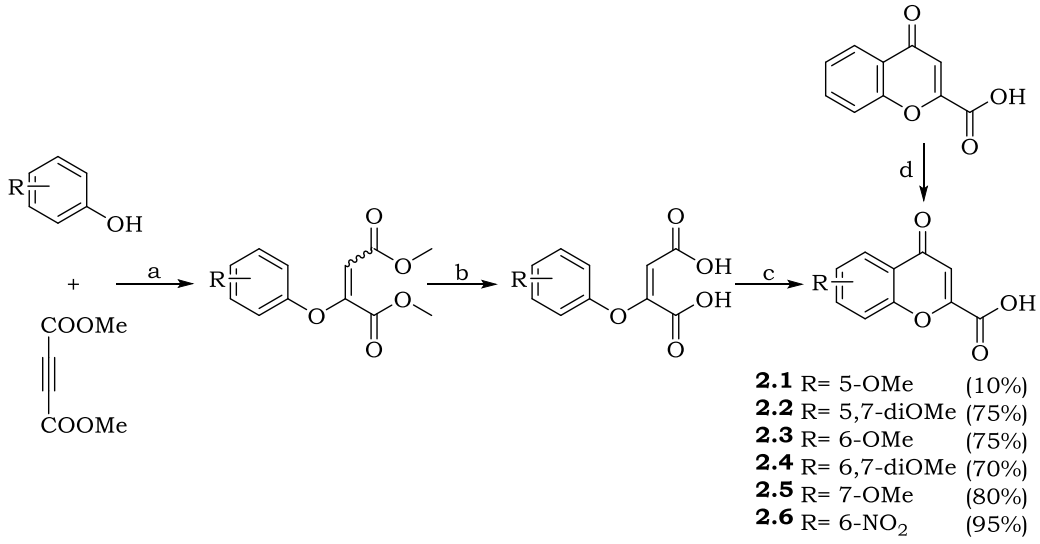

Scheme 2.1 Reagents and conditions. (a)Et_2O, Et_3N, overnight, rt; (b) Acethyl chloride, H_2SO_4, reflux 30 min; (c) NaOH, reflux 30 min; (d) HNO_3:H_2SO_4 (1:6), 70 °C, 3h.

The nitro derivative **2.6** was obtained as a sole product by a classical nitration of the commercially available chromone-2-carboxylic acid in a mixture of nitric and sulphuric acids (scheme 2.1).[222]

NBP and DMBA amine intermediates (**1.2** and **1.4**) were synthesized as described in chapter 1, (scheme 1.1). Alcohol **2.7**, was synthesized as described in scheme 2.2 from commercially available 2-(piperidin-4-yl)ethan-1-ol and benzyl bromide; amines where n= 0, 2 and alcohols where n= 0, 1 are commercially available.

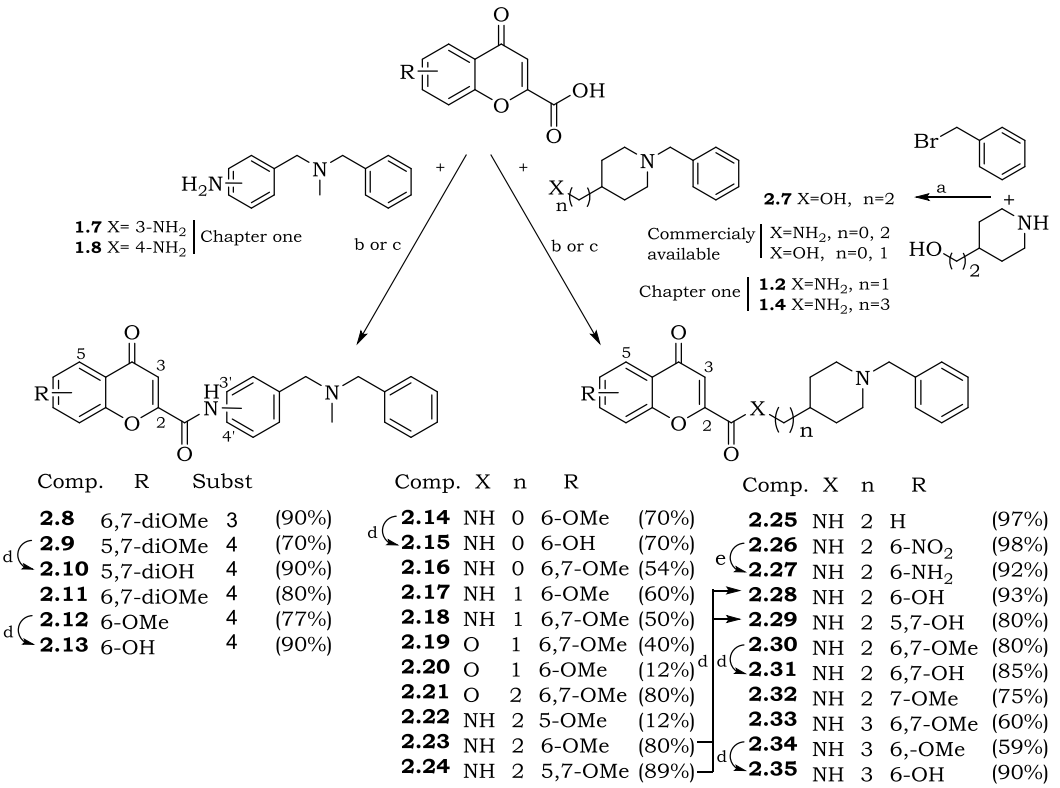

Scheme 2.2 Reagents and conditions. (a)ACN, K_2CO_3, Tetrabutyl ammonium iodide (TBAI), reflux 24h; (b) DMF, CDI, mw 120 °C; (c) BOP, Et_3N, DMF, overnight, rt. (d) BBr_3, THF, overnight, rt. (e) H_2/Pd(5%), EtOH, overnight, rt.

The synthesis of the chromone-based hybrids was developed by reaction between the corresponding alcohols or amines with acids **2.1-2.6** or chromone-2-carboxylic acid (commercially available). Two different methods where used according to the availability of the coupling agent. A microwave assisted reaction with CDI as activating agent and a coupling reaction at room temperature (rt) with BOP and Et_3N (CDI is preferred due to the easier work up; see experimental section). In both cases the

best solvent was DMF due to the low solubility of the chromone carboxylic acids in less polar solvents, although when activation is carried out with BOP, other solvents could be used (i.e. THF or DCM) because the Et_3N helps to solubilize the acids. Deprotection of methoxylated derivatives was carried out by overnight treatment with boron tibromide (BBr_3) at rt. It is worth to mention that 1 equivalent for each ether group and one additional equivalent for each heteroatom present in the molecule was used to obtain good yields (70-90 %).[140,223]

Regarding to characterization of final compounds, it is important to mention the case of nitro derivative **2.26**. Although the exact mass corresponds to the desired product; the CH group at position 3 of the chromone system was not observed either in ^{13}C or ^{1}H NMR spectra. However, amine derivative **2.27**, obtained by hydrogenation of **2.26** exhibited all the expected signals and exact mass, allowing us to confirm the structure of **2.26**.

Biological Evaluation

All derivatives were evaluated initially as inhibitors of human cholinesterases (AChE and BuChE), as described in chapter one. In order to establish their ability to reach the CNS and to determine whether or not they exhibit antioxidant properties, they were evaluated simultaneously in ORAC and PAMPA assays. Results are gathered in tables 2.1 and 2.2 for DBMA and NBP series respectively.

AChE inhibition test, demonstrated that both series (chromone-NBP and chromone-DBMA) are selective inhibitors of AChE with IC_{50} values between the low micromolar and two-digit nanomolar range. Chromone-DBMA hybrids are weaker AChE inhibitors and totally lack of affinity for BuChE, consequently a shorter series was prepared. (Table 2.1)

Table 2.1 Inhibition of h-AChE, h-BuChE (IC_{50}, μM) and prediction of CNS-Permeation by the PAMPA-BBB Assay.[a]

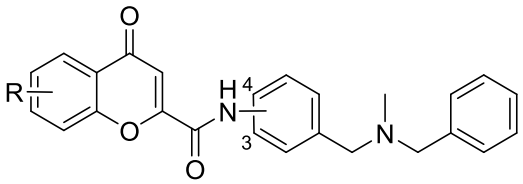

			IC_{50} (μM)		PAMPA[b]
Comp.	R	Subst.	**h-AChE**	**h-BuChE**	P_e 10^{-6} cm s^{-1}
2.8	6,7-diOMe	3	4.5±0.8	>10	30.6±0.8 CNS +
2.9	5,7-diOMe	4	3.2±0.4	>10	31.4±0.9 CNS +
2.10	5,7-diOH	4	1.9±0.6	>10	25.3±1.7 CNS +
2.11	6,7-diOMe	4	0.99±0.3	>10	31.0±0.1 CNS +
2.12	6-OMe	4	1.5±0.2	>10	28.4±1.1 CNS +
2.13	6-OH	4	1.3±0.3	>10	12.6±0.3 CNS +

[a]Results are expressed as mean ± SD (n =3). [b]CNS+: compounds predicted to reach CNS.

As seen in table 2.2, the most potent AChE inhibitors belong to chromone-NBP series, showing more potency when the linker chain holds 2 or 3 methylene groups.

The nature of the substituent in the chromone system did not exert a significant effect on the potency, 6.7-diMeO, 6-OH, 6-NO_2, and 6-NH_2 substituted compounds showed IC_{50} values in the low nanomolar range, as long as the substituted positions are 6 and 7. Replacement of the amide by an ester bong did not affect significantly the inhibitory potency as evident comparing compounds **2.21** and **2.30**, with IC_{50} values in the same range, 56 nM and 46 nM respectively.

Table 2.2 Inhibition of h-AChE, h-BuChE (IC_{50}, μM) and prediction of CNS-Permeation by the PAMPA-BBB Assay.[a]

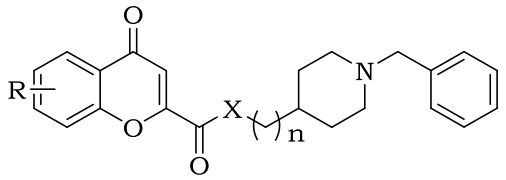

				IC_{50} (μM)		**PAMPA[b]**
Comp.	**X**	**n**	**R**	**h-AChE**	**h-BuChe**	P_e 10^{-6} cm s^{-1}
2.14	NH	0	6-OMe	0.97±0.14	>10	17.4±1.1 CNS +
2.15	NH	0	6-OH	2.36±0.54	>10	8.8±0.9 CNS -
2.16	NH	0	6,7-diOMe	0.66±0.09	>10	18.0±0.4 CNS +
2.17	NH	1	6-OMe	3.61±0.09	>10	16.1±0.5 CNS +
2.18	NH	1	6,7-diOMe	1.46±0.17	>10	nd
2.19	O	1	6,7-OMe	0.30±0.06	>10	10.7±0.8 CNS ±
2.20	O	1	6-OMe	7.49±0.12	>10	15.1±0.4 CNS +
2.21	O	2	6,7-diOMe	0.056±0.015	>10	14.3±0.4 CNS +
2.22	NH	2	5-OMe	0.87±0.14	>10	nd
2.23	NH	2	6-OMe	0.17±0.01	6.5±0.7	20.9±0.3 CNS +
2.24	NH	2	5,7-diOMe	0.32±0.02	6.3±0.5	11.5±0.7 CNS ±
2.25	NH	2	H	0.11±0.03	5.2±0.4	16.0±0.8 CNS +
2.26	NH	2	6-NO_2	0.021±0.009	9.3±0.7	18.2±0.2 CNS +
2.27	NH	2	6-NH_2	0.041±0.006	4.3±0.4	11.3±0.3 CNS ±
2.28	NH	2	6-OH	0.091±0.014	>10	10.1±0.6 CNS ±
2.29	NH	2	5,7-diOH	0.58±0.04	>10	19.1±0.7 CNS +
2.30	NH	2	6,7-OMe	0.046±0.007	>10	14.8±1.2 CNS +
2.31	NH	2	6,7-diOH	4.13±0.79	>10	10.7±0.4 CNS ±
2.32	NH	2	7-OMe	0.033±0.009	9.9±0.99	nd
2.33	NH	3	6,7-diOMe	0.11±0.04	>10	13.4±0.5 CNS +
2.34	NH	3	6-OMe	0.37±0.13	5.8±0.5	21.8±0.2 CNS +
2.35	NH	3	6-OH	0.023±0.012	>10	12.7±0.5 CNS +

[a]Results are expressed as mean ± SD (n =3). [b]CNS+: compounds predicted to reach CNS. nd: not determined.

In chromone-NBP series, the best dual profile combining AChE inhibition and antioxidant properties was shown by compounds **2.27** (6-NH_2, n=2 IC_{50}=41 nM), **2.28** (6-OH, n=2, IC_{50}=91 nM) and **2.35** (6-OH, n=3, IC_{50}=23 nM), they were selected besides to **2.30** (6,7-diMeO, n=2, IC_{50}=46 nM) and **2.9** (6,7-diOMe-4'-DBMA, IC_{50}=0.99 µM), to determine the mechanism of the inhibition of AChE. For example, Lineweaver-Burk plots for several compounds (fig 2.3), show how $1/V_{max}$ (y intercept) and $1/K_m$ (x intercept) increase with increasing concentrations of inhibitor; the prototypical pattern of a mixed-type of inhibition (competitive and non-competitive); possibly due to the interaction of compounds with both catalytic anionic site (CAS) and peripheral anionic site (PAS) of AChE.

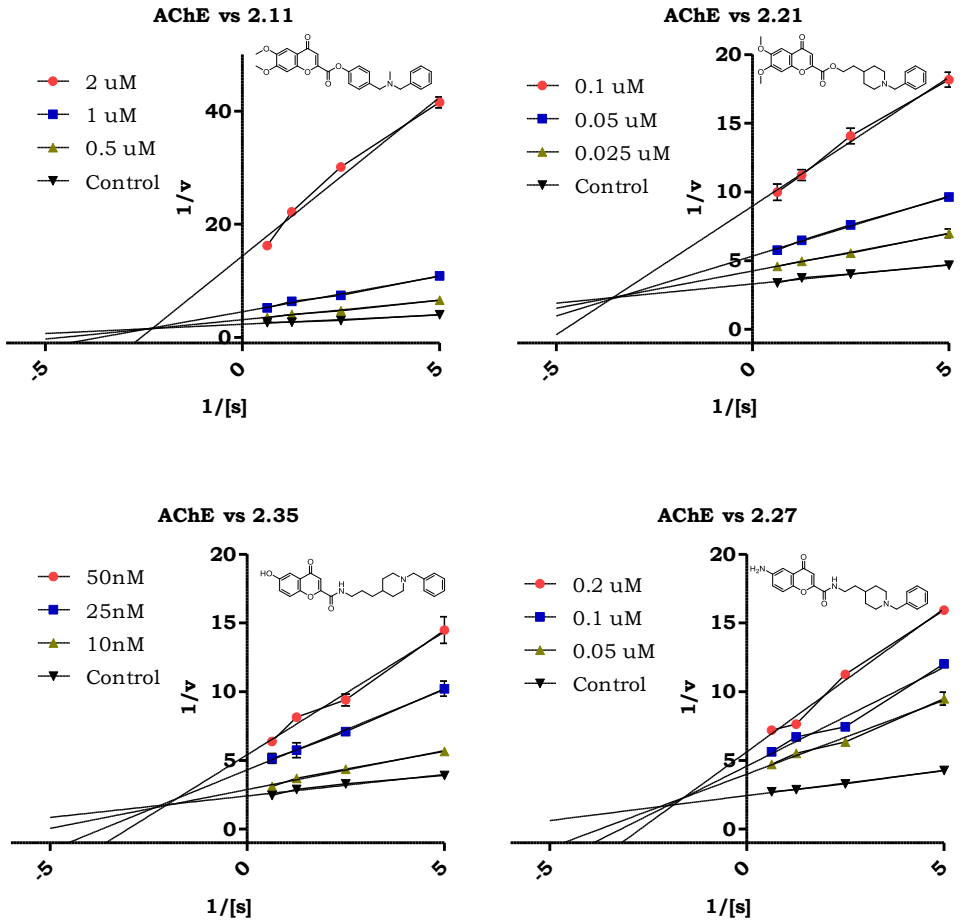

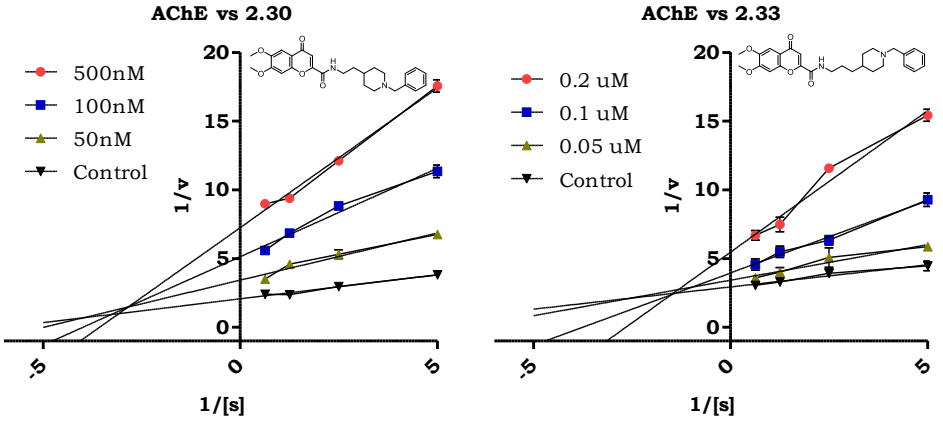

Fig 2.3 Lineweaver-Burk plot of reciprocals for velocity and increasing concentrations of inhibitor. Lines were derived from a weighted least-squares analysis of data.

According to PAMPA assay results, most of nanomolar AChE inhibitors are able to cross the BBB. In the case of **2.27** and **2.28**, permeability values in the upper limit of the calculated range of uncertainty (8.9-11.5; figure 2.4) were obtained, 11.3 and 10.1 respectively.

Table 2.3 Permeability values (P_e 10^{-6} cm s^{-1}) for commercial drugs used in the PAMPA-BBB Validation Experiment.

Compound	Bibl.[a]	Exp.[b]
Testosterone	17.0	26.5 ± 0.3
Verapamil	16.0	29.5 ± 0.2
Imipramine	13.0	20.6 ± 1.0
Desipramine	12.0	22.9 ± 1.7
Promazine	8.8	20.8 ± 0.5
Corticosterone	5.1	11.0 ± 0.2
Piroxicam	2.5	10.0 ± 0.1
Hydrocortisone	1.9	10.2 ± 0.1
Caffeine	1.3	7.9± 0.3
Ofloxacin	0.8	6.1 ± 0.1

[a]Taken from Ref 225 [b]Data are the mean ± SD of three independent experiments

In general, chromone-DBMA hybrids exhibited higher values of permeability than chromone-NBP derivatives and hydroxy-substituted hybrids showed lower permeability than methoxylated compounds.

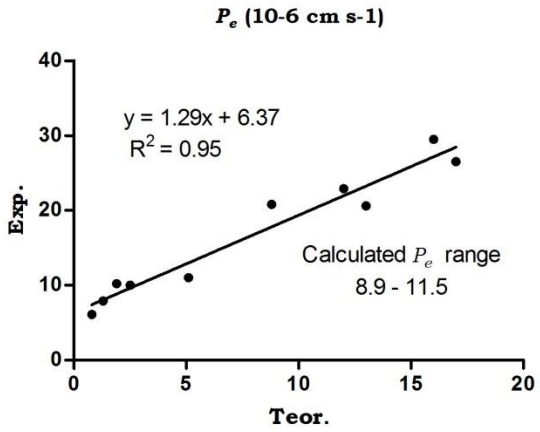

Figure 2.4 Correlation of permeability of experimental and theoretical values of standard compounds used in PAMPA assay in PBS:EtOH (70:30) as solvent and the calculated range of permeability values to determine whether or not a given compound is able to reach CNS.

Inhibition of human MAO's and BACE and the antioxidant properties

To continue the assessment of the multitarget profile of these new hybrids, we evaluated their ability to inhibit both isoforms of human recombinant MAO, expressed in baculovirus infected BTI insect cells.

Table 2.4 summarizes the results of those compounds which exhibited activity towards MAO-A and MAO-B. Interestingly, most potent MAO inhibitors belong to chromone-DBMA series. Compounds **2.12** and **2.13** inhibit MAO-A, with comparable potency than iproniazide, and higher potency than moclobemide; drugs which exert antidepressant effects with potencies in the micromolar range (*in vitro*) and have been clinically used in humans to treat depression.

Table 2.4 IC_{50} values for the inhibitory effects new compounds and reference inhibitors on the enzymatic activity of human recombinant MAO isoforms expressed in baculovirus infected BTI insect cells.

		IC_{50} (µM)			
	Comp.	**MAO-A**	**MAO-B**	**BACE1** (% Inh[b])	**ORAC** Trolox Equiv.
NBP	**2.26**	20.5±1.3	**	(3.5)	NA
	2.27	***	**	(5.1)	0.9±0.1
	2.28	39.3±2.8*	51.2±4.3	(0.2)	1.2±0.1
	2.31	70.5±8.6*	37.9±4.2*	(14.8)	1.7±0.2
	2.35	***	**	ND	1.3±0.1
DBMA	**2.8**	**	**	6.7±0.8 µM	NA
	2.9	**	**	(30.9)	ND
	2.10	22.8±1.5	**	(20.6)	1.2±0.1
	2.11	**	**	(27.4)	NA
	2.12	1.6±0.4	59.8±3.7*	(22.1)	ND
	2.13	7.0±0.8	9.7±1.6	(3.3)	1.6±0.1
	R-Deprenyl	68.7±4.2[a]	0.017±0.002	nd	nd
	Iproniazide	6.6±0.8	7.5±0.36	nd	nd
	Moclobemide	361.4±19.4	*	nd	nd

IC_{50} values shown in this table are the mean ± SEM. from five experiments. Level of statistical significance: [a]$P < 0.01$ versus the corresponding IC_{50} values obtained against MAO-B, as determined by ANOVA/Dunnett´s. [b]Percent of inhibition at 10 uM. *Maximum inhibition achieved with compound was about 50% of total enzymatic activity. ** Inactive at 200 µM (highest concentration tested). *** Inactive at 1 mM (highest concentration tested).NA: not antioxidant. nd: not determined

Regarding to BACE1 inhibition, we observed that chromone-NBP hybrids completely lack of affinity for the enzyme, while chromone-DBMA series are poor BACE1 inhibitors with inhibition percentages around 30% at 10 μM, except compound **2.8**, in this case we observed a notorious effect of changing the position of the amide group linking the DBMA fragment to the chromone scaffold, shifting from 27% of inhibition at 10 μM in the case of **2.11** to an IC_{50} value of 6.7 μM in the case of **2.8**.

The antioxidant activities of selected chromone-based hybrids were evaluated by ORAC assay. As expected, compounds bearing methoxy or nitro groups in the chromone scaffold were inactive, while hybrids with amine, or better hydroxyl groups, exhibited interesting antioxidant capacities, ranging from 0.9 to 1.7-fold the trolox value. In the NBP series, the best antioxidant agent was **2.31** with two hydroxyl groups in positions 6 and 7 of the chromone core, but moderated AChE inhibitory potency. On the other hand, **2.35** combines a good value of antioxidant capacity (1.3 trolox equivalents.) and a potent inhibitory activity towards AChE (IC_{50} 23 nM). Among the DBMA-based hybrids, the best radical scavenger was **2.13** (6-hydroxy substituted), a dual AChE-MAO inhibitor in the low micromolar range.

Inhibition of $A\beta_{42}$ and *tau* aggregation in intact *Escherichia coli* cells

A selection of compounds, including **2.12** and **2.13** (chromone-DBMA), with a good dual profile AChE-MAO and the potent AChE inhibitors **2.28** and **2.30** (chromone-NBP) were evaluated as anti-aggregating agents in independent assays on cells overexpressing $A\beta_{42}$ and *tau* protein. In the NBP series, very low anti-aggregating activities were found, and only the nanomolar AChE inhibitor **2.30** showed percentages of inhibition around 10%. By contrast, the chromone-DBMA hybrids **2.12** and **2.13**, which also showed a good dual inhibition of hAChE – hMAO, displayed a

moderated anti-aggregating effect of 21% and 19% for $A\beta_{42}$ and 33% and 27% for *tau* protein respectively. (Table 2.5)

Table 2.5 Inhibitory activities of chromone-based hybrids (20 µM) monitored by Th-S staining of bacterial cells overexpressing Aβ42 peptide

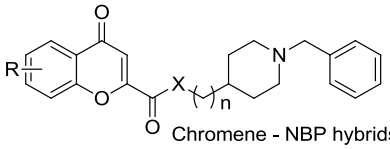

Chromene - NBP hybrids

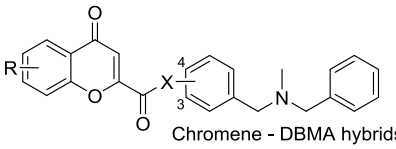

Chromene - DBMA hybrids

	Comp.	R	X	n or subst.	% Inhibition[a]	
					$A\beta_{42}$ aggr.	*tau* aggr.
NBP	**2.14**	6-OMe	NH	0	<10	<10
	2.16	6,7-diOMe	NH	0	<10	<10
	2.19	6,7-diOMe	O	1	<10	<10
	2.28	6-OH	NH	2	<10	<10
	2.29	5,7-diOH	NH	2	<10	<10
	2.30	6,7-diOMe	NH	2	11.9 ± 4.9	9.6 ± 5.4
DBMA	**2.12**	6-OMe	NH	4	21.8 ± 3.4	33.5 ± 7.5
	2.13	6-OH	NH	4	19.3 ± 5.8	27.0 ± 2.2

[a]Values are expressed as mean ± SEM of four independent experiments (n = 4). Inhibitor concentration: 20 µM

Neuro-protectant properties of some selected compounds including **2.13** with an antioxidant capacity of 1.2 trolox equivalents and **2.30** inactive in ORAC but a potent AChE inhibitor, were evaluated in a cell viability test using SH-SY5Y cells co-cultured with a toxic mixture of rotenone-oligomycin during 24 hours.

Unexpectedly, **2.30** with negative results in ORAC exhibited the better neuro-protective profile in a concentration-dependent manner, increasing concentrations from 0.1 to 3 µM protected between 11% and 22% of cells (table 2.6, figure 2.5). Melatonin, with antioxidant capacity of 2.8 trolox equivalents, was used as a positive control, protecting 38 % of cells at 10

nM. **2.13** exhibited a statistically significant protection of 17 % at 0.3 μM and **2.19** at 0.1 and 0.3 μM.

Table 2.6 Percentage of neuroprotection in the human neuroblastoma cell line SH-SY5Y against the combination of rotenone (30 μM) and oligomycin A (10 μM) by selected chromene-based hybrids at indicated concentrations.

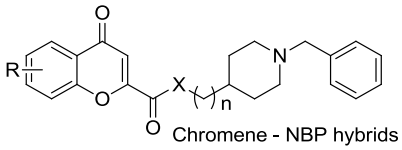

Chromene - NBP hybrids

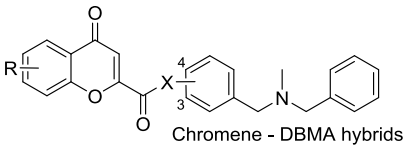

Chromene - DBMA hybrids

			Neuroprotection (%)[a]			
	Comp.	n/sust.	0.1 μM	0.3 μM	1 μM	3 μM
NBP	**2.14**	0	9.8±1.1^{ns}	13.9±3.1^{ns}	14.6±1.2^{ns}	8.6±1.7^{ns}
	2.16	0	5.7±3.6^{ns}	18.0±3.1^{ns}	12.3±2.5^{ns}	12.6±3.1^{ns}
	2.19	1	19.4±0.7*	19.6±3.0*	6.8±1.2^{ns}	12.4±3.6^{ns}
	2.28	2	15.0±2.9^{ns}	18.8±3.8^{ns}	8.6±3.0^{ns}	15.2±4.9^{ns}
	2.30	2	11.5±1.5*	18.1±1.6**	17.1±1.9*	22.4±2.5**
DBMA	**2.13**	4	13.5±2.6^{ns}	17.4±1.1*	12.2±2.6^{ns}	15.3±2.4^{ns}

[a]Cell viability was measured as MTT reduction and data were normalized as % control. Data are expressed as the means ± SEM of triplicate of at least three different cultures. All compounds were assayed at increasing concentrations (0.1-3 μM). **P≤ 0.01 and *P≤0.05 with respect to control group. Comparisons between drugs and control group were performed by one-way ANOVA followed by the Newman–Keuls post-hoc test.

According to these results, it is probable that the protection exerted by **2.30** could involve a mechanism different than the radical scavenging capacity. Even though the rest of compounds did not exhibited neuro-protectant properties, it is worth to mention that in any case, they potentiated the toxicity of rotenone/oligomycin.

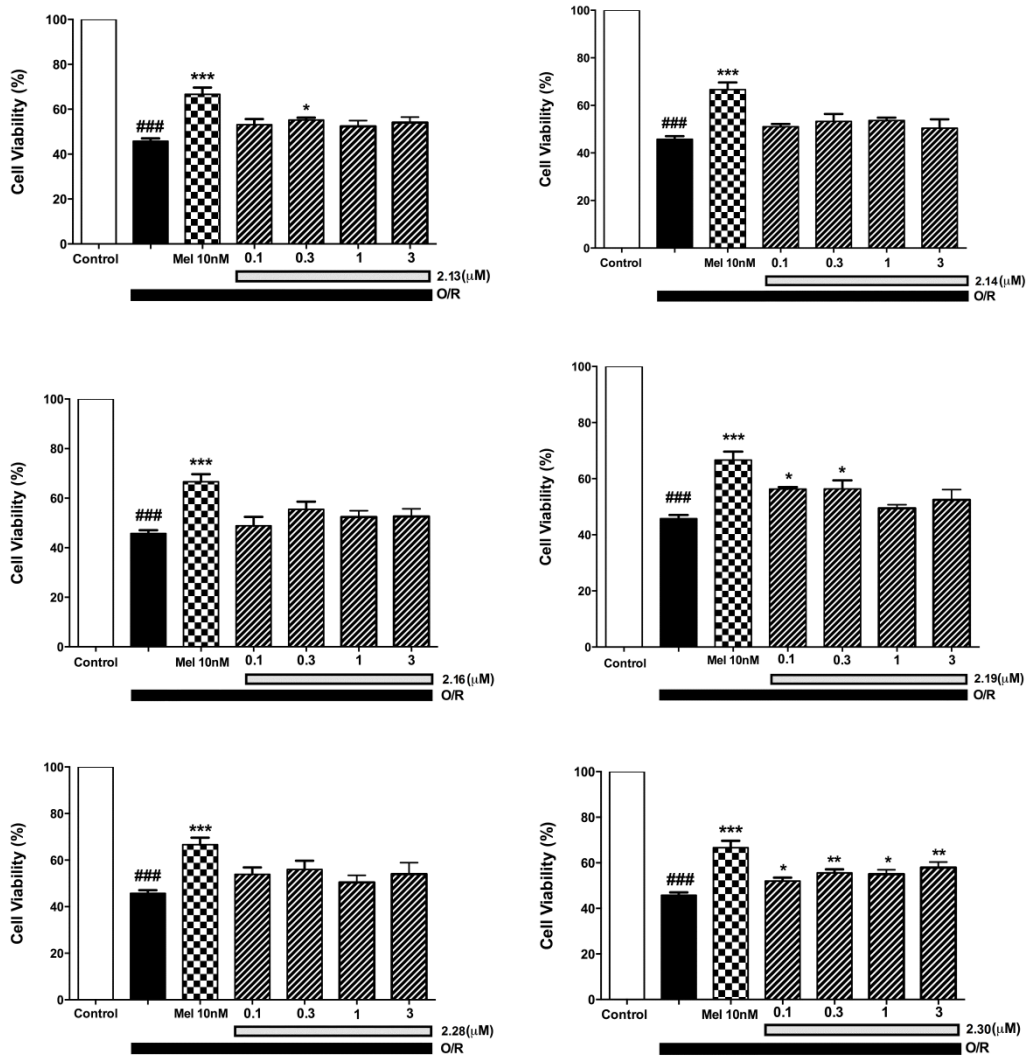

Figure 2.5 Cell viability was measured as MTT reduction and data were normalized as % of control. Data are expressed as the means ± SEM. of triplicate of at least three different cultures. All compounds were assayed at increasing concentrations (0.1-3 μM).

Preliminary evaluation *in vivo* of MAO-B inhibitory properties in the model of reversion of hypokinesia induced by reserpine

Taking into account that inhibition of MAO's could exert antidepressant or antiparkinsonian effects *in vivo*. We decided to evaluate some of the most potent MAO inhibitors in the murine model of reserpine. This model

is based on the monoaminergic hypothesis which states that depression and extrapyramidal symptoms of PD are caused by an unbalance in the levels of monoamine neurotransmitters, i.e serotonin or dopamine.[224-226]

Reserpine, an indole based alkaloid with antihypertensive and antipsychotic properties, has ability to deplete catecholamines by inhibition of vesicular monoamine transporter (VMAT). Free catecholamines are introduced by VMAT from the cytosol to presynaptic vesicles for subsequent exocytosis. As a consequence of VMAT inhibition, free intracellular unprotected amines are metabolized by MAO's and never reach the synaptic cleft and consequently the postsynaptic neuron. These undesired effects are believed to be responsible for the depressant and parkinsonian effects of reserpine, and are the basis of the model of hypokinesia induced by reserpine.[227,228]

In this preliminary evaluation, a single dose of 100 mg/Kg of compounds **2.12**, **2.13** (MAO-B IC_{50} 9.7 μM) and **2.30** (it was introduced in this experiment as a control since it does not inhibit MAO's) were administered intraperitoneally (i.p.) to ICR albino mice to counteract the hypokinetic effects of reserpine (3mg/Kg) as described by Tadaiesky et. al (2006), with minor adaptations.[229]

The spontaneous locomotion of the animals was measured 2 h and 24 h after administration of compounds. As described in figure 2.6, control animals did not recover the mobility; even after 24 hours because of the long lasting effects of reserpine.

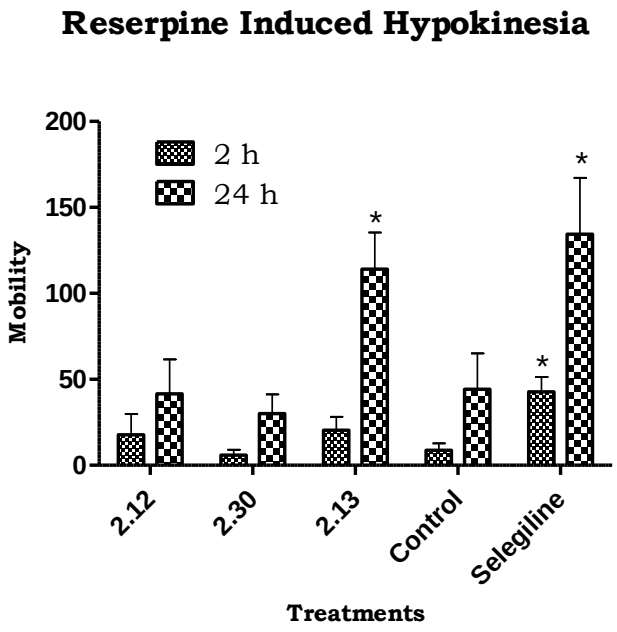

Figure 2.6 Locomotion measured 2 and 24 hours after administration of compounds (100 mg/Kg), control (vehicle) and selegiline (10 mg/Kg). All animals were administered with reserpine (3 mg/Kg). Statistical significance ($p<0.05$)

However, compound **2.13** (100 mg/Kg) and MAO-B inhibitor, selegiline (10 mg/Kg), reverted significantly the effects, allowing to the animals to recover the natural locomotion. In future experiments it will be determined whether or not these effects are dose dependent.

The capacity of **2.13** to counteract the hypokinesia in a similar manner to selegiline corroborates the MAO-B inhibitory effects observed in the previous *in vitro* assays.

σ1R Agonist radioligand displacement

The most potent AChE inhibitors in the series of chromone-NBP hybrids and chromone-DBMA derivative **2.8**, with dual AChE-BACE1inhibitory activity, were selected to evaluate their ability to displace [^{3}H]pentazocine from σ1R at a concentration of 10 μM.

Table 2.7 [^{3}H]pentazocine binding inhibition by newly synthesized compounds

Compound	% Inhibition of agonist radioligand binding to σ1R (10 μM)
2.8	39
2.26	95
2.27	88
2.30	83
2.35	83

Percent values obtained by CEREP Co. at a single dose of 10 μM[230]

High inhibition percentages (83-95%) (table 2.7) were obtained in the series of chromone-NBP hybrids. The nitro-derivative **2.26**, was the most potent displacing 95%, of agonist radioligand; while the chromone-DBMA derivative **2.8** displaced a moderated 39% of [^{3}H]pentazocine.

Determination of affinity constants and the agonist or antagonist character of each compound remain to be determined, in order to learn about their potential to exert neuroprotective effects trough σ1R modulation.

Conclusions

In this chapter we have synthesized and evaluated as multitarget compounds several hybrids based on the chromone scaffold combined with the NBP and DBMA fragments. We have obtained potent and selective inhibitors of AChE with IC_{50} values in the low nanomolar range. Although these new compounds reminds the structure and activity of donepezil, especially di-methoxy substituted compound **2.30**, they exhibit additional pharmacological properties such as neuroprotection, radical scavenging capacity, MAO inhibition.

Chromone-NBP derived compounds substituted with hydroxyl and amino groups, exhibited the better antioxidant properties, among them, **2.27** and **2.35**, demonstrated to be effective in three targets of interest in this work, AChE, anti-oxidation and affinity σ1R. In agreement with these results, and the fact that they were predicted to reach the CNS, we can argue that these new hybrids have the potential to become useful drugs in AD treatment. They could be able to restore the cholinergic homeostasis and therefore alleviate the cognitive symptoms in a manner similar to currently used cholinergic drugs including donepezil, but with the advantage of their radical scavenging properties and their potential activity as agonists of σ1R, which activation is essential for mitochondrial health and neuronal survival.

The chromone-NBP series yielded three moderated MAO inhibitors, **2.28**, **2.31** and the multitarget compound **2.26** with affinity for σ1R and the ability to inhibit potently AChE. Even though, IC_{50} values for MAO enzymes are in the low micromolar range, it is worth to mention that high potencies (*in vitro*) for MAO-A are not required to exert therapeutic antidepressant effects (*in vivo*). Some drugs such as moclobemide or iproniazide exhibit IC_{50} values in the low micromolar range but significant antidepressant effects in humans.

On the other hand, in the series of chromone-DBMA hybrids, **2.12** and **2.13**, which behave as MAO-A inhibitors with potencies comparable to the reference drugs, are at the same time, moderated inhibitors of AChE in the low micromolar range (IC_{50}=1.5 μM). Results in the rest of targets could be considered moderated, inhibiting 20% of BACE activity at 10 μM, 21% and 33% of Aβ and *tau* aggregation at 20 μM. In the case of **2.13**, their potent antioxidant properties (1.6 trolox equivalents) acting synergistically with its ability to inhibit MAO-B (IC_{50} = 9.7 μM) could be able to reduce oxidative stress, distinctive of neurodegenerative disorders such as AD and PD. These results are in agreement with those observed *in vivo* in the model of reserpine. They corroborate the MAO-B inhibitory activity and the ability to reach the CNS predicted in PAMPA.

These findings support the continuation of the investigation of these new hybrids with further *in vivo* experiments in order to determine the antidepressant effects which could give an additional value to their pharmacological profile.

Finally, we present in this work, **2.8**, a new dual hit with activity in AChE and BACE1; even though, this compound inhibits both enzymes with moderated potency (IC_{50} = 6.7 μM AChE, 4.5 μM BACE1). We can argue that these values are susceptible to be improved by structural modifications, similar to those made in chromone-NBP hybrids; the substituents in the chromone ring, the length of the chain linker and introduction of new substituents in the DBMA rings.

Experimental section

Chemical Synthesis

General procedure 2.1 Synthesis of 4-oxo-4*H*-chromene-2-carboxylic acids (2.1-2.5) A mixture of the corresponding phenol (24 mmol) dissolved in 50 mL of Et_2O with an equimolar quantity of dimethyl acetylenedicarboxylate and 29 mmol of Et_3N, was stirred overnight at room temperature. After completion of reaction, this mixture was washed with HCl (1N) (3 x 5 mL), water (3 x 5 mL) and brine (3 x 5 mL), dried over $MgSO_4$ and concentrated under reduced pressure to yield the corresponding mixture of isomers (*Z* and *E*) of dimethyl 2-(phenoxy)but-2-enedioates. To the flask containing the intermediate esters, 20 mL of NaOH 2M (40 mmol) were added and the mixture was refluxed during 30 min ; afterward, the reaction mixture was cooled into an ice bath and concentrated HCl was added dropwise until pH 1 to precipitate the corresponding dicarboxylic acid which was separated by filtration and washed with distilled water. Once the solid got dried, it was dissolved in 20 mL of acetyl chloride (290 mmol) and cooled to 0 °C. To this mixture, 4 mL of concentrated H_2SO_4 (77 mmol) were added carefully to subsequently reflux during 30 min. The crude was cooled again and water was added dropwise under gentle stirring to precipitate the desired product (**2.1-2.5**). The dried solid was partially dissolved in EtOAc and precipitated again with hexane, filtrated and washed again several times with hexane, obtaining the desired products pure enough to characterization and to be used in the next reactions.

General Procedure 2.2. Synthesis of chromone-NBP and chromone-DBMA hybrids 1.0 mmol of the corresponding 4-oxo-4*H*-chromene-2-carboxylic acid and 1.3 mmol of CDI were mixed into a 10 mL microwave vial under N_2 atmosphere. The vial was sealed and 5 mL of anhydrous DMF were added using a syringe to dissolve the mixture ($CO_2\uparrow$). This solution was heated into a mw reactor at 120 °C during 10 min to

complete the activation of the acid. Afterward, a solution of 1.2 mmol of the corresponding amine in 2 mL of DMF was added with a syringe; this final solution was heated during 10 min at 150 °C to obtain the desired amide. After completion of the reaction, the DMF was evaporated under reduced pressure; the crude was re-dissolved in 25 mL of EtOAc and washed five times with water, dried over $MgSO_4$ and concentrated. The crude was purified by column chromatography using EtOAc:MeOH (9:1) as eluent.

General Procedure 2.3. Synthesis of chromone-NBP and chromone-DBMA hybrids

Into a round bottom flask, 1.0 mmol of the corresponding acid were mixed with 10 mL of anhydrous DCM under N_2 atmosphere; to this mixture, 3 mmol of BOP were added to stir during 5 min; subsequently, 2.5 mmoL of triethylamine were added to dissolve utterly the reagents. The mixture was stirred again during 5 min and finally, 1.1 mmol of the amine was added to stir overnight at room temperature. The mixture of reaction was washed with HCl (0.5 M) (3 x 5 mL), saturated solution of $NaHCO_3$ (3 x 5 mL) and brine (3 x 5 mL), dried over $MgSO_4$, filtered and concentrated. The crude was purified by column chromatography using EtOAc/MeOH (9:1) as eluent.

General procedure 2.4 Deprotection of methoxy-substituted hybrids

To the corresponding methoxy-derivative (0.1 mmol) dissolved in 3 mL of anhydrous THF, was added slowly under magnetic stirring, 1 equivalent of BBr_3 per each heteroatom present in the molecule; air was displaced by N_2 and the mixture was allowed to react overnight at room temperature. Reaction was quenched with MeOH (dropwise until end of effervescence) and the solvent evaporated under reduced pressure to eliminate the remaining BBr_3, this process was repeated several times depending on the quantity of BBr_3 used, until no fumes were observed when adding MeOH. When necessary, purification was carried out by

column chromatography using a gradient of EtOAc/MeOH 0→10% as eluent.

5-methoxy-4-oxo-4H-chromene-2-carboxylic acid. (2.1)

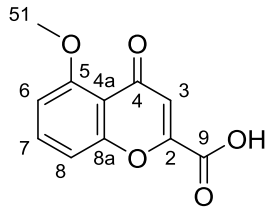

Acid **2.1** was obtained as a secondary product in the synthesis of **2.5**, as described in the general procedure 2.1. 3 g (24 mmol) of 3-methoxyphenol and 3.4 g (24 mmol) of dimethyl acetylenedicarboxylate, 0,5 g (10%). White amorphous solid. ^{1}H NMR (500 MHz, DMSO-d_6) δ 7.73 (t, J = 8.4 Hz, 1H, H_7), 7.18 (dd, J = 8.5, 0.9 Hz, 1H, H_6), 7.03 (dd, J = 8.5, 0.9 Hz, 1H, H_8), 6.70 (s, 1H, H_3), 3.86 (s, 3H, H_{51}).^{13}C NMR (126 MHz, DMSO-d_6) δ 176.69 (C_4), 161.51 (C_9), 159.21 (C_5), 157.37 (C_{8a}), 151.08 (C_2), 135.27 (C_7), 115.20 (C_3), 114.34 (C_{4a}), 110.13 (C_6), 107.60 (C_8), 56.25 (C_{61}). HPLC-MS (Water-ACN 15→95%, g.t. 5 min), retention time 2.82 min, m/z = 221.2 $[M + H]^+$, calcd for $[C_{11}H_8O_5 + H]^+$ 221.18

5,7-Dimethoxy-4-oxo-4*H*-chromene-2-carboxylic acid. (2.2)

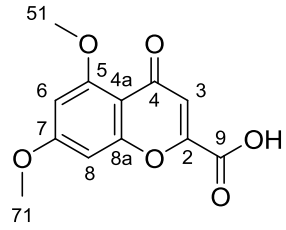

Compound **2.2** was obtained from 3 g of 3,5-dimethoxyphenol (19.5 mmol) and 2.76 (19.5 mmol) of dimethyl acetylenedicarboxylate, as described in the general procedure 2.1. Light brown solid, 5.3 g (75%). ^{1}H NMR (500 MHz, DMSO-d_6) δ 6.72 (d, J = 2.3 Hz, 1H, H_8), 6.64 (s, 1H, H_3), 6.54 (d, J = 2.3 Hz, 1H, H_6), 3.89 (s, 3H, H_{71}), 3.83 (s, 3H, H_{51}). ^{13}C NMR (126 MHz DMSO-d_6) δ 175.53 (C_4), 164.41 (C_7), 161.46 (C_9), 160.38 (C_5), 159.07 (C_{8a}), 150.71 (C_2), 115.33 (C_3), 109.08 (C_{4a}), 96.72 (C_6), 93.37 (C_8), 56.21 (C_{51}), 56.15 (C_{71}). HPLC-MS (Water-ACN 15→95%, g.t. 5 min), retention time 3.17 min, m/z =251.2 $[M + H]^+$, calcd for $[C_{12}H_{10}O_6 + H]^+$ 251.2

6-Methoxy-4-oxo-4*H*-chromene-2-carboxylic acid. (2.3)

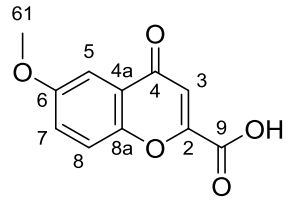

According to the general procedure 2.1, compound **2.3** was synthesized from 3 g (24 mmol) of 4-methoxyphenol and 3.4 g (24 mmol) of dimethyl acetylenedicarboxylate. Light yellow amorphous solid, 5.01 g (78%). ^{1}H NMR (300 MHz, DMSO-d_6) δ 7.70 (d, J = 9.1 Hz, 1H, H_8), 7.46 (dd, J = 9.1, 3.1 Hz, 1H, H_7), 7.40 (d, J = 3.1 Hz, 1H, H_5), 6.88 (s, 1H, H_3), 3.87 (s, 3H, H_{61}). ^{13}C NMR (75 MHz, DMSO-d_6) δ 177.27 (C_4), 161.47 (C_9), 156.99 (C_6), 152.96 (C_2), 150.18 (C_{8a}), 124.55 (C_{4a}), 124.42 (C_7), 120.56 (C_8), 112.56 (C_3), 104.53 (C_5), 55.82 (C_{61}). HPLC-MS (Water-ACN 15→95%, g.t. 5 min), retention time 3.62 min, m/z = 221.2 $[M + H]^+$, calcd for $[C_{11}H_8O_5 + H]^+$ 221.2

5,7-Dimethoxy-4-oxo-4*H*-chromene-2-carboxylic acid. (2.4)

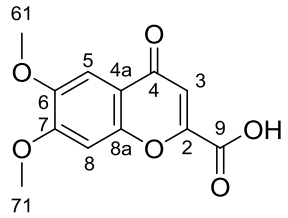

2.4 was obtained from 3 g (19.5 mmol) of 3,4-dimethoxyphenol and 2.76 (19.5 mmol) of dimethyl acetylenedicarboxylate, as described in the general procedure. Brown amorphous solid, 4.9 g (69%). ^{1}H NMR (300 MHz, DMSO-d_6) δ 7.33 (s, 1H, H_5), 7.23 (s, 1H, H_8), 6.72 (s, 1H, H_3), 3.92 (s, 3H, H_{71}), 3.86 (s, 3H, H_{61}). ^{13}C NMR (75 MHz, DMSO-d_6) δ 176.96 (C_4), 161.79 (C_9), 157.35 (C_2), 154.70 (C_7), 151.72 (C_{8a}), 147.57 (C_6), 117.07 (C_{4a}), 111.22 (C_3), 103.44 (C_5), 100.81 (C_8), 56.43 (C_{61}), 55.79 (C_{71}). HPLC-MS (Water-ACN 15→95%, g.t. 5 min), retention time 3.13 min, m/z =251.2 $[M + H]^+$, calcd for $[C_{12}H_{10}O_6 + H]^+$ 251.2

7-methoxy-4-oxo-4H-chromene-2-carboxylic acid. (2.5)

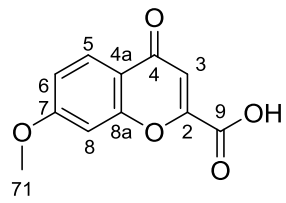

2.5 was obtained from 3 g (24 mmol) of 3-methoxyphenol and 3.4 g (24 mmol) of dimethyl acetylenedicarboxylate. White amorphous solid, 4.25 g (80%). ^{1}H NMR (500 MHz, DMSO-d_6) δ 7.91 (d, J = 8.9 Hz, 1H, H_5), 7.16 (d, J = 2.4 Hz, 1H, H_8), 7.06 (dd, J = 8.9, 2.4 Hz, 1H, H_6), 6.82 (s, 1H, H_3), 3.90 (s, 3H, H_{71}). ^{13}C NMR (126 MHz, DMSO-d_6) δ 176.62 (C_4), 164.52 (C_7), 161.45 (C_9), 157.40 (C_{8a}), 152.87 (C_2), 126.33 (C_5), 117.63 (C_{4a}), 115.54 (C_6), 113.70 (C_3), 100.96 (C_8), 56.27 (C_{71}). HPLC-MS (Water-ACN 15→95%, g.t. 5 min), retention time 4.26 min, m/z = 221.2 $[M + H]^+$, calcd for $[C_{11}H_8O_5 + H]^+$ 221.18.

6-Nitro-4-oxo-4*H*-chromene-2-carboxylic acid. (2.6)

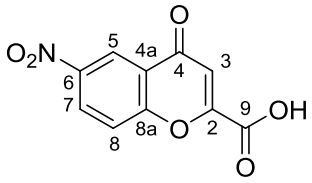

Over an ice bath, 1 g (5.26 mmol) of 4-oxo-4*H*-chromene-2-carboxylic acid was dissolved in 1.5 mL of HNO_3 (34.2 mmol), to this solution 10 mL of concentrated H_2SO_4 (190 mmol) were carefully added; the reaction mixture was first heated until 75 °C during 3 hours and then cooled over an ice bath to add water dropwise to precipitate **2.6** as a white amorphous solid, 1.1 g (90%). mp: 273 - 275 °C. ^{1}H NMR (300 MHz, DMSO-d_6) δ 8.71 (d, J = 2.8 Hz, 1H, H_5), 8.61 (dd, J = 9.2, 2.8 Hz, 1H, H_7), 8.00 (d, J = 9.2 Hz, 1H, H_8), 7.02 (s, 1H, H_3). ^{13}C NMR (75 MHz, DMSO-d_6) δ 176.88 (C_4), 160.96 (C_9), 158.47 (C_6), 153.99 (C_2), 144.65 (C_{8a}), 129.16 (C_7), 123.73 (C_{4a}), 121.23 (C_8), 120.93 (C_5), 113.72 (C_3). HPLC-MS (Water-ACN 15→95%, g.t. 10 min), retention time 5.75 min, m/z =236.1 $[M + H]^+$, calcd for $[C_{10}H_5NO_6 + H]^+$ 236.1

2-(1-Benzylpiperidin-4-yl)ethan-1-ol. (2.7)

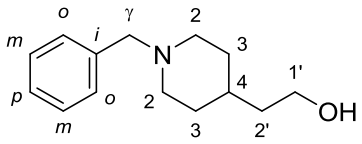

4-Piperidineethanol (0.3 g, 2.32 mmol) and benzyl bromide (276 µL, 1 eq), were dissolved in 20 mL of acetonitrile. Then, anhydrous K_2CO_3 (320.65 mg, 1 eq) and tetrabutylammonium iodide (TBAI, 8.6 mg, 0.01 eq) were added. The reaction mixture was refluxed for 24 h. The inorganic salt was filtered and washed with MeOH, the filtrate was evaporated and purified by column chromatography using a mixture of DCM: MeOH. ^{1}H NMR (300 MHz, ^{1}H NMR (300 MHz, $CDCl_3$) δ 7.51 – 7.15 (m, 5H, Ph), 3.80 – 3.57 (m, 4H, $H_{\alpha\ \beta}$), 3.51 (s, 1H, H_γ), 2.90 (d, J = 11.6 Hz, 2H, H_{2eq}), 1.99 (dt, J = 12.4, 6.2 Hz, 2H, H_{2ax}), 1.73 – 1.58 (m, 2H, H_{3eq}), 1.52 (q, J = 6.2 Hz, 1H, H_4), 1.31 (qd, J = 11.1, 10.2, 3.6 Hz, 1H, H_{3ax}). ^{13}C NMR (75 MHz, $CDCl_3$) δ 138.05 (C_i), 129.50 (C_o), 128.31 (C_m), 127.19 (C_p), 70.70 (C_α), 63.51 (C_γ), 60.66 (C_β), 53.86 (C_2), 32.36 (C_4), 32.26 (C_3).

***N*-(3-((Benzyl(methyl)amino)methyl)phenyl)-6,7-dimethoxy-4-oxo-4*H*-chromene-2-carboxamide. (2.8)**

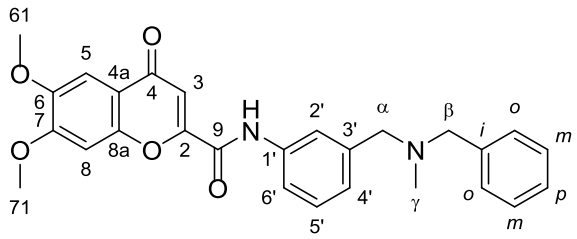

(2.8) was obtained as described in the general procedure 2.2, from 0.12 g (0.48 mmol) of **(2.4)** and 0.13 g (0.58 mmol) of **1.7.** Light brown amorphous solid, 0.2 g (90%), mp: 105 -108 °C. ^{1}H NMR (400 MHz, MeOD) δ 7.79 (bs, 1H, $H_{2'}$), 7.71 (dd, J = 8.2, 1.6 Hz, 1H, $H_{6'}$), 7.46 (s, 1H, H_5), 7.39 – 7.31 (m, 6H, $H_{o,\ m,\ p,\ 8}$), 7.29 – 7.21 (m, 1H, $H_{5'}$), 7.20 (dt, J = 8.2, 1.5 Hz, 1H, $H_{4'}$), 7.03 (s, 1H, H_3), 4.01 (s, 3H, H_{61}), 3.92 (s, 3H, H_{71}), 3.55 (bs, 4H, $H_{\alpha,\ \beta}$), 2.19 (s, 3H, H_γ). ^{13}C NMR (101 MHz, MeOD) δ 179.43 (C_4), 159.40 (C_9), 157.41 (C_6), 156.94 (C_2), 153.48 (C_{8a}), 150.11

(C_7), 140.93 (C_i), 139.68 ($C_{3'}$), 138.69 ($C_{1'}$), 130.40 (C_o), 129.89 (C_p), 129.34 (C_m), 128.29 ($C_{5'}$), 127.37 ($C_{4'}$), 123.17 ($C_{2'}$), 121.27 ($C_{6'}$), 118.50 (C_{4a}), 111.78 (C_3), 104.68 (C_5), 101.45 (C_8), 62.79 (C_α), 62.57 (C_β), 57.10 (C_{61}), 56.67 (C_{71}), 42.42 (C_γ). HRMS [ESI+] *m/z* =458.1840 $[M]^+$, calcd for $[C_{27}H_{26}N_2O_5]^+$ 458.1841. HPLC purity 100%

_N_-(4-((Benzyl(methyl)amino)methyl)phenyl)-5,7-dimethoxy-4-oxo-4_H_-chromene-2-carboxamide. (2.9)

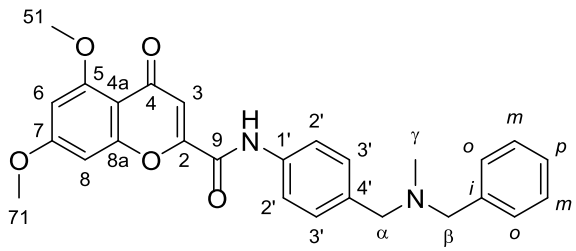

According to the general procedure, **2.9** was obtained from 0.2 g (0.8 mmol) of **2.2** and 0.22 g (0.96 mmol) of **1.8** White amorphous solid (70%), mp: 99.3-101.2 ºC. ^{1}H NMR (300 MHz, $CDCl_3$) δ 8.81 (s, 1H, NH), 7.88 (d, *J* = 8.4 Hz, 2H, $H_{2'}$), 7.60 (d, *J* = 8.4 Hz, 2H, $H_{3'}$), 7.56 – 7.41 (m, 5H, Ph), 7.26 (s, 1H, H_3), 6.75 (d, *J* = 2.3 Hz, 1H, H_6), 6.58 (d, *J* = 2.3 Hz, 1H, H_8), 4.11 (s, 3H, H_{71}), 4.09 (s, 3H, H_{51}), 3.73 (s, 2H, H_β), 3.72 (s, 2H, H_α), 2.39 (s, 3H, H_γ). ^{13}C NMR (75 MHz, $CDCl_3$) δ 176.96 (C_4), 164.84 (C_7), 161.28 (C_5), 159.02 (C_{8a}), 157.16 (C_9), 152.57 (C_2), 139.22 (C_i), 136.85 ($C_{1'}$), 135.48 ($C_{4'}$), 129.81 ($C_{3'}$), 129.05 (C_o), 128.38 (C_m), 127.13 (C_p), 120.47 ($C_{2'}$), 114.39 (C_3), 109.85 (C_{4a}), 96.86 (C_6), 93.03 (C_8), 61.94 (C_β), 61.37 (C_α), 56.55 (C_{51}), 56.05 (C_{71}), 42.34 (C_γ). HRMS [ESI+] *m/z* =458.1863 $[M]^+$, calcd for $[C_{27}H_{26}N_2O_5]^+$ 458.1842. HPLC purity 99%

***N*-(4-((Benzyl(methyl)amino)methyl)phenyl)-5,7-dihydroxy-4-oxo-4*H*-chromene-2-carboxamide. 2.10**

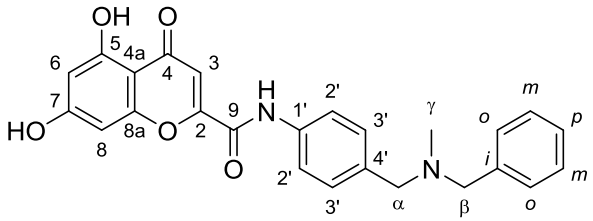

2.10 was obtained as described in the above C, from 0.1 g (0.25 mmol) of **2.9** and 0.3 g (1.2 mmol) BBr_3. Bright yellow solid, 0.84 g (90%), mp: 199 - 233 °C. ^{1}H NMR (500 MHz, MeOD) δ 7.75 (d, *J* = 8.5 Hz, 2H, $H_{2'}$), 7.41 (d, *J* = 8.5 Hz, 2H, $H_{3'}$), 7.39 – 7.33 (m, 4H, $H_{o, m}$), 7.30 – 7.26 (m, 1H, H_p), 6.94 (s, 1H, H_3), 6.63 (d, *J* = 2.1 Hz, 1H, H_8), 6.28 (d, *J* = 2.1 Hz, 1H, H_6), 3.59 (s, 4H, $H_{\alpha, \beta}$), 2.22 (s, 3H, H_γ). ^{13}C NMR (126 MHz, MeOD) δ 183.60 (C_4), 167.44 (C_7), 163.42 (C_5), 159.15 (C_9), 159.00 (C_{8a}), 157.45 (C_2), 139.22 (C_i), 137.77 ($C_{1'}$), 136.59 ($C_{4'}$), 130.98 ($C_{3'}$), 130.48 (C_o), 129.40 (C_m), 128.46 (C_p), 122.50 ($C_{2'}$), 111.22 (C_3), 106.32 (C_{4a}), 100.92 (C_6), 95.94 (C_8), 62.60 (C_α), 62.07 (C_β), 42.22 (C_γ). HRMS [ESI+] *m/z* =430.1517 $[M]^+$, calcd for $[C_{25}H_{22}N_2O_5]^+$ 430.1529. HPLC purity 100%

***N*-(4-((Benzyl(methyl)amino)methyl)phenyl)-6,7-dimethoxy-4-oxo-4*H*-chromene-2-carboxamide. 2.11**

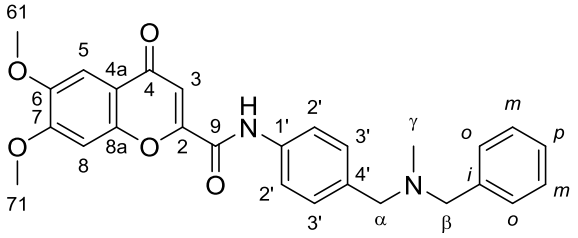

2.11 was obtained as described in the general procedure 2.2, from 0.2 g (0.80 mmol) of **2.4** and 0.18 g (0.88 mmol) of **1.8**. White amorphous solid, 0.29 g (80%), mp: 119.5-120.3 °C. ^{1}H NMR (300 MHz, MeOD) δ 7.89 (d, *J* = 8.6 Hz, 2H, $H_{2'}$), 7.53 – 7.35 (m, 9H, Ph, $H_{3', 5, 8}$), 7.06 (s, 1H, H_3), 4.04 (s, 3H, H_{61}), 3.98 (bs, 4H, $H_{\alpha, \beta}$), 3.95 (s, 3H, H_{71}), 2.49 (s, 3H, H_γ). ^{13}C NMR (75 MHz, MeOD) δ 179.39 (C_4), 159.50 (C_9), 157.48 (C_6), 156.76 (C_2), 153.49 (C_{8a}), 150.17 (C_7), 139.17 ($C_{1'}$), 136.52 ($C_{4'}$), 134.41 (C_i), 131.99 ($C_{3'}$),

131.33 (C_o), 129.93 (C_m), 129.84 (C_p), 122.53 ($C_{2'}$), 118.53 (C_{4a}), 111.87 (C_3), 104.71 (C_5), 101.48 (C_8), 61.77 (C_α), 61.30 (C_β), 57.14 (C_{61}), 56.69 (C_{71}), 40.87 (C_γ). HRMS [ESI+] *m/z* =458.1848 $[M]^+$, calcd for $[C_{27}H_{26}N_2O_5]^+$ 450.1842. HPLC purity 100%

_N_-(4-((Benzyl(methyl)amino)methyl)phenyl)-6-methoxy-4-oxo-4_H_-chromene-2-carboxamide. (2.12)

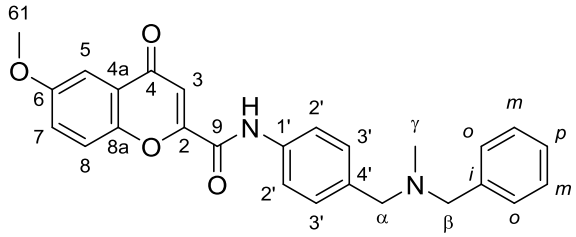

According to the general procedure 2.2, **2.12** was obtained from 0.2 g (0.91 mmol) of **2.3** and 0.27 g (1.18 mmol) of **1.8.** White amorphous solid, 0.3 g (77%), mp: 145.7-146.7 °C. ^{1}H NMR (300 MHz, $CDCl_3$) δ 8.55 (s, 1H, NH), 7.67 (d, *J* = 8.5 Hz, 2H, $H_{2'}$), 7.59 (d, *J* = 3.1 Hz, 1H, H_5), 7.54 (d, *J* = 9.1 Hz, 1H, H_7), 7.42 (d, *J* = 8.5 Hz, 2H, $H_{3'}$), 7.39 – 7.29 (m, 5H, $H_{8,\ o,\ m}$), 7.28 – 7.23 (m, 2H, $H_{3,\ p}$), 3.91 (s, 3H, H_{61}), 3.54 (s, 2H, H_β), 3.53 (s, 2H, H_α), 2.20 (s, 3H, H_γ).^{13}C NMR (75 MHz, $CDCl_3$) δ 178.02 (C_4), 157.78 (C_6), 157.06 (C_9), 154.52 (C_2), 150.02 (C_{8a}), 139.28 (C_i), 137.14 ($C_{1'}$), 135.26 ($C_{4'}$), 129.86 ($C_{3'}$), 129.05 (C_m), 128.39 (C_p), 127.13 (C_o), 125.24 (C_{4a}), 124.90 (C_8), 120.47 ($C_{2'}$), 119.60 (C_7), 111.84 (C_3), 105.34 (C_5), 61.99 (C_β), 61.37 (C_α), 56.16 (C_{61}), 42.37 (C_γ). HRMS [ESI+] *m/z* =428.1754 $[M]^+$, calcd for $[C_{26}H_{24}N_2O_4]^+$ 428.1736. HPLC purity 99%

***N*-(4-((Benzyl(methyl)amino)methyl)phenyl)-6-hydroxy-4-oxo-4*H*-chromene-2-carboxamide. 2.13**

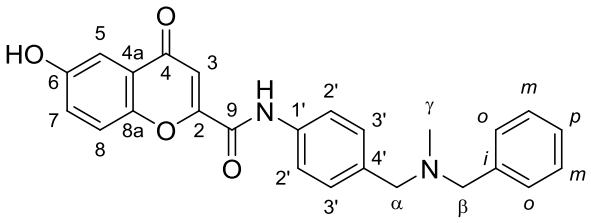

2.13 was obtained as described in the general procedure C, from 0.05 g (0.1 mmol) of **2.12** and 0.3 g (1.2 mmol) BBr_3. Yellow solid, 0.043 g (90%), mp: 186 -189 °C. ^{1}H NMR (500 MHz, MeOD) δ 7.77 (d, *J* = 8.6 Hz, 2H, $H_{2'}$), 7.73 (d, *J* = 9.1 Hz, 1H, H_8), 7.45 (d, *J* = 2.9 Hz, 1H, H_5), 7.41 (d, *J* = 8.6 Hz, 2H, $H_{3'}$), 7.38 – 7.31 (m, 5H, $H_{7,\ o,\ m}$), 7.29 – 7.25 (m, 1H, H_p), 7.05 (s, 1H, H_3), 3.56 (s, 4H, $H_{\alpha,\ \beta}$), 2.20 (s, 3H, H_γ).^{13}C NMR (126 MHz, MeOD) δ 180.41 (C_4), 159.57 (C_9), 157.38 (C_2), 157.29 (C_{8a}), 151.03 (C_6), 139.51 (C_i), 137.75 ($C_{1'}$), 136.84 ($C_{4'}$), 130.92 (C_o), 130.42 ($C_{3'}$), 129.36 (C_m), 128.36 (C_p), 126.09 (C_{4a}), 125.57 (C_7), 122.39 ($C_{2'}$), 121.32 (C_8), 111.16 (C_3), 108.72 (C_5), 62.65 (C_β), 62.13 (C_α), 42.30 (C_γ).HRMS [ESI+] *m/z* =414.1583 $[M]^+$, calcd for $[C_{25}H_{22}N_2O_4]^+$ 414.1580. HPLC purity 100%

***N*-(1-Benzylpiperidin-4-yl)-6-methoxy-4-oxo-4H-chromene-2-carboxamide. 2.14**

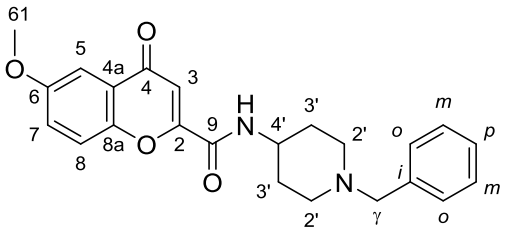

2.14 was obtained as described in the general procedure method A, from 0.20 g (0.91 mmol) of **2.3** and 0.19 g (1 mmol) of 1-benzylpiperidin-4-amine**.** White amorphous solid, 0.25 g (70%), mp: 196 -199 °C. ^{1}H NMR (300 MHz, MeOD) δ 7.72 (d, *J* = 9.2 Hz, 1H, H_8), 7.53 (d, *J* = 3.1 Hz, 1H, H_5), 7.46 (dd, *J* = 9.2, 3.1 Hz, 1H, H_7), 7.38 – 7.28 (m, 5H, Ph), 6.96 (s, 1H, H_3), 3.92 (s, 4H, $H_{4',\ 61'}$), 3.58 (s, 2H, H_γ), 2.99 (d, *J* = 11.9 Hz, 2H, $H_{2'eq}$), 2.20

(td, J = 11.9, 2.5 Hz, 2H, $H_{2'ax}$), 2.03 – 1.88 (m, 2H, $H_{3'eq}$), 1.78 (tt, J = 13.3, 6.6 Hz, 2H, $H_{3'ax}$). ^{13}C NMR (75 MHz, MeOD) δ 180.23 (C_4), 160.81 (C_9), 159.21 (C_6), 157.30 (C_2), 151.86 (C_{8a}), 138.52 (C_i), 130.73 (C_o), 129.33 (C_m), 128.47 (C_p), 125.88 (C_7), 125.83 (C_{4a}), 121.37 (C_8), 111.08 (C_3), 105.68 (C_5), 63.93 (C_γ), 56.42 (C_{61}), 53.53 ($C_{2'}$), 49.17 ($C_{4'}$) 32.04 ($C_{3'}$). HRMS [ESI+] m/z =392.1742 $[M]^+$, calcd for $[C_{23}H_{24}N_2O_4]^+$ 392.1736. HPLC purity 100%

_N_-(1-Benzylpiperidin-4-yl)-6-hydroxy-4-oxo-4_H_-chromene-2-carboxamide. 2.15

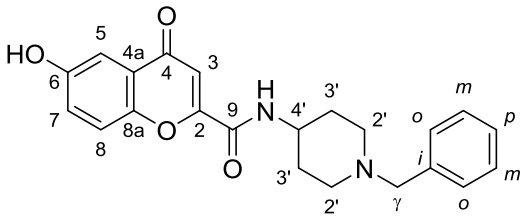

2.15 was obtained as described in the general procedure from 0.05 g (0.013 mmol) of 2.14 and 0.1 mmol of BBr_3. white amorphous solid, 0.013 g (70%), mp: 302 - 304 °C. ^{1}H NMR (500 MHz, MeOD) δ 7.65 (d, J = 9.1 Hz, 1H, H_8), 7.56 – 7.51 (m, 5H, Ph), 7.43 (d, J = 3.0 Hz, 1H, H_5), 7.34 (dd, J = 9.1, 3.0 Hz, 1H, H_7), 6.94 (s, 1H, H_3), 4.35 (s, 2H, H_γ), 4.25 – 4.15 (m, 1H, $H_{4'}$), 3.66 – 3.50 (m, 2H, $H_{2'eq}$), 3.25 – 3.13 (m, 2H, $H_{2'ax}$), 2.29 – 2.17 (m, 2H, $H_{3'eq}$), 2.09 – 1.96 (m, 2H, $H_{3'ax}$). ^{13}C NMR (126 MHz, MeOD) δ 180.33 (C_4), 161.28 (C_9), 157.26 (C_{8a}), 156.84 (C_2), 150.97 (C_6), 132.35 (C_o), 131.33 (C_p), 130.44 (C_m), 130.44 (C_i) 126.06 (C_{4a}), 125.59 (C_7), 121.13 (C_8), 110.96 (C_3), 108.72 (C_5), 61.88 (C_γ), 52.86 ($C_{2'}$), 29.75 ($C_{3'}$). HRMS [ESI+] m/z =378.15814 $[M]^+$, calcd for $[C_{22}H_{22}N_2O_4]^+$ 378.1579. HPLC purity 97%

***N*-(1-Benzylpiperidin-4-yl)-6,7-dimethoxy-4-oxo-4*H*-chromene-2-carboxamide. 2.16**

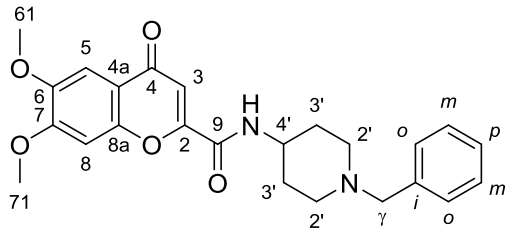

2.16 was obtained as described in the general procedure 2.3, from 0.05 g (0.2 mmol) of **2.4** and 0.42 g (0.22 mmol) of 1-benzylpiperidin-4-amine. White solid, 0.04 g (54%), mp: 183-185 °C. ^{1}H NMR (300 MHz, MeOD) δ 7.45 (s, 1H, H_8), 7.42 – 7.29 (m, 5H, Ph), 7.26 (s, 1H, H_5), 6.93 (s, 1H, H_3), 4.01 (s, 3H, H_{71}), 3.98 – 3.83 (m, 4H, $H_{4', 61}$), 3.65 (s, 2H, H_γ), 3.05 (d, *J* = 11.9 Hz, 2H, $H_{2'eq}$), 2.36 – 2.21 (m, 2H, $H_{2'ax}$), 2.06 – 1.93 (m, 2H, $H_{3'eq}$), 1.90 – 1.70 (m, 2H $H_{3'ax}$). ^{13}C NMR (75 MHz, MeOD) δ 179.42 (C_4), 160.78 (C_9), 157.36 (C_7), 156.75 (C_2), 153.43 (C_{8a}), 150.02 (C_6), 137.96 (C_i), 130.85 (C_o), 129.41 (C_m), 128.67 (C_p), 118.40 (C_{4a}), 111.38 ($C_{4'}$), 104.68 (C_8), 101.31 (C_5), 63.76 (C_γ), 57.07 (C_{71}), 56.66 (C_{61}), 53.44 ($C_{2'}$), 31.89 ($C_{3'}$). HRMS [ESI+] *m/z* =422.1850 $[M]^+$, calcd for $[C_{24}H_{26}N_2O_5]^+$ 422.1842. HPLC purity 97%

***N*-((1-Benzylpiperidin-4-yl)methyl)-6-methoxy-4-oxo-4*H*-chromene-2-carboxamide. 2.17**

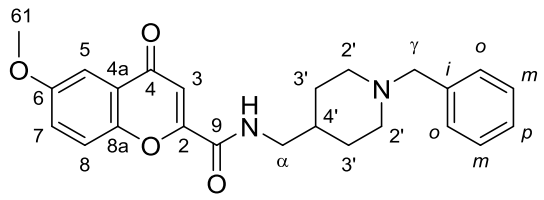

2.17 was obtained as described in the general procedure 2.2, from 0.05 g (0.23 mmol) of **2.3** and 0.051 g (0.25 mmol) of **1.2**. White amorphous solid, 0.055 g (60%). mp: 116.1-118.3 ºC. ^{1}H NMR (500 MHz, $CDCl_3$) δ 7.55 (d, *J* = 3.1 Hz, 1H, H_5), 7.42 (d, *J* = 9.1 Hz, 1H, H_8), 7.31 – 7.20 (m, 6H, Ph, H_7), 7.12 (s, 1H, H_3), 6.90 (t, *J* = 6.2 Hz, 1H, NH), 3.88 (s, 3H, H_{61}), 3.48 (s, 2H, H_γ), 3.37 (t, *J* = 6.2 Hz, 2H, H_α), 2.90 (d, *J* = 11.4 Hz, 2H, $H_{2'eq}$), 1.96 (dt, *J* = 11.4, 6.1 Hz, 2H, $H_{2'ax}$), 1.71 (d, *J* = 12.7 Hz, 2H, $H_{3'eq}$), 1.67 – 1.50 (m, 1H, $H_{4'}$),

1.45 – 1.26 (m, 2H, $H_{3'ax}$). ^{13}C NMR (126 MHz, $CDCl_3$) δ 178.14 (C_4), 159.58 (C_9), 157.65 (C_6), 154.59 (C_2), 150.08 (C_{8a}), 138.42 (C_i), 129.33 (C_o), 128.34 (C_m), 127.17 (C_p), 125.23 (C_{4a}), 124.77 (C_7), 119.56 (C_8), 111.46 (C_3), 105.28 (C_5), 63.45 (C_γ), 56.16 (C_{61}), 53.36 ($C_{3'}$), 45.56 (C_α), 36.17 ($C_{4'}$), 30.12 ($C_{2'}$). HRMS [ESI+] *m/z* =406.1908 $[M]^+$, calcd for $[C_{24}H_{26}N_2O_4]^+$ 406.1893. HPLC purity 98%

_N_-((1-Benzylpiperidin-4-yl)methyl)-6,7-dimethoxy-4-oxo-4_H_-chromene-2-carboxamide. 2.18

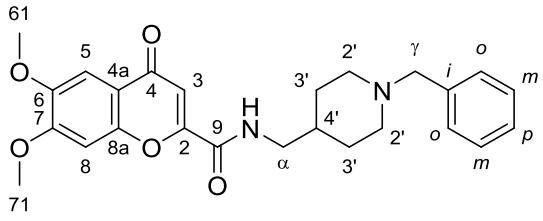

2.18 was obtained as described in the general procedure 2.3, from 0.20 g (0.80 mmol) of **2.4** and 0.18 g (0.88 mmol) of **1.2**. White amorphous solid, 0.17 g (50%), mp: 172 - 174 °C. ^1H NMR (500 MHz, MeOD) δ 7.44 (s, 1H, H_5), 7.35 – 7.24 (m, 5H, Ph), 7.20 (s, 1H, H_8), 6.92 (s, 1H, H_3), 3.99 (s, 3H, H_{71}), 3.92 (s, 3H, H_{61}), 3.56 (s, 2H, H_γ), 3.33 (bs, 2H, H_α), 2.97 (dt, *J* = 12.0, 3.2 Hz, 2H, $H_{2'eq}$), 2.08 (td, *J* = 12.0, 2.5 Hz, 2H, $H_{2'ax}$), 1.84 – 1.76 (m, 2H, $H_{3'eq}$), 1.72 (tq, *J* = 7.6, 3.7 Hz, 1H, $H_{4'}$), 1.43 – 1.32 (m, 2H, $H_{3'ax}$). ^{13}C NMR (126 MHz, MeOD) δ 179.44 (C_4), 161.50 (C_9), 157.37 (C_7), 156.74 (C_2), 153.41 (C_{8a}), 150.03 (C_6), 137.97 (C_i), 130.92 (C_o), 129.32 (C_m), 128.55 (C_p), 118.37 (C_{4a}), 111.34 (C_3), 104.68 (C_5), 101.22 (C_8), 64.17 (C_γ), 57.06 (C_{71}), 56.66 (C_{61}), 54.25 ($C_{2'}$), 46.23 (C_α), 37.06 ($C_{4'}$), 30.50 ($C_{3'}$). HPLC-MS (Water-ACN 2→95%, g.t. 10 min), retention time 6.27 min, *m/z* =437.2 $[M + H]^+$, calcd for $[C_{25}H_{28}N_2O_5 + H]^+$ 437.2. HPLC purity 100%.

(1-Benzylpiperidin-4-yl)methyl 6,7-dimethoxy-4-oxo-4*H*-chromene-2-carboxylate. 2.19

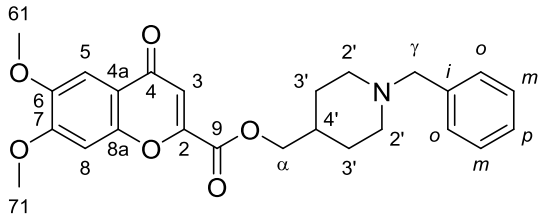

2.19 was synthesized as described in the general procedure 2.3, from 0.05 g (0.20 mmol) of **2.4** and 0.05 g (0.24 mmol) (1-benzylpiperidin-4-yl)methanol. White solid, 0.035 g (40%), mp: 138 -140 °C. ^{1}H NMR (500 MHz, $CDCl_3$) δ 7.65 – 7.60 (m, 2H, H_o), 7.48 (s, 1H, H_8), 7.48 – 7.42 (m, 3H, $H_{m,\,p}$), 7.33 (s, 1H, H_5), 7.06 (s, 1H, H_3), 4.30 (d, J = 5.4 Hz, 2H, H_α), 4.18 (s, 2H, H_γ), 4.06 (s, 3H, H_{71}), 3.97 (s, 3H, H_{61}), 3.59 – 3.53 (m, 2H, $H_{2'eq}$), 2.75 – 2.63 (m, 2H, $H_{2'ax}$), 2.49 – 2.34 (m, 2H, H $H_{3'eq}$), 2.04 – 1.97 (m, 1H, $H_{4'}$), 1.97 – 1.91 (m, 2H, $H_{3'ax}$). ^{13}C NMR (126 MHz, $CDCl_3$) δ 177.34 (C_4), 160.64 (C_9), 155.79 (C_7), 152.57 (C_{8a}), 151.13 (C_2), 148.55 (C_6), 131.63 (C_o), 130.46 (C_p), 129.55 (C_m), 127.91 (C_i), 118.21 (C_{4a}), 114.71 (C_3), 103.93 (C_8), 101.00 (C_5), 69.04 (C_α), 61.23 (C_γ), 57.31 (C_{71}), 56.53 (C_{61}), 51.97 ($C_{2'}$), 33.78 ($C_{4'}$), 25.69 ($C_{3'}$). HRMS [ESI+] *m/z* =437.1859 $[M]^+$, calcd for $[C_{25}H_{27}NO_6]^+$ 437.1838. HPLC purity 97%

(1-Benzylpiperidin-4-yl)methyl 6-methoxy-4-oxo-4*H*-chromene-2-carboxylate. 2.20

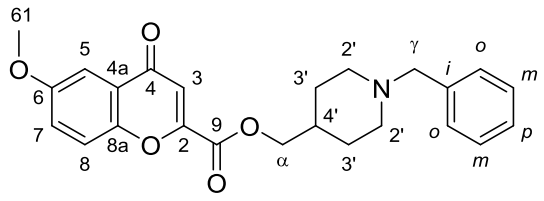

2.20 was obtained as described in the general procedure 2.2, from 0.05 g (0.23 mmol) of **2.3** and 0.055 g (0.27 mmol) (1-benzylpiperidin-4-yl)methanol. White amorphous solid, 0.11 g (12%), mp: 185 -188 °C. ^{1}H NMR (500 MHz, $CDCl_3$) δ 7.64 – 7.60 (m, 3H, $H_{o,\,8}$), 7.52 (d, J = 3.2 Hz, 1H, H_5), 7.47 – 7.44 (m, 3H, $H_{m,\,p}$), 7.34 (dd, J = 9.2, 3.2 Hz, 1H, H_7), 7.05 (s, 1H, H_3),

4.30 (d, J = 6.3 Hz, 2H, H_{α}), 4.17 (s, 2H, H_{γ}), 3.89 (s, 3H, H_{61}),3.54 (d, J = 12.1 Hz, 2H, $H_{2'eq}$), 2.70 – 2.61 (m, 2H, $H_{2'ax}$), 2.38 – 2.24 (m, 2H, $H_{3'eq}$), 2.08 – 1.87 (m, 3H, $H_{3'ax,\ 4'}$). ^{13}C NMR (126 MHz, $CDCl_3$) δ 178.26 (C_4), 160.46 (C_9), 157.74 (C_6), 151.49 (C_2), 150.97 (C_{8a}), 131.64 (C_o), 130.43 (C_p), 129.53 (C_m), 127.93 (C_i), 125.32 (C_7), 120.59 (C_8), 120.40 (C_{4a}), 114.17 (C_3), 104.66 (C_5), 69.30 (C_{α}), 61.23 (C_{γ}), 56.12 (C_{61}), 51.85 ($C_{2'}$), 33.85 ($C_{4'}$), 25.76 ($C_{3'}$). HRMS [ESI+] m/z =407.1741 $[M]^+$, calcd for $[C_{24}H_{25}NO_5]^+$ 407.1733. HPLC purity 98%

2-(1-Benzylpiperidin-4-yl)ethyl 6,7-dimethoxy-4-oxo-4*H*-chromene-2-carboxylate. 2.21

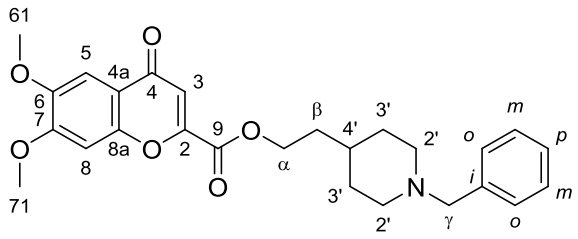

2.21 was obtained as described in the general procedure 2.3, from 0.2 g (0.80 mmol) of **2.4** and 0.191 g (0.88 mmol) of 2-(1-benzylpiperidin-4-yl)ethan-1-amine**.** White amorphous solid, 0.29 g (80%), mp: 129 -130 °C. ^{1}H NMR (500 MHz, $CDCl_3$) δ 7.51 (s, 1H, H_8), 7.39 – 7.24 (m, 5H, Ph), 7.06 (s, 1H, H_3), 7.03 (s, 1H, H_5), 4.43 (t, J = 6.6 Hz, 2H, H_{α}), 3.99 (s, 3H, H_{71}), 3.98 (s, 3H, H_{61}), 3.60 (s, 2H, H_{γ}), 2.99 (s, 2H, $H_{2'eq}$), 2.15 – 1.99 (m, 2H, $H_{2'ax}$), 1.82 – 1.67 (m, 4H, $H_{3'eq,\ \beta}$), 1.53 – 1.24 (m, 3H, $H_{3'ax,\ 4'}$). ^{13}C NMR (126 MHz, $CDCl_3$) δ 177.49 (C_4), 160.77 (C_9), 155.52 (C_7), 152.42 (C_{8a}), 151.46 (C_2), 148.48 (C_6), 129.70 (C_o), 129.14 (C_i), 128.51 (C_m), 126.20 (C_p), 118.31 (C_{4a}), 114.61 (C_3), 104.19 (C_8), 100.33 (C_5), 64.83 (C_{α}), 63.15 (C_{γ}), 56.80 (C_{71}), 56.57 (C_{61}), 53.50 ($C_{2'}$), 35.00 (C_{β}), 32.53 ($C_{4'}$), 29.85 ($C_{3'}$). HRMS [ESI+] m/z =451.2005 $[M]^+$, calcd for $[C_{26}H_{29}NO_6]^+$ 451.1995. HPLC purity 96%

_N_-(2-(1-Benzylpiperidin-4-yl)ethyl)-6-methoxy-4-oxo-4_H_-chromene-2-carboxamide. 2.23

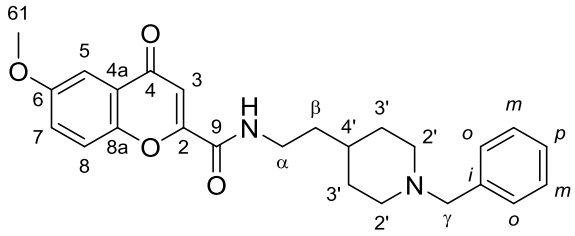

According to the general procedure 2.2, **2.23** was obtained from 0.15 g (0.7 mmol) of **2.3** and 0.18 g (0.82 mmol) of 2-(1-benzylpiperidin-4-yl)ethan-1-amine. White amorphous solid, 0.23 g (80%), mp: 136.7-138.8 ºC. ^{1}H NMR (300 MHz, $CDCl_3$) δ 7.69 (d, *J* = 3.1 Hz, 1H, H_5), 7.57 (d, *J* = 9.2 Hz, 1H, H_7), 7.47 – 7.32 (m, 6H, Ph, H_8), 7.26 (s, 1H, H_3), 7.00 (t, *J* = 5.0 Hz, 1H, NH), 4.02 (s, 3H, H_{61}), 3.69 – 3.59 (m, 4H, $H_{\alpha,\gamma}$), 3.02 (d, *J* = 10.7 Hz, 2H, $H_{2'eq}$), 2.10 (t, *J* = 10.7 Hz, 2H, $H_{2'ax}$), 1.84 (d, *J* = 9.5 Hz, 2H, $H_{3'eq}$), 1.73 (p, *J* = 6.1 Hz, 2H, H_β), 1.57 – 1.38 (m, 3H, $H_{3'ax,\ 4'}$). ^{13}C NMR (75 MHz, $CDCl_3$) δ 178.14 (C_4), 159.39 (C_9), 157.63 (C_6), 154.65 (C_2), 150.09 (C_{8a}), 138.28 (C_i), 129.40 (C_o), 128.30 (C_m), 127.14 (C_p), 125.20 (C_{4a}), 124.72 (C_8), 119.54 (C_7), 111.33 (C_3), 105.26 (C_5), 63.52 (C_γ), 56.13 (C_{61}), 53.74 ($C_{2'}$), 37.91 (C_α), 36.29 (C_β), 33.69 ($C_{4'}$), 32.23 ($C_{3'}$). HRMS [ESI+] *m/z* =420.2068 $[M]^+$, calcd for $[C_{25}H_{28}N_2O_4]^+$ 420.2049. HPLC purity 100%

_N_-(2-(1-Benzylpiperidin-4-yl)ethyl)-5,7-dimethoxy-4-oxo-4_H_-chromene-2-carboxamide. 2.24

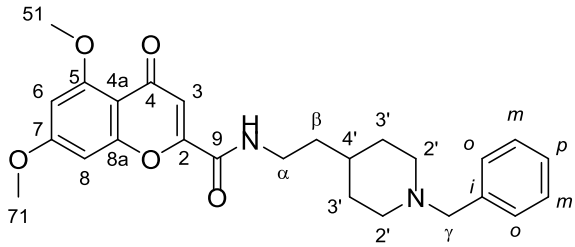

According to the general procedure 2.2, **2.24** was obtained from 0.15 g (0.60 mmol) of **2.2** and 0.157 g (0.72 mmol) of 2-(1-benzylpiperidin-4-yl)ethan-1-amine. White amorphous solid, 0.24 g (89%), mp: 82 - 84 °C. ^{1}H NMR (300 MHz, $CDCl_3$) δ 7.37 – 7.21 (m, 5H, Ph), 6.95 (s, 1H, H_3), 6.83 (t, *J* = 5.9 Hz, NH), 6.48 (d, *J* = 2.3 Hz, 1H, H_8), 6.37 (d, *J* = 2.3 Hz,

1H, H_6), 3.92 (s, 3H, H_{71}), 3.88 (s, 3H, H_{51}), 3.53 – 3.44 (m, 4H, $H_{\alpha,\gamma}$), 2.89 (d, *J* = 10.7 Hz, 2H, $H_{2'eq}$), 1.97 (t, *J* = 10.7 Hz, 2H, $H_{2'ax}$), 1.70 (d, *J* = 9.5 Hz, 2H, $H_{3'eq}$), 1.63 – 1.54 (m, 2H, H_β), 1.40 – 1.28 (m, 3H, $H_{3'ax,\ 4'}$). ^{13}C NMR (75 MHz, $CDCl_3$) δ 177.05 (C_4), 164.68 (C_7), 161.29 (C_5), 159.39 (C_9), 159.05 (C_{8a}), 152.55 (C_2), 138.25 (C_i), 129.39 (C_o), 128.29 (C_m), 127.13 (C_p), 113.91 (C_3), 109.89 (C_{4a}), 96.67 (C_6), 92.94 (C_8), 63.51 (C_γ), 56.56 (C_{71}), 55.96 (C_{51}), 53.73 ($C_{2'}$), 37.84 (C_α), 36.29 (C_β), 33.66 ($C_{4'}$), 32.22 ($C_{3'}$). HRMS [ESI+] *m/z* =450.2169 $[M]^+$, calcd for $[C_{26}H_{30}N_2O_5]^+$ 450.2155. HPLC purity 100%

N-(2-(1-Benzylpiperidin-4-yl)ethyl)-4-oxo-4*H*-chromene-2-carboxamide. 2.25

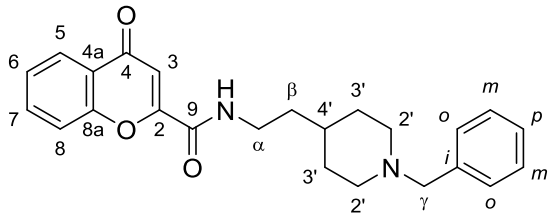

2.25 was obtained as described in the general procedure 2.2, from 0.2 g (1 mmol) of 4-oxo-4H-chromene-2-carboxylic acid and 0.275 g (1.2mmol) of 2-(1-benzylpiperidin-4-yl)ethan-1-amine. White amorphous solid, 0.5 g (97%). mp: 163 - 165 °C. ^{1}H NMR (300 MHz, MeOD) δ 8.14 (dd, *J* = 8.1, 1.7 Hz, 1H, H_5), 7.85 (ddd, *J* = 8.6, 7.1, 1.7 Hz, 1H, H_6), 7.72 (dd, *J* = 8.6, 1.2 Hz, 1H, H_8), 7.52 (ddd, *J* = 8.1, 7.1, 1.2 Hz, 1H, H_7), 7.42 – 7.22 (m, 5H, Ph), 6.97 (s, 1H, H_3), 3.52 (s, 2H, H_γ), 3.45 (t, *J* = 7.4 Hz, 2H, H_α), 2.91 (d, *J* = 11.5 Hz, 2H, $H_{2'eq}$), 2.05 (t, *J* = 11.4 Hz, 2H, $H_{2'ax}$), 1.78 (d, *J* = 12.3 Hz, 2H, $H_{3'eq}$), 1.67 – 1.53 (m, 2H, H_β), 1.45 – 1.18 (m, 3H, $H_{3'ax,\ 4'}$). ^{13}C NMR (126 MHz, MeOD) δ 180.43 (C_4), 161.24 (C_9), 157.52 (C_2), 157.13 (C_{8a}), 138.01 (C_i), 136.31 (C_6), 130.97 (C_o), 129.29 (C_m), 128.51 (C_p), 127.29 (C_7), 126.37 (C_5), 125.07 (C_{4a}), 119.81 (C_8), 111.88 (C_3), 64.29 (C_γ), 54.60 ($C_{2'}$), 38.64 (C_α), 36.90 (C_β), 34.47 ($C_{4'}$), 32.66 ($C_{3'}$). HRMS [ESI+] *m/z* =390.1944 $[M]^+$, calcd for $[C_{24}H_{26}N_2O_3]^+$ 390.1943. HPLC purity 100%

_N_-(2-(1-Benzylpiperidin-4-yl)ethyl)-6-nitro-4-oxo-4_H_-chromene-2-carboxamide. 2.26

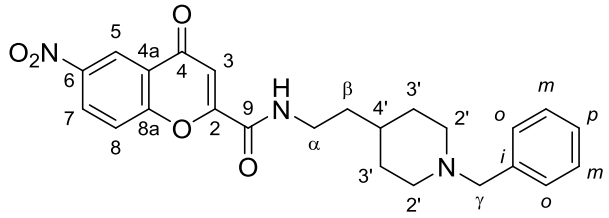

2.26 was obtained as described in the general procedure 2.2, from 0.2 g (0.85 mmol) of **2.6** and 0.23 g (1 mmol) of 2-(1-benzylpiperidin-4-yl)ethan-1-amine**.** Light brown amorphous solid, 0.34 g (92%), mp: 173 - 175 °C. ^{1}H NMR (500 MHz, MeOD) δ 8.94 (d, *J* = 2.8 Hz, 1H, H_5), 8.65 (dd, *J* = 9.2, 2.8 Hz, 1H, H_7), 7.92 (d, *J* = 9.2 Hz, 1H, H_8), 7.35 – 7.31 (m, 5H, $H_{o,\ m,}$ H_3), 7.35 – 7.25 (m, 1H, H_p), 3.55 (s, 2H, H_γ), 3.48 (dd, *J* = 8.1, 6.7 Hz, 2H, H_α), 2.94 (dt, *J* = 12.0, 3.1 Hz, 2H, $H_{2'eq}$), 2.07 (td, *J* = 11.9, 2.5 Hz, 2H, $H_{2'ax}$), 1.82 – 1.76 (m, 2H, H, $H_{3'eq}$), 1.61 (dt, *J* = 8.1, 6.7 Hz, 2H, H_β), 1.41 (ddt, *J* = 12.9, 6.7, 3.4 Hz, 1H, $H_{4'}$), 1.38 – 1.27 (m, 2H, $H_{3'ax}$). ^{13}C NMR (126 MHz, MeOD) δ 178.83 (C_4), 160.66 (C_9), 159.84 (C_6), 157.83 (C_2), 146.65 (C_{8a}), 137.98 (C_i), 130.97 (C_o), 130.13 (C_7), 129.30 (C_m), 128.52 (C_p), 125.30 (C_{4a}), 122.57 (C_5), 121.83 (C_8), 64.28 (C_γ), 54.58 ($C_{2'}$), 38.71 (C_α), 36.87 (C_β), 34.44 ($C_{4'}$), 32.65 ($C_{3'}$). HRMS [ESI+] *m/z* =435.1795 $[M]^+$, calcd for $[C_{24}H_{25}N_3O_5]^+$ 435.1794. HPLC purity 100% C-3 not observed

6-Amino-_N_-(2-(1-benzylpiperidin-4-yl)ethyl)-4-oxo-4_H_-chromene-2-carboxamide. 2.27

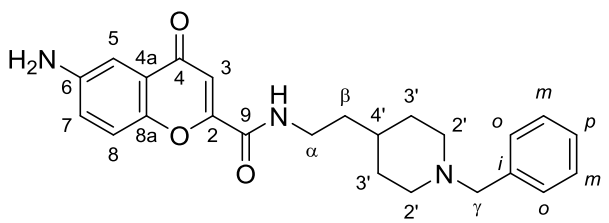

2.26 0.2 g (0.46 mmol) was dissolved in 5 mL of EtOH into a 50 mL round bottom flask, to this dissolution a catalytic amount of Pd/charcoal 5% was added under N_2 atmosphere; subsequently, N_2 was

displaced by H_2 and the flask was sealed up with a rubber septum; a balloon containing H_2 was connected with a needle trough the septum to stir overnight at 30 °C; once reaction was completed, the catalyser was eliminated by filtration and the solvent evaporated under reduced pressure. Yellow amorphous solid, 0.18 g (98%). mp: 215 - 217 °C. ^{1}H NMR (400 MHz, MeOD) δ 7.50 (dd, *J* = 8.9, 0.5 Hz, 1H, H_8), 7.35 – 7.31 (m, 4H, $H_{o,\,m}$), 7.31 – 7.26 (m, 1H, H_p), 7.25 (dd, *J* = 2.9, 0.5 Hz, 1H, H_5), 7.21 (dd, *J* = 8.9, 2.9 Hz, 1H, H_7), 6.89 (s, 1H, H_3), 3.55 (s, 2H, H_γ), 3.44 (t, *J* = 7.4 Hz, 2H, H_α), 2.94 (dt, *J* = 12.1, 3.2 Hz, 2H, $H_{2'eq}$), 2.12 – 2.04 (m, 2H, $H_{2'ax}$), 1.83 – 1.75 (m, 2H, $H_{3'eq}$), 1.64 – 1.54 (m, 2H, H_β), 1.47 – 1.25 (m, 3H, $H_{3'ax,\,4'}$). ^{13}C NMR (101 MHz, MeOD) δ 180.68 (C_4), 161.57 (C_9), 156.84 (C_2), 150.04 (C_6), 148.37 (C_i), 131.01 (C_o), 129.32 (C_m), 128.58 (C_p), 125.92 (C_{4a}), 124.78 (C_7), 120.42 (C_8), 110.52 (C_3), 106.95 (C_5), 64.21 (C_γ), 54.57 ($C_{2'}$), 38.56 (C_α), 36.90 (C_β), 34.40 ($C_{4'}$), 32.58 ($C_{3'}$). HRMS [ESI+] *m/z* =405.2063 $[M]^+$, calcd for $[C_{24}H_{27}N_3O_3]^+$ 405.2054. HPLC purity 100%

_N_-(2-(1-Benzylpiperidin-4-yl)ethyl)-6-hydroxy-4-oxo-4_H_-chromene-2-carboxamide. 2.28

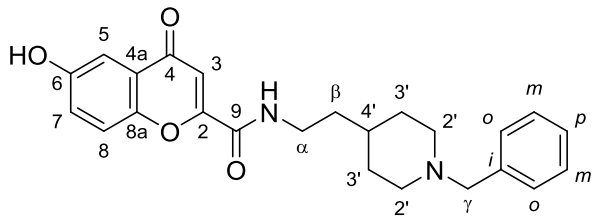

2.28 was obtained as described in the general procedure from 0.05 g (0.12 mmol) of **2.23** and 0.3 g (1.2 mmol) BBr_3. Pale yellow solid, 0.045 g (93%), mp: 204.5 (desc.) °C. ^{1}H NMR (500 MHz, MeOD) δ 7.67 (d, *J* = 9.1 Hz, 1H, H_8), 7.55 – 7.52 (m, 2H, H_o), 7.50 – 7.47 (m, 3H, $H_{m,\,p}$), 7.43 (d, *J* = 2.9 Hz, 1H, H_5), 7.34 (dd, *J* = 9.1, 2.9 Hz, 1H, H_7), 6.94 (s, 1H, H_3), 4.26 (s, 2H, H_γ), 3.50 (t, *J* = 6.8 Hz, 2H, H_α), 3.43 (d, *J* = 12.5 Hz, 2H, $H_{2'eq}$), 2.97 (t, *J* = 12.5 Hz, 2H, $H_{2'ax}$), 2.06 (d, *J* = 13.4 Hz, 2H, $H_{3'eq}$), 1.77 – 1.70 (m, 1H, $H_{4'}$), 1.67 (q, *J* = 6.8 Hz, 2H, H_β), 1.59 – 1.48 (m, 2H,

$H_{3'ax}$). ^{13}C NMR (126 MHz, MeOD) δ 180.43 (C_4), 161.54 (C_9), 157.21 (C_{8a}), 157.07 (C_2), 150.98 (C_6), 132.26 (C_o), 131.19 (C_i), 130.94 (C_p), 130.23 (C_m), 125.98 (C_{4a}), 125.54 (C_7), 121.21 (C_8), 110.73 (C_3), 108.71 (C_5), 61.73 (C_γ), 53.51 ($C_{2'}$), 38.09 (C_α), 36.09 (C_β), 32.39 ($C_{4'}$), 30.34 ($C_{3'}$). HRMS [ESI+] *m/z* =406.1893 M]$^+$, calcd for $[C_{24}H_{26}N_2O_4]^+$ 406.1893. HPLC purity 99%

_N_-(2-(1-Benzylpiperidin-4-yl)ethyl)-5,7-dihydroxy-4-oxo-4_H_-chromene-2-carboxamide. 2.29

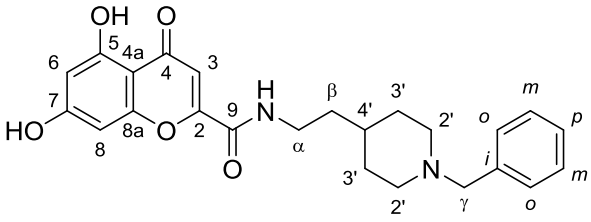

2.29 was obtained as described in the general procedure from 0.05 g (0.11 mmol) of **2.24** and 0.3 g (1.2 mmol) BBr_3. Pale yellow solid, 0.037 g (80%), mp: 267.0 (desc.) °C. ^1H NMR (500 MHz, MeOD) δ 7.56 – 7.52 (m, 2H, H_o), 7.51 – 7.47 (m, 3H, $H_{m, p}$), 6.83 (s, 1H, H_3), 6.56 (d, *J* = 2.2 Hz, 1H, H_8), 6.26 (d, *J* = 2.2 Hz, 1H, H_6), 4.27 (s, 2H, H_γ), 3.48 (t, *J* = 6.9 Hz, 2H, H_α), 3.44 (d, *J* = 12.6 Hz, 2H, $H_{2'eq}$), 3.00 (t, *J* = 12.6 Hz, 2H, $H_{2'ax}$), 2.06 (d, *J* = 14.3 Hz, 2H, $H_{3'eq}$), 1.80 – 1.68 (m, 1H, $H_{4'}$), 1.65 (q, *J* = 6.9 Hz, 2H, H_β), 1.57 – 1.47 (m, 2H, $H_{3'ax}$). ^{13}C NMR (126 MHz, MeOD) δ 183.66 (C_4), 167.08 (C_7), 163.41 (C_5), 161.04 (C_9), 158.90 (C_{8a}), 157.15 (C_2), 132.30 (C_o), 131.10 (C_i), 130.99 (C_p), 130.25 (C_m), 110.75 (C_3), 106.30 (C_{4a}), 100.75 (C_6), 95.68 (C_8), 61.68 (C_γ), 53.48 ($C_{3'}$), 38.06 (C_α), 36.03 (C_β), 32.33 ($C_{4'}$), 30.24 ($C_{3'}$). HRMS [ESI+] *m/z* =422.1852 M]$^+$, calcd for $[C_{24}H_{26}N_2O_5]^+$ 422.1842. HPLC purity 98%

***N*-(4-((Benzyl(methyl)amino)methyl)phenyl)-6,7-dimethoxy-4-oxo-4*H*-chromene-2-carboxamide. 2.30**

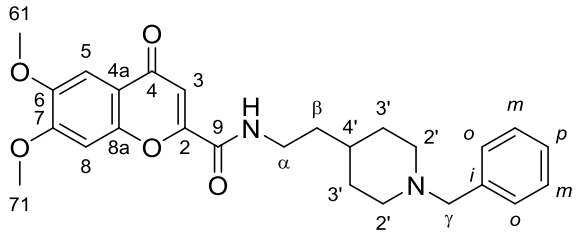

2.30 was obtained as described in the general procedure 2.3, from 0.2 g (0.80 mmol) of **2.4** and 0.191 g (0.88 mmol) of 2-(1-benzylpiperidin-4-yl)ethan-1-amine. White amorphous solid, 0.28 (80%), mp: 129 - 132 °C. ^{1}H NMR (300 MHz, $CDCl_3$) δ 7.46 (s, 1H, H_5), 7.32 – 7.18 (m, 5H, Ph), 7.05 (s, 1H, H_8), 6.90 (s, 2H, NH, H_3), 3.94 (s, 3H, H_{71}), 3.92 (s, 3H, H_{61}), 3.53 – 3.38 (m, 4H, $H_{\alpha,\ \gamma}$), 2.88 (dd, J = 11.5, 3.9 Hz, 2H, $H_{2'eq}$), 1.97 (t, J = 11.5 Hz, 2H, $H_{2'ax}$), 1.75 – 1.63 (m, 2H, $H_{3'eq}$), 1.63 – 1.44 (m, 2H, H_β), 1.39 – 1.22 (m, 3H, $H_{3'ax,\ 4'}$). ^{13}C NMR (75 MHz, $CDCl_3$) δ 177.30 (C_4), 159.42 (C_9), 155.19 (C_7), 154.37 (C_{8a}), 151.39 (C_2), 148.29 (C_6), 137.73 (C_i), 129.46 (C_o), 128.31 (C_m), 127.26 (C_p), 117.97 (C_{4a}), 111.61 (C_8), 104.51 (C_5), 99.77 (C_3), 63.34 (C_γ), 56.67 (C_{61}), 56.49 (C_{71}), 53.60 ($C_{2'}$), 37.85 (C_α), 36.20 (C_β), 33.51 ($C_{4'}$), 32.02 ($C_{3'}$). HRMS [ESI+] m/z =450.2176 $[M]^+$, calcd for $[C_{26}H_{30}N_2O_5]^+$ 450.2155. HPLC purity 100%

***N*-(2-(1-Benzylpiperidin-4-yl)ethyl)-6,7-dihydroxy-4-oxo-4*H*-chromene-2-carboxamide. 2.31**

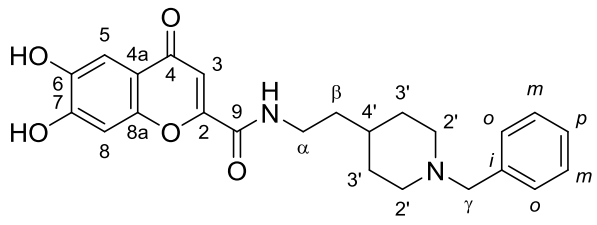

2.31 was obtained as described in the general procedure from 0.05 g (0.12 mmol) of **2.23** and 0.3 g (1.2 mmol) BBr_3. Pale yellow solid, 0.04 g (85%), mp: 204.5 (desc.) °C. ^{1}H NMR (300 MHz, MeOD) δ 7.54 – 7.46 (m, 2H, H_o), 7.45 – 7.39 (m, 3H, $H_{m,\ p}$), 7.32 (s, 1H, H_8), 7.03 (s, 1H, H_5), 6.81 (s, 1H, H_3), 4.21 (s, 2H, H_γ), 3.48 – 3.34 (m, 4H, $H_{2'eq,\ \alpha}$), 2.93 (td,

J = 12.5, 2.8 Hz, 2H, $H_{2'ax}$), 2.00 (d, *J* = 13.8 Hz, 2H, $H_{3'eq}$), 1.71 – 1.38 (m, 5H, $H_{3'ax,\ \beta,\ 4'}$). ^{13}C NMR (75 MHz, MeOD) δ 179.57 (C_4), 161.58 (C_9), 156.33 (C_2), 155.69 (C_7), 152.96 (C_6), 146.97 (C_{8a}), 132.34 (C_o), 131.04 (C_p), 130.80 (C_i), 130.24 (C_m), 117.87 (C_{4a}), 110.85 (C_3), 108.13 (C_8), 104.19 (C_5), 61.55 (C_γ), 53.41 ($C_{2'}$), 38.02 (C_α), 35.98 (C_β), 32.22 ($C_{4'}$), 30.12 ($C_{3'}$ HRMS [ESI+] *m/z* =422.1852 M]$^+$, calcd for $[C_{24}H_{26}N_2O_5]^+$ 422.1842. HPLC purity 97%

_N_-(2-(1-Benzylpiperidin-4-yl)ethyl)-7-methoxy-4-oxo-4H-chromene-2-carboxamide. 2.32

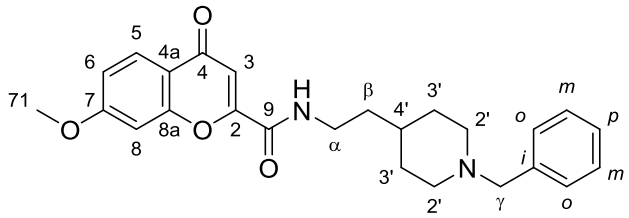

2.32 was obtained as described in the general procedure 2.2, from 0.22 g (1 mmol) of 7-methoxy-4-oxo-4H-chromene-2-carboxylic acid and 0.26 g (1.2mmol) of 2-(1-benzylpiperidin-4-yl)ethan-1-amine. White amorphous solid, 0.38 g (90%). mp: 141 - 143 °C. ^1H NMR (500 MHz, MeOD) δ 7.99 (d, *J* = 8.9 Hz, 1H, H_5), 7.32 – 7.29 (m, 4H, $H_{o,\ m}$), 7.25 (ddd, *J* = 8.9, 5.0, 3.8 Hz, 1H, H_p), 7.13 (d, *J* = 2.4 Hz, 1H, H_8), 7.06 (dd, *J* = 8.9, 2.4 Hz, 1H, H_6), 6.88 (s, 1H, H_3), 3.94 (s, 3H, H_{71}), 3.51 (s, 2H, H_γ), 3.44 (dd, *J* = 8.1, 6.6 Hz, 2H, H_α), 2.90 (dt, *J* = 12.1, 3.3 Hz, 3H, $H_{2'eq}$), 2.03 (td, *J* = 11.7, 2.5 Hz, 2H, $H_{2'ax}$), 1.77 (d, *J* = 12.9 Hz, 2H, $H_{3'eq}$), 1.59 (dt, *J* = 8.1, 6.6 Hz, 2H, H_β), 1.39 (ddtd, *J* = 16.4, 9.5, 6.6, 3.3 Hz, 1H, $H_{4'}$), 1.30 (qd, *J* = 12.1, 3.8 Hz, 2H, $H_{3'ax}$). ^{13}C NMR (126 MHz, MeOD) δ 178.24 (C_4), 165.35 (C_7), 159.75 (C_9), 157.56 (C_{8a}), 155.69 (C_2), 136.73 (C_i), 129.49 (C_o), 127.85 (C_m), 127.03 (C_p), 126.30 (C_5), 117.32 (C_{4a}), 115.30 (C_6), 110.47 (C_3), 100.34 (C_8), 62.90 (C_γ), 55.26 (C_{71}), 53.18 ($C_{2'}$), 37.21 (C_α), 35.49 (C_β), 33.06 ($C_{4'}$), 31.28 ($C_{3'}$).HRMS [ESI+] *m/z* =420.2090 [M]$^+$, calcd for $[C_{25}H_{28}N_2O4]^+$ 420.2049. HPLC purity 100%

***N*-(3-(1-Benzylpiperidin-4-yl)propyl)-6,7-dimethoxy-4-oxo-4*H*-chromene-2-carboxamide. 2.33**

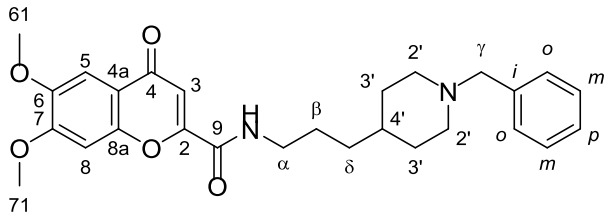

2.33 was obtained as described in the general procedure 2.3, from 0.21 g (1 mmol) of **2.4** and 0.22 g (1.1 mmol) of 3-(1-benzylpiperidin-4-yl)propan-1-amine **1.4**. Light yellow amorphous solid, 0.23 g (60%), mp: 98 - 102 °C. ^{1}H NMR (500 MHz, MeOD) δ 7.46 (s, 1H, H_5), 7.35 – 7.31 (m, 4H, $H_{o,\ m}$), 7.30 – 7.26 (m, 1H, H_p), 7.20 (s, 1H, H_8), 6.92 (s, 1H, H_3), 3.99 (s, 3H, H_{61}), 3.93 (s, 3H, H_{71}), 3.58 (s, 2H, H_γ), 3.40 (t, *J* = 7.2 Hz, 2H, H_α), 2.95 (dt, *J* = 12.2, 3.1 Hz, 2H, $H_{2'eq}$), 2.10 (td, *J* = 12.2, 11.5, 2.5 Hz, 2H, $H_{2'ax}$), 1.75 (d, *J* = 12.8 Hz, 2H, $H_{3'eq}$), 1.67 (p, *J* = 7.7 Hz, 2H, H_β), 1.39 – 1.32 (m, 3H, $H_{\delta,\ 4'}$), 1.31 – 1.23 (m, 2H, $H_{3'ax}$). ^{13}C NMR (126 MHz, MeOD) δ 179.46 (C_4), 161.29 (C_9), 157.38 (C_6), 156.80 (C_2), 153.42 (C_{8a}), 150.04 (C_7), 137.50 (C_i), 131.06 (C_o), 129.35 (C_m), 128.68 (C_p), 118.37 (C_{4a}), 111.29 (C_3), 104.70 (C_5), 101.21 (C_8), 64.12 (C_γ), 57.07 (C_{61}), 56.67 (C_{71}), 54.63 ($C_{2'}$), 41.12 (C_α), 36.35 ($C_{4'}$), 34.70 (C_δ), 32.64 ($C_{3'}$), 27.53 (C_β). HRMS [ESI+] *m/z* =464.2304 $[M]^+$, calcd for $[C_{27}H_{32}N_2O_5]^+$ 464.2311. HPLC purity 100%

***N*-(3-(1-Benzylpiperidin-4-yl)propyl)-6-methoxy-4-oxo-4*H*-chromene-2-carboxamide. 2.34**

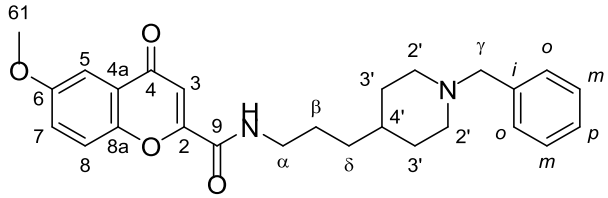

2.34 was obtained as described in the general procedure for the synthesis of 4-oxo-4H-chromene-2-carboxamides (method B) from 0.25 g (1.11 mmol) of **2.3** and 0.29 g (1.25 mmol) of 3-(1-benzylpiperidin-4-yl)propan-1-amine **1.4**. Light yellow amorphous solid,

0.28 (59%), mp: 149 - 151 °C. ^{1}H NMR (500 MHz, MeOD) δ 7.67 (d, *J* = 9.3 Hz, 1H, H_8), 7.53 (d, *J* = 3.1 Hz, 1H, H_5), 7.45 (dd, *J* = 9.3, 3.1 Hz, 1H, H_7), 7.35 – 7.30 (m, 4H, $H_{o,\ m}$), 7.30 – 7.25 (m, 1H, H_p), 6.96 (s, 1H, H_3), 3.91 (s, 3H, H_{61}), 3.56 (s, 2H, H_γ), 3.40 (t, *J* = 7.4 Hz, 2H, H_α), 2.94 (dt, *J* = 12.0, 3.3 Hz, 2H, $H_{2'eq}$), 2.08 (td, *J* = 12.0, 11.4, 2.5 Hz, 2H, $H_{2'ax}$), 1.74 (d, *J* = 13.1 Hz, 2H, $H_{3'eq}$), 1.67 (p, *J* = 7.4 Hz, 2H, H_β), 1.37 – 1.25 (m, 5H, $H_{3'ax,\ 4',\ \delta}$). ^{13}C NMR (126 MHz, MeOD) δ 180.23 (C_4), 161.29 (C_9), 159.21 (C_6), 157.26 (C_2), 151.82 (C_{8a}), 137.68 (C_i), 131.03 (C_o), 129.32 (C_m), 128.61 (C_p), 125.90 (C_7), 125.79 (C_{4a}), 121.30 (C_8), 110.98 (C_3), 105.68 (C_5), 64.19 (C_γ), 56.42 (C_{61}), 54.65 ($C_{2'}$), 41.15 (C_α), 36.38 ($C_{4'}$), 34.72 (C_δ), 32.69 ($C_{3'}$), 27.52 (C_β). HRMS [ESI+] *m/z* =434.2214 $[M]^+$, calcd for $[C_{26}H_{30}N_2O_4]^+$ 434.2206. HPLC purity 100%

_N_-(3-(1-Benzylpiperidin-4-yl)propyl)-6-hydroxy-4-oxo-4_H_-chromene-2-carboxamide. 2.35

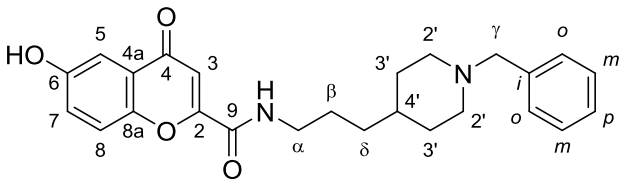

2.35 was obtained as described in the general procedure from 0.05 g (0.09 mmol) of **2.34** and 0.3 g (1.2 mmol) BBr_3. Pale brown solid, 0.043 g (90%), mp: 208 - 210 °C. ^{1}H NMR (500 MHz, MeOD) δ 7.65 (d, *J* = 9.1 Hz, 1H, H_8), 7.56 – 7.52 (m, 2H, H_o), 7.49 – 7.47 (m, 3H, $H_{m,\ p}$), 7.41 (d, *J* = 3.0 Hz, 1H, H_5), 7.33 (dd, *J* = 9.1, 3.0 Hz, 1H, H_7), 6.92 (s, 1H, H_3), 4.30 (s, 2H, H_γ), 3.47 – 3.40 (m, 4H, $H_{2'eq,\ \alpha}$), 3.02 (td, *J* = 12.8, 3.1 Hz, 2H, $H_{2'ax}$), 2.02 – 1.97 (m, 2H, $H_{3'eq}$), 1.73 – 1.65 (m, 3H, $H_{4',\ \beta}$), 1.54 – 1.44 (m, 2H, $H_{3'ax}$), 1.43 – 1.36 (m, 2H, H_δ). ^{13}C NMR (126 MHz, MeOD) δ 180.44 (C_4), 161.47 (C_9), 157.18 (C_{8a}), 157.13 (C_2), 150.97 (C_6), 132.36 (C_o), 131.11 (C_p), 130.72 (C_i), 130.29 (C_m), 125.95 (C_{4a}), 125.54 (C_7), 121.19 (C_8), 110.69 (C_3), 108.71 (C_5), 61.57 (C_γ), 53.54 ($C_{2'}$), 40.81 (C_α), 34.32 ($C_{4'}$), 33.66 (C_δ), 30.33 ($C_{3'}$),

27.30 (C_β). HRMS [ESI+] *m/z* =420.2045 M]$^+$, calcd for $[C_{25}H_{28}N_2O_4]^+$ 420.2049. HPLC purity 99%

Biochemical protocols used in this chapter but not described in the previous one are explained next.

Biochemical Studies

Inhibition of human monoamino oxidases (h-MAO-A and h-MAO-B) MAO inhibition measurements were evaluated following the general procedure previously described previously[231]. Briefly, test drugs and adequate amounts of recombinant hMAO-A or hMAO-B (Sigma-Aldrich Quiímica S.A., Alcobendas, Spain) required and adjusted to oxidize 165 pmol of p-tyramine/min in the control group, were incubated for 15 min at 37 ºC in a flat-black-bottom 96-well microtest plate (BD Biosciences, Franklin Lakes, NJ) placed in the dark fluorimeter chamber. The reaction was started by adding 200 mM Amplex Red reagent (Molecular Probes, Inc., Eugene, OR), 1 U/mL horseradish peroxidase, and 1 mM *p*-tyramine and the production of resorufin, was quantified at 37 ºC in a multidetection microplate fluorescence reader (FLX800, Bio-Tek Instruments, Inc., Winooski, VT) based on the fluorescence generated (excitation, 545 nm; emission, 590 nm). The specific fluorescence emission was calculated after subtraction of the background activity, which was determined from wells containing all components except the h-MAO isoforms, which were replaced by a sodium phosphate buffer solution.

Antagonism of reserpine-induced hypokinesia. Adult ICR albino mice (10 weeks, 25-30 g) from the Department of Pharmarcy of Universidad Nacional de Colombia were group housed at 22±1 °C on a 12-hours light/dark cycle with *ad libitum* access to food and water until two hours prior to the experiment. All experiments were approved by an Ethical Committee and are in accordance with the current accepted methods of

research in the field. The procedure used is the same described by tadaievsky et al.[229]

The animals were randomly distributed into the following groups: vehicle, selegiline and testing compounds; ten animals per group. The mice were orally administered with the corresponding treatment as follows, saline, 0.1 mL/10g, selegiline, 10 mg/Kg and compounds **2.12**, **1.13**, **2.30**, 100 mg/Kg.

2 and 24 hours after administration, the locomotor activity was evaluated in the open field test. The animals were located at the center of an acrylic box of 50 x 50 cm with 20 cm high walls and immediately the time of movement and inactivity was determined during five minutes. Statistical comparisons were carried out by a Kruskal-Wallis one way analysis of variance (ANOVA). Differences were considered statistically significant when $P<0.05$

σ1R Radioligand displacement. Evaluation of the affinity of the derivatives obtained in this chapter was developed in JURKAT cells by CEREP co.[230] Cell membrane homogenates (150 µg protein) are incubated for 120 min at 37°C with 15 nM [^{3}H]pentazocine in the absence or presence of the test compound in a buffer containing 50 mM Tris-HCl (pH 8). Nonspecific binding is determined in the presence of 10 µM haloperidol. Following incubation, the samples are filtered rapidly under vacuum through glass fiber filters (GF/B, Packard) presoaked with 0.3% PEI and rinsed several times with ice-cold 50 mM Tris-HCl using a 96-sample cell harvester (Unifilter, Packard). The filters are dried then counted for radioactivity in a scintillation counter (Topcount, Packard) using a scintillation cocktail (Microscint 0, Packard). The results are expressed as a percent inhibition of the control radioligand specific binding. The standard reference compound is haloperidol, which is tested in each experiment at several concentrations to obtain a competition curve from which its IC_{50} is calculated.

Chapter 3

Synthesis of Kynurenic Acid-based Hybrids, a Failed Attempt to Obtain NMDA Receptor Antagonists

Introduction

NMDA Receptor

Glutamate is the main excitatory neurotransmitter in CNS, it is used by almost 70% of excitatory synapses, especially in cerebral tissue; Glutamate plays a key role in neural survival, differentiation and migration; at the same time, is the precursor of γ-aminobutyric acid (GABA), the main inhibitory neurotransmitter in the CNS. Glutamatergic neurons take part in important processes such as learning, memory and neuronal communication. Glutamate released from presynaptic cells binds receptors located on the cell membrane of postsynaptic neurons. These glutamate receptors are divided into ionotropic and metabotropic, depending on the mechanism of activation. Ionotropic glutamate receptors are cationic channels which respond to glutamate binding allowing the entrance of Na^{+}, K^{+} or Ca^{2+}. On the other hand, metabotropic glutamate receptors allow the flow of cations by a signal transduction system involving associated G-proteins and second messengers.

Ionotropic glutamate receptors are named by their preferred agonists, kaynate, *N*-methyl-D-aspartate (NMDA), and α-amino-3-hydroxy-5-methyl-4-isoxazol propionic acid (AMPA). NMDA receptors participate in physiological processes such as long term potentiation (LTP) and in pathological ones, such as excitotoxicity. It is a ligand-gated and voltage-dependent ion channel which simultaneously requires a co-ligand such as glycine, or D-serine to be activated. This activation leads to an increase of free intracellular Ca^{+2} levels required for LTP, neuronal plasticity,

learning and memory. Disruptions in glutamatergic system including NMDA receptors are implicated in several neurodegenerative processes such AD.[232-234]

NMDA receptors in AD

Excitotoxicity has been postulated to be the link between the glutamate signaling system and several neurodegenerative processes including AD. It is a phenomenon elicited by over-stimulation of NMDA receptors due to an excessive secretion or an impaired uptake of glutamate. This over-stimulation entails an intense influx of calcium ions, which subsequently produces the signaling events resulting in ER stress and cell death.[235,236]

It has been proved that Aβ is able to affect the homeostasis of the glutamatergic system. Enlarged release of glutamate from presynaptic neurons and inhibition of glutamate uptake/recycling in perisynaptic glial cells are some effects of toxic Aβ fragments.[237-239] $A\beta_{(25-35)}$ increases glutamate levels and exerts toxicity in cultured neurons; interestingly, neurons with an enhanced glutamate uptake capacity are able to survive Aβ insult.[240] Oxidative damage might be involved in these effects, it has been proved that Aβ impairs glutamate uptake increasing the conjugation of 4-hydroxy-2-nonenal (HNE), a product from lipid peroxidation, to glutamate transporters.[241] Indeed, Aβ species are able to interact directly with the NMDA receptor; in cortical cultured neurons Aβ oligomeric species evoke an immediate rise of Ca^{2+} influx through activation of NMDA receptors.[242] Moreover, these receptors seem to be required for Aβ oligomers to target synapses, since knocking-down of NMDA receptor abolishes $A\beta_{1-42}$ oligomer binding to dendrites.[243] Although the mechanisms by Aβ species interact with NMDA receptors are not fully understood, it is widely accepted that they are valid targets in AD.[236,244,245] Proof of this is memantine, an NMDAr antagonist currently used in clinical treatment of AD. Several studies have shown that memantine is capable to counteract the deleterious effects of Aβ

species; for instance, reduction of neurite outgrowth, cyclic relationship Aβ administration-NMDAr activation-Aβ production or Aβ induced ROS.[246-248] Even though it is widely accepted that memantine effects are mediated by NMDA receptor, some studies suggest additional properties for this drug, such as enhancing of non amyloidogenic pathway, since memantine increases the levels of soluble APPα in cultured human neuroblastoma cells, attenuation of tau phosphorylation and potentiation of the effects of donepezil in AD patients, according to different clinical trials.[191,249,250]

Kynurenic acid and derivatives in AD

Kynurenic acid (KA, figure 3.1) is a naturally occurring NMDAr antagonist, resulting from the normal metabolism of L-tryptophan. KA and several derivatives have been evaluated as antagonists of different glutamate receptors including NMDAr; furthermore KA derivatives are able to interact with the glycine binding site, especially 5- and 7-substituted derivatives.[251,252] 4-Benzylpiperidine amides of KA inhibit in the nanomolar range the influx of Ca^{+2} mediated by NMDA receptor in rat cortical cell cultures, proving that the acidic moiety is susceptible to be modified without losing activity.[253] On this basis, we decided to combine the KA structure with NBP or DBMA fragments in a single small molecule aiming to obtain new NMDAr antagonists with affinity for the general targets evaluated in previous chapters (cholinesterases, BACE1, and oxidative stress).

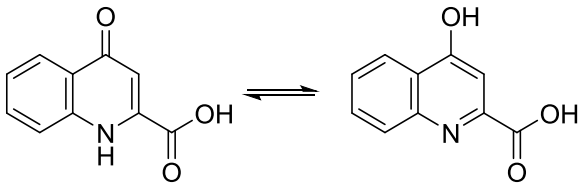

Fig 3.1 Kynurenic Acid

Results and discussion

Synthesis of KA-based Hybrids

Diesters **3.1-3.4** were synthesized from the corresponding methoxy aniline and dimethyl acetylenedicarboxylate at room temperature in Et_2O; (Scheme 3.1). Subsequently, compounds **3.1-3.4** (100 mg) were heated in DMF at 225 °C into a microwave reactor to yield the desired products **3.5-3.8**; however, when scaled up to 500 mg, this reaction allowed the isolation of byproducts **3.9-3.12** (10-12%). This methodology was selected instead the procedure used in the previous chapter because of the susceptibility of derivatives **3.1-3.4** to the acid-base hydrolysis.

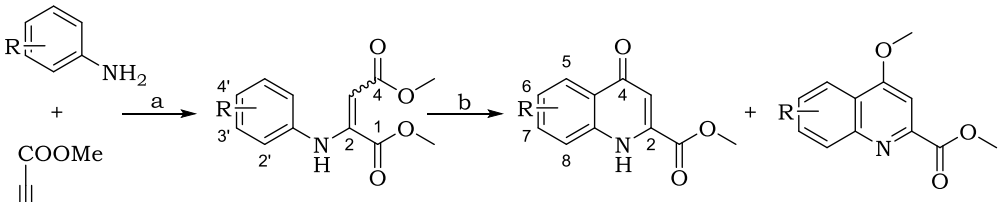

Compd	R		Compd	R		Compd	R	
3.1	2'-OMe	(97%)	3.5	6-OMe	(60%)	3.9	6-OMe	(12%)
3.2	3'-OMe	(95%)	3.6	6',7'-OMe	(90%)	3.10	6',7'-OMe	(5%)
3.3	4'-OMe	(94%)	3.7	7-OMe	(55%)	3.11	7-OMe	(10%)
3.4	3',4'-diOMe	(90%)	3.8	8-OMe	(68%)	3.12	8-OMe	(12%)

Scheme 3.1 Synthesis of starting products (a) Et_2O, rt, overnight; (b) DMF, microwave, 225 °C, 30 min

Additionally, **3.2** yielded a mixture of **3.7** (7-OMe) (55%) with the 5-OMe substituted derivative (13%) which was not isolated. However, a mixture of these two products was used to obtain final compounds **3.20** and **3.23**.

Target compounds **3.13-3.26** were obtained by trimethylaluminium ($Al(CH_3)_3$) mediated amide formation between the corresponding methyl ester (**3.2-3.8**) and the proper amine (**1.7**, **1.8** or 2-(1-benzylpiperidin-4-yl)ethan-1-amine) (Scheme 3.2). This procedure allowed us to obtain the desired products directly from the kynurenic methyl esters in 1.5 min

with good yields (50-90%). Hydroxy-substituted derivatives were obtained by treatment of the corresponding methoxy derivative with BBr_3 in THF at rt as described previously.

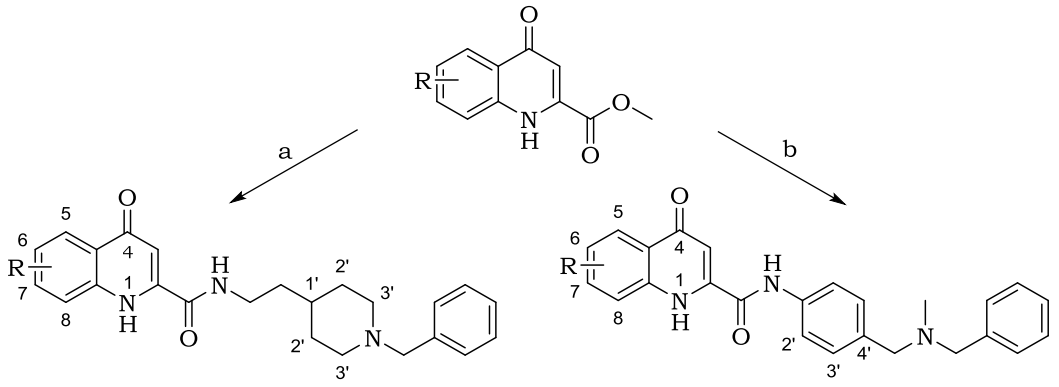

Compd	R		Compd	R	
3.13	6-OMe	(80%)	3.20	5-OMe	(60%)
c 3.14	6-OH	(70%)	3.21	6-OMe	(80%)
3.15	6,7-OMe	(50%)	c 3.22	6-OH	(52%)
3.16	7-OMe	(50%)	3.23	7-OMe	(65%)
3.17	8-OMe	(55%)	3.24	6,7-diOMe	(50%)
c 3.18	8-OH	(55%)	c 3.25	6,7 OH	(57%)
3.19	4,6,7'-triOMe	(50%)	3.26	6,7-OMe (*3'*-subst)	(90%)

Scheme 3.2 Synthesis of KA-based hybrids (a) THF, 2-(1-benzylpiperidin-4-yl)ethan-1-amine, $Al(CH_3)_3$, mw, 1.5 min, 120 °C; (b) THF, **1.7-1.8**, $Al(CH_3)_3$, microwave, 3 min, 120 °C; (c) THF, BBr_3, r.t., overnight

In regard to characterization of final products, it must be taken into account that unlike the chromone scaffold, the 4-quinolinone structure can exist in the tautomeric forms illustrated in the figure 3.2

In tautomer B, H-3 possesses higher aromatic character compared to H-3 in tautomer A; given the similarity of compounds **3.9-3.12** with tautomer B, we inferred that A is the favored tautomer in target compounds by comparison of the chemical shifts for H-3 in the pairs **3.6** – **3.10** and **3.19** - **3.15**. In most of cases H-3 presented chemical shifts around 6.8-7.30 (when an accurate assignation of the corresponding peak was achieved, see experimental section).

Probably, because of this tautomerism, in some final compounds, quaternary carbons were not detected and the multiplicity of some signals corresponding to the aromatic protons in the quinolinone scaffold were not well defined, appearing as broad signals. However, high resolution mass spectroscopy confirmed the exact mass of the desired products. It is detailed in the experimental section, for each case.

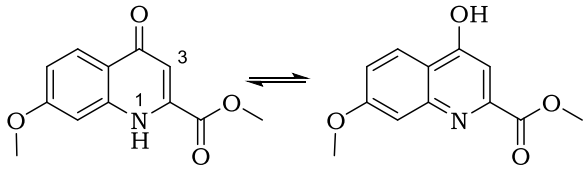

Tauromeric forms of Kynurenic esters

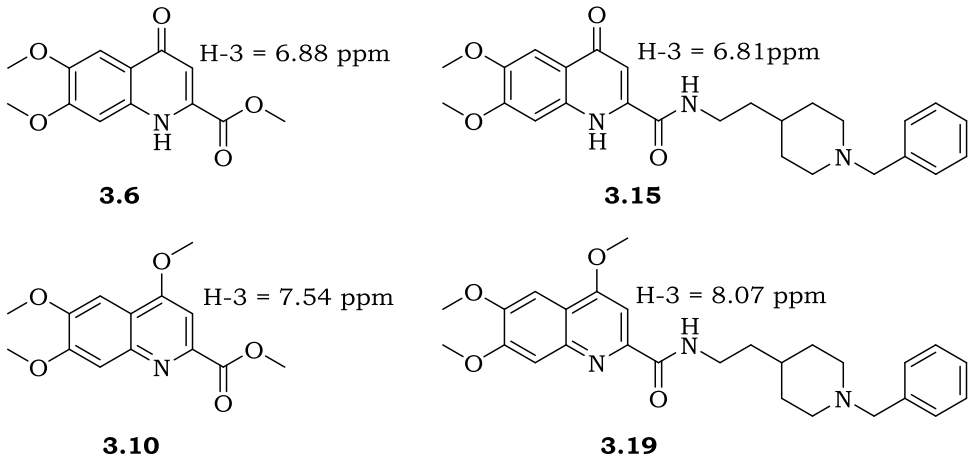

3.6 **3.15**

3.10 **3.19**

Fig 3.2 Tautomeric forms of starting esters and ^{1}H-NMR chemical shifts for H-3 in the target products

Biological Evaluation

As described above, the main objective of this chapter was the synthesis of multitarget ligands with affinity for NMDA receptors. In a first stage, we evaluated these new hybrids in the battery of assays available in our group, inhibition of cholinesterases and antioxidant capacity, in order to

select the most active compounds for further evaluation as NMDA receptor antagonists. Results are summarized in tables 3.1-2

Table 3.1 Inhibition of h-AChE, h-BuChE, MAO-A/B (IC_{50}, μM)

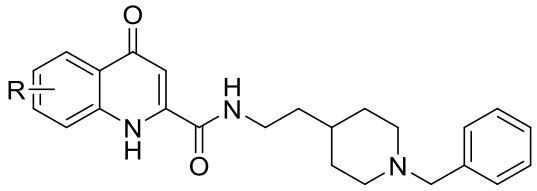

		IC_{50} (μM)			
Comp.	R	**h-AChE**[a]	**h-BuChE**[a]	**h-MAO-A**[b]	**h-MAO-B**[b]
3.13	6-OMe	0.88±0.14	>10	**	**
3.14	6-OH	0.30±0.06	9.88±0.9	51.3±6.2*	59.9±6.7
3.15	6,7-OMe	0.17±0.01	>10	**	**
3.16	7-OMe	0.45±0.05	>10	72.7±6.5*	56.4±4.5
3.17	8-OMe	1.64±0.07	>10	52.4±3.1*	71.6±5.4*
3.18	8-OH	1.15±0.41	>10	***	13.6±0.9
3.19	4,6,7-OMe	0.62±0.05	8.79±0.5	nd	nd

Results are expressed as mean ± SD ([a]n =3, [b]n =5), **Inactive at 200 μM, *** inactive at 1 mM, nd: not determined

Similarly to the chromone based hybrids in the former chapter, the most potent AChE inhibitors belong to the KA-NBP hybrids family. Compound **3.15**, bearing two methoxy groups at positions 6 and 7, was the most potent inhibitor with an IC_{50} value of 170 nM.

Regarding to BuChE, only compounds **3.14** and **3.19** exhibited a modest inhibitory activity with IC_{50}'s of 9.8 and 8.8 μM respectively; this represents selectivity for AChE of about two orders of magnitude.

In the KA-DBMA family, the whole series inhibited selectively AChE in the low micromolar range, except compound **3.26**; here, the change of

the amide bond position from 4' (**3.24**) to position 3', resulted in a complete loss of activity. The same was observed when 6,7-methoxy groups were reduced to obtain the corresponding di-hydroxy substituted compound **3.25**.

Table 3.2 Inhibition of h-AChE, h-BuChE, MAO-A/B (IC_{50}, μM)

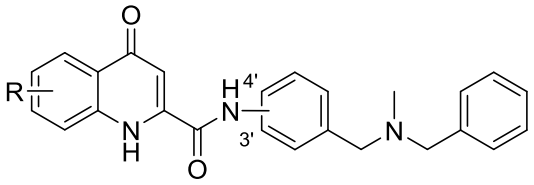

		IC_{50} (μM)		% at 10 μM	% at 20 μM	
Comp.	R	**h-AChE**[a]	**MAO-B**[b]	**h-BACE1**[a]	**Aβ**[a]	**Tau**[a]
3.20	5-OMe	4.0±0.4	15.2±1	10.4	nd	nd
3.21	6-OMe	2.3±0.1	**	26.6	25.1	15.0
3.22	6-OH	3.1±0.3	**	26.5	26.3	27.4
3.23	7-OMe	2.3±0.2	**	33.5	nd	nd
3.24	6,7-OMe	4.5±0.3	nd	28.7	nd	nd
3.25	6,7-OH	>10	**	27.8	nd	nd
3.26 (3')	6,7-OMe	>10	**	32.5	nd	nd

Results are expressed as mean ± SD ([a]n =3, [b]n =5), **Inactive at 200 μM, nd: not determined

Likewise to chromone based hybrids, **3.15** inhibited AChE with a mixed mechanism as inferred from figure 3.3

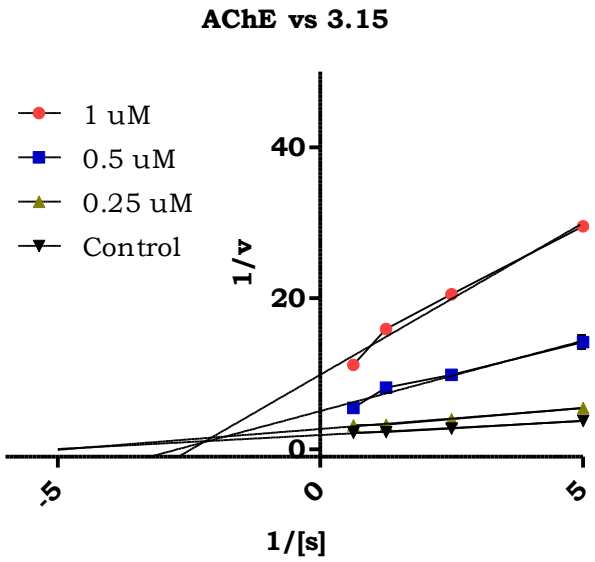

Fig 3.3 Lineweaver-Burk plot of reciprocals for velocity and different concentrations of **3.15**, 0.5 - 1 µM. Lines were derived from a weighted least-squares analysis of data.

At this point, a selection of compounds (**3.13**, **3.16**, **3.14**, **3.15**, **3.24**, **3.23**, **3.21**, **3.22**), including the most potent AChE inhibitors, were tested in a radioligand displacement assay ([^{3}H]CGP 39653, CEREP Co.[254]) to determine whether or not they are able to antagonize NMDA receptor. Unfortunately, none of the selected compounds exhibited affinity for this receptor. Highest radioligand displacement percentage was reached by **3.13** with a poor 6%.

Continuing with biological assessment of our compounds, we evaluated their MAO inhibitory activity. As shown in table 3.1, four of the newly synthesized KA-NBP hybrids displayed unselective MAO inhibitory activity (IC_{50}'s = 52-72 µM). **3.18** (8-OH substituted) was the most potent and the unique selective towards MAO-B, IC_{50} = 13.6 µM. In the KA-DBMA series, only 5-methoxy substituted compound **3.20**, was able to inhibit selectively **MAO-B** with an IC_{50} value of 15.2 µM (table 3.2). The rest of the series was inactive towards both MAO isoforms.

Concerning to BACE1 inhibition, KA-NBP series was utterly inactive, while in KA-DBMA series, almost all derivatives inhibited modestly this enzyme with percentages around 30% at 10 μM. The highest inhibition was reached by **3.23** (7-OMe) with 33% (table 3.2).

Complementary assays were carried out with some compounds depending on the availability. Anti-aggregating effect of compounds **3.13**, **3.15, 3.16** (KA-BP), **3.21**, **3.22** (KA-DBMA) were evaluated in a culture of bacterial cells overexpressing $A\beta_{42}$ peptide or *tau* protein. While KA-NBP compounds were completely inactive, KA-DBMA hybrid **3.22**, inhibited modestly and simultaneously the self-aggregation of amyloid peptide and *tau* protein, 26 - 27% respectively (table 3.2).

All derivatives were tested in PAMPA assay and were predicted to cross the BBB. On the other hand, all hydroxy substituted derivatives were evaluated as radical scavengers in ORAC assay, obtaining good antioxidant properties with values around 1 equivalent of trolox; **3.17** = 0.97, **3.14** = 1.4, **3.25** = 0.5, **3.22** = 1.2.

Finally, compound **3.14**, with dual AChE-MAO inhibitory activity and the highest antioxidant capacity, exhibited neuroprotective properties in SH-SY5Y cells treated with rotenone-oligomycin as described in the previous chapter; the highest cconcentration tested, 3 μM protected around 30% of the cells.

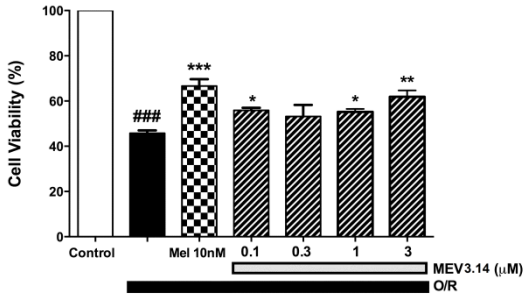

Figure 3.4 Cell viability was measured as MTT reduction and data were normalized as % of control. Data are expressed as the means ± SEM. of triplicate of at least three different cultures. All compounds were assayed at increasing concentrations (0.1-3 μM).

Conclusions

New hybrids based on the combination of KA and NBP or DBMA fragments were obtained and evaluated in several enzymes related to AD. This new molecules required a different approach in the synthesis compared to the chromone based derivatives described in chapter two. The susceptibility of intermediate diesters to hydrolysis demanded a more direct but less efficient method consistent in microwave assisted cyclization to obtain the corresponding kynurenic methyl esters.

Taking into account that previous works have demonstrated the ability of KA containing compounds to antagonize the NMDA receptor,[251,255-257] here we attempted to combine this structure with NBP and DBMA fragments in order to obtain new multitarget anti-AD compounds. Although, we failed in our attempt to achieve molecules able to antagonize NMDA receptor, we obtained several compounds with antioxidant properties and dual affinity AChE/MAO-B.

An interesting conclusion in regard to AChE inhibition could be drawn from the comparison between potencies of **3.15** (6,7-OMe) and the equivalent chromone based hybrid **2.30** (Chapter 2, IC_{50}=41 nM). It

highlights the relevance of the endocyclic oxygen and/or the stability of the exocyclic carbonyl group (position 4) for the interaction with the enzyme, since the substitution by a group susceptible of tautomerization was detrimental for activity.

In KA-DBMA series, the loss of activity observed in the changes from **3.24** to **3.25** (6,7-diOMe→6,7-diOH) and from **3.24** to **3.26** (4'subst.→3'subst.) reveal that the nature of the substituents in KA scaffold and the position of DBMA fragment contribute to the interaction with the enzyme. On the basis of these findings we believe that future modifications on the position, size and substitution of the intermediate ring could improve the potency towards AChE.

In the case of MAO, either KA-NBP as KA-DBMA series gave inhibitors in the same order of magnitude, which could be interpreted as a dependence of the activity on the nature of substituents in the KA scaffold more than on the nature of the moiety bearing the tertiary amine and the benzyl group. Conversely, BACE1 inhibitory activity was independent of the kynurenic moiety (as well as the chromone scaffold in last chapter) but dependent on the fragment containing the tertiary amine, only DBMA derivatives were able to inhibit modestly this enzyme.

Despite the fact that our results in NMDA receptor were negative and very modest in the rest of assays, we believe that there is still a region of the molecules that could be explored in the search for a better multitarget profile in KA-DBMA compounds, modifications in the position and substitution of the central ring could influence the interaction with the enzyme and exert better results in BACE1, and Aβ or tau aggregation; these modifications remain to be developed.

Experimental Part

General Procedure 3.1 Synthesis of diesters (3.1-3.4) 1 mL (0.89 mmol) of the corresponding methoxy aniline was dissolved in 20 mL of Et_2O; to this solution, 0.10 mL (0.89 mmol) of dimethyl acetylenedicarboxylate and 0.11 mL (0.89 mmol) of Et_3N were added, to stir overnight at room temperature. The reaction mixture was washed with HCl (1N) (3x5 mL), water (3x5 mL) and brine (3x5 mL), dried over $MgSO_4$ and concentrated under reduced pressure. Purification was carried out recrystallizing the crude from a mixture of Et_2O-Hexane, or column chromatography using a mixture of ethyl acetate in hexane (0→100%).

General procedure 3.2 Synthesis of KA-methyl esters (3.5-3.8). Into a 20 mL microwave vial, 0.2 g (0.76 mmol) of the corresponding dimethyl 2-(phenylamino)but-2-enedioate were dissolved in 15 mL (193 mmol) of DMF; this dissolution was heated at 225 °C during 15 min in a microwave reactor. The solvent was evaporated under reduced pressure at 80 °C and purification was carried out by column chromatography using a gradient of methanol in EtOAc (0→10%) as eluent. The proportion between reagents and solvent is important to avoid undesired byproducts or decomposition.

General Procedure 3.3 Synthesis of KA-amides. Into a 5 mL microwave vial, the corresponding esther (0.40 mmol) was dissolved in 2 mL of dry THF; to this dissolution, the corresponding amine (1 mmol) previously dissolved in 1.5 mL of THF, was added; air was displaced by N_2 and the tube was sealed up; afterward, 3 mmol of $Al(CH_3)_3$ (2M in heptane) was injected with a syringe; this mixture was heated into a microwave reactor at 120 °C during 1.5 min. The crude was treated with HCl 2M (dropwise) until the end of effervescence, the mixture was neutralized with NaOH 2M and the liquid phase evaporated until dryness; the solid was washed with EtOAc (5x5 mL) and methanol (2x5 mL), these fractions were mixed

and concentrated under reduced pressure. The product was purified by column chromatography using a gradient of EtOAc in hexane (0→65%) as eluent.

General Procedure 3.4 Demethoxylation of KA-amides To 3 mL of a solution of the corresponding KA-amide in anhydrous DCM was added slowly under magnetic stirring, 1 equivalent of BBr_3 per each heteroatom present in the molecule; air was displaced by N_2 and the mixture was allowed to react overnight at room temperature. Reaction was quenched with methanol (dropwise until end of effervescence) and the solvent evaporated under reduced pressure to eliminate the remaining BBr_3, this process was repeated several times depending on the quantity of BBr_3 used, until no fumes were observed when adding methanol. When necessary, purification was carried out by column chromatography using a gradient of MeOH in EtOAc (0→10%) as eluent.

Dimethyl 2-((2-methoxyphenyl)amino)but-2-enedioate. 3.1

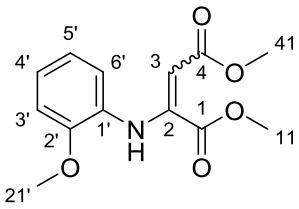

3.1 was obtained from equimolar quantities of 2-methoxy aniline and dimethyl acetylenedicarboxylate (0.89 mmol) as described in the general procedure 3.1. HPLC-MS (Water-ACN 15→95%, g.t. 5 min) was used to control the reaction, observing the majoritarian formation of one of the two possible isomers, retention time 4.17 min (3%), 4.90 min (97%). The main product was recrystallized from ether. Yellow crystals, 0.22 g (94%), mp:72 °C. ^{1}H NMR (300 MHz, $CDCl_3$) δ 9.66 (s, 1H, NH), 7.03 (ddd, *J* = 8.4, 7.1, 1.7 Hz, 1H, $H_{3'}$), 6.90 – 6.80 (m, 2H, $H_{4', 5'}$), 6.80 – 6.70 (m, 1H, $H_{6'}$), 5.39 (s, 1H, H_3), 3.84 (s, 3H, $H_{21'}$), 3.74 (s, 3H, H_{41}), 3.71 (s, 3H, H_{11}). ^{13}C NMR (75 MHz, $CDCl_3$) δ 169.96 (C_4), 164.92 (C_1), 150.62 ($C_{2'}$), 147.84 (C_2), 129.50 ($C_{1'}$), 124.56 ($C_{3'}$), 120.74 ($C_{4'}$), 120.16 ($C_{6'}$), 111.12 ($C_{5'}$), 92.80 (C_3), 55.68

($C_{21'}$), 52.73 (C_{11}), 51.26 (C_{41}). HPLC-MS *m/z* =266.2 $[M + H]^+$, calcd for $[C_{13}H_{15}NO_5 + H]^+$ 266.2

Dimethyl 2-((3-methoxyphenyl)amino)but-2-enedioate. 3.2

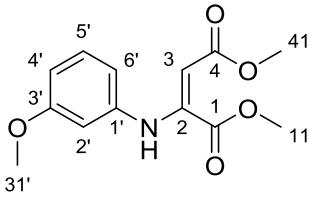

3.2 was obtained from equimolar quantities of 3-methoxy aniline and dimethyl acetylenedicarboxylate (0.89 mmol) as described in the general procedure 3.1. HPLC-MS (Water-ACN 15→95%, g.t. 5 min) was used to control the reaction, observing the formation the two possible isomers. Retention time 4.17 min (20%), 4.88 min (80%) (Yield of mixture 95%), however, this proportion changed to 3%-97% after work up. The main product was purified by column chromatography, obtaining **3.2** as a brown oil, 0.21 g (90%). ^{1}H NMR (300 MHz, $CDCl_3$) δ 9.62 (s, 1H, NH), 7.21 – 7.10 (m, 1H, $H_{5'}$), 6.71 – 6.56 (m, 1H, $H_{4'}$), 6.48 – 6.39 (m, 2H, $H_{2', 6'}$), 5.37 (s, 1H, H_3), 3.75 (s, 3H, $H_{31'}$), 3.72 (s, 3H, H_{41}), 3.70 (s, 3H, H_{11}). ^{13}C NMR (75 MHz, $CDCl_3$) δ 169.91 (C_4), 165.01 (C_1), 160.46 ($C_{3'}$), 148.08 (C_2), 141.57 ($C_{1'}$), 129.96 ($C_{5'}$), 113.01 ($C_{2'}$), 110.10 ($C_{4'}$), 106.50 ($C_{6'}$), 93.83 (C_3), 55.34 ($C_{31'}$), 52.92 (C_{11}), 51.31 (C_{41}). HPLC-MS *m/z* =266.2 $[M + H]^+$, calcd for $[C_{13}H_{15}NO_5 + H]^+$ 266.2

Dimethyl 2-((4-methoxyphenyl)amino)but-2-enedioate. 3.3

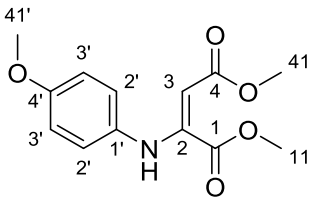

3.3 was obtained from equimolar quantities of 4-methoxy aniline and dimethyl acetylenedicarboxylate (0.89 mmol) as described in the general procedure 3.1. HPLC-MS (Water-ACN 15→95%, g.t. 5 min) was used to control the reaction, observing the formation of the two possible isomers, retention time 4.07 min (20%), 4.81 min (80%) (Yield of mixture of isomers 94%), the main product was isolated by column chromatography as a brown

oil, 0.19 g (80%). ^{1}H NMR (300 MHz, $CDCl_3$) δ 9.56 (s, 1H, NH), 6.93 – 6.76 (m, 4H, $H_{2',3'}$), 5.28 (s, 1H, H_3), 3.75 (s, 3H, $H_{41'}$), 3.70 (s, 3H, H_{41}), 3.64 (s, 3H, H_{11}). ^{13}C NMR (75 MHz, $CDCl_3$) δ 170.09 (C_4), 164.81 (C_1), 156.93 ($C_{4'}$), 149.04 (C_2), 133.43 ($C_{1'}$), 122.98 ($C_{2'}$), 114.39 ($C_{3'}$), 91.69 (C_3), 55.42 ($C_{41'}$), 52.69 (C_{11}), 51.07(C_{41}). HPLC-MS *m/z* =266.2 $[M + H]^+$, calcd for $[C_{13}H_{15}NO_5 + H]^+$ 266.2

Dimethyl 2-((3,4-dimethoxyphenyl)amino)but-2-enedioate. 3.4

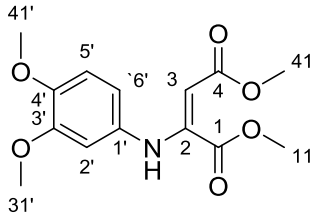

3.4 was obtained from 1 g (6.53 mmol) of 3, 4-dimethoxy aniline and 0.8 mL (6.53 mmol) of dimethyl acetylenedicarboxylate as described in the general procedure 3.1. HPLC-MS (Water-ACN 15→95%, g.t. 5 min) was used to control the reaction, observing the majoritarian formation of one of the two possible isomers, retention time 3.74 min (10%), 4.49 min (90%) (Yield of isomers mixture 95%), the main product was isolated by column chromatography as a brown oil, 1.7 g (87%). ^{1}H NMR (300 MHz, $CDCl_3$) δ 9.53 (s, 1H, NH), 6.70 (d, *J* = 8.5 Hz, 1H, $H_{5'}$), 6.47 (d, *J* = 2.5 Hz, 1H, $H_{2'}$), 6.40 (dd, *J* = 8.5, 2.6 Hz, 1H, $H_{6'}$), 5.23 (s, 1H, H_3), 3.78 (s, 3H, $H_{41'}$), 3.77 (s, 3H, $H_{31'}$), 3.66 (s, 3H, H_{41}), 3.61 (s, 3H, H_{11}). ^{13}C NMR (75 MHz, $CDCl_3$) δ 169.93 (C_4), 164.86 (C_1), 149.28 ($C_{3'}$), 148.90 (C_2), 146.35 ($C_{4'}$), 133.71 ($C_{1'}$), 113.24 ($C_{6'}$), 111.35 ($C_{5'}$), 105.96 ($C_{2'}$), 91.91 (C_3), 55.96 ($C_{41'}$), 55.77 ($C_{31'}$), 52.67 (C_{11}), 51.02 (C_{41}). HPLC-MS *m/z* =296.3 $[M + H]^+$, calcd for $[C_{14}H_{17}NO_6 + H]^+$ 296.3

Methyl 6-methoxy-4-oxo-1,4-dihydroquinoline-2-carboxylate. 3.5

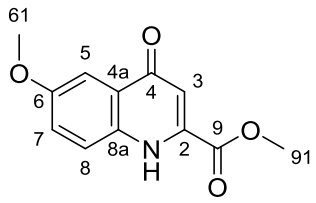

3.3, (0.2 g) was reacted as described in the general procedure 3.2. The crude was purified by column chromatography, obtaining **3.5** as brown needles, 0.105 (60%), mp: 254 °C ^{1}H NMR (300 MHz, MeOD) δ 7.80 (d, *J* = 9.2 Hz, 1H, H_8), 7.62 (d, *J* = 2.9 Hz, 1H, H_5), 7.40 (dd, *J* = 9.2, 2.9 Hz, 1H, H_7), 6.93 (s, 1H, H_3), 4.02 (s, 3H, H_{91}), 3.91 (s, 3H, H_{61}). ^{13}C NMR (126 MHz, MeOD) δ 180.26 (C_4), 163.75 (C_9), 158.97 (C_6), 139.13 (C_2), 136.49 (C_{8a}), 128.32 (C_{4a}), 125.93 (C_7), 122.37 (C_8), 109.84 (C_3), 104.31 (C_5), 56.16 (C_{61}), 54.02 (C_{91}). HPLC-MS (Water-ACN 2→30%, g.t. 10 min), retention time 6.39 min, *m/z* =233.3 $[M + H]^+$, calcd for $[C_{12}H_{11}NO_4 + H]^+$ 233.2

Methyl 6,7-dimethoxy-4-oxo-1,4-dihydroquinoline-2-carboxylate. 3.6

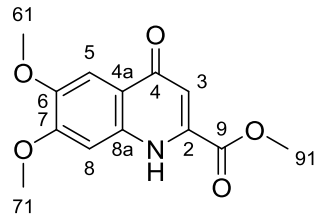

3.4 (0.2 g) was reacted as described in the general procedure 3.2. The crude was purified by column chromatography, obtaining **3.6** as a pale brown solid, 0.16 g (90%), mp: 267 - 269 °C. ^{1}H NMR (300 MHz, MeOD) δ 7.55 (s, 1H, H_8), 7.26 (s, 1H, H_5), 6.88 (s, 1H, H_3), 4.01 (s, 3H, H_{91}), 3.96 (s, 3H, H_{61}), 3.92 (s, 3H, H_{71}). ^{13}C NMR (126 MHz, MeOD) δ 179.38 (C_4), 163.78 (C_9), 156.59 (C_7), 150.23 (C_6), 146.71 (C_2), 138.04 (C_{8a}), 121.71 (C_{4a}), 110.25 (C_3), 104.46 (C_8), 100.63 (C_5), 56.72 (C_{71}), 56.48 (C_{61}), 53.96 (C_{91}). HPLC-MS (Water-ACN 15→95%, g.t. 5 min), retention time 2.64 min HPLC-MS *m/z* =264.2 $[M + H]^+$, calcd for $[C_{13}H_{13}NO_5 + H]^+$ 264.2

Methyl 7-methoxy-4-oxo-1, 4-dihydroquinoline-2-carboxylate. 3.7

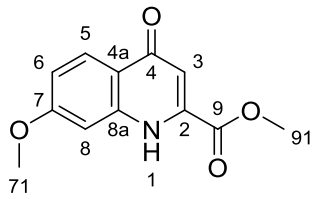

3.2 (0.2 g) was reacted as described in the general procedure 3.2. The crude was purified by column chromatography, obtaining **3.7** as pale brown needles, 0.097 g (55%), mp: 242 °C. ^{1}H NMR (500 MHz, DMSO-d_6) δ 11.84 (bs, 1H, NH), 7.98 (d, J = 9.0 Hz, 1H, H_5), 7.41 (d, J = 2.4 Hz, 1H, H_8), 6.98 (dd, J = 9.0, 2.4 Hz, 1H, H_6), 6.56 (s, 1H, H_3), 3.95 (s, 3H, H_{91}), 3.85 (s, 3H, H_{71}). ^{13}C NMR (126 MHz, DMSO-d_6) δ 176.88 (C_4), 162.70 (C_9), 162.46 (C_7), 141.90 (C_{8a}), 137.44 (C_2), 126.52 (C_5), 120.43 (C_{4a}), 114.34 (C_6), 110.31 (C_3), 100.27 (C_8), 55.49 (C_{71}), 53.46 (C_{91}). HPLC-MS (Water-ACN 15→95%, g.t. 5 min), retention time 2.88 min, m/z =234.2 $[M + H]^+$, calcd for $[C_{12}H_{11}NO_4 + H]^+$ 234.2

Methyl 8-methoxy-4-oxo-1, 4-dihydroquinoline-2-carboxylate. 3.8

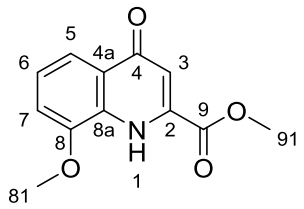

3.1 (0.2 g) was reacted as described in the general procedure 3.2. The crude was purified by column chromatography, obtaining **3.8** as brown needles 0.12 g (68%) mp: 132 °C. ^{1}H NMR (300 MHz, $CDCl_3$) δ 9.41 (s, 1H, NH), 7.89 (d, J = 8.1 Hz, 1H, H_5), 7.36 – 7.23 (m, 1H, H_6), 7.08 (dd, J = 8.1, 1.2 Hz, 1H, H_7), 6.97 (d, J = 2.0 Hz, 1H, H_3), 4.04 (s, 6H, $H_{81,91}$). ^{13}C NMR (75 MHz, $CDCl_3$) δ 179.51 (C_4), 163.42 (C_9), 148.46 (C_8), 135.63 (C_2), 130.59 (C_{8a}), 127.22 (C_{4a}), 124.14 (C_6), 117.50 (C_5), 112.09 (C_3), 111.33 (C_7), 56.28 (O-CH_3), 53.87(O-CH_3). HPLC-MS (Water-ACN 15→95%, g.t. 10 min), retention time 4.8 min, m/z =234.2 $[M + H]^+$, calcd for $[C_{12}H_{11}NO_4 + H]^+$ 234.2

Methyl 4,6-dimethoxyquinoline-2-carboxylate. 3.9

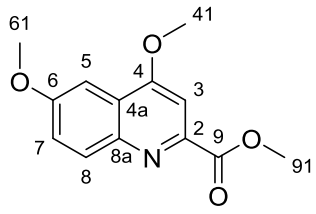

3.9 was obtained as a secondary product from the synthesis of **3.5** (starting from 0.5 g of **3.3** in 15 mL of DMF), pale brown needles, 0.042 g (12%), mp: 135 °C. ^{1}H NMR (300 MHz, $CDCl_3$) δ 8.13 (d, *J* = 9.2 Hz, 1H, H_8), 7.59 (s, 1H, H_3), 7.46 (d, *J* = 2.9 Hz, 1H, H_5), 7.40 (dd, *J* = 9.2, 2.9 Hz, 1H, H_7), 4.13 (s, 3H, H_{41}), 4.07 (s, 3H, H_{91}), 3.96 (s, 3H, H_{61}). ^{13}C NMR (75 MHz, $CDCl_3$) δ 166.58 (C_9), 162.18 (C_4), 159.16 (C_6), 146.72 (C_2), 144.47 (C_{8a}), 131.98 (C_8), 123.49 (C_{4a}), 123.42 (C_7), 100.67 (C_3), 99.55 (C_5), 56.18 (C_{41}), 55.84 (C_{61}), 53.34 (C_{91}). HPLC-MS (Water-ACN 15→95%, g.t. 10 min), retention time 6.42 min, *m/z* =248.2 $[M + H]^+$, calcd for $[C_{13}H_{13}NO_4 + H]^+$ 248.2

Methyl 4,6,7-trimethoxyquinoline-2-carboxylate. 3.10

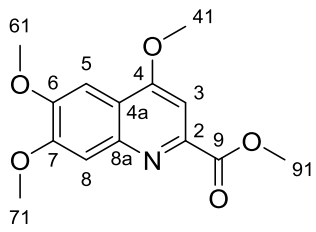

3.10 was obtained as a secondary product from the synthesis of **3.6** (starting from 0.5 g of **3.4** in 15 mL of DMF), pale brown solid, 0.024 g (5%), mp: 255 - 258 °C ^{1}H NMR (300 MHz, $CDCl_3$) δ 7.55 (s, 1H, H_8), 7.54 (s, 1H, H_3), 7.43 (s, 1H, H_5), 4.11 (s, 3H, H_{91}), 4.06 (s, 3H, H_{41}), 4.04 (s, 3H, H_{71}), 4.02 (s, 3H, H_{61}). ^{13}C NMR (75 MHz, $CDCl_3$) δ 166.62 (C_9), 161.92 (C_4), 153.19 (C_6), 150.89 (C_7), 147.06 (C_2), 145.63 (C_{4a}), 117.53 (C_{8a}), 109.07 (C_8), 99.83 (C_3), 99.61 (C_5), 56.41 (OCH_3), 56.34 (OCH_3), 56.12 (C_{91}), 53.30 (C_{41}). HPLC-MS (Water-ACN 15→95%, g.t. 5 min), retention time 2.99 min, *m/z* =278.3 $[M + H]^+$, calcd for $[C_{14}H_{15}NO_5 + H]^+$ 278.3

Methyl 4,7-dimethoxyquinoline-2-carboxylate. 3.11

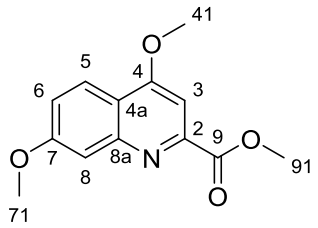

3.11 was obtained as a secondary product of the synthesis of **3.7** (starting from 0.5 g of **3.2** in 15 mL of DMF). Pale yellow needles, 0.046 g (10%), mp: 157 °C ^{1}H NMR (500 MHz, DMSO-d_6) δ 8.06 (d, J = 9.1 Hz, 1H, H_5), 7.47 (d, J = 2.5 Hz, 1H, H_8), 7.43 (s, 1H, H_3), 7.30 (dd, J = 9.2, 2.6 Hz, 1H, H_6), 4.09 (s, 3H, H_{41}), 3.93 (s, 3H, H_{91}), 3.92 (s, 3H, H_{71}). ^{13}C NMR (126 MHz, DMSO-d_6) δ 165.66 (C_9), 162.71 (C_4), 161.08 (C_7), 149.88 (C_{8a}), 149.30 (C_2), 122.76 (C_5), 120.30 (C_6), 116.03 (C_{4a}), 107.98 (C_8), 99.08 (C_3), 56.33 (C_{41}), 55.64 (C_{71}), 52.61 (C_{91}) HPLC-MS (Water-ACN 15→95%, g.t. 5 min), retention time 3.54 min, m/z =248.3 $[M + H]^+$, calcd for $[C_{13}H_{13}NO_4 + H]^+$ 248.3

Methyl 4,8-dimethoxyquinoline-2-carboxylate. 3.12

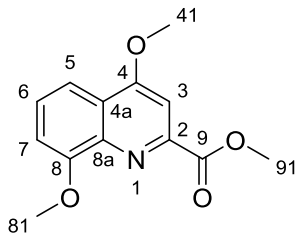

3.12 was obtained as a secondary product from the synthesis of **3.8** (starting from 0.5 g of **3.1** in 15 mL of DMF). White flakes, 0.056g (12%) mp: 143 °C. ^{1}H NMR (300 MHz, $CDCl_3$) δ 7.77 (dd, J = 8.1, 1.3 Hz, 1H, H_5), 7.63 (s, 1H, H_3), 7.51 (t, J = 8.1 Hz, 1H, H_6), 7.08 (d, J = 8.0 Hz, 1H, H_7), 4.11 (s, 3H, H_{41}), 4.06 (s, 3H, H_{81}), 4.04 (s, 3H, H_{91}). ^{13}C NMR (75 MHz, $CDCl_3$) δ 166.50 (C_9), 163.42 (C_4), 155.92 (C_8), 147.89 (C_2), 140.43 (C_{8a}), 128.18 (C_6), 123.52 (C_{4a}), 113.35 (C_5), 108.56 (C_7), 100.88 (C_3), 56.28 (C_{41}), 56.17 (C_{81}), 53.23 (C_{91}) HPLC-MS (Water-ACN 15→95%, g.t. 10 min), retention time 3.94 min, m/z =248.2 $[M + H]^+$, calcd for $[C_{13}H_{13}NO_4 + H]^+$ 248.2

***N*-(2-(1-benzylpiperidin-4-yl)ethyl)-6-methoxy-4-oxo-1,4-dihydroquinoline-2-carboxamide. 3.13**

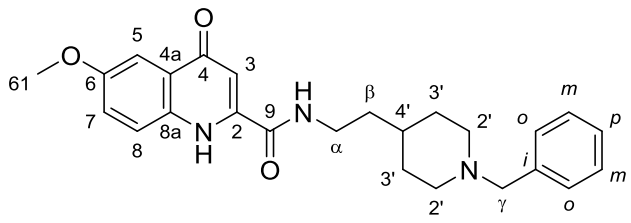

Product **3.13** was obtained According to the general procedure 3.3, from 0.1 g (0,43 mmol) of **3.5** and 0.23 g (1,07 mmol) of 2-(1-benzylpiperidin-4-yl)ethan-1-amine as a white amorphous solid, 0.143g (80%), mp: 184 - 186 °C. ^{1}H NMR (300 MHz, MeOD) δ 8.16 (d, *J* = 9.3 Hz, 1H, H_8), 7.75 – 7.41 (m, 8H, Ph, $H_{3,\,7,\,5}$), 4.30 (s, 2H, H_{γ}), 3.99 (s, 3H, H_{61}), 3.62 – 3.38 (m, 4H, $H_{\alpha,\,2'eq}$), 3.04 (t, *J* = 13.0 Hz, 2H, $H_{2'ax}$), 2.07 (d, *J* = 14.2 Hz, 2H, $H_{3'eq}$), 1.93 – 1.61 (m, 3H, $H_{\beta,\,4'}$), 1.61 – 1.42 (m, 2H, $H_{3'ax}$). ^{13}C NMR (75 MHz, MeOD) δ 171.74 (C_4), 161.25 (C_9), 160.95 (C_6), 144.92 (C_2), 136.53 (C_{8a}), 132.47 (C_{o}), 131.19 (C_{p}), 130.42 (C_{i}), 130.30 (C_{m}), 129.05 (C_7), 124.45 (C_{4a}), 123.40 (C_8), 104.38 (C_3), 102.42 (C_5), 61.78 (C_{γ}), 56.69 (C_{61}), 53.71 ($C_{2'}$), 38.63 (C_{α}), 35.95 (C_{β}), 32.35 ($C_{4'}$), 30.35 ($C_{3'}$). HRMS [ESI+] *m/z* =419.2203 $[M]^+$, calcd for $[C_{25}H_{29}N_3O_3]^+$ 419.2209. HPLC purity 100%

***N*-(2-(1-benzylpiperidin-4-yl)ethyl)-6-hydroxy-4-oxo-1,4-dihydroquinoline-2-carboxamide. 3.14**

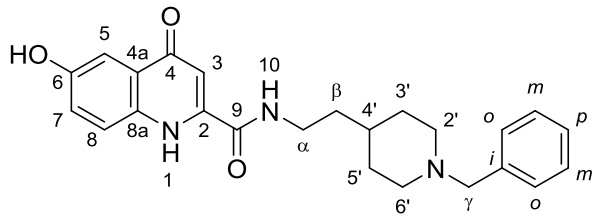

According to the general procedure 3.4, product **3.14** was obtained from 0.03 g (0.07 mmol) of **3.13** and 0.5 mmol of BBr_3 (1M in DCM, 0.5 mL). Purification was carried out by preparative TLC using EtOAc/MeOH 9:1 as eluent. White amorphous powder, 0,02 g (70%), mp:167 – 169 °C . ^{1}H NMR (500 MHz, DMSO-d_6) δ 11.71 (s, 1H, NH_1), 9.77 (s, 1H, OH), 8.93 (t, *J* = 5.7 Hz, 1H, NH_{10}), 7.82 (d, *J* = 8.7 Hz, 1H,

H_8), 7.56 – 7.42 (m, 5H, Ph), 7.36 (d, J = 2.9 Hz, 1H, H_5), 7.18 (dd, J = 8.7, 2.9 Hz, 1H, H_7), 6.59 (s, 1H, H_3), 4.28 (s, 2H, H_γ), 3.33 (s, 4H, $H_{\alpha,\ 2'eq}$), 2.98 – 2.84 (m, 2H, $H_{2'ax}$), 1.97 – 1.87 (m, 2H, $H_{3'eq}$), 1.63 – 1.45 (m, 3H, $H_{\beta,\ 4'}$), 1.44 – 1.34 (m, 2H, $H_{3'ax}$). ^{13}C NMR (126 MHz, DMSO-d_6) δ 177.38 (C_4), 162.40 (C_9), 154.51 (C_6), 140.61 (C_2), 133.75 (C_{8a}), 131.82 (C_o), 129.99 (C_i), 129.37 (C_p), 129.26 (C_m), 127.56 (C_{4a}), 123.12 (C_7), 121.57 (C_8), 107.32 (C_5), 105.44 (C_3), 59.60 (C_γ), 52.01 ($C_{2'}$), 37.02 (C_α), 35.09 (C_β), 30.87 ($C_{4'}$), 29.06 ($C_{3'}$). HRMS [ESI+] m/z =405.2059 $[M]^+$, calcd for $[C_{24}H_{27}N_3O_3]^+$ 405.2052. HPLC purity 100%

N-(2-(1-benzylpiperidin-4-yl)ethyl)-6,7-dimethoxy-4-oxo-1,4-dihydroquinoline-2-carboxamide. 3.15.

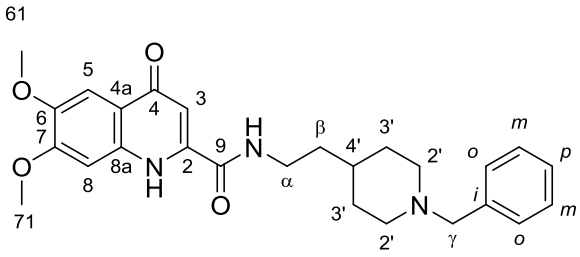

3.15 was synthesized as described in the general procedure 3.3, from esther **3.6** (0.12 g, 0.40 mmol) and 0.22 g (0.9 mmol) of 2-(1-benzylpiperidin-4-yl)ethan-1-amine). White amorphous solid, 0.1 g (50%), mp:254 - 256 °C. ^{1}H NMR (500 MHz, MeOD) δ 7.59 (s, 1H, H_8), 7.54 – 7.50 (m, 2H, H_o), 7.47 – 7.43 (m, 3H, $H_{m,\ p}$), 7.35 (s, 1H, H_5), 6.81 (s, 1H, H_5), 4.16 (s, 2H, H_γ), 4.00 (s, 3H, H_{71}), 3.96 (s, 3H, H_{61}), 3.50 (t, J = 6.7 Hz, 2H, H_{15}), 3.39 – 3.33 (m, 2H, $H_{2'eq}$), 2.85 (t, J = 12.6 Hz, 2H, $H_{2'ax}$), 2.01 (d, J = 13.2 Hz, 2H, $H_{3'eq}$), 1.70 – 1.63 (m, 3H, $H_{\beta,\ 4'}$), 1.60 – 1.48 (m, 2H, $H_{3'ax}$). ^{13}C NMR (126 MHz, MeOD) δ 163.85 (C_9), 156.23 (C_7), 150.05 (C_6), 142.81 (C_2), 138.37 (C_{8a}), 132.11 (C_o), 130.56 (C_p), 130.07 (C_m), 120.88 (C_{4a}), 106.42 (C_3), 104.27 (C_8), 101.21 (C_6), 62.03 (C_{23}), 56.78 (C_{71}), 56.50 (C_{61}), 53.64 ($C_{2'}$), 38.38 (C_α), 36.14 (C_β), 32.74 ($C_{4'}$), 30.60 ($C_{3'}$). C4a, C2 Ci not observed. HRMS [ESI+] m/z =449.2315 $[M]^+$, calcd for $[C_{26}H_{31}N_3O_4]^+$ 449.2315. HPLC purity 100%

***N*-(2-(1-benzylpiperidin-4-yl)ethyl)-7-methoxy-4-oxo-1,4-dihydroquinoline-2-carboxamide. 3.16**

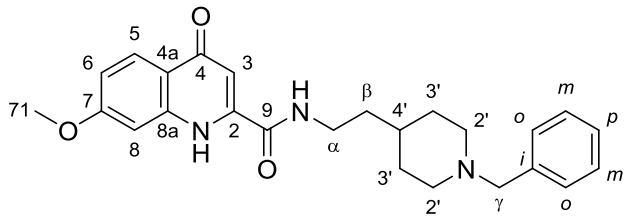

According to the general procedure 3.3, compound **3.16** was obtained from 0.1 g (0,43 mmol) of **3.7** and 0.23 g (1,07 mmol) of 2-(1-benzylpiperidin-4-yl)ethan-1-amine as a white amorphous solid, 0.116 g (65%), mp:200 -203 °C. ^{1}H NMR (300 MHz, MeOD) δ 8.27 (d, *J* = 9.4 Hz, 1H, H_5), 7.69 – 7.39 (m, 7H, Ph, $H_{3,\ 8}$), 7.37 (dd, *J* = 9.4, 2.3 Hz, 1H, H_6), 4.30 (s, 2H, H_γ), 4.02 (s, 3H, H_{71}), 3.58 – 3.41 (m, 4H, $H_{\alpha,\ 2'eq}$), 3.05 (t, *J* = 12.5 Hz, 2H, $H_{2'ax}$), 2.06 (d, *J* = 14.2 Hz, 2H, $H_{3'eq}$), 1.80 – 1.44 (m, 5H, $H_{\beta,\ 4',\ 3'ax}$). ^{13}C NMR (75 MHz, MeOD) δ 172.32 (C_4), 167.01 (C_7), 160.96 (C_9), 146.61 (C_2), 143.66 (C_{8a}), 132.49 (C_o), 131.14 (C_p), 130.45 (C_i), 130.26 (C_m), 126.58 (C_5), 122.17 (C_6), 117.00 (C_{4a}), 103.81 (C_3), 100.32 (C_8), 61.73 (C_γ), 57.04 (C_{71}), 53.68 ($C_{2'}$), 38.64 (C_α), 35.88 (C_β), 32.29 ($C_{4'}$), 30.32 ($C_{3'}$). HRMS [ESI+] *m/z* =419.2212 $[M]^+$, calcd for $[C_{25}H_{29}N_3O_3]^+$ 419.2209. HPLC purity 100%

***N*-(2-(1-benzylpiperidin-4-yl)ethyl)-8-methoxy-4-oxo-1,4-dihydroquinoline-2-carboxamide. 3.17**

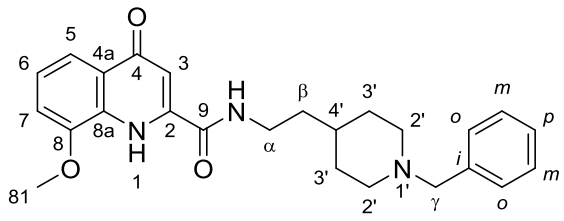

According to the general procedure 3.3, amide **3.17** was obtained from 0.1 g (0,43 mmol) of **3.8** and 0.23 g (1,07 mmol) of 2-(1-benzylpiperidin-4-yl)ethan-1-amine as a white amorphous solid, 0.108 g (60%), mp: 187 - 189 °C. ^{1}H NMR (500 MHz, MeOD) δ 7.80 (bs, 1H, CH), 7.56 – 7.49 (m, 6H, CH, Ph), 7.41 (bs, 1H, CH), 7.37 – 7.32 (m, 1H, CH), 6.89 (bs, 1H, NH), 4.30

(s, 2H, H_{γ}), 4.11 (s, 3H, H_{81}), 3.54 – 3.49 (m, 4H, $H_{\alpha,\ 2'eq}$), 3.06 – 2.98 (m, 2H, $H_{2'ax}$), 2.09 (d, *J* = 13.7 Hz, 2H, $H_{3'eq}$), 1.78 – 1.62 (m, 3H, $H_{4',\beta}$), 1.59 – 1.45 (m, 2H, $H_{3'ax}$). ^{13}C NMR (126 MHz, MeOD) δ 172.97 (C_4), 163.29 (C_9), 150.74 (C_8), 132.47 (C_o), 132.05 (C), 131.26 (C_p), 130.50 (C), 130.37 (C_i), 130.36 (C_m), 126.28 (CH), 116.99 (CH), 112.78 (CH), 61.95 (C_{γ}), 57.10 (C_{81}), 53.88 ($C_{2'}$), 38.38 (C_{α}), 36.16 (C_{β}), 32.44 ($C_{4'}$), 30.43 ($C_{3'}$). HRMS [ESI+] *m/z* =419.2207 $[M]^+$, calcd for $[C_{25}H_{29}N_3O_3]^+$ 419.2209. HPLC purity 100% CH's not assignable, CH-3 in ^{13}C not detected

_N_-(2-(1-benzylpiperidin-4-yl)ethyl)-8-hydroxy-4-oxo-1,4-dihydroquinoline-2-carboxamide. 3.18

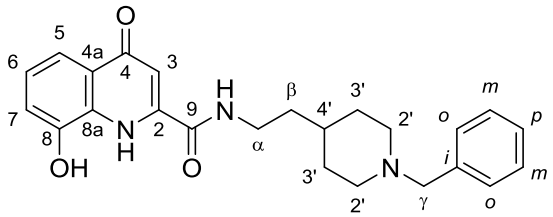

According to the general procedure 3.4; product **3.18** was obtained from 0.07 g (0.17 mmol) of **3.17** and 1.17 mmol of BBr_3 (1M in DCM, 1.2 mL). After column chromatography purification (DCM:MeOH 9:1), the product was obtained as a white amorphous powder 0,061 g (90%), mp: 184 - 187 °C. ^{1}H NMR (500 MHz, MeOD) δ 7.72 (dd, *J* = 8.4, 1.2 Hz, 1H, H_5), 7.57 – 7.46 (m, 6H, Ph, H_3), 7.41 (dd, *J* = 8.4, 7.6 Hz, 1H, H_6), 7.24 (bs, 1H, NH), 7.19 (dd, *J* = 7.6, 1.2 Hz, 1H, H_7), 4.30 (s, 2H, H_{γ}), 3.54 (t, *J* = 6.8 Hz, 2H, H_{α}), 3.52 – 3.48 (m, 2H, $H_{2'eq}$), 3.08 – 2.99 (m, 2H, $H_{2'ax}$), 2.11 (d, *J* = 14.5 Hz, 2H, $H_{3'eq}$), 1.80 – 1.71 (m, 1H, $H_{4'}$), 1.68 (q, *J* = 6.8 Hz, 2H, H_{β}), 1.54 – 1.43 (m, 2H, $H_{3'ax}$). ^{13}C NMR (126 MHz, MeOD) δ 164.66 (C_9), 132.38 (C_o), 131.29 (C_p), 130.37 (C_m), 127.84 (C_6), 114.76 (CH), 61.87 (C_{γ}), 53.77 ($C_{2'}$), 38.08 (C_{α}), 36.29 (C_{β}), 32.37 ($C_{4'}$), 30.45 ($C_{3'}$). HRMS [ESI+] *m/z* =405.2053 $[M]^+$, calcd for $[C_{24}H_{27}N_3O_3]^+$ 405.2052. HPLC purity 99% quaternary carbons not observed

***N*-(2-(1-benzylpiperidin-4-yl)ethyl)-4,6,7-trimethoxyquinoline-2-carboxamide. 3.19.**

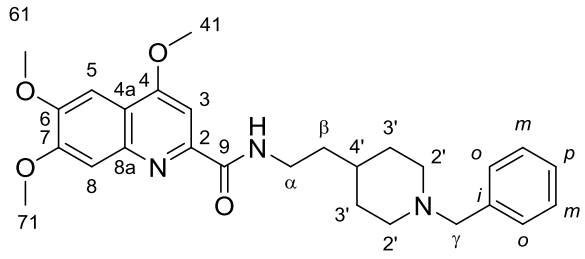

According to the general procedure 3.4, product **3.19** was obtained from 0.05 g (0.18 mmol) of **3.10** and 0.059 g (0.27 mmol) of 2-(1-benzylpiperidin-4-yl)ethan-1-amine as a white amorphous solid, 0.054 g (65%), mp:182 - 184 °C. ^{1}H NMR (500 MHz, $CDCl_3$) δ 8.45 (s, 1H, H_8), 8.07 (s, 1H, H_3), 7.67 – 7.56 (m, 2H, H_m), 7.44 (s, 1H, H_5), 7.40 – 7.33 (m, 3H, $H_{o,\,p}$), 4.35 (s, 3H, H_{41}), 4.11 (s, 5H, $H_{71,\,\gamma}$), 4.05 (s, 3H, H_{61}), 3.66 – 3.52 (m, 2H, H_α), 3.51 – 3.38 (m, 2H, $H_{2'eq}$), 2.90 – 2.62 (m, 2H, $H_{2'ax}$), 2.06 – 1.92 (m, 5H, $H_{4',\,3'}$), 1.78 – 1.60 (m, 2H, H_β). ^{13}C NMR (126 MHz, $CDCl_3$) δ 167.05 (C_4), 158.28 (C_9), 157.03 (C_7), 152.21 (C_6), 143.69 (C_2), 137.12 (C_{8a}), 131.62 (C_m), 130.03 (C_p), 129.25 (C_o), 128.48 (C_i), 116.90 (C_{4a}), 101.10 (C_3), 100.09 (C_8), 77.41 (C_5), 61.15 (C_γ), 58.62 (C_{41}), 57.35 (C_{71}), 56.72 (C_{61}), 52.79 ($C_{2'}$), 37.67 (C_α), 34.32 (C_β), 30.98 ($C_{4'}$), 28.80 ($C_{3'}$). HRMS [ESI+] *m/z* =463.24746 $[M]^+$, calcd for $[C_{27}H_{33}N_3O_4]^+$ 463.24711. HPLC purity 100%

***N*-(4-((benzyl(methyl)amino)methyl)phenyl)-5-methoxy-4-oxo-1,4-dihydroquinoline-2-carboxamide. 3.20**

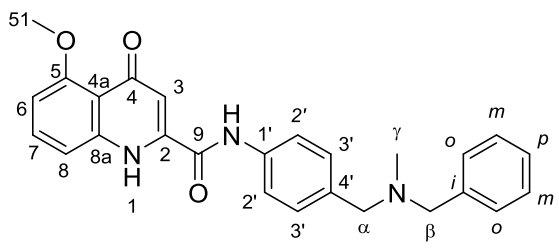

3.20 was synthesized as described in the general procedure 3.3, from 0.11 g (0.48 mmol) of amine **1.8** and a mixture containing 80% of **3.7** and 20% of its isomer bearing the methoxy group at position 5. This reaction yielded both **3.23** 0,04 g (60%) and **3.20** 0,01 g (61%). Light

brown amorphous solid. mp 263 - 265 °C. ^{1}H NMR (500 MHz, $CDCl_3$) δ 10.20 (s, 1H NH_{10}), 9.88 (s, 1H, NH_1), 7.80 (d, *J* = 8.3 Hz, 2H, $H_{2'}$), 7.75 (s, 1H, H_3), 7.73 (d, *J* = 0.9 Hz, 1H, H_8), 7.63 (t, *J* = 7.8 Hz, 1H, H_7), 7.46 – 7.36 (m, 4H, $H_{3', o}$), 7.34 (t, *J* = 7.5 Hz, 2H, H_m), 7.29 – 7.26 (m, 1H, H_p), 6.92 (dd, *J* = 7.8, 0.9 Hz, 1H, H_6), 4.13 (s, 3H, H_{51}), 3.57 (s, 4H, $H_{\alpha, \beta}$), 2.23 (s, 3H, H_γ). ^{13}C NMR (126 MHz, $CDCl_3$) δ 164.19 (C_4), 162.09 (C_9), 156.07 (C_5), 152.06 (C_2), 149.81 (C_{8a}), 136.90 ($C_{1'}$), 135.49 ($C_{4'}$), 130.07 (C_7), , 129.88 ($C_{3'}$), 129.23 (C_o), 128.45 (C_m), 127.25 (C_p), 1213.37 (C_8), 119.77 ($C_{2'}$), 112.61 (C_{4a}), 105.39 (C_6), 104.34 (C_3), 61.84 (C_α), 61.49 (C_β), 56.76 (C_{51}), 42.24 (C_γ). C*i* not detected. HRMS [ESI+] *m/z* =427.1900 $[M]^+$, calcd for $[C_{26}H_{25}N_3O_3]^+$ 427.1896. HPLC purity 99%

_N_-(4-((benzyl(methyl)amino)methyl)phenyl)-6-methoxy-4-oxo-1,4-dihydroquinoline-2-carboxamide. 3.21

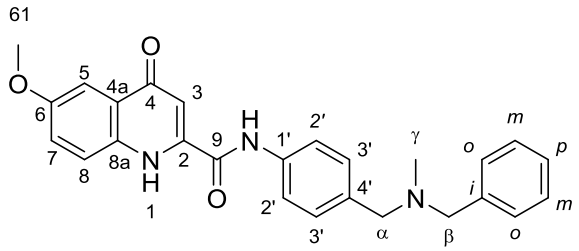

3.21 was synthesized as described in the general procedure 3.3, from 0.22 g of **1.8** and **3.5** (0.1 g, 0.43 mmol). White amorphous solid, 0.049 g (60%), mp:261 - 264 °C. ^{1}H NMR (500 MHz, DMSO-d_6) δ 10.61 (s, 1H, NH), 7.96 (d, *J* = 9.1 Hz, 1H_8), 7.82 (d, *J* = 8.0 Hz, 2H, $H_{2'}$), 7.49 (d, *J* = 2.9 Hz, 1H, H_5), 7.40 (dd, *J* = 9.1, 2.9 Hz, 1H, H_7), 7.38 – 7.30 (m, 7H, $H_{3, 3', o, m}$), 7.28 – 7.23 (m, 1H, H_p), 3.89 (s, 3H, H_{61}), 3.50 (s, 2H, H_β), 3.48 (s, 2H, H_α), 2.08 (s, 3H, H_γ). ^{13}C NMR (126 MHz, DMSO-d_6) δ 157.07 (C_6), 139.09 (C_i), 136.99 ($C_{4'}$), 134.98 ($C_{1'}$), 128.98 ($C_{3'}$), 128.60 (C_m), 128.20 (C_o), 126.88 (C_p), 122.98 (C_7), 120.18 ($C_{2'}$), 60.97 (C_β), 60.57 (C_α), 55.43 (C_{61}), 41.63 (C_γ). C_3 and quaternary carbons of chromone ring not detected. HRMS [ESI+] *m/z* =427.1905 $[M]^+$, calcd for $[C_{26}H_{25}N_3O_3]^+$ 427.1896. HPLC purity 99%

***N*-(4-((benzyl(methyl)amino)methyl)phenyl)-6-hydroxy-4-oxo-1,4-dihydroquinoline-2-carboxamide. 3.22**

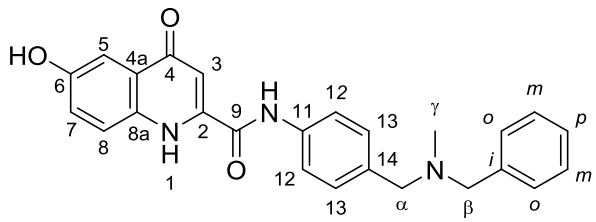

According to the general procedure 3.4, product **3.22** was obtained from 0.022 g (0.051 mmol) of **3.21** and 0.4 mmol of BBr_3 (0.4 mL, 1M in DCM). Purification MeOH in EtOAc (0→80%), white amorphous powder (90%). mp: 248 -251 °C. ^{1}H NMR (300 MHz, DMSO-d_6) δ 10.56 (s, 1H, NH), 7.90 (s, 1H), 7.82 (d, J = 8.3 Hz, 2H), 7.53 – 7.15 (m, 9H), 3.50 (s, 2H, CH_2), 3.48 (s, 2H, CH_2), 2.08 (s, 3H, CH_3). ^{13}C NMR (75 MHz, DMSO-d_6) δ 139.08 (C), 137.00 (C), 128.96 ($C_{3'}$), 128.58 (C_o), 128.18 (C_m), 126.86 (C_p), 122.80 (CH), 120.14 ($C_{2'}$), 60.95 (CH_2), 60.56(CH_2), 41.61(CH_3). Some quaternary carbons detected but not assignable just one CH detected. HRMS [ESI+] *m/z* =413.1751 $[M]^+$, calcd for $[C_{25}H_{23}N_3O_3]^+$ 413.1739. HPLC purity 99%

***N*-(4-((benzyl(methyl)amino)methyl)phenyl)-7-methoxy-4-oxo-1,4-dihydroquinoline-2-carboxamide. 3.23**

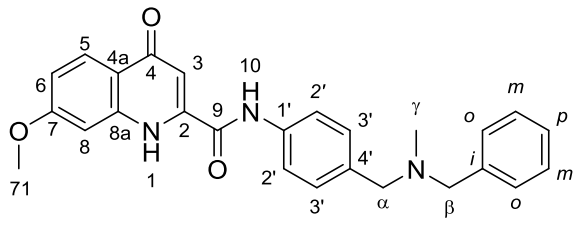

Compound **3.23** was synthesized as described in the general procedure 3.3, from 0.105 g (0.48 mmol) of amine **1.8** and **3.7** (0.045 g, 0.19 mmol). Light brown amorphous solid, 0.051 g (62%). mp: 240 - 243 °C. ^{1}H NMR (300 MHz, DMSO-d_6) δ 11.73 (s, 1H, NH_1), 10.63 (s, 1H, NH_{10}), 8.01 (d, J = 9.0 Hz, 1H, H_5), 7.79 (d, J = 8.1 Hz, 2H, $H_{2'}$), 7.50 – 7.42 (m, 1H, H_8), 7.40 – 7.29 (m, 6H, $H_{3',\ o,\ m}$), 7.28 – 7.19 (m, 1H, H_p), 6.99 (bs, 1H, H_6), 6.86 (bs, 1H, H_3), 3.87 (s, 3H, H_{71}), 3.50 (s, 2H, H_β), 3.49 (s, 2H,

H_{α}), 2.08 (s, 3H, H_{γ}). ^{13}C NMR (75 MHz, DMSO-d_6) δ 177.03 (C_4), 162.28 (C_7), 160.65 (C_9), 139.04 (C_i), 136.88 ($C_{1'}$), 135.22 ($C_{4'}$), 128.98 ($C_{3'}$), 128.59 (C_m), 128.18 (C_o), 126.87 (C_p), 126.44 (C_5), 120.43 ($C_{2'}$), 113.96 (C_6), 107.56 (C_3), 100.31 (C_8), 60.96 (C_{β}), 60.53 (C_{α}), 55.45 (C_{71}), 41.59 (C_{γ}). HRMS [ESI+] *m/z* =427.1898 $[M]^+$, calcd for $[C_{26}H_{25}N_3O_3]^+$ 427.1896. HPLC purity 99%

_N_-(4-((benzyl(methyl)amino)methyl)phenyl)-6,7-dimethoxy-4-oxo-1,4-dihydroquinoline-2-carboxamide. 3.24

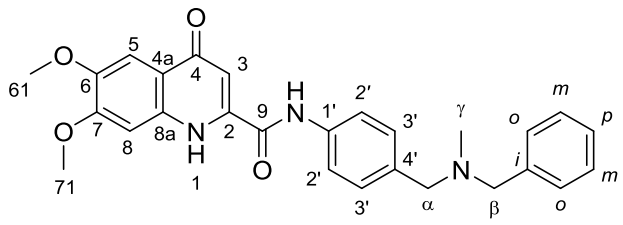

Product **3.24** was synthesized as described in the general procedure 3.3, starting from 0.045 g (0.19 mmol) of **3.6** and 0.11 g, (0.48 mmol) of amine **1.7**. White amorphous solid, 0,028 g (35%), mp:245 - 248 °C. ^{1}H NMR (500 MHz, MeOD) δ 7.79 (d, *J* = 8.2 Hz, 2H, $H_{2'}$), 7.59 (s, 1H, $H_{(5 \text{ or } 8)}$), 7.42 (d, *J* = 8.2 Hz, 2H, $H_{3'}$), 7.48 – 7.25 (m, 7H, $H_{(8 \text{ or } 5),\ 3,\ o,\ m,\ p}$), 7.05 (bs, 1H, NH), 4.00 (s, 3H, O-CH_3), 3.96 (s, 3H, O-CH_3), 3.70 (bs, 4H, $H_{\alpha,\ \beta}$), 2.30 (s, 3H, H_{γ}). ^{13}C NMR (126 MHz, MeOD) δ 156.16 (C-OCH_3), 150.33 (C-OCH_3), 138.73 (C_{14}), 137.98 (C_i), 134.68 (C_{11}), 131.33 (C_{13}), 130.76 (C_o), 129.57 (C_m), 128.89 (C_p), 122.06 (C_{12}), 103.89 (CH), 62.32 (C_{17}), 61.85 (C_{15}), 56.70 (C_{71}), 56.48 (C_{61}), 41.82 (C_{16}). CH's and quaternary carbons not detected. HRMS [ESI+] *m/z* =457.2009 $[M]^+$, calcd for $[C_{27}H_{27}N_3O_4]^+$ 457.2002. HPLC purity 100%

***N*-(4-((benzyl(methyl)amino)methyl)phenyl)-6,7-dihydroxy-4-oxo-1,4-dihydroquinoline-2-carboxamide. 3.25**

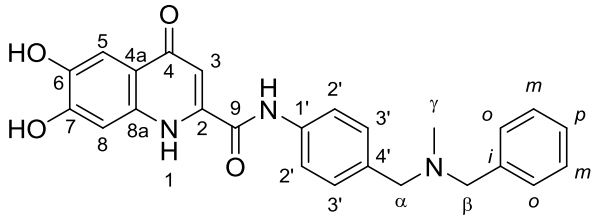

According to the general procedure 3.4, product **3.25** was obtained from 0.018 g (0.04 mmol) of **3.24** and 0.4 mmol of BBr_3 (0.4 mL, 1M in DCM). Purification (MeOH in EtOAc 0→60%), white amorphous powder, 0,015 (90%), mp: 248 -251 °C. ^{1}H NMR (500 MHz, MeOD) δ 7.99 (d, *J* = 8.1 Hz, 2H, $H_{2'}$), 7.64 (d, *J* = 8.1 Hz, 2H, $H_{3'}$), 7.62 (s, 1H, H_3), 7.60 – 7.55 (m, 2H, H_m), 7.54 – 7.50 (m, 5H, $H_{5,\ 8,\ o,\ p}$), 4.58 – 4.51 (m, 2H, H_α), 4.39 – 4.30 (m, 2H, H_β), 2.77 (s, 3H, H_γ). ^{13}C NMR (126 MHz, MeOD) δ 194.03 (C_4), 170.55 (C_9), 160.79 (C), 156.94 (C_7), 150.15 (C_6), 143.73 (C), 140.71 ($C_{4'}$), 133.97 (C), 133.26 ($C_{3'}$), 132.39 (C_o), 131.31 (C_p), 130.77 (C_i), 130.45 (C_m), 127.38 ($C_{1'}$), 122.65 ($C_{2'}$), 118.34 (C_8), 111.41 (C), 105.80 (C_3), 103.76 (C_5), 60.76 (C_α), 60.30 (C_β), 39.55 (C_γ). HRMS [ESI+] *m/z* =429.1700 $[M]^+$, calcd for $[C_{25}H_{23}N_3O_4]^+$ 429.1689. HPLC purity 99%

***N*-(3-((benzyl(methyl)amino)methyl)phenyl)-6,7-dimethoxy-4-oxo-1,4-dihydroquinoline-2-carboxamide. 3.26**

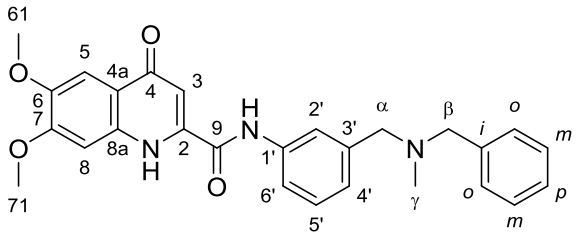

Product **3.26** was synthesized as described in the general procedure 3.3, from 0.05 g (0.19 mmol) of **3.6** and 0.085 g of **1.7** (0.38 mmol). Light brown amorphous solid, 0.078 g (90%). mp: 131 - 133 °C.^{1}H NMR (500 MHz, MeOd) δ 7.92 (s, 1H, $H_{2'}$), 7.76 (dd, *J* = 7.6, 1.3 Hz, 1H, $H_{6'}$), 7.55 (s, 1H, CH), 7.50 – 7.38 (m, 7H, Ph, CH, $H_{5'}$), 7.31 (s, 1H, CH), 7.27 (dt, *J* = 7.7, 1.3 Hz, 1H, $H_{4'}$), 4.04 – 4.00 (bs, 4H, $H_{\alpha,\ \beta}$), 3.99 – 3.98 (m, 3H, OCH_3),

3.94 (s, 3H, OCH_3), 2.51 (s, 3H, H_γ). ^{13}C NMR (126 MHz, MeOD) δ 156.08 (C_6), 150.35 (C_7), 139.66 ($C_{1'}$), 131.43 (C_o), 130.54 (C_p), 129.98 (C_m), 129.98 ($C_{5'}$), 127.84 ($C_{4'}$), 123.80 ($C_{2'}$), 122.42 ($C_{6'}$), 103.75 (CH), 61.75 (C_β), 61.58 (C_α), 56.68 (O-CH_3), 56.45 (O-CH_3), 41.00 (C_γ). Quaternary carbons not observed and just one CH detected HRMS [ESI+] *m/z* =457.2002 $[M]^+$, calcd for $[C_{27}H_{27}N_3O_3]^+$ 457.2001. HPLC purity 100%

NMDA receptor agonist radioligand displacement. Affinity of compounds for the NMDA receptor was carried out in the rat cerebral cortex by CEREP Co.[258] Membrane homogenates of cerebral cortex (1 mg protein) are incubated for 60 min at 4°C with 5 nM [^{3}H]CGP 39653 in the absence or presence of the test compound in a buffer containing 5 mM Tris-HCl (pH 7.7) and 10 mM EDTA-Tris. Nonspecific binding is determined in the presence of 100 μM

L-glutamate. Following incubation, the samples are filtered rapidly under vacuum through glass fiber filters (GF/B, Whatman) and rinsed several times with ice-cold incubation buffer using a 48-sample cell harvester (Brandel). The filters are dried then counted for radioactivity in a scintillation counter (LS series, Beckman) using a scintillation cocktail (Formula 989, Packard). The results are expressed as a percent inhibition of the control radioligand specific binding. The standard reference compound is CGS 19755, which is tested in each experiment at several concentrations to obtain a competition curve from which its IC_{50} is calculated.

Chapter 4

Cinnamic-Based Antioxidants as Multitarget Compounds for the Treatment of Alzheimer's disease

Introduction

Although nowadays it is widely accepted that neuronal loss in neurodegenerative diseases is the outcome of a wide variety of factors, one of the most accepted factors explaining the origin of diseases like AD or PD is the oxidative stress.[259] The oxidative stress hypothesis states that neuronal death results from the toxicity exerted by free radical species. These reactive entities are able to interact with lipidic molecules in cellular membranes, altering their composition, function and permeability. Not only unsaturated fatty acids in membranes are affected by free radicals; arachidonic acid and docosahexaenoic acid, two important molecules which concentration reaches the highest levels in brain, are susceptible to be oxidized under oxidative conditions. Byproducts from peroxidation of unsaturated acids include highly reactive and toxic species such as 4-hydroxynonenal (HNE), malondialdehyde (MDA) and acrolein, which seems to be especially increased in AD.[260-262]

In spite of the effective system of the human body to counteract the harmful effects of oxidative metabolism (superoxide dismutase (SOD), aldehyde dehydrogenase and glutathione peroxidase), the brain is particularly sensitive to oxidative damage due to its great requirement of oxygen, its high levels of unsaturated acids and relatively low levels of antioxidant enzymes.[263]

Several investigations have demonstrated a correlation between the severity and advance of AD and free radicals. Moreover, Aβ has been proven to induce the production of H_2O_2 by reduction of metals such as iron and copper.[264] Simultaneously, Aβ is able to stimulate glial cells, enhancing the production of an oxidative environment and pro-inflammatory molecules.[10,265,266]

According to the oxidative stress hypothesis, antioxidants and metal chelators could play an important role in prevention and therapy of AD. Among the most investigated natural antioxidants, are some derivatives of cinnamic acid (e.g., ferulic, caffeic, coumaric and umbellic acid) and natural molecules containing its structure, such as curcumin or some bioactive chalcones.[267-272] (Figure 4.1)

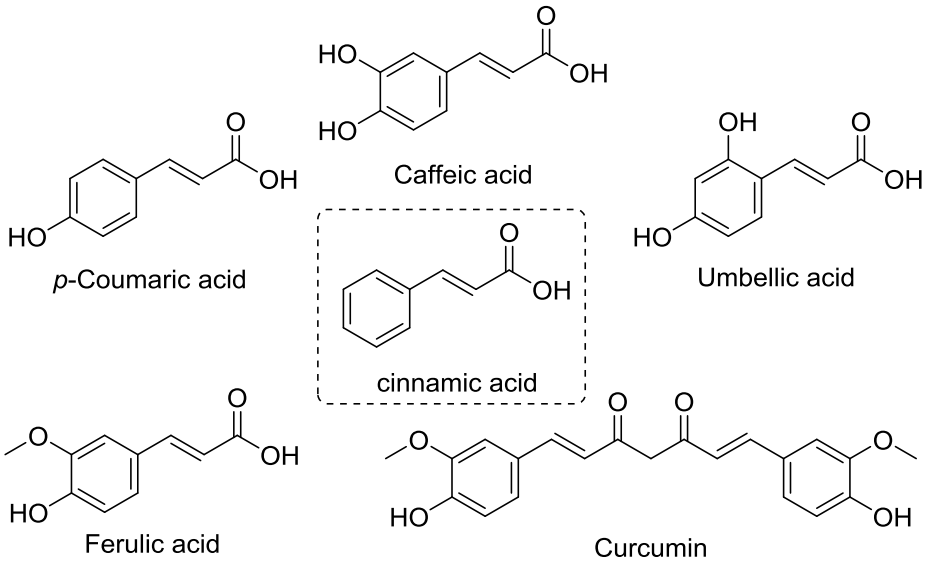

Figure 4.1 Natural antioxidants containing the cinnamic acid structure

Antioxidant molecules *per se* might not be sufficient to treat or prevent AD, as shown by the ambiguous results obtained from several clinical trials with this kind of compounds.[273] In light of this, here we propose the synthesis of hybrid molecules resulting from the combination of the privileged structures NBP and DBMA with several natural antioxidant

molecules derived from the cinnamic acid, in order to obtain multitarget directed molecules with enhanced antioxidant capacity and able to inhibit simultaneously cholinesterases, MAO or BACE1.

Results and discussion

Synthesis of Cinnamic acid-based Hybrids

Commercially available cinnamic-derived acids were used to be coupled to amines carrying the NBP and DBMA fragments used along this work. Coupling reaction was carried out by activation of the corresponding acids with CDI in THF at 120 °C during 10 min and subsequent reaction with the proper amine during 10-40 min depending on its character, aliphatic or aromatic (scheme 4.1).

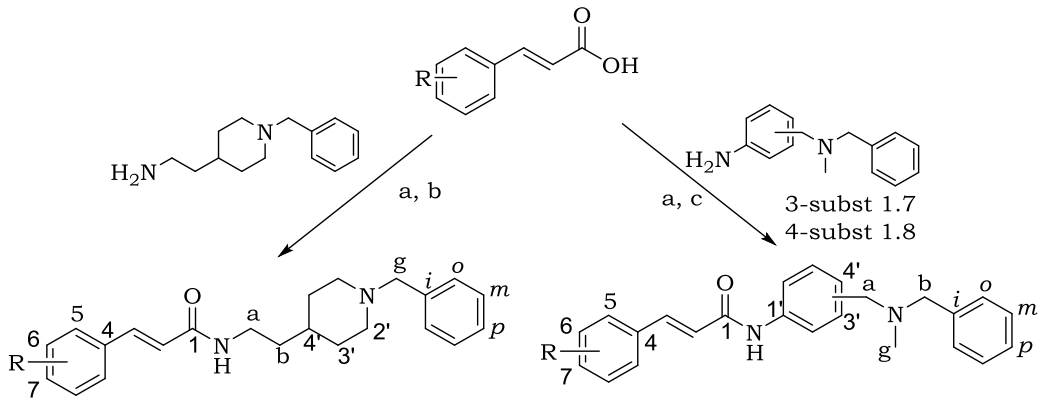

4.1, R = 6,7-diOMe (75%)
4.2, R = 6-OMe (70%)
4.3, R = 7-OMe (77%)
4.4, R = 5,7-diOMe (90%)
4.5, R = 6-OMe,7-OH (85%)
4.6, R = 6-OH (97%)
4.7, R = 7-OH (85%)
4.8, R = 5,7-diOH (55%)
4.9, R = 6,7-diOH (55%)

4.10, R = 5,7-diOMe (60%)
4.11, R = 6,7-diOMe (60%)
4.12, R = 6-OMe,7-OH (3'-subst) (65%)
4.13, R = 6-OMe,7-OH (63%)
4.14, R = 6-OMe (80%)
4.15, R = 7-OMe (65%)
4.16, R = 6-OH (65%)
4.17, R = 7-OH (57%)

(All DBMA derivatives are 4'-substituted, except **4.12**)

Scheme 4.1 Synthesis of Cinnamic acid-based hybrids (a) CDI, THF, mw, 5 min, 120 °C; (b) 2-(1-benzylpiperidin-3-yl)ethan-1-amine, mw, 10 min, 120 °C; (c) Amine (**1.7**, **1.8**), mw, 40 min, 120 °C; (d) BBr_3, THF, rt, overnight

Deprotection of the methoxy groups was accomplished by treatment with BBr_3, as described in previous chapters. Scheme 4.1

Biological Evaluation

As explained above, we aimed to obtain better antioxidants than the chromone-based compounds synthesized in chapter two, improving, or at least preserving affinity for MAO and cholinesterases. Although we found that NBP containing hybrids (**4.4**) are included in an patent of year 1989,[274] we decided to synthesize a short series of these compounds, besides DBMA hybrids, in order to evaluate them as MAO inhibitors, since the privileged structure of cinnamic acid is contained in several chalcones with MAO inhibitory activity as explained above.[271,272]

Table 4.1 Inhibition of human cholinesterases (hAChE and hBuChE) and monoaminoxidases (MAO-A and MAO-B) (IC_{50}, μM); ORAC, trolox equivalents.

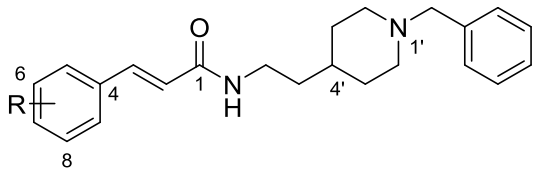

		IC_{50} (μM)		**ORAC**
Comp.	R	**hAChE**	**hBuChE**	Trolox Eq.
4.1	6,7-OMe	0.26±0.04	0.69±0.10	0.4±0.04
4.2	6-OMe	0.75±0.10	0.98±0.12	NA
4.3	7-OMe	0.49±0.06	0.76±0.20	NA
4.4	5,7-OMe	0.63±0.08	4.39±0.86	NA
4.5	6-OMe,7-OH	0.39±0.05	0.076±0.01	1.8±0.2
4.6	6-OH	1.12±0.10	1.02±0.21	2.2±0.1
4.7	7-OH	1.01±0.08	0.93±0.16	1.7±0.1
4.8	5,7-OH	0.99±0.10	0.26±0.08	1.3±0.6
4.9	6,7-OH	1.75±0.12	0.69±0.12	1.0±0.1

Results are expressed as mean ± SD ([a]n =3, [b]n =5), **Inactive at 200 μM, *** inactive at 1 mM, NA: not antioxidant

Although we preferred the hydroxy substituted compounds because their potential antioxidant capacity, all derivatives were assessed as inhibitors of MAO, AChE and BuChE.

Hydroxy derivatives exhibited good antioxidant capacity in both series (NBP and DBMA). *m*-Coumaric derived hybrids **4.6** and **4.16** (6-OH substituted), exhibited the best results in ORAC assay, with trolox equivalents up to 2.2 and 3.2 in the NBP and DBMA series respectively. Simultaneously, they inhibit both cholinesterases in the low micromolar range but were unable to inhibit any isoform of MAO (Table 4.1).

In the NBP series, the best multitarget profile was achieved by ferulic-based compound **4.5**, with antioxidant capacity of 1.8 trolox equivalents, potent inhibitory activity towards BuChE and moderate none-selective inhibitory activity towards MAO-A and MAO-B (IC_{50} = 76 nM, 11 µM and 13 µM respectively). Di-hydroxy substituted compounds **4.9** and **4.8** exhibited a similar profile with IC_{50}'s in the low micromolar range for the cholinesterases and both isoforms of MAO (Tables 4.2 and 4.3). Although less potent, **4.7** was the one of this series able to inhibit selectively MAO-A with an IC_{50} of 57 µM.

The cinnamic-DBMA series provided moderated inhibitors of AChE with low micromolar IC_{50}'s (table 4.3). **4.17** was inactive towards the cholinesterases but a moderated inhibitor of MAO-A and MAO-B (IC_{50} = 29.7 and 29.0 µM respectively). Interestingly, in this series only compound **4.12** (ferulic derivative with a DBMA fragment at position 3') exhibited a multitarget profile, with low micromolar IC_{50}'s in all tested targets (h-AChE: 6.0 µM; h-BuChE: 5.9 µM; MAO-A: 4.5 µM; MAO-B: 7.7 µM) and antioxidant capacity of 1.5 trolox equivalents. The rest of compounds were inactive as MAO inhibitors.

Table 4.2 Inhibition of h-AChE, h-BuChE (IC_{50}, μM); ORAC

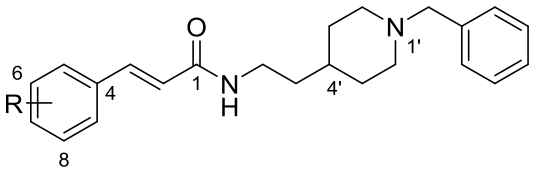

		IC_{50} (μM)		**ORAC**
Comp.	R	**MAO-A**[b]	**MAO-B**[b]	Trolox Eq.
4.1	6,7-OMe	**	**	0.4±0.04
4.2	6-OMe	**	**	NA
4.3	7-OMe	**	**	NA
4.4	5,7-OMe	**	**	NA
4.5	6-OMe,7-OH	11.37±0.76	13.13±0.88	1.8±0.2
4.6	6-OH	***	**	2.2±0.1
4.7	7-OH	57.45 ± 3.8	**	1.7±0.6
4.8	5,7-OH	5.48±0.37	8.31 ± 0.55	1.3±0.6
4.9	6,7-OH	3.50±0.23	5.98 ± 0.4	1.04±0.1

Results are expressed as mean ± SD ([a]n =3, [b]n =5), **Inactive at 200 μM, *** inactive at 1 mM, NA: not antioxidant

Both series resulted inactive as BACE1 inhibitors. Only compounds **4.14**, **4.15**, **4.13** and **4.12** were capable to inhibit poorly this enzyme with percentages around 23-33% at 10 μM (table 4.3).

Table 4.3 Inhibition of h-AChE, h-BuChE, MAO-A/B (IC_{50}, μM)

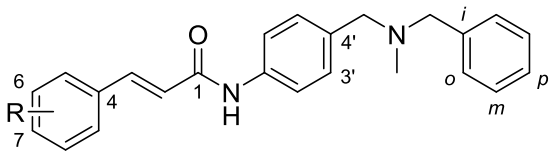

		IC_{50} (μM)		**ORAC**	**hBACE1**
Comp.	R	**h-AChE**[a]	**h-BuChE**[b]	Trolox Eq	%inh*
4.10	5,7-OMe	8.73±0.92	>10	0.5±0.10	14%
4.11	6,7-OMe	3.98±0.29	>10	0.4±0.08	18%
4.12	6-OMe,7-OH	5.99±0.49	5,89±0,48	1.4±0.11	23%
4.13	6-OMe,7-OH	33%*	45%*	1.5±0.18	33%
4.14	6-OMe	4.67±0.31	35%*	0.6±0.06	32%
4.15	7-OMe	5.76±0.40	25%*	NA	25%
4.16	6-OH	3.49±0.31	46%*	3.2±0.2	8%
4.17	7-OH	46%*	30%*	1.8±0.14	5%

* % at a concentration of 10 μM; results are expressed as mean ± SD where n =3, NA: not antioxidant.

4.16 the best antioxidant, **4.5**, the most potent BuChE inhibitor and **4.13**, were evaluated as neuro-protectants in the MTT assay described previously. These compounds protected around 30-35% of cells at a concentration of 0.3 μM; however, a dose dependent relationship was not observed in these experiments, higher doses were not able to protect the cells. Nevertheless, in any case they did not potentiate the toxicity exerted by rotenone/oligomycin, which could be assumed as a lack of toxicity of our newly obtained hybrids.

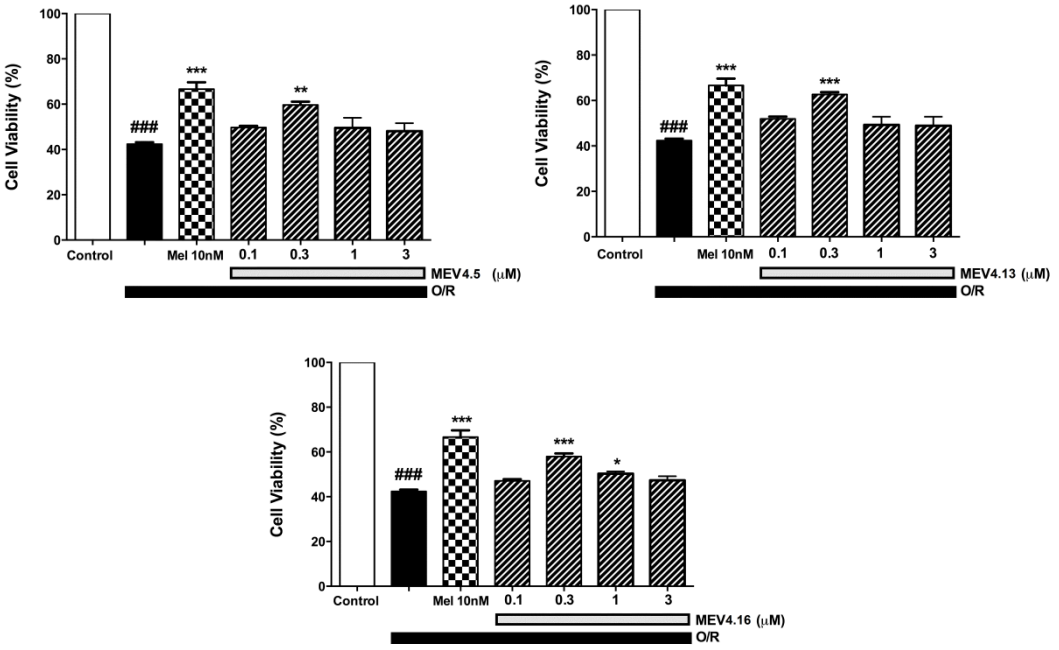

Figure 4.2 Cell viability was measured as MTT reduction and data were normalized as % of control. Data are expressed as the means ± SEM. of triplicate of at least three different cultures. All compounds were assayed at increasing concentrations (0.1-3 μM)

4.5, **4.6**, **4.16** and **4.13** were evaluated as anti-aggregating agents in bacterial cells overexpressing *tau* protein and $A\beta_{42}$ peptide. All compounds resulted inactive at 20 μM except **4.16**; it was able to inhibit 23% and 21% of the self-catalyzed aggregation of *tau* and $A\beta_{42}$ respectively.

A selection of compounds including methoxy, hydroxy and di-hydroxy-substituted derivatives from both series was evaluated in PAMPA assay. Table 4.4 summarizes the values of permeability for these products and those predicted for 10 known standard drugs. All DBMA derivatives were predicted to cross the BBB, while in NBP series, only methoxy substituted derivatives could reach the CNS; the rest of compounds gave permeability values included in the range of uncertainty, P_e (10^{-6} cm s^{-1}) = 9.8 – 12.3, r^2= 0.95.

Table 4.4 Permeability (P_e 10^{-6} cm s^{-1}) of 10 Commercial drugs used in the experiment validation, [a]Taken from Ref.147. [b]Mean ± SD of three independent experiments

Compd.	Bibl.[a]	Exp.[b]	Compd	P_e (10^{-6}cm s^{-1})[b]	Predict.
Testosterone	17.0	26.5 ± 1.1	**4.5**	9.4 ± 0.8	CNS ±
Verapamil	16.0	29.5 ± 1.0	**4.1**	12.4 ± 0.5	CNS +
Imipramine	13.0	20.6 ± 3.0	**4.9**	9.7 ± 0.2	CNS ±
Desipramine	12.0	22.9 ± 1.7	**4.8**	9.8 ± 0.8	CNS ±
Promazine	8.8	20.8 ± 0.9	**4.6**	11.9 ± 0.2	CNS ±
Corticosterone	5.1	11.0 ± 0.2	**4.14**	14.8 ± 0.5	CNS +
Piroxicam	2.5	10.0 ± 0.1	**4.15**	14.9 ± 0.8	CNS +
Hydrocortisone	1.9	10.2 ± 0.1	**4.16**	13.2 ± 1.2	CNS +
Caffeine	1.3	7.9 ± 0.3	**4.13**	14.2 ± 0.5	CNS +
Ofloxacin	0.8	6.11 ± 0.9	**4.12**	14.1 ± 1.2	CNS +

Finally, caffeic – NBP hybrid **9**, with a balanced multifunctional profile in hChEs, hMAOs and ORAC (h-AChE: 1.75 μM; h-BuChE: 0.69 μM; h-MAO-A: 3.5 μM; h-MAO-B: 6.0 μM; ORAC: 1.0 trolox equivalents), was chosen to evaluate the ability of new cinnamic-based hybrids in promoting the differentiation of neural stem-cells towards a neuronal phenotype. To that purpose, neural stem cells (NSC) isolated from one of the main neurogenic niches in the adult, the subgranular zone (SGZ) of the dentate gyrus, were used as described chapter one. NSC were grown as neurospheres in the presence of hybrid **9** (10 μM) during 7 days and later on allowed for 3 days to differentiate when adhered on a substrate in the presence of serum and compound. At this point, immunocytochemical analysis was performed to evaluate the ability of tested compound to promote neuronal differentiation. Our results summarized in figure 4.3 showed that the new caffeic-based hybrid **9**

clearly induced the differentiation of adult SGZ-derived NSC into a neuronal phenotype. After treatment with compound **9** a significant increase in the number of β-III-tubulin (early neurogenesis marker) and MAP-2 (microtubule-associated protein expressed in mature neurons) expressing cells in the neurospheres in shown. These results suggest that the new caffeic – NBP hybrid **9** has the ability to induce the differentiation of adult neural stem cells into neurons, promoting its maturation *in vitro* and showing a great neurogenic effect.

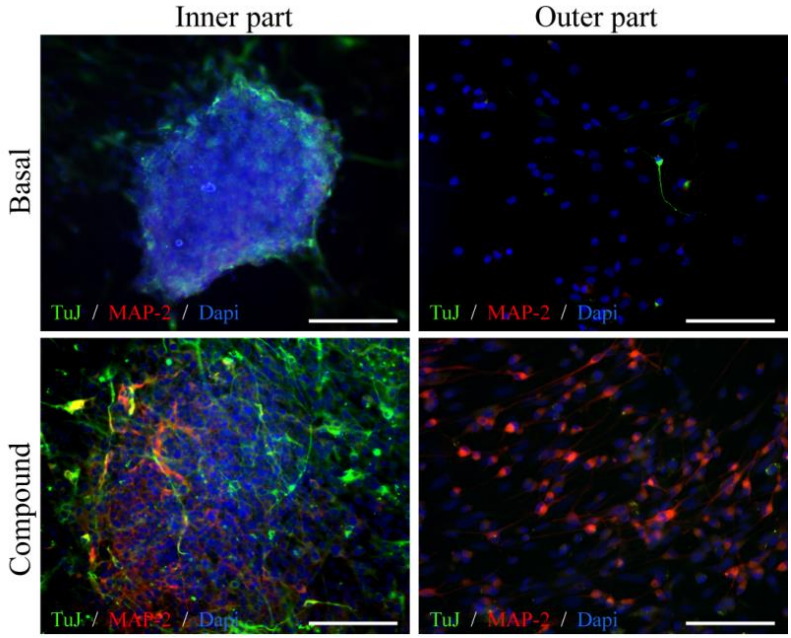

Figure 4.3. Caffeic-based hybrid **9** promotes neuronal differentiation *in vitro*. Adult murine neural stem cells isolated from the neurogenic niche of the SGZ of the hippocampus were grown as NS during 7 days in the presence of compound **9** (10 μM). Then, NS were allowed to differentiate on a substrate for another 3 days in the presence of tested compound. Immunocytochemical analysis shows the expression of two well-known neuronal markers: β-III-tubulin (TuJ clone; green) and MAP-2 (red) inside the NS (inner part) and in the distal area (outer part). DAPI was used for nuclear staining. Scale bar, 200μm.

At this point, we decided to explore additional structural modifications in order to improve the antioxidant capacity of the hybrids obtained in this chapter. Based on compound **4.5**, the new derivative **4.18** was synthesized as described in scheme 4.2.

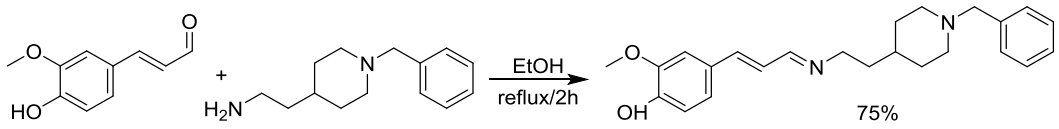

Scheme 4.2 Synthesis of ferulic acid-based compound **4.18**

The effect of this modification over AChE inhibition and antioxidant capacity was minimal, AChE (IC_{50})= 0.76 ± 0.2 µM, ORAC (trolox equivalents) = 1.70 ± 0.05. However, it was detrimental to affinity for BuChE; IC_{50} shifted from 76 nM in **4.5** to 27% of inhibition at 10 µM in **4.18**. Regarding to BACE1, a very interesting change was observed, while **4.5** was utterly inactive, **4.18** was able to inhibit a 34 % of this enzyme at a concentration of 10 µM. Even though, it represents a modest percentage of inhibition; it is a remarkable change that should be studied in the future. In regard of BBB permeability, **4.18** was not predicted to reach the CNS, however, a simple change of methoxy group by a larger chain could be sufficient to solve this problem.

Given that it is well known that BACE1 has a large active site, another modification we decided to explore was the length of the entire molecule. Taking advantage of the remaining hydroxy group in molecules such as **4.12**, we resolved to add an extra ferulic acid fragment to obtain compound **4.19**. (Figure 4.3).

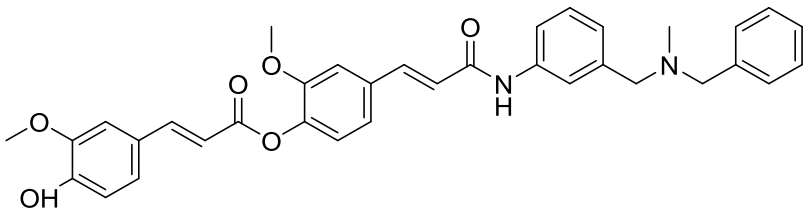

Figure 4.3 Structure of **4.19**, BACE1 inhibitor, IC_{50} 1.5 μM

A remarkable change of activity from 23% at 10 μM in the case of **4.12** to an IC_{50} value of 1.5 μM for **4.19** was observed. At this point, this new derivative has been tested only as BACE1 inhibitor and remains to be evaluated in the rest of targets explored in this work.

Taken together, these modifications open a new range of possibilities to improve the biological activity and the multitarget character of this kind of hybrids; however, these new compounds are out of the scope of this thesis and remain to be developed.

Conclusions

The combination of cinnamic structure with NBP and DBMA fragments gave hybrids with enhanced antioxidant capacity, compared to the chromone-based compounds obtained previously. As we have aimed along this work, we obtained several hybrids with multitarget profile; here, we highlight compounds **4.5**, **4.9, 4.8** and **4.7** in the cinnamic-NBP and **4.12** in the cinnamic-DBMA series, as dual AChE-MAO inhibitors. The feature shared for all compounds with affinity for MAO is the hydroxy group at position 7; it seems to be crucial for their inhibitory activity.

Regarding to the antioxidant capacity, hydroxy group at position 6 was the best improving the ORAC values, although it was detrimental for the affinity towards MAO; notwithstanding, the compounds exhibiting

concurrent affinity for cholinesterases and MAO, still display values up to 1.8 equivalents of trolox.

Although it has been formerly proposed that cinnamic-NBP hybrids could be good inhibitors of AChE, it has not been evaluated if this combination could inhibit MAO and simultaneously protect the cells against oxidative stress. This could be the mechanism involved in protection against rotenone/oligomycin toxicity observed in the MTT assay; however, complementary studies must be developed in this regard.

Newly synthesized compound **4.19** represents a new hit in the search of BACE1 inhibitors; if this hybrid preserves the activity of the smaller analogue **4.12** in cholinesterases and MAO, it could represent a new opportunity in the search of disease modifying drugs for AD treatment.

Experimental Part

General Procedure 4.1 Synthesis of Cinnamic-based Hybrids. The corresponding acid (1 mmol) and CDI (1.15 mmol) were mixed into a microwave tube under nitrogen atmosphere. The tube was sealed up and 3 mL of anhydrous THF were added using a syringe to dissolve the mixture ($CO_2\uparrow$). This solution of activated acid was heated into a microwave reactor at 120 ^{0}C during 7 min to complete the activation. Afterward, a solution of 1.2 mmol of the corresponding amine in 2 mL of THF was added with a syringe into the tube; this solution was heated at 120 ^{0}C during 10 min for NBP derivatives and 40 min for DBMA hybrids. After evaporation of the THF under reduced pressure the crude obtained was re-dissolved in 25 mL of EtOAc and washed 3x5 mL with water and 3x5 mL with brine; dried over $MgSO_4$ and concentrated under reduced pressure. The crude was purified by column chromatography using EtOAc:MeOH (9:1) or hexane/EtOAc (0→70%) as eluent.

***(E)-N*-(2-(1-benzylpiperidin-4-yl)ethyl)-3-(3,4-dimethoxyphenyl)acrylamide. 4.1**

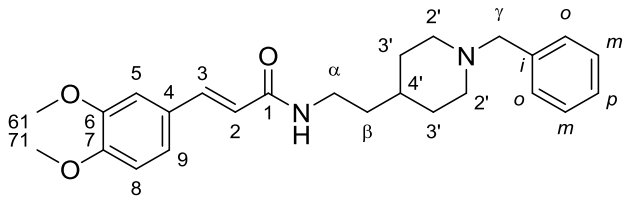

4.1 was obtained from 0.1 g of 4,5-dimethoxy cinnamic acid (0.48 mmol) and 0.126 g (0.58 mmol) of 2-(1-benzylpiperidin-4-yl)ethan-1-amine. Ligth yellow solid, 0.170 g (90%) mp: 108.1-110.5^{0}C. ^{1}H NMR (500 MHz, MeOD) δ 7.46 (d, *J* = 15.7 Hz, 1H, H_3), 7.32 (s, 2H, H_m), 7.31 (s, 2H, H_o), 7.29 – 7.24 (m, 1H, H_p), 7.14 (d, *J* = 2.0 Hz, 1H, H_5), 7.12 (ddd, *J* = 8.2, 2.0, 0.5 Hz, 1H, H_9), 6.96 (d, *J* = 8.2 Hz, 1H, H_8), 6.47 (d, *J* = 15.7 Hz, 1H, H_2), 3.86 (s, 3H, H_{71}), 3.85 (s, 3H, H_{61}), 3.51 (s, 2H, H_γ), 3.35 – 3.32 (m, 2H, H_α), 2.90 (dt, *J* = 12.1, 3.5 Hz, 2H, $H_{2'eq}$), 2.05 – 1.99 (m, 2H, $H_{2'ax}$), 1.76 – 1.71 (m, 2H, $H_{3'eq}$), 1.50 (dt, *J* = 7.9, 6.6 Hz, 2H, H_β), 1.37 (dddd, *J* = 16.4, 9.7, 6.4, 3.5 Hz, 1H, $H_{4'}$), 1.28 (qd, *J* = 12.1, 3.5 Hz, 2H, $H_{3'ax}$). ^{13}C NMR (126 MHz, MeOD) δ 168.86 (C_1), 152.20 (C_6), 150.70 (C_7), 141.56 (C_3), 138.19 (C_i), 130.92 (C_o), 129.36 (C_4), 129.26 (C_m), 128.43 (C_p), 123.16 (C_9), 119.67 (C_2), 112.71 (C_8), 111.31 (C_5), 64.34 (C_γ), 56.42 (C_{61}), 56.40 (C_{71}), 54.64 ($C_{2'}$), 38.10 (C_α), 37.10 (C_β), 34.44 ($C_{4'}$), 32.72 ($C_{3'}$). HRMS [ESI+] m/z =408.2407 [M] $^+$, Calcd for $[C_{25}H_{32}N_2O_3]^+$ 408.2413. HPLC purity 99%

***(E)-N*-(2-(1-benzylpiperidin-4-yl)ethyl)-3-(3-methoxyphenyl)acrylamide. 4.2**

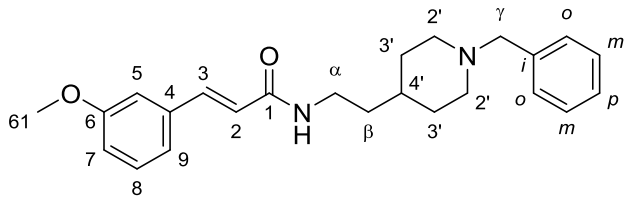

4.2 was obtained from 0.25 g of 5-methoxy cinnamic acid (1.4 mmol) and 0.36 g (1.61 mmol) of 2-(1-benzylpiperidin-4-yl)ethan-1-amine. White amorphous solid, 0.430 g (80%) mp: 68-70 ^{0}C. ^{1}H NMR

(300 MHz, MeOD) δ 7.48 (d, *J* = 15.8 Hz, 1H, H_3), 7.39 – 7.21 (m, 6H, Ph, H_7), 7.18 – 7.06 (m, 2H, $H_{5,9}$), 6.94 (ddd, *J* = 8.2, 2.6, 1.0 Hz, 1H, H_8), 6.58 (d, *J* = 15.8 Hz, 1H, H_2), 3.82 (s, 3H, H_{61}), 3.51 (s, 2H, H_γ), 3.38 – 3.32 (m, 2H, H_α), 2.90 (d, *J* = 11.4 Hz, $2H_{2'eq}$), 2.02 (t, *J* = 11.3 Hz, 2H, $H_{2'ax}$), 1.74 (d, *J* = 12.2 Hz, 2H, $H_{3'eq}$), 1.51 (q, *J* = 6.8 Hz, 2H, H_β), 1.42 – 1.19 (m, 3H, $H_{3'ax,\ 4'}$). ^{13}C NMR (75 MHz, MeOD) δ 168.47 (C_1), 161.53 (C_6), 141.51 (C_3), 138.28 (C_i), 137.68 (C_4), 130.92 (C_7), 130.90 (C_o), 129.25 (C_m), 128.40 (C_p), 122.16 (C_2), 121.32 (C_9), 116.48 (C_8), 113.83 (C_5), 64.37 (C_γ), 55.73 (C_{61}), 54.66 ($C_{2'}$), 38.13 (C_α), 37.06 (C_β), 34.46 ($C_{4'}$), 32.75 ($C_{3'}$). HRMS [ESI+] m/z =378.2304 $[M]^+$, Calcd for $[C_{24}H_{30}N_2O_2]^+$ 378.2307. HPLC purity 100%

***(E)-N*-(2-(1-benzylpiperidin-4-yl)ethyl)-3-(4-methoxyphenyl)acrylamide. 4.3**

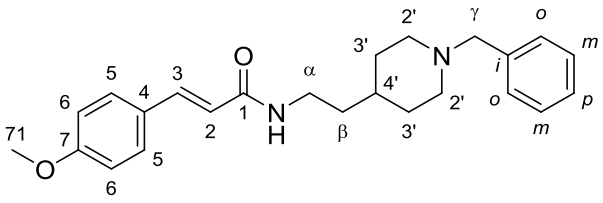

4.3 was obtained from 0.25 g of 4-methoxy cinnamic acid (1.4 mmol) and 0.36 g (1.7 mmol) of 2-(1-benzylpiperidin-4-yl)ethan-1-amine. White amorphous solid, 0.424 g (80%) mp: 103-105 ^{0}C. ^{1}H NMR (500 MHz, MeOD) δ 7.49 (d, *J* = 8.5 Hz, 2H, H_5), 7.45 (d, *J* = 15.7 Hz, 1H, H_3), 7.34 – 7.28 (m, 4H, $H_{o,\ m}$), 7.28 – 7.23 (m, 1H, H_p), 6.93 (d, *J* = 8.5 Hz, 2H, H_6), 6.44 (d, *J* = 15.7 Hz, 1H, H_2), 3.81 (s, 3H, H_{71}), 3.50 (s, 2H, H_γ), 3.32 – 3.30 (m, 2H, H, H_α), 2.89 (dt, *J* = 12.2, 3.5 Hz, 2H, $H_{2'eq}$), 2.01 (td, *J* = 11.8, 2.4 Hz, 2H, $H_{2'ax}$), 1.73 (d, *J* = 12.3 Hz, 2H, $H_{3'eq}$), 1.50 (q, *J* = 6.9 Hz, 2H, H_β), 1.37 (dtq, *J* = 13.9, 6.9, 3.5 Hz, 1H, $H_{4'}$), 1.27 (qd, *J* = 12.2, 3.5 Hz, 2H, $H_{3'ax}$). ^{13}C NMR (126 MHz, MeOD) δ 168.95 (C_1), 162.56 (C_7), 141.34 (C_5), 138.25 (C_i), 130.92 (C_o), 130.37 (C_5), 129.25 (C_m), 128.87 (C_4), 128.41 (C_p), 119.30 (C_2), 115.33 (C_6), 64.37 (C_γ), 55.82 (C_{71}), 54.65 ($C_{2'}$), 38.10 (C_α), 37.10 (C_β), 34.45 ($C_{4'}$), 32.74 ($C_{3'}$). HRMS [ESI+]

m/z =378.2304 [M] $^{+}$, Calcd for $[C_{24}H_{30}N_2O_2]^{+}$ 378.2307. HPLC purity 100%

***(E)-N*-(2-(1-benzylpiperidin-4-yl)ethyl)-3-(2,4-dimethoxyphenyl)acrylamide. 4.4**

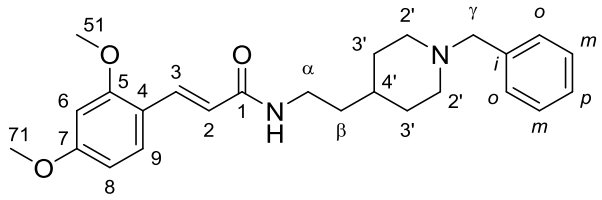

4.4 was obtained from 0.30 g of 4,6-dimethoxy cinnamic acid (1.44 mmol) and 0.37 g (1.73 mmol) of 2-(1-benzylpiperidin-4-yl)ethan-1-amine. Beige solid, 0.517 g (91%) mp: 90-93 ^{0}C. ^{1}H NMR (300 MHz, MeOD) δ 7.74 (d, *J* = 15.8 Hz, 1H, H_3), 7.44 (d, *J* = 8.2 Hz, 1H, H_9), 7.36 – 7.28 (m, 4H, $H_{o,\ m}$), 7.29 – 7.18 (m, 1H, H_p), 6.62 – 6.48 (m, 3H, H_2, H_6, H_8), 3.87 (s, 3H, H_{51}), 3.82 (s, 3H, H_{71}) 3.49 (s, 2H, H_γ), 3.37 – 3.26 (m, 2H, H_α), 2.97 – 2.78 (m, 2H, $H_{2'eq}$), 2.00 (t, *J* = 11.2 Hz, 2H, $H_{2'ax}$), 1.80 – 1.62 (m, 2.5 Hz, 2H, $H_{3'eq}$), 1.49 (q, *J* = 6.9 Hz, 2H, H_β), 1.39 - 1.19 (m, 3H, $H_{4'}$, $H_{3'ax}$). ^{13}C NMR (75 MHz, MeOD) δ 169.64 (C_1), 163.96 (C_7), 161.03 (C_5), 138.27(C_i), 136.98 (C_3), 130.91 (C_o), 130.83 (C_9), 129.24 (C_m), 128.39 (C_p), 119.53 (C_2), 117.83 (C_4), 106.69 (C_6), 99.23 (C_8), 64.37 (C_γ), 56.01 (C_{51}), 55.91(C_{71}), 54.66 ($C_{2'}$), 38.08 (C_α), 37.13 (C_β), 34.44 ($C_{4'}$), 32.74 ($C_{3'}$). HRMS [ESI+] m/z =408.2416 [M] $^{+}$, Calcd for $[C_{25}H_{32}N_2O_3]^{+}$ 408.2413. HPLC purity 99%

***(E)-N*-(2-(1-benzylpiperidin-4-yl)ethyl)-3-(4-hydroxy-3-methoxyphenyl)acrylamide. 4.5**

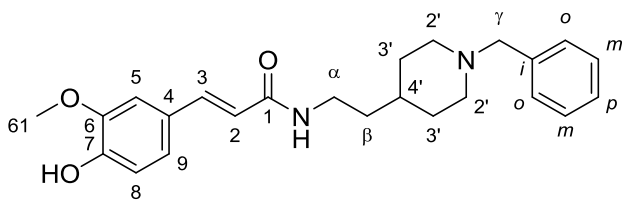

4.5 was obtained from 0.1 g of ferulic acid (0.5 mmol) and 0.135 g (0.6 mmol) of

2-(1-benzylpiperidin-4-yl)ethan-1-amine, according to the general procedure 4.1. Bright yellow solid, 0.193 g (95%), mp: 83.1-84.5 ^{0}C. ^{1}H NMR (500 MHz, MeOD) δ 7.43 (d, *J* = 15.7 Hz, 1H, H_3), 7.35 – 7.31 (m, 4H, $H_{o, m}$), 7.30 – 7.24 (m, 1H, H_p), 7.12 (d, *J* = 2.0 Hz, 1H, H_5), 7.03 (dd, *J* = 8.2, 2.0 Hz, 1H, H_9), 6.80 (d, *J* = 8.2 Hz, 1H, H_8), 6.42 (d, *J* = 15.7 Hz, 1H, H_2), 3.89 (s, 3H, H_{61}), 3.54 (s, 2H, H_γ), 3.35 – 3.33 (m, 2H, H_α), 2.92 (dt, *J* = 11.9, 3.5 Hz, 2H, $H_{2'eq}$), 2.05 (td, *J* = 11.9, 2.5 Hz, 2H, $H_{2'ax}$), 1.75 (dt, *J* = 13.0, 2.5 Hz, 2H, $H_{3'eq}$), 1.51 (q, *J* = 7.0 Hz, 2H, H_β), 1.39 (dtt, *J* = 13.5, 6.6, 3.5 Hz, 1H, $H_{4'}$), 1.30 (td, *J* = 12.5, 3.5 Hz, 2H, $H_{3'ax}$). ^{13}C NMR (126 MHz, MeOD) δ 169.11 (C_1), 149.90 (C_7), 149.30 (C_6), 141.97 (C_3), 138.01 (C_i), 130.97 (C_o), 129.29 (C_m), 128.51 (C_p), 128.23 (C_4), 123.16 (C_9), 118.70 (C_2), 116.49 (C_8), 111.52 (C_5), 64.29 (C_γ), 56.36 (C_{61}), 54.63 ($C_{2'}$), 38.06 (C_α), 37.10 (C_β), 34.39 ($C_{4'}$), 32.67 ($C_{3'}$). HRMS [ESI+] m/z =394.2260 $[M]^+$, Calcd for $[C_{24}H_{30}N_2O_3]^+$ 394.2256. HPLC purity 99%

***(E)-N*-(2-(1-benzylpiperidin-4-yl)ethyl)-3-(3-hydroxyphenyl)acrylamide. 4.6**

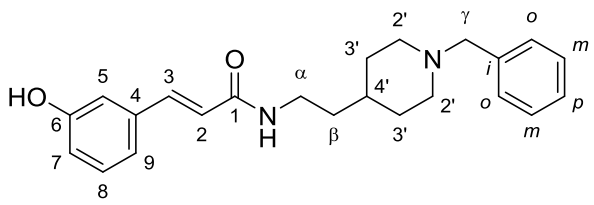

4.6 was obtained from 0.1 g (0.26 mmol) of **4.2** and 7 mmol of BBr_3 as described in general procedure 2.4. Light brown amorphous solid 93 mg (97%) mp: 190-193^{0}C. ^{1}H NMR (500 MHz, MeOD) δ 7.53 – 7.50 (m, 2H, H_o), 7.48 – 7.46 (m, 3H, $H_{m, p}$), 7.42 (d, *J* = 15.7 Hz, 1H, H_3), 7.18 (t, *J* = 7.8 Hz, 1H, H_8), 6.99 (dt, *J* = 7.8, 1.2 Hz, 1H, H_9), 6.95 (t, *J* = 2.0 Hz, 1H, H_5), 6.78 (ddd, *J* = 7.9, 2.5, 1.0 Hz, 1H), 6.55 (d, *J* = 15.7 Hz, 1H, H_2), 4.29 (s, 2H, H_γ), 3.49 – 3.45 (m, 2H, $H_{2'eq}$), 3.37 – 3.33 (m, 2H, H_α), 3.01 (td, *J* = 13.0, 3.0 Hz, 2H, $H_{2'ax}$), 2.05 – 1.99 (m, 2H, $H_{3'eq}$), 1.74 – 1.61 (m, 1H, H_4), 1.53 (q, *J* = 6.9 Hz, 2H, H_β), 1.50 – 1.40 (m, 2H, $H_{3'ax}$). ^{13}C NMR (126 MHz, MeOD) δ 168.74 (C_1), 159.01 (C_6), 141.96 (C_3), 137.49 (C_4),

132.43 (C_o), 131.22 (C_p), 130.95 (C_6), 130.38 (C_i), 130.32 (C_m), 121.56 (C_2), 120.37 (C_9), 118.00 (C_7), 115.06 (C_5), 61.78 (C_γ), 53.73 ($C_{2'}$), 37.55 (C_α), 36.36 (C_β), 32.33 ($C_{4'}$), 30.36 ($C_{3'}$). HRMS [ESI+] *m/z* =364.2150 $[M]^+$, Calcd for $[C_{23}H_{28}N_2O_2]^+$ 364.2151. HPLC purity 98%

***(E)-N*-(2-(1-benzylpiperidin-4-yl)ethyl)-3-(4-hydroxyphenyl)acrylamide. 4.7.**

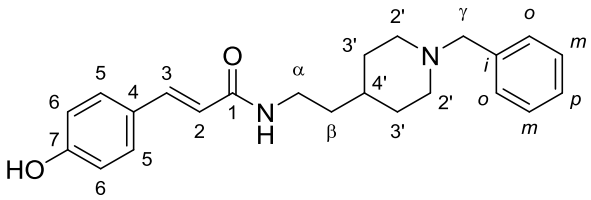

4.7 was obtained from 0.1 g (0.26 mmol) of **4.3** and 7 mmol of BBr_3 as described in general procedure 2.4. white amorphous solid 83 mg (87%) mp: 164-166^{0}C. ^{1}H NMR (500 MHz, MeOD) δ 7.50 – 7.46 (m, 5H, Ph), 7.44 (d, *J* = 15.7 Hz, 1H, H_3), 7.40 (d, *J* = 8.7 Hz, 2H, H_6), 6.79 (d, *J* = 8.6 Hz, 2H, H_5), 6.40 (d, *J* = 15.7 Hz, 1H, H_2), 4.21 (s, 2H, H_γ), 3.42 – 3.37 (m, 2H, $H_{2'eq}$), 3.34 (t, *J* = 7.0 Hz, 2H, H_α), 2.91 (m, 2H, $H_{2'ax}$), 2.00 (d, *J* = 14.0 Hz, 2H, $H_{3'eq}$), 1.65 (bs, 1H, $H_{4'}$), 1.55 (q, *J* = 7.0 Hz, 2H, H_β), 1.48 – 1.44 (m, 2H, $H_{3'ax}$). ^{13}C NMR (126 MHz, MeOD) δ 167.84 (C_1), 159.20 (C_7), 140.48 (C_3), 130.77 (C_o), 130.74 (C_i), 129.49 (C_p), 129.13 (C_5), 128.80 (C_m), 126.14 (C_4), 116.79 (C_2), 115.30 (C_6), 60.46 (C_γ), 52.23 ($C_{2'}$), 36.13 (C_α), 35.01 (C_β), 31.04 ($C_{4'}$), 29.08 ($C_{3'}$). HRMS [ESI+] *m/z* =364.2158 $[M]^+$, Calcd for $[C_{23}H_{28}N_2O_2]^+$ 364.2151. HPLC purity 98%

***(E)-N*-(2-(1-benzylpiperidin-4-yl)ethyl)-3-(3,4-dihydroxyphenyl)acrylamide. 4.9**

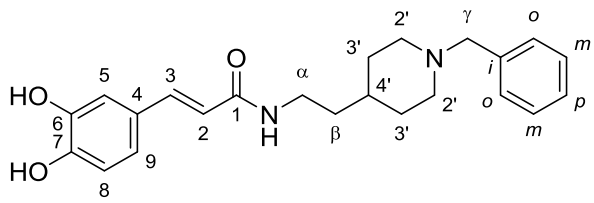

4.9 was obtained from 0.1 g (0.25 mmol) of **4.5** and 7 mmol of BBr_3 as described in general procedure 2.4; white amorphous solid 0.06 g (60%) mp: 164-166^{0}C.^{1}H NMR (500 MHz, MeOD) δ 7.48 – 7.40 (m, 5H, Ph), 7.37 (d, *J* = 15.7 Hz, 1H, H_3), 7.01 (d, *J* = 2.1 Hz, 1H, H_5), 6.90 (dd, *J* = 8.2, 2.1 Hz, 1H, H_9), 6.77 (d, *J* = 8.2 Hz, 1H, H_8), 6.39 (d, *J* = 15.7 Hz, 1H, H_2), 4.00 (s, 2H, H_γ), 3.34 (t, *J* = 6.9 Hz, 2H, H_α), 3.24 (d, *J* = 12.3 Hz, 2H, $H_{2'eq}$), 2.64 (t, *J* = 11.6 Hz, 2H, $H_{2'ax}$), 1.95 – 1.82 (m, 2H, $H_{3'eq}$), 1.56 (m, 1H, $H_{4'}$), 1.53 (q, *J* = 6.7 Hz, 2H, H_β), 1.47 – 1.33 (m, 2H, $H_{3'ax}$). ^{13}C NMR (126 MHz, MeOD) δ 169.23 (C_1), 148.77 (C_7), 146.72 (C_6), 142.15 (C_3), 133.40 (C_i), 131.86 (C_o), 130.13 (C_p), 129.90 (C_m), 128.21 (C_4), 122.15 (C_9), 118.33 (C_2), 116.44 (C_8), 114.93 (C_5), 62.49 (C_γ), 53.83 ($C_{2'}$), 37.70 (C_α), 36.52 (C_β), 32.99 ($C_{4'}$), 31.01 ($C_{3'}$). HRMS [ESI+] *m/z* =380.2104 [M]$^+$, Calcd for $[C_{23}H_{28}N_2O_3]^+$ 380.2100. HPLC purity 99%

***(E)-N*-(4-((Benzyl(methyl)amino)methyl)phenyl)-3-(2,4-dimethoxyphenyl)acrylamide. 4.10**

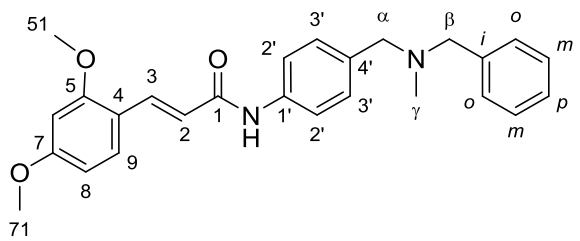

4.10 was synthesized as described in the general procedure 4.1, starting from 0.150 g (0.72 mmol) of 2,4-dimethoxy cinnamic acid and 0.195 g (0.86 mmol) of **1.8** White amorphous solid, 0.18 g (60%) mp: 105-107 ^{0}C. ^{1}H NMR (300 MHz, MeOD) δ 7.90 (d, *J* = 15.8 Hz, 1H, H_3), 7.65 (d, *J* = 8.2 Hz, 2H, $H_{2'}$), 7.51 (d, *J* = 8.7 Hz, 1H, H_9), 7.35 – 7.23 (m,

7H, Ph, $H_{3'}$), 6.77 (d, *J* = 15.7 Hz, 1H, H_2), 6.62 – 6.49 (m, 2H, $H_{8,6}$), 3.91 (s, 3H, H_{51}), 3.85 (s, 3H, H_{71}), 3.52 (s, 2H, H_β), 3.50 (s, 2H, H_α), 2.18 (s, 3H, H_γ). ^{13}C NMR (75 MHz, MeOD) δ 167.83 (C_1), 164.21 (C_7), 161.26 (C_5), 139.69 (C_i), 139.33 ($C_{1'}$), 138.31 (C_3), 135.31 ($C_{4'}$), 131.19 (C_9), 130.84 ($C_{3'}$), 130.40 (C_o), 129.30 (C_m), 128.25 (C_p), 121.05 ($C_{2'}$), 119.82 (C_2), 117.83 (C_4), 106.81 (C_6), 99.27 (C_8), 62.61 (C_β), 62.21 (C_α), 56.05 (C_{51}), 55.93 (C_{71}), 42.31 (C_γ). HRMS [ESI+] m/z =416.2099 $[M]^+$, Calcd for $[C_{26}H_{28}N_2O_3]^+$ 416.2100. HPLC purity 100%

***(E)-N*-(4-((Benzyl(methyl)amino)methyl)phenyl)-3-(3,4-dimethoxyphenyl)acrylamide. 4.11**

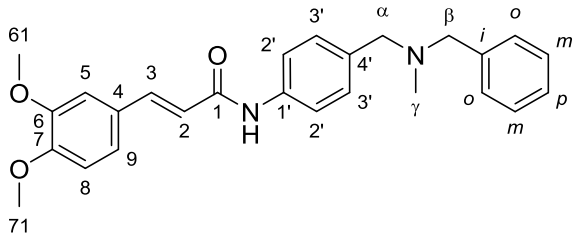

0.050 g (0.24 mmol) of 4,5-dimethoxy cinnamic acid, 0.044 g and 0.065 g (0.28 mmol) of **1.8**, were reacted as described in general procedure 4.1 to obtain **4.11** as a white amorphous solid, 60 mg (60%) mp: 107-110 ^{0}C. ^{1}H NMR (300 MHz, MeOD) δ 7.68 – 7.57 (m, 3H, $H_{3,2'}$), 7.38 – 7.24 (m, 7H, Ph, $H_{3'}$), 7.22 – 7.13 (m, 2H, $H_{5,9}$), 6.98 (d, *J* = 8.0 Hz, 1H, H_8), 6.67 (d, *J* = 15.5 Hz, 1H, H_2), 3.89 (s, 3H, H_{61}), 3.87 (s, 3H, H_{71}), 3.52 (s, 2H, H_α), 3.50 (s, 2H, H_β), 2.17 (s, 3H, H_γ). ^{13}C NMR (75 MHz, MeOD) δ 166.97 (C_1), 152.44 (C_7), 150.73 (C_6), 142.78 (C_3), 139.66 (C_i), 139.18 ($C_{1'}$), 135.47 ($C_{4'}$), 130.88 ($C_{3'}$), 130.40 (C_o), 129.36 (C_4), 129.31 (C_m), 128.26 (C_p), 123.43 (C_9), 121.03 ($C_{2'}$), 119.98 (C_2), 112.74 (C_8), 111.43 (C_5), 62.62 (C_α), 62.20 (C_β), 56.44 (C_{61}), 56.42 (C_{71}), 42.31 (C_γ). HRMS [ESI+] m/z =416.2112 $[M]^+$, Calcd for $[C_{26}H_{28}N_2O_3]^+$ 416.2100. HPLC purity 100%

***(E)-N*-(3-((benzyl(methyl)amino)methyl)phenyl)-3-(4-hydroxy-3-methoxyphenyl)acrylamide. 4.12**

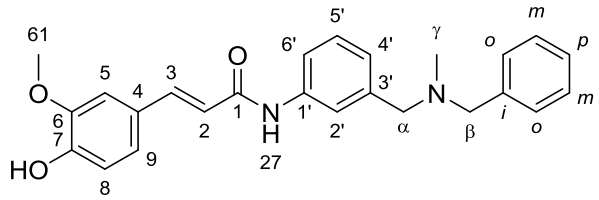

4.13 was obtained from 0.1 g of ferulic acid (0.5 mmol) and 0.18 g (0.8 mmol) of amine **1.7**, according to the general procedure 4.1. Bright yellow solid, 0.18 g (65%), mp: 72-74 ^{0}C. ^{1}H NMR (400 MHz, MeOD) δ 7.64 (s, 1H, $H_{2'}$), 7.56 (s, 1H, $H_{6'}$), 7.56 (d, *J* = 15.7 Hz, 1H, H_3), 7.36 – 7.21 (m, 6H, Ph, $H_{5'}$), 7.15 (d, *J* = 2.0 Hz, 1H, H_5), 7.10 – 7.05 (m, 2H, H_2, $H_{4'}$), 6.80 (d, *J* = 8.1 Hz, 1H, H_8), 6.60 (d, *J* = 15.6 Hz, 1H, H_2), 3.88 (s, 3H, H_{61}), 3.51 (s, 2H, H_β), 3.49 (s, 2H, H_α), 2.16 (s, 3H, H_γ). ^{13}C NMR (101 MHz, MeOD) δ 167.27 (C_1), 150.16 (C_7), 149.33 (C_6), 143.25 (C_3), 140.66 ($C_{3'}$), 140.18 (C_i), 139.70 ($C_{1'}$), 130.40 (C_o), 129.78 (C_p), 129.32 (C_m), 128.27 ($C_{5'}$), 128.18 (C_4), 126.08 ($C_{4'}$), 123.42 (C_9), 121.97 ($C_{2'}$), 120.06 ($C_{6'}$), 119.04 (C_2), 116.54 (C_8), 111.65 (C_5), 62.74 (C_β), 62.62 (C_α), 56.36 (C_{61}), 42.41 (C_γ). HRMS [ESI+] m/z =402.1934 [M] $^{+}$, Calcd for $[C_{25}H_{26}N_2O_3]^{+}$ 402.1943. HPLC purity 99%

***(E)-N*-(4-((benzyl(methyl)amino)methyl)phenyl)-3-(4-hydroxy-3-methoxyphenyl)acrylamide 4.13**

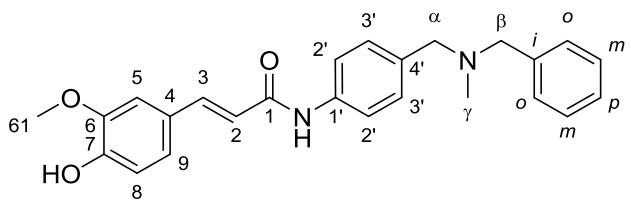

4.13 was obtained from 0.1 g of ferulic acid (0.5 mmol) and 0.18 g (0.8 mmol) of amine **1.8**, according to the general procedure 4.1. Bright yellow solid, 0.16 g (64%), mp: 80-83 ^{0}C.^{1}H NMR (500 MHz, MeOD) δ 7.63 (d, *J* = 8.5 Hz, 2H, $H_{2'}$), 7.57 (d, *J* = 15.6 Hz, 1H, $H_{3'}$), 7.36 – 7.31 (m, 6H, Ph, $H_{3'}$), 7.29 – 7.23 (m, 1H, H_p), 7.17 (d, *J* = 2.1 Hz, 1H, H_5), 7.08 (dd, *J* = 8.2, 2.2 Hz, 1H, H_9), 6.82 (d, *J* = 8.2 Hz, 1H,

H_8), 6.61 (d, J = 15.6 Hz, 1H, H_2), 3.90 (s, 3H, H_{61}), 3.56 (s, 2H, H_β), 3.55 (s, 2H, H_α), 2.20 (s, 3H, H_γ). ^{13}C NMR (126 MHz, MeOD) δ 167.23 (C_1), 150.16 (C_6), 149.33 (C_7), 143.26 (C_3), 139.44 (C_i), 136.29 ($C_{1'}$), 134.77 ($C_{4'}$), 131.03 ($C_{3'}$), 130.54 (C_o), 129.40 (C_m), 128.48 (C_4), 128.19 (C_p), 123.43 (C_9), 121.05 ($C_{2'}$), 119.00 (C_2), 116.55 (C_8), 111.67 (C_5), 62.50 (C_α), 62.09 (C_β), 56.38 (C_{61}), 42.12 (C_γ). HRMS [ESI+] m/z =402.1902 [M] $^+$, Calcd for $[C_{25}H_{26}N_2O_3]^+$ 402.1943. HPLC purity 97%

***(E)-N*-(4-((Benzyl(methyl)amino)methyl)phenyl)-3-(3-methoxyphenyl)acrylamide. 4.14**

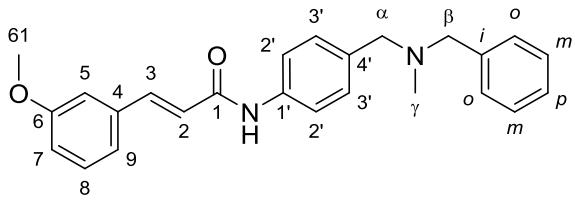

3-Methoxy cinamic acid, 0.150 g and 0.22 g (1.0 mmol) of **1.8**, were reacted as described in the general procedure 4.1 to obtain **4.14** as a white amorphous solid, 0.255 g (79%) mp: 90-93 ^{0}C. ^{1}H NMR (300 MHz, MeOD) δ 7.68 – 7.60 (m, 3H, $H_{3,\,2'}$), 7.38 – 7.25 (m, 8H, Ph, $H_{8,\,3'}$), 7.21 – 7.12 (m, 2H, $H_{5,\,9}$), 6.97 (dd, J = 8.1, 2.6 Hz, 1H, H_7), 6.79 (d, J = 15.7 Hz, 1H, H_2), 3.84 (s, 3H, H_{61}), 3.52 (s, 2H, H_β), 3.50 (s, 2H, H_α), 2.17 (s, 3H, H_γ). ^{13}C NMR (75 MHz, MeOD) δ 166.55 (C_1), 161.56 (C_6), 142.70 (C_3), 139.70 (C_i), 139.07 ($C_{1'}$), 137.60 (C_4), 135.67 ($C_{4'}$), 130.99 (C_8), 130.87 ($C_{3'}$), 130.39 (C_o), 129.30 (C_m), 128.25 (C_p), 122.55 (C_2), 121.48 (C_9), 121.08 ($C_{2'}$), 116.72 (C_7), 113.98 (C_5), 62.64 (C_β), 62.20 (C_α), 55.75 (C_{61}), 42.32 (C_γ). HRMS [ESI+] m/z =386.1998 [M] $^+$, Calcd for $[C_{25}H_{26}N_2O_2]^+$ 386.1994. HPLC purity 99%

***(E)-N*-(4-((benzyl(methyl)amino)methyl)phenyl)-3-(4-methoxyphenyl)acrylamide. 4.15**

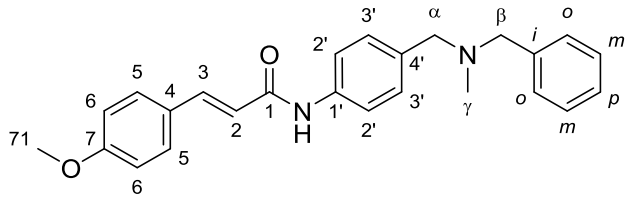

4-Methoxy cinnamic acid, 0.150 g (0.84 mmol) and 0.22 g (1.0 mmol) of **1.8**, were reacted as described in the general procedure 4.1 to obtain **4.15** as a white amorphous solid, 0.23 g (70%) mp: 131-134 ^{0}C. ^{1}H NMR (300 MHz, , MeOD) δ 7.70 – 7.60 (m, 3H, $H_{3,2'}$), 7.57 (d, *J* = 8.6 Hz, 2H, H_5), 7.39 – 7.27 (m, 7H, Ph, $H_{3'}$), 6.99 (d, *J* = 8.6 Hz, 2H, H_6), 6.67 (d, *J* = 15.6 Hz, 1H, H_2), 3.86 (s, 3H, H_{71}), 3.54 (s, 2H, H_β), 3.52 (s, 2H, H_α), 2.19 (s, 3H, H_γ). ^{13}C NMR (75 MHz, MeOD) δ 167.09 (C_1), 162.80(C_7), 142.58(C_3), 139.70(C_i), 139.20($C_{1'}$), 135.51($C_{4'}$), 130.87($C_{3'}$), 130.59(C_o), 130.39(C_5), 129.31(C_m), 128.85(C_4), 128.26(C_p), 121.08($C_{2'}$), 119.65(C_2), 115.42(C_6), 62.64(C_β), 62.21(C_α), 55.85(C_{71}), 42.32(C_γ). HRMS [ESI+] m/z =386.2000 [M] $^+$, Calcd for $[C_{25}H_{26}N_2O_2]^+$ 386.1994. HPLC purity 99%

***(E)-N*-(4-((benzyl(methyl)amino)methyl)phenyl)-3-(3-hydroxyphenyl)acrylamide 4.16**

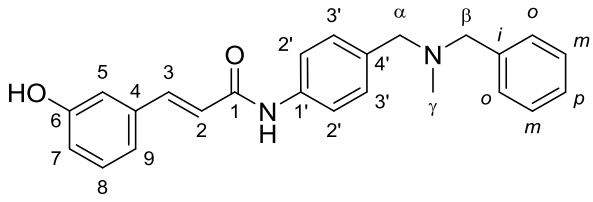

4.16 was obtained from 0.1 g (0.26 mmol) of **4.14** and 7 mmol of BBr_3 as described in general procedure 2.4. Light brown amorphous solid 69 mg (72%) mp: 156-158^{0}C. ^{1}H NMR (300 MHz, MeOD) δ 7.84 (d, *J* = 8.6 Hz, 2H, $H_{2'}$), 7.62 (d, *J* = 15.7 Hz, 1H, H_3), 7.56 – 7.44 (m, 7H, Ph, $H_{3'}$), 7.25 (t, *J* = 7.7 Hz, 1H, H_8), 7.09 (d, *J* = 7.7 Hz, 1H, H_9), 7.04 (t, *J* = 2.1 Hz, 1H, H_5), 6.85 (dd, *J* = 7.8, 2.2 Hz, 1H, H_7), 6.85 (d, *J* = 15.6 Hz, 1H, H_2), 4.50 (dd, *J* = 13.1, 10.3 Hz, 2H, $H_{\alpha,\ \beta}$), 4.28 (d, *J* = 13.2 Hz, 2H, $H_{\alpha,\ \beta}$),

2.73 (s, 3H, H_{γ}). ^{13}C NMR (75 MHz, MeOD) δ 166.91 (C_1), 159.10 (C_6), 143.60 (C_3), 142.00 ($C_{1'}$), 137.38 (C_4), 133.08 (C_m), 132.29 (C_o), 131.33 (C_p), 131.02 (C_8), 130.77 (C_i), 130.48 ($C_{3'}$), 125.82 ($C_{4'}$), 121.76 (C_2), 121.53 ($C_{2'}$), 120.58 (C_9), 118.33 (C_7), 115.28 (C_5), 60.72 (CH_2), 60.52 (CH_2), 39.49 (C_{γ}). HRMS [ESI+] m/z =372.1844 $[M]^+$, Calcd for $[C_{24}H_{24}N_2O_2]^+$ 372.1838. HPLC purity 99%

***(E)-N*-(4-((benzyl(methyl)amino)methyl)phenyl)-3-(4-hydroxyphenyl)acrylamide 4.17**

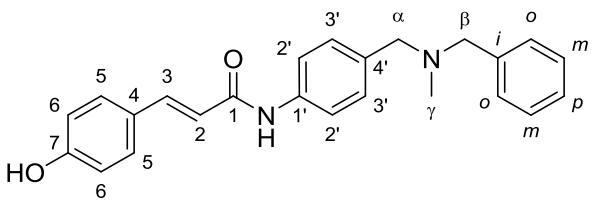

4.17 was obtained from 0.1 g (0.26 mmol) of **4.15** and 7 mmol of BBr_3 as described in general procedure 2.4. White amorphous solid 58 mg (60%) mp: 160-163^{0}C. ^1H NMR (300 MHz, MeOD) δ 7.82 (d, *J* = 8.7 Hz, 2H, $H_{2'}$), 7.63 (d, *J* = 15.6 Hz, 1H, H_3), 7.55 – 7.45 (m, 5H, $H_{5,\ 3',\ p}$), 7.20 (d, *J* = 8.5 Hz, 2H, H_o), 6.84 (d, *J* = 8.5 Hz, 2H, H_6), 6.76 (d, *J* = 8.4 Hz, 1H, H_m), 6.63 (d, *J* = 15.6 Hz, 1H, H_2), 4.35 (bs, 4H, $H_{\alpha,\ \beta}$), 2.69 (s, 3H, H_{γ}). ^{13}C NMR (75 MHz, MeOD) δ 167.51 (C_1), 161.00 (C_7), 143.65 (C_3), 142.13 ($C_{1'}$), 133.20 (C_o), 132.21 ($C_{3'}$), 131.28 (C_i), 131.20 ($C_{4'}$), 130.89 ($C_{5'}$), 130.46 (C_p), 127.51 (C_4), 121.46 ($C_{2'}$), 118.33 (C_2), 116.84 (C_6), 116.07 (C_m), 60.96 (CH_2), 60.36 (CH_2), 39.39 (C_{γ}). HRMS [ESI+] m/z =372.1846 $[M]^+$, Calcd for $[C_{24}H_{24}N_2O_2]^+$ 372.1838. HPLC purity 96%

4-((1*E*,3*E*)-3-((2-(1-benzylpiperidin-4-yl)ethyl)imino)prop-1-en-1-yl)-2-methoxyphenol. 4.18

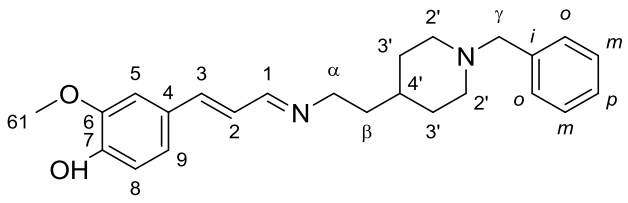

A mixture of 0.13 g (0.61 mmol) of 2-(1-benzylpiperidin-4-yl)ethan-1-amine and 0.1 g (0.56 mmol) of 4-hydroxy-3-methoxy cinnamaldehyde was refluxed during 2 hours in 20 mL of ethanol, when reactants were consumed, the solvent was evaporated and the crude was purified by column chromathography using a mixture of EtOAc:MeOH 9:1. Brown amorphous solid, 0.18 g (85%). ^{1}H NMR (300 MHz, MeOD) δ 8.02 (dq, *J* = 9.0, 1.4 Hz, 1H, H_1), 7.38 – 7.21 (m, 5H, Ph), 7.13 (d, *J* = 1.9 Hz, 1H, H_5), 7.07 – 7.01 (m, 1H, H_8), 7.01 – 6.99 (m, 1H, H_9), 6.79 (d, *J* = 8.2 Hz, 1H, H_3), 6.70 (dd, *J* = 15.8, 9.1 Hz, 1H, H_2), 3.88 (d, *J* = 2.1 Hz, 3H, H_6), 3.51 (d, *J* = 2.1 Hz, 4H, $H_{\alpha,\gamma}$), 2.90 (dd, *J* = 11.7, 3.0 Hz, 2H, $H_{2'eq}$), 2.01 (t, *J* = 11.7 Hz, 2H, $H_{2'ax}$), 1.72 (d, *J* = 11.6 Hz, 2H, $H_{3'eq}$), 1.57 (q, *J* = 6.8 Hz, 2H, H_β), 1.45 – 1.20 (m, 3H, $H_{3'ax,\ 4'}$). ^{13}C NMR (75 MHz, MeOD) δ 166.25 (C_1), 150.26 (C_7), 149.46 (C_6), 145.56 (C_8), 138.21 (C_i), 130.93 (C_m), 129.26 (C_o), 128.77 (C_4), 128.44 (C_p), 124.35 (C_2), 123.22 (C_9), 116.59 (C_3), 111.08 (C_5), 64.35 (C_γ), 58.60 (C_α), 56.38 (C_{61}), 54.66 ($C_{2'}$), 38.64 (C_β), 34.49 ($C_{4'}$), 32.78 ($C_{3'}$).

4-((*E*)-3-((3-((benzyl(methyl)amino)methyl)phenyl)amino)-3-oxoprop-1-en-1-yl)-2-methoxyphenyl (*E*)-3-(4-hydroxy-3-methoxyphenyl)acrylate. 4.19

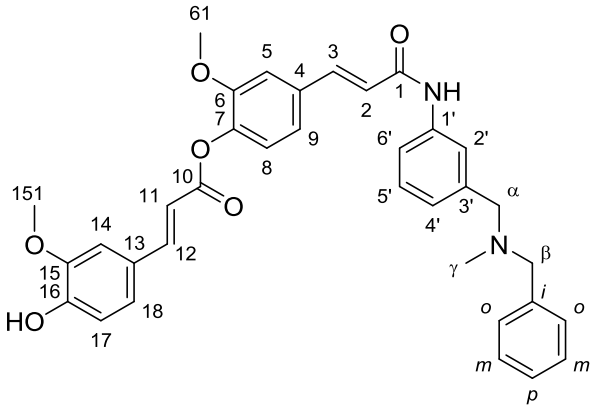

A mixture of ferulic acid 0.055 g (0.29 mmol) and 0.048 g (0.30 mmol) of CDI dissolved in 5 mL of DMF was heated at 120 °C into a microwave reactor during 10 min ; to this mixture was added **4.12**, 0.1 g (0.25 mmol) dissolved in 5 mL of DMF to heat at 120 °C for 40 additional minutes. The DMF was evaporated under reduced pressure and the crude was purified by column chromatography in a mixture of EtOAc in hexane (0→65%). Yellow solid, 0.13 g (90%). m.p: 86-89 ^{0}C ^{1}H NMR (500 MHz, MeOD) δ 7.81 (d, *J* = 15.9 Hz, 1H, H_3), 7.74 – 7.72 (m, 1H, $H_{4'}$), 7.68 (d, *J* = 15.7 Hz, 1H, H_{12}), 7.62 (ddd, *J* = 8.2, 2.3, 1.1 Hz, 1H, $H_{5'}$), 7.41 – 7.32 (m, 6H, Ph, H_7), 7.31 – 7.28 (m, 2H, H_5, $H_{6'}$), 7.26 (dd, *J* = 8.2, 1.9 Hz, 1H, H_{18}), 7.19 – 7.13 (m, 3H, $H_{2', 9, 17}$), 6.86 (dd, *J* = 8.3, 0.8 Hz, 1H, H_8), 6.80 (d, *J* = 15.7 Hz, 1H, H_{11}), 6.59 (d, *J* = 15.9 Hz, 1H, H_2), 3.93 (s, 3H, H_{61}), 3.89 (s, 3H, H_{151}), 3.63 (s, 2H$_\beta$), 3.62 (s, 2H, H_α), 2.25 (s, 3H, H_γ). ^{13}C NMR (126 MHz, MeOD) δ 167.01 (C_1), 166.56 (C_{10}), 153.19 (C_{15}), 151.12 (C_7), 149.47 (C_6), 148.82 (C_3), 142.79 (C_{16}), 142.19 (C_{12}), 140.13 ($C_{1'}$), 139.90 ($C_{3'}$), 138.90 (C_i), 135.22 (C_{13}), 130.57 (C_o), 129.93 (C_p), 129.44 (C_m), 128.56 ($C_{6'}$), 127.53 (C_4), 126.40 (C_9), 124.61 (C_{17}), 124.44 (C_{11}), 122.54 ($C_{4'}$), 122.19 (C_{18}), 121.74 ($C_{5'}$), 120.37 (C_8), 116.55 (C_8), 114.11 (C_2), 112.67 (C_{14}), 111.90 (C_5), 62.58 (C_β), 62.46 (C_α), 56.49 (C_{61}), 49.51 (C_{151}), 42.17 (C_γ). HRMS [ESI+] m/z =578.2425 [M]$^+$, Calcd for $[C_{35}H_{34}N_2O_6]^+$ 578.2417. HPLC purity 99%

The biological evaluation was developed according to the experimental protocols described in previous chapters.

Concluding Remarks

As described in the general objective of this work, we aimed to obtain new molecules able to interact simultaneously with some of the most important enzymes related to AD. With this idea in mind, we to take advantage of the *N*-benzyl piperidine and the *N, N*-dibenzyl amine fragments which are present in several bioactive molecules as found in the initial bibliographic review and described in the general approach section.

In order to achieve this objective, we resolved to apply the multitarget strategy and the privileged structure concept. Synthetic ease and accessibility to the biological experiments was always kept in mind to develop in the most rapid and efficient way this research. New hybrids were obtained combining the NBP and DBMA fragments with different scaffolds endowed with antioxidant properties and which could play a complementary role to give to the resulting hybrids a multitarget profile.

Along this work we have demonstrated that NBP and DBMA fragments are able to give to the new hybrids affinity the cholinesterases, as we expected from the very beginning according to the initial bibliographic review. Depending on the complementary scaffold, newly obtained hybrids exhibit affinity for the several enzymes related to AD.

We have found that the combination of these two fragments with LA give molecules with affinity for the σ1R, and consequently, with the potential to preserve the health of the neurons affected in AD. As explained in the in the introduction and conclusions sections of the first chapter, we believe that agonizing the σ1R could be beneficial to maintain the communication between ER and mitochondria, the proper functioning of calcium channels and to avoid excitotoxicity.

In this first approximation we effectively obtained molecules with a multitarget profile. Even though, more experiments are needed to corroborate the agonist character the σ1R ligands obtained here, they are starting point to continue the investigation in order to improve the activity towards AChE and BACE1. On the other hand, we believe that further experiments should be addressed in order to determine the possible antidepressant effects of these molecules, since there is enough evidence demonstrating that σ1R could be involved in the mechanism of some antidepressants such as fluvoxamine. [275]

In the second and fourth chapter we successfully combined the fragments of interest with the chromone scaffold and the cinnamic structure respectively. Once more, naturally occurring scaffolds were the inspiration to obtain the desired multitarget products. These new hybrids exhibited the desired MAO inhibitory activity and the radical scavenger capacity; apart from the ability to inhibit simultaneously AChE and BACE1.

Yet again, complementary experiments must be carried out in order to take this new hybrids one step further. Taking into account their ability to inhibit MAO-A and MAO-B, the antidepressant activity must be explored; as well as their antiparkinsonian effects. MAO-B inhibitors are valuable tools in the pharmacotherapy of PD. However, drugs with additional properties are urgently needed and this kind of compounds could be a starting point.

The neurogenic properties exhibited by compounds of chapter one and four were a nice discovery. Although these are qualitative results, it is clear that a neurogenic effect was observed. Even though, the role of neurogenesis in adults is not yet fully understood and the usefulness of the neurogenic agents is still a topic of discussion; it is worth to continue the study of this kind of compounds. Maybe their ability to influence this

process could be a valuable tool that may help us to increase our understanding in this field.

In regard of the lack of affinity of hybrids obtained in the third chapter, it is true that more substituents could have been used to obtain a wider series. However we must admit that the current model of research, sometimes force the researchers to sweep aside some projects in order to focus their efforts in the most promising ones in order to use resources in the most efficient manner. Although it was a disappointment, a conclusion can be drawn from this chapter: not always you hit the target you aimed to. Maybe this is the case; maybe this combination of privileged scaffolds in the way it was developed has not affinity for NMDA receptors. The results are the results.

Summarizing, the *N*-benzyl piperidine and the *N*, *N*-dibenzyl-*N*-methyl amine fragments have proved to behave as privileged structures providing four series of new compounds with affinity for the targets aimed in this work. The new molecules presented in this work intend to be a small contribution in the quest for the urgently needed disease modifying drug to treat Alzheimer's disease.

.

Resumen

Introducción

La enfermedad de Alzheimer (EA) es una patología que se caracteriza por una pérdida progresiva de neuronas en áreas específicas tales como la corteza frontal, el neocórtex, y las proyecciones subcorticales del *nucleus basalis* de Meynert. Dicha pérdida de neuronas colinérgicas produce niveles bajos de acetilcolina, ocasionando una interrupción de la transmisión entre las células implicadas en los procesos de memoria y aprendizaje. Esta interrupción es el origen de los síntomas cognitivos de la EA, tales como pérdida de memoria, incapacidad para pensar, para razonar y hacer juicios, así como dificultades de comunicación.

El conocimiento de la disfunción en el sistema colinérgico condujo a proponer a la acetilcolinesterasa como la primera diana farmacológica en la búsqueda de agentes terapéuticos para el tratamiento del alzheimer. Los inhibidores de la acetilcolinesterasa fueron la primera clase de fármacos usados con éxito en el tratamiento sintomático de esta enfermedad. Sin embargo, a pesar de mejorar los indicadores cognitivos y comportamentales en pacientes tratados con inhibidores de acetilcolinesterasa, esta clase de fármacos ha sido incapaz de detener la degeneración neuronal.

Es por esto que una explicación del origen de los síntomas cognitivos no basta para saber lo que causa realmente la pérdida de neuronas en la EA. Actualmente, el péptido beta amiloide (Aβ) es considerado la sustancia que inicia el proceso que lleva a la muerte neuronal. Las fibrillas insolubles de este péptido son el componente principal de las placas seniles, consideradas como el elemento tóxico que desencadena la cascada de respuestas celulares que finalmente producirán la

neurodegeneración. Algunos de estos eventos moleculares y celulares son la inflamación neural, la producción de especies reactivas de oxígeno y la hiperfosforilación de la proteína *tau*. Una estrategia importante en la búsqueda de nuevos fármacos capaces de prevenir la formación del péptido Aβ y la consecuente formación de placas seniles ha sido la síntesis de inhibidores de la beta secretasa, una de las tres enzimas responsable del procesamiento de la proteína precursora de amiloide.

Por otra parte, además de la disminución de los niveles de acetilcolina, se ha demostrado una disminución en los niveles cerebrales de otros neurotransmisores tales como: dopamina, serotonina y noradrenalina, en comparación con los niveles observados en el envejecimiento saludable. Simultáneamente, se sabe que los niveles de MAO-B se incrementan con la edad, tanto en personas saludables como en personas con EA. Este incremento se correlaciona con una producción exagerada de especies reactivas de oxígeno, responsables del ambiente tóxico que caracteriza las enfermedades neurodegenerativas. La inhibición de MAO se ha evaluado también como una alternativa en la búsqueda de nuevos fármacos para tratar la EA, tanto para reducir los niveles de estrés oxidativo, inhibiendo MAO-B, como para tratar la depresión asociada esta enferemedad, inhibiendo MAO-A.

Esta breve descripción pone de manifiesto que la EA es una compleja red influenciada por una extensa variedad de factores. En el resto de esta memoria se explicará de una manera más profunda el papel de cada una de las enzimas que se ha seleccionado como diana farmacológica, así como la estrategia utilizada y los resultados obtenidos. Dicha complejidad de factores nos ha llevado a proponer el desarrollo del siguiente objetivo general.

Objetivo

En este trabajo se ha propuesto evaluar la utilidad de los fragmentos de *N*-bencilpiperidina (NBP) y de *N, N*-dibencil-*N*-metilamina (DBMA) para el diseño, síntesis y evaluación farmacológica de nuevos compuestos multidiana con afinidad por enzimas relevantes en la aparición y desarrollo de la EA. Para lograr este objetivo, algunas estructuras químicas de origen natural (cromona, 4-quinolinona, ácido lipóico y ácido cinámico) han sido combinadas con los fragmentos de NBP y DBMA en moléculas sencillas buscando un perfil multidiana. La sencillez en las rutas de síntesis y la accesibilidad a los ensayos biológicos fue tenida en cuenta para desarrollar de la manera más eficiente y rápida este proyecto. Los nuevos compuestos obtenidos en este trabajo fueron evaluados en varios ensayos biológicos, *in vivo* e *in vitro*, así como en experimentos *in sílico* con el fin de encontrar una relación entre la estructura química y la actividad biológica.

Resultados

Los fragmentos de NBP y DBMA fueron útiles en la síntesis de nuevos híbridos con afinidad por acetilcolinesterasa, tal como se esperaba desde la revisión bibliográfica inicial. Dependiendo de la estructura complementaria con la que estos fragmentos fueron combinados, los nuevos compuestos presentan actividad sobre varias enzimas relacionadas con la EA.

La combinación de los fragmentos de NBP o DBMA con el ácido lipóico permitió la obtención de nuevas moléculas con afinidad por el receptor sigma 1. Gracias a esta propiedad, estos compuestos pueden ayudar a preservar la salud de las neuronas afectadas en la EA, ayudando a evitar, o al menos retrasar, los procesos neurodegenerativos. Simultáneamente, estos compuestos son capaces de inhibir a la beta-secretasa y estimular procesos neurogénicos.

En el segundo y cuarto capítulos de esta tesis, se combinaron con éxito los fragmentos de interés con la estructura de la cromona y el ácido cinámico. Nuevamente, los compuestos obtenidos estuvieron inspirados en estructuras de origen natural. Estos nuevos híbridos demostraron tener actividad en AChE y MAO, así como capacidad antioxidante, tal como se esperaba de su diseño. Los compuestos basados en el ácido cinámico demostraron ser antioxidantes más efectivos que aquellos basados en la cromona, así como poseer también propiedades neurogénicas.

Los compuestos del tercer capítulo, combinando la estructura del ácido kinurénico con los fragmentos de NBP y de DBMA, fueron completamente inactivos en el receptor de NMDA para el cual fueron diseñados. Sin embargo son inhibidores de AChE y MAO.

Los efectos neurogénicos observados en los compuestos del capítulo primero y tercero, fueron un agradable descubrimiento. Aunque estos son resultados cualitativos, un efecto neurogénico fue claramente observado. A pesar de que el papel de la neurogénesis en adultos no está entendido completamente y de que la utilidad de agentes neurogénicos sigue siendo tema de debate, vale la pena continuar con su estudio. Es posible que su habilidad de intervenir en este proceso los convierta en una herramienta que nos ayude a incrementar nuestro conocimiento en esta área.

Conclusiones

Los fragmentos de NBP y DBMA han demostrado ser estructuras privilegiadas en la búsqueda de nuevas moléculas con posible aplicación en la EA. Con base en estas estructuras se han generado ocho familias de nuevos compuestos bioactivos.

La estrategia de hibridación utilizada a lo largo de este trabajo, fue efectiva en la obtención de nuevos compuestos con perfil multidiana.

Todos los compuestos fueron diseñados bajo esta estrategia, acoplando en una molécula pequeña dos estructuras privilegiadas. Los compuestos resultantes de esta combinación presentaron en la mayoría de los casos la actividad biológica esperada.

Las moléculas presentadas en esta tesis doctoral, pretenden ser una pequeña contribución en la gesta por encontrar el tan necesitado fármaco capaz de modificar el avance de la enfermedad de Alzheimer.

Bibliography

(1) Francis, P. T.; Palmer, A. M.; Snape, M.; Wilcock, G. K. The cholinergic hypothesis of Alzheimer's disease: a review of progress. *J. Neurol. Neurosurg. Psychiatry* **1999**, *66* (2), 137-147.

(2) Tagliavini, F.; Pilleri, G. Basal nucleus of meynert: A neuropathological study in Alzheimer's disease, simple senile dementia, Pick's disease and Huntington's chorea. *J. Neurol. Sci.* **1983**, *62* (1–3), 243-260.

(3) Nagai, T.; McGeer, P. L.; Peng, J. H.; McGeer, E. G.; Dolman, C. E. Choline acetyltransferase immunohistochemistry in brains of alzheimer's disease patients and controls. *Neurosci. Lett.* **1983**, *36* (2), 195-199.

(4) Liu, A.; Chang, R. C.; Pearce, R. B.; Gentleman, S. Nucleus basalis of Meynert revisited: anatomy, history and differential involvement in Alzheimer's and Parkinson's disease. *Acta Neuropathol.* **2015**, *129* (4), 527-540.

(5) Murphy, M. P.; LeVine, H. Alzheimer's disease and the amyloid-beta peptide. *J. Alzheimers Dis.* **2010**, *19* (1), 311-323.

(6) Deshpande, A.; Mina, E.; Glabe, C.; Busciglio, J. Different conformations of amyloid beta induce neurotoxicity by distinct mechanisms in human cortical neurons. *J. Neurosci.* **2006**, *26* (22), 6011-6018.

(7) Gasic-Milenkovic, J.; Dukic-Stefanovic, S.; Deuther-Conrad, W.; Gartner, U.; Munch, G. beta-Amyloid peptide potentiates inflammatory responses induced by lipopolysaccharide, interferon -gamma and 'advanced glycation endproducts' in a murine microglia cell line. *Eur. J. Neurosci.* **2003**, *17* (4), 813-821.

(8) Couturier, J.; Paccalin, M.; Morel, M.; Terro, F.; Milin, S.; Pontcharraud, R.; Fauconneau, B.; Page, G. Prevention of the beta-amyloid peptide-induced inflammatory process by inhibition of double-

stranded RNA-dependent protein kinase in primary murine mixed co-cultures. *J. Neuroinflamm.* **2011**, *8*, 72.

(9) Mamelak, M. Alzheimer' s disease, oxidative stress and gammahydroxybutyrate. *Neurobiol. Aging* **2007**, *28* (9), 1340-1360.

(10) Rosini, M.; Simoni, E.; Milelli, A.; Minarini, A.; Melchiorre, C. Oxidative stress in Alzheimer's disease: are we connecting the dots? *J. Med. Chem.* **2014**, *57* (7), 2821-2831.

(11) Melo, A.; Monteiro, L.; Lima, R. M.; Oliveira, D. M.; Cerqueira, M. D.; El-Bacha, R. S. Oxidative stress in neurodegenerative diseases: mechanisms and therapeutic perspectives. *Oxid. Med. Cell. Longev.* **2011**, *2011*, 467180.

(12) Lloret, A.; Fuchsberger, T.; Giraldo, E.; Vina, J. Molecular mechanisms linking amyloid beta toxicity and Tau hyperphosphorylation in Alzheimers disease. *Free Radic. Biol. Med.* **2015**, *83*, 186-191.

(13) Adolfsson, R.; Gottfries, C. G.; Roos, B. E.; Winblad, B., *Changes in the Brain Catecholamines in Patients with Dementia of Alzheimer type*. 1979; p 216-223.

(14) Fowler, C. J., Wiberg, A., Oreland, L., Marcusson, J., and Winblad, B The effect of age on the activity and molecular properties of human brain monoamine oxidase. . *J. Neural. Transm.* **1980**, *49*, 1-20.

(15) Fowler, J. S. V., N.D. Wang, G.J. Logan, J. Pappas, N. Shea, C. MacGregor, R. Age related increases in brain monoamine oxidase B in living healthy human subjects. *Neurobiol. Aging.* **1997**, *(18)*, 431-435.

(16) Strolin Benedetti, M. D., P. Monoamine oxidase, brain ageing and degenerative diseases. *Biochem. Pharmacol.* **1989**, *38*, 555-561.

(17) Aluf, Y.; Vaya, J.; Khatib, S.; Loboda, Y.; Finberg, J. P. M. Selective inhibition of monoamine oxidase A or B reduces striatal oxidative stress in rats with partial depletion of the nigro-striatal dopaminergic pathway. *Neuropharmacology* **2013**, *65*, 48-57.

(18) Vermeiren, Y.; Van Dam, D.; Aerts, T.; Engelborghs, S.; De Deyn, P. P. Monoaminergic neurotransmitter alterations in postmortem brain

regions of depressed and aggressive patients with Alzheimer's disease. *Neurobiol. Aging.* **2014**, *35* (12), 2691-2700.

(19) Finberg, J. P. M. Update on the pharmacology of selective inhibitors of MAO-A and MAO-B: Focus on modulation of CNS monoamine neurotransmitter release. *Pharmacol. Ther.* **2014**, *143* (2), 133-152.

(20) Coulson, D. T.; Beyer, N.; Quinn, J. G.; Brockbank, S.; Hellemans, J.; Irvine, G. B.; Ravid, R.; Johnston, J. A. BACE1 mRNA expression in Alzheimer's disease postmortem brain tissue. *J. Alzheimers Dis.* **2010**, *22* (4), 1111-1122.

(21) Martinez, A.; Gil, C.; Perez, D. I. Glycogen synthase kinase 3 inhibitors in the next horizon for Alzheimer's disease treatment. *Int. J. Alzheimers Dis.* **2011**, (10), 30.

(22) Green, R. C.; Schneider, L. S.; Amato, D. A.; Beelen, A. P.; Wilcock, G.; Swabb, E. A.; Zavitz, K. H.; the Tarenflurbil Phase 3 Study, G. Effect of Tarenflurbil on Cognitive Decline and Activities of Daily Living in Patients With Mild Alzheimer Disease: A Randomized Controlled Trial. *J. Am. Med. Assoc.* **2009**, *302* (23), 2557-2564.

(23) Siemers, E.; Henley, D.; Sundell, K.; Sethuraman, G.; Dean, R.; Wrobleski, K.; Mohs, R. Evaluating semagacestat, a gamma-secretase inhibitor, in a phase III trial. *Alzheimers Dement.* **2011**, *7* (4, Supplement), S484-S485.

(24) Cummings, J. What Can Be Inferred from the Interruption of the Semagacestat Trial for Treatment of Alzheimer's Disease? *Biol. Psychiatry* **2010**, *68* (10), 876-878.

(25) Holmes, C.; Boche, D.; Wilkinson, D.; Yadegarfar, G.; Hopkins, V.; Bayer, A.; Jones, R. W.; Bullock, R.; Love, S.; Neal, J. W.; Zotova, E.; Nicoll, J. A. R. Long-term effects of Aβ42 immunisation in Alzheimer's disease: follow-up of a randomised, placebo-controlled phase I trial. *The Lancet* **2008**, *372* (9634), 216-223.

(26) Evin, G.; Barakat, A. Critical analysis of the use of beta;-site amyloid precursor protein-cleaving enzyme 1 inhibitors in the treatment of Alzheimer's disease. *Degener. Neurol. Neuromuscul. Dis.* **2014**, 1.

(27) Ghosh, A. K.; Osswald, H. L. BACE1 (beta-secretase) inhibitors for the treatment of Alzheimer's disease. *Chem. Soc. Rev.* **2014**, *43* (19), 6765-6813.

(28) Godyń, J.; Jończyk, J.; Panek, D.; Malawska, B. Therapeutic strategies for Alzheimer's disease in clinical trials. *Pharmacol. Rep.* **2015**, 127-138.

(29) Jia, Q.; Deng, Y.; Qing, H. Potential therapeutic strategies for Alzheimer's disease targeting or beyond beta-amyloid: insights from clinical trials. *Biomed. Res. Int.* **2014**, *2014*, 837157.

(30) Hong, L.; Koelsch, G.; Lin, X.; Wu, S.; Terzyan, S.; Ghosh, A. K.; Zhang, X. C.; Tang, J. Structure of the Protease Domain of Memapsin 2 (β-Secretase) Complexed with Inhibitor. *Science* **2000**, *290* (5489), 150-153.

(31) Gijsen, H. J. M.; Bischoff, F. P., Chapter Five - Secretase Inhibitors and Modulators as a Disease-Modifying Approach Against Alzheimer's Disease. In *Annu. Rep. Med. Chem.*, Academic Press: 2012; Vol. 47, pp 55-69.

(32) Olson, R. E.; Marcin, L. R., Secretase Inhibitors and Modulators for the Treatment of Alzheimer's Disease. In *Annu. Rep. Med. Chem.*, John, E. M., Ed. Academic Press: 2007; Vol. 42, pp 27-47.

(33) Evin, G.; Lessene, G.; Wilkins, S. BACE inhibitors as potential drugs for the treatment of Alzheimer's disease: focus on bioactivity. *Recent. Pat. CNS. Drug Discov.* **2011**, *6* (2), 91-106.

(34) Ghosh, A. K.; Brindisi, M.; Tang, J. Developing beta-secretase inhibitors for treatment of Alzheimer's disease. *J. Neurochem.* **2012**, *120 Suppl 1*, 71-83.

(35) Stamford, A.; Strickland, C. Inhibitors of BACE for treating Alzheimer's disease: a fragment-based drug discovery story. *Curr. Opin. Chem. Biol.* **2013**, *17* (3), 320-328.

(36) Lucas, F.; Fukushima, T.; Nozaki, Y. Novel BACE1 inhibitor, E2609, lowers Aβ levels in the cerebrospinal fluid and plasma in nonhuman primates. *Alzheimers Dement.* **2012**, *8* (4, Supplement), P224.

(37) Vassar, R. BACE1 inhibitor drugs in clinical trials for Alzheimer's disease. *Alzheimers Res. Ther.* **2014**, *6* (9), 89.

(38) Bolognesi, M. L.; Matera, R.; Minarini, A.; Rosini, M.; Melchiorre, C. Alzheimer's disease: new approaches to drug discovery. *Curr. Opin. Chem. Biol.* **2009**, *13* (3), 303-308.

(39) Cummings, J. L. Defining and labeling disease-modifying treatments for Alzheimer's disease. *Alzheimers Dement.* **2009**, *5* (5), 406-418.

(40) Agis-Torres, A.; Solhuber, M.; Fernandez, M.; Sanchez-Montero, J. M. Multi-Target-Directed Ligands and other Therapeutic Strategies in the Search of a Real Solution for Alzheimer's Disease. *Curr. Neuropharmacol.* **2014**, *12* (1), 2-36.

(41) Cavalli, A.; Bolognesi, M. L.; Minarini, A.; Rosini, M.; Tumiatti, V.; Recanatini, M.; Melchiorre, C. Multi-target-directed ligands to combat neurodegenerative diseases. *J. Med. Chem.* **2008**, *51* (3), 347-372.

(42) Han, H. J.; Kim, B. C.; Lee, J. Y.; Ryu, S. H.; Na, H. R.; Yoon, S. J.; Park, H. Y.; Shin, J. H.; Cho, S. J.; Yi, H. A.; Choi, M. S.; Heo, J. H.; Park, K. W.; Kim, K. K.; Choi, S. H. Response to rivastigmine transdermal patch or memantine plus rivastigmine patch is affected by apolipoprotein E genotype in Alzheimer patients. *Dement. Geriatr. Cogn. Disord.* **2012**, *34* (3-4), 167-173.

(43) Farrimond, L. E.; Roberts, E.; McShane, R. Memantine and cholinesterase inhibitor combination therapy for Alzheimer's disease: a systematic review. *BMJ Open* **2012**, *2* (3), e000917.

(44) Rodríguez-Rodríguez, C.; Telpoukhovskaia, M.; Orvig, C. The art of building multifunctional metal-binding agents from basic molecular scaffolds for the potential application in neurodegenerative diseases. *Coord. Chem. Rev.* **2012**, *256* (19-20), 2308-2332.

(45) Van der Schyf, C. J.; Geldenhuys, W. J. Multimodal drugs and their future for Alzheimer's and Parkinson's disease. *Int. Rev. Neurobiol.* **2011**, *100*, 107-125.

(46) Muller-Schiffmann, A.; Sticht, H.; Korth, C. Hybrid compounds: from simple combinations to nanomachines. *BioDrugs* **2012**, *26* (1), 21-31.

(47) Korcsmáros, T.; Szalay, M. S.; Böde, C.; Kovács, I. A.; Csermely, P. How to design multi-target drugs. *Expert Opin. Drug Dis.* **2007**, *2* (6), 799-808.

(48) Evans, B. E.; Rittle, K. E.; Bock, M. G.; DiPardo, R. M.; Freidinger, R. M.; Whitter, W. L.; Lundell, G. F.; Veber, D. F.; Anderson, P. S. Methods for drug discovery: development of potent, selective, orally effective cholecystokinin antagonists. *J. Med. Chem.* **1988**, *31* (12), 2235-2246.

(49) Welsch, M. E.; Snyder, S. A.; Stockwell, B. R. Privileged scaffolds for library design and drug discovery. *Curr. Opin. Chem. Biol.* **2010**, *14* (3), 347-361.

(50) Duarte, C. D.; Barreiro, E. J.; Fraga, C. A. Privileged structures: a useful concept for the rational design of new lead drug candidates. *Mini Rev. Med. Chem.* **2007**, *7* (11), 1108-1119.

(51) Williams, K. Ifenprodil, a novel NMDA receptor antagonist: site and mechanism of action. *Curr. Drug Targets* **2001**, *2* (3), 285-298.

(52) Cheung, J.; Rudolph, M. J.; Burshteyn, F.; Cassidy, M. S.; Gary, E. N.; Love, J.; Franklin, M. C.; Height, J. J. Structures of Human Acetylcholinesterase in Complex with Pharmacologically Important Ligands. *J. Med. Chem.* **2012**, *55* (22), 10282-10286.

(53) Zampieri, D.; Grazia Mamolo, M.; Laurini, E.; Zanette, C.; Florio, C.; Collina, S.; Rossi, D.; Azzolina, O.; Vio, L. Substituted benzo[d]oxazol-2(3H)-one derivatives with preference for the sigma1 binding site. *Eur. J. Med. Chem.* **2009**, *44* (1), 124-130.

(54) Laurini, E.; Col, V. D.; Mamolo, M. G.; Zampieri, D.; Posocco, P.; Fermeglia, M.; Vio, L.; Pricl, S. Homology Model and Docking-Based

Virtual Screening for Ligands of the σ1 Receptor. *ACS Med. Chem. Lett.* **2011**, *2* (11), 834-839.

(55) Laurini, E.; Da Col, V.; Wünsch, B.; Pricl, S. Analysis of the molecular interactions of the potent analgesic S1RA with the σ1 receptor. *Bioorg. Med. Chem. Lett.* **2013**, *23* (10), 2868-2871.

(56) Yang, W.; Fucini, R. V.; Fahr, B. T.; Randal, M.; Lind, K. E.; Lam, M. B.; Lu, W.; Lu, Y.; Cary, D. R.; Romanowski, M. J.; Colussi, D.; Pietrak, B.; Allison, T. J.; Munshi, S. K.; Penny, D. M.; Pham, P.; Sun, J.; Thomas, A. E.; Wilkinson, J. M.; Jacobs, J. W.; McDowell, R. S.; Ballinger, M. D. Fragment-Based Discovery of Nonpeptidic BACE-1 Inhibitors Using Tethering. *Biochemistry* **2009**, *48* (21), 4488-4496.

(57) Asadipour, A.; Alipour, M.; Jafari, M.; Khoobi, M.; Emami, S.; Nadri, H.; Sakhteman, A.; Moradi, A.; Sheibani, V.; Homayouni Moghadam, F.; Shafiee, A.; Foroumadi, A. Novel coumarin-3-carboxamides bearing N-benzylpiperidine moiety as potent acetylcholinesterase inhibitors. *Eur. J. Med. Chem.* **2013**, *70*, 623-630.

(58) Tsao, L.-i.; Su, T.-P. Naloxone-sensitive, haloperidol-sensitive, [3H] (+) SKF-10047-binding protein partially purified from rat liver and rat brain membranes: An opioid/sigma receptor? *Synapse* **1997**, *25* (2), 117-124.

(59) Seth, P.; Fei, Y.-J.; Li, H. W.; Huang, W.; Leibach, F. H.; Ganapathy, V. Cloning and Functional Characterization of a σ Receptor from Rat Brain. *J. Neurochem.* **1998**, *70* (3), 922-931.

(60) Kekuda, R.; Prasad, P. D.; Fei, Y. J.; Leibach, F. H.; Ganapathy, V. Cloning and functional expression of the human type 1 sigma receptor (hSigmaR1). *Biochem. Biophys. Res. Commun.* **1996**, *229* (2), 553-558.

(61) Martin, W. R.; Eades, C. G.; Thompson, J. A.; Huppler, R. E.; Gilbert, P. E. The effects of morphine- and nalorphine- like drugs in the nondependent and morphine-dependent chronic spinal dog. *J. Pharmacol. Exp. Ther.* **1976**, *197* (3), 517-532.

(62) Vaupel, D. B. Naltrexone fails to antagonize the sigma effects of PCP and SKF 10,047 in the dog. *Eur. J. Pharmacol.* **1983**, *92* (3-4), 269-274.

(63) Herling, S.; Shannon, H. E. Discriminative effects of ethylketazocine in the rat: Stereospecificity and antagonism by naloxone. *Life Sci.* **1982**, *31* (20–21), 2371-2374.

(64) Quirion, R.; Chicheportiche, R.; Contreras, P. C.; Johnson, K. M.; Lodge, D.; William Tam, S.; Woods, J. H.; Zukin, S. R. Classification and nomenclature of phencyclidine and sigma receptor sites. *Trends Neurosci.* **1987**, *10* (11), 444-446.

(65) Gundlach, A. L.; Largent, B. L.; Snyder, S. H. Phencyclidine and σ opiate receptors in brain: Biochemical and autoradiographical differentiation. *Eur. J. Pharmacol.* **1985**, *113* (3), 465-466.

(66) Hellewell, S. B.; Bowen, W. D. A sigma-like binding site in rat pheochromocytoma (PC12) cells: decreased affinity for (+)-benzomorphans and lower molecular weight suggest a different sigma receptor form from that of guinea pig brain. *Brain Res.* **1990**, *527* (2), 244-253.

(67) Quirion, R.; Bowen, W. D.; Itzhak, Y.; Junien, J. L.; Musacchio, J.; Rothman, R. B.; Tsung-Ping, S.; Tam, S. W.; Taylor, D. P. A proposal for the classification of sigma binding sites. *Trends Pharmacol. Sci.* **1992**, *13*, 85-86.

(68) Hanner, M.; Moebius, F. F.; Flandorfer, A.; Knaus, H. G.; Striessnig, J.; Kempner, E.; Glossmann, H. Purification, molecular cloning, and expression of the mammalian sigma1-binding site. *Proc. Natl. Acad. Sci. U S A* **1996**, *93* (15), 8072-8077.

(69) Mei, J.; Pasternak, G. W. Molecular cloning and pharmacological characterization of the rat sigma1 receptor1. *Biochem. Pharmacol.* **2001**, *62* (3), 349-355.

(70) Kekuda, R.; Prasad, P. D.; Fei, Y.-J.; Leibach, F. H.; Ganapathy, V. Cloning and Functional Expression of the Human Type 1 Sigma Receptor (hSigmaR1). *Biochem. Biophys. Res. Commun.* **1996**, *229* (2), 553-558.

(71) Hayashi, T.; Su, T. P. Sigma-1 receptor chaperones at the ER-mitochondrion interface regulate Ca(2+) signaling and cell survival. *Cell* **2007**, *131* (3), 596-610.

(72) Su, T. P.; Hayashi, T.; Maurice, T.; Buch, S.; Ruoho, A. E. The sigma-1 receptor chaperone as an inter-organelle signaling modulator. *Trends Pharmacol. Sci.* **2010**, *31* (12), 557-566.

(73) Ono, Y.; Tanaka, H.; Takata, M.; Nagahara, Y.; Noda, Y.; Tsuruma, K.; Shimazawa, M.; Hozumi, I.; Hara, H. SA4503, a sigma-1 receptor agonist, suppresses motor neuron damage in in vitro and in vivo amyotrophic lateral sclerosis models. *Neurosci. Lett.* **2014**, *559*, 174-178.

(74) Mancuso, R.; Olivan, S.; Rando, A.; Casas, C.; Osta, R.; Navarro, X. Sigma-1R agonist improves motor function and motoneuron survival in ALS mice. *Neurotherapeutics : the journal of the American Society for Experimental NeuroTherapeutics* **2012**, *9* (4), 814-826.

(75) Francardo, V.; Bez, F.; Wieloch, T.; Nissbrandt, H.; Ruscher, K.; Cenci, M. A. Pharmacological stimulation of sigma-1 receptors has neurorestorative effects in experimental parkinsonism. *Brain* **2014**, *137* (7), 1998-2014.

(76) Miki, Y.; Tanji, K.; Mori, F.; Wakabayashi, K. Sigma-1 receptor is involved in degradation of intranuclear inclusions in a cellular model of Huntington's disease. *Neurobiol. Dis.* **2015**, *74*, 25-31.

(77) Ruscher, K.; Wieloch, T. The involvement of the sigma-1 receptor in neurodegeneration and neurorestoration. *J. Pharmacol. Sci.* **2015**, *127* (1), 30-35.

(78) Miki, Y.; Mori, F.; Kon, T.; Tanji, K.; Toyoshima, Y.; Yoshida, M.; Sasaki, H.; Kakita, A.; Takahashi, H.; Wakabayashi, K. Accumulation of the sigma-1 receptor is common to neuronal nuclear inclusions in various neurodegenerative diseases. *Neuropathology* **2014**, *34* (2), 148-158.

(79) Weissman, A. D.; Su, T. P.; Hedreen, J. C.; London, E. D. Sigma receptors in post-mortem human brains. *J. Pharmacol. Exp. Ther.* **1988**, *247* (1), 29-33.

(80) Jansen, K. L. R.; Faull, R. L. M.; Dragunow, M.; Leslie, R. A. Autoradiographic distribution of sigma receptors in human neocortex, hippocampus, basal ganglia, cerebellum, pineal and pituitary glands. *Brain Res.* **1991**, *559* (1), 172-177.

(81) Seth, P.; Ganapathy, M. E.; Conway, S. J.; Bridges, C. D.; Smith, S. B.; Casellas, P.; Ganapathy, V. Expression pattern of the type 1 sigma receptor in the brain and identity of critical anionic amino acid residues in the ligand-binding domain of the receptor. *BBA - Mol. Cell Res.* **2001**, *1540* (1), 59-67.

(82) Seth, P.; Fei, Y. J.; Li, H. W.; Huang, W.; Leibach, F. H.; Ganapathy, V. Cloning and functional characterization of a sigma receptor from rat brain. *J. Neurochem.* **1998**, *70* (3), 922-931.

(83) Hayashi, T.; Su, T. P. The Sigma Receptor: Evolution of the Concept in Neuropsychopharmacology. *Curr. Neuropharmacol.* **2005**, *3* (4), 267-280.

(84) Palacios, G.; Muro, A.; Verdú, E.; Pumarola, M.; Vela, J. M. Immunohistochemical localization of the sigma1 receptor in Schwann cells of rat sciatic nerve. *Brain Res.* **2004**, *1007* (1–2), 65-70.

(85) Hayashi, T.; Su, T. P. Sigma-1 receptors at galactosylceramide-enriched lipid microdomains regulate oligodendrocyte differentiation. *Proc. Natl. Acad. Sci. U S A* **2004**, *101* (41), 14949-14954.

(86) Matsumoto, R. R. B., W. D., Su, T.P. Sigma Receptors Chemistry, Cell Biology and Clinical Implications. *Springer* **2007**.

(87) Monnet, F. P.; Debonnel, G.; Junien, J.-L.; De Montigny, C. N-methyl-D-aspartate-induced neuronal activation is selectively modulated by σ receptors. *Eur. J. Pharmacol.* **1990**, *179* (3), 441-445.

(88) Matsuno, K.; Matsunaga, K.; Mita, S. Increase of extracellular acetylcholine level in rat frontal cortex induced by (+)N-allylnormetazocine as measured by brain microdialysis. *Brain Res.* **1992**, *575* (2), 315-319.

(89) Senda, T.; Matsuno, K.; Okamoto, K.; Kobayashi, T.; Nakata, K.; Mita, S. Ameliorating effect of SA4503, a novel σ1 receptor agonist, on

memory impairments induced by cholinergic dysfunction in rats. *Eur. J. Pharmacol.* **1996**, *315* (1), 1-10.

(90) Jarrard, L. E. On the use of ibotenic acid to lesion selectively different components of the hippocampal formation. *J. Neurosci. Methods* **1989**, *29* (3), 251-259.

(91) Maurice, T. Beneficial effect of the σ1 receptor agonist PRE-084 against the spatial learning deficits in aged rats. *Eur. J. Pharmacol.* **2001**, *431* (2), 223-227.

(92) Meunier, J.; Ieni, J.; Maurice, T. The anti-amnesic and neuroprotective effects of donepezil against amyloid beta25-35 peptide-induced toxicity in mice involve an interaction with the sigma1 receptor. *Br. J. Pharmacol.* **2006**, *149* (8), 998-1012.

(93) Villard, V.; Espallergues, J.; Keller, E.; Vamvakides, A.; Maurice, T. Anti-amnesic and neuroprotective potentials of the mixed muscarinic receptor/sigma 1 (sigma1) ligand ANAVEX2-73, a novel aminotetrahydrofuran derivative. *J. Psychopharmacol.* **2011**, *25* (8), 1101-1117.

(94) Villard, V.; Espallergues, J.; Keller, E.; Alkam, T.; Nitta, A.; Yamada, K.; Nabeshima, T.; Vamvakides, A.; Maurice, T. Antiamnesic and neuroprotective effects of the aminotetrahydrofuran derivative ANAVEX1-41 against amyloid beta(25-35)-induced toxicity in mice. *Neuropsychopharmacology* **2009**, *34* (6), 1552-1566.

(95) Lahmy, V.; Meunier, J.; Malmstrom, S.; Naert, G.; Givalois, L.; Kim, S. H.; Villard, V.; Vamvakides, A.; Maurice, T. Blockade of Tau hyperphosphorylation and Abeta1-42 generation by the aminotetrahydrofuran derivative ANAVEX2-73, a mixed muscarinic and sigma(1) receptor agonist, in a nontransgenic mouse model of Alzheimer's disease. *Neuropsychopharmacology* **2013**, *38* (9), 1706-1723.

(96) Jansen, K. L.; Faull, R. L.; Storey, P.; Leslie, R. A. Loss of sigma binding sites in the CA1 area of the anterior hippocampus in Alzheimer's disease correlates with CA1 pyramidal cell loss. *Brain Res.* **1993**, *623* (2), 299-302.

(97) Mishina, M.; Ohyama, M.; Ishii, K.; Kitamura, S.; Kimura, Y.; Oda, K.; Kawamura, K.; Sasaki, T.; Kobayashi, S.; Katayama, Y.; Ishiwata, K. Low density of sigma1 receptors in early Alzheimer's disease. *Ann. Nucl. Med.* **2008**, *22* (3), 151-156.

(98) Pal, A.; Fontanilla, D.; Gopalakrishnan, A.; Chae, Y. K.; Markley, J. L.; Ruoho, A. E. The sigma-1 receptor protects against cellular oxidative stress and activates antioxidant response elements. *Eur. J. Pharmacol.* **2012**, *682* (1-3), 12-20.

(99) Zhang, X. J.; Liu, L. L.; Jiang, S. X.; Zhong, Y. M.; Yang, X. L. Activation of the zeta receptor 1 suppresses NMDA responses in rat retinal ganglion cells. *Neuroscience* **2011**, *177*, 12-22.

(100) Lesage, A. S.; De Loore, K. L.; Peeters, L.; Leysen, J. E. Neuroprotective sigma ligands interfere with the glutamate-activated NOS pathway in hippocampal cell culture. *Synapse* **1995**, *20* (2), 156-164.

(101) Tchedre, K. T.; Huang, R. Q.; Dibas, A.; Krishnamoorthy, R. R.; Dillon, G. H.; Yorio, T. Sigma-1 receptor regulation of voltage-gated calcium channels involves a direct interaction. *Invest. Ophthalmol. Vis. Sci.* **2008**, *49* (11), 4993-5002.

(102) Lobner, D.; Lipton, P. σ-Ligands and non-competitive NMDA antagonists inhibit glutamate release during cerebral ischemia. *Neurosci. Lett.* **1990**, *117* (1–2), 169-174.

(103) Moritz, C.; Berardi, F.; Abate, C.; Peri, F. Live imaging reveals a new role for the sigma-1 (sigma1) receptor in allowing microglia to leave brain injuries. *Neurosci. Lett.* **2015**, *591*, 13-18.

(104) Ishikawa, M. H., K. The role of sigma-1 receptors in the pathophysiology of neuropsychiatric diseases. *J. Receptor Ligand Channel Res.* **2010**, *3*, 25-36.

(105) Reed, L. J.; De, B. B.; Gunsalus, I. C.; Hornberger, C. S., Jr. Crystalline alpha-lipoic acid; a catalytic agent associated with pyruvate dehydrogenase. *Science* **1951**, *114* (2952), 93-94.

(106) Reed, L. J.; Gunsalus, I. C.; Schnakenberg, G. H. F.; Soper, Q. F.; Boaz, H. E.; Kern, S. F.; Parke, T. V. Isolation, Characterization and Structure of α-Lipoic Acid1. *J. Am. Chem. Soc.* **1953**, *75* (6), 1267-1270.

(107) Duprè, S.; Spoto, G.; Matarese, R. M.; Orlando, M.; Cavallini, D. Biosynthesis of lipoic acid in the rat: Incorporation of 35S- and 14C-labeled precursors. *Arch. Biochem. Biophys.* **1980**, *202* (2), 361-365.

(108) Carreau, J.-P., [32] Biosynthesis of lipoic acid via unsaturated fatty acids. In *Meth. Enzymol.*, Donald B. McCormick, L. D. W., Ed. Academic Press: 1979; Vol. 62, pp 152-158.

(109) Reed, L. J.; DeBusk, B. G.; Gunsalus, I. C.; Hornberger, C. S. Crystalline α-Lipoic Acid: A Catalytic Agent Associated with Pyruvate Dehydrogenase. *Science* **1951**, *114* (2952), 93-94.

(110) Handelman, G. J.; Han, D.; Tritschler, H.; Packer, L. α-Lipoic acid reduction by mammalian cells to the dithiol form, and release into the culture medium. *Biochem. Pharmacol.* **1994**, *47* (10), 1725-1730.

(111) Packer, L.; Witt, E. H.; Tritschler, H. J. Alpha-lipoic acid as a biological antioxidant. *Free Radic. Biol. Med.* **1995**, *19* (2), 227-250.

(112) Maczurek, A.; Hager, K.; Kenklies, M.; Sharman, M.; Martins, R.; Engel, J.; Carlson, D. A.; Munch, G. Lipoic acid as an anti-inflammatory and neuroprotective treatment for Alzheimer's disease. *Adv. Drug Deliv. Rev.* **2008**, *60* (13-14), 1463-1470.

(113) Rosini, M.; Simoni, E.; Bartolini, M.; Tarozzi, A.; Matera, R.; Milelli, A.; Hrelia, P.; Andrisano, V.; Bolognesi, M. L.; Melchiorre, C. Exploiting the lipoic acid structure in the search for novel multitarget ligands against Alzheimer's disease. *Eur. J. Med. Chem.* **2011**, *46* (11), 5435-5442.

(114) Prezzavento, O.; Arena, E.; Parenti, C.; Pasquinucci, L.; Arico, G.; Scoto, G. M.; Grancara, S.; Toninello, A.; Ronsisvalle, S. Design and synthesis of new bifunctional sigma-1 selective ligands with antioxidant activity. *J. Med. Chem.* **2013**, *56* (6), 2447-2455.

(115) Muller, U.; Krieglstein, J. Prolonged Pretreatment with [alpha]-Lipoic Acid Protects Cultured Neurons Against Hypoxic, Glutamate-, or Iron-Induced Injury. *J. Cereb. Blood Flow Metab.* **1995**, *15* (4), 624-630.
(116) Bobermin, L. D.; Wartchow, K. M.; Flores, M. P.; Leite, M. C.; Quincozes-Santos, A.; Goncalves, C. A. Ammonia-induced oxidative damage in neurons is prevented by resveratrol and lipoic acid with participation of heme oxygenase 1. *Neurotoxicology* **2015**, *49*, 28-35.
(117) Ali, Y. F.; Desouky, O. S.; Selim, N. S.; Ereiba, K. M. Assessment of the role of α-lipoic acid against the oxidative stress of induced iron overload. *J. Radiat. Res. Appl. Sci.* **2015**, *8* (1), 26-35.
(118) Fava, A.; Pirritano, D.; Plastino, M.; Cristiano, D.; Puccio, G.; Colica, C.; Ermio, C.; De Bartolo, M.; Mauro, G.; Bosco, D. The Effect of Lipoic Acid Therapy on Cognitive Functioning in Patients with Alzheimer's Disease. *J. Neurodegener. Dis.* **2013**, *2013*, 1-7.
(119) Hager, K.; Kenklies, M.; McAfoose, J.; Engel, J.; Munch, G. Alpha-lipoic acid as a new treatment option for Alzheimer's disease: a 48 months follow-up analysis. *J. Neural Transm. Suppl.* **2007**, *72*, 189-193.
(120) Hager, K.; Marahrens, A.; Kenklies, M.; Riederer, P.; Munch, G. Alpha-lipoic acid as a new treatment option for Alzheimer type dementia. *Arch. Gerontol. Geriatr.* **2001**, *32* (3), 275-282.
(121) Haugaard, N.; Levin, R.; Surname, F. Regulation of the activity of choline acetyl transferase by lipoic acid. *Mol. Cell. Biochem.* **2000**, *213* (1-2), 61-63.
(122) Haugaard, N.; Levin, R. Activation of choline acetyl transferase by dihydrolipoic acid. *Mol. Cell. Biochem.* **2002**, *229* (1-2), 103-106.
(123) Zhang, L.; Xing, G. q.; Barker, J. L.; Chang, Y.; Maric, D.; Ma, W.; Li, B.-s.; Rubinow, D. R. α-lipoic acid protects rat cortical neurons against cell death induced by amyloid and hydrogen peroxide through the Akt signalling pathway. *Neurosci. Lett.* **2001**, *312* (3), 125-128.
(124) Lovell, M. A.; Xie, C.; Xiong, S.; Markesbery, W. R. Protection against amyloid beta peptide and iron/hydrogen peroxide toxicity by alpha lipoic acid. *J. Alzheimers Dis.* **2003**, *5* (3), 229-239.

(125) Seaton, T. A.; Jenner, P.; Marsden, C. D. The isomers of thioctic acid alter C-deoxyglucose incorporation in rat basal ganglia. *Biochem. Pharmacol.* **1996**, *51* (7), 983-986.

(126) Steen, E.; Terry, B. M.; Rivera, E. J.; Cannon, J. L.; Neely, T. R.; Tavares, R.; Xu, X. J.; Wands, J. R.; de la Monte, S. M. Impaired insulin and insulin-like growth factor expression and signaling mechanisms in Alzheimer's disease: Is this type 3 diabetes? *J. Alzheimers Dis.* **2005**, *7* (1), 63-80.

(127) de la Monte, S. M.; Wands, J. R. Alzheimer's Disease Is Type 3 Diabetes–Evidence Reviewed. *J. Diabetes Sci. Technol.* **2008**, *2* (6), 1101-1113.

(128) Matera, R. Design and Synthesis of Novel Non Peptidomimetic Beta-Secretase Inhibitors in the Treatment of Alzheimer's Disease. *Uniiversiittà dii Bollogna* **2009**.

(129) Bolognesi, M. L.; Rosini, M.; Andrisano, V.; Bartolini, M.; Minarini, A.; Tumiatti, V.; Melchiorre, C. MTDL design strategy in the context of Alzheimer's disease: from lipocrine to memoquin and beyond. *Curr. Pharm. Des.* **2009**, *15* (6), 601-613.

(130) Bolognesi, M. L.; Cavalli, A.; Bergamini, C.; Fato, R.; Lenaz, G.; Rosini, M.; Bartolini, M.; Andrisano, V.; Melchiorre, C. Toward a Rational Design of Multitarget-Directed Antioxidants: Merging Memoquin and Lipoic Acid Molecular Frameworks. *J. Med. Chem.* **2009**, *52* (23), 7883-7886.

(131) Rosini, M.; Andrisano, V.; Bartolini, M.; Bolognesi, M. L.; Hrelia, P.; Minarini, A.; Tarozzi, A.; Melchiorre, C. Rational Approach To Discover Multipotent Anti-Alzheimer Drugs. *J. Med. Chem.* **2005**, *48* (2), 360-363.

(132) Kates, S. A.; Casale, R. A.; Baguisi, A.; Beeuwkes, R., 3rd Lipoic acid analogs with enhanced pharmacological activity. *Bioorg. Med. Chem.* **2014**, *22* (1), 505-512.

(133) Koufaki, M.; Kiziridi, C.; Nikoloudaki, F.; Alexis, M. N. Design and synthesis of 1,2-dithiolane derivatives and evaluation of their

neuroprotective activity. *Bioorg. Med. Chem. Lett.* **2007**, *17* (15), 4223-4227.

(134) Tarozzi, A.; Bartolini, M.; Piazzi, L.; Valgimigli, L.; Amorati, R.; Bolondi, C.; Djemil, A.; Mancini, F.; Andrisano, V.; Rampa, A. From the dual function lead AP2238 to AP2469, a multi-target-directed ligand for the treatment of Alzheimer's disease. *Pharmacol. Res. Perspect.* **2014**, *2* (2), e00023.

(135) Ellman, G. L.; Courtney, K. D.; Andres, V. J.; Feather-Stone, R. M. A new and rapid colorimetric determination of acetylcholinesterase activity. *Biochem. Pharmacol.* **1961**, *7*, 88-95.

(136) Dávalos, A.; Gómez-Cordovés, C.; Bartolomé, B. Extending Applicability of the Oxygen Radical Absorbance Capacity (ORAC−Fluorescein) Assay. *J. Agric. Food. Chem.* **2004**, *52* (1), 48-54.

(137) Mancini, F.; Naldi, M.; Cavrini, V.; Andrisano, V. Multiwell fluorometric and colorimetric microassays for the evaluation of beta-secretase (BACE-1) inhibitors. *Anal. Bioanal. Chem.* **2007**, *388* (5), 1175-1183.

(138) Piazzi, L.; Cavalli, A.; Belluti, F.; Bisi, A.; Gobbi, S.; Rizzo, S.; Bartolini, M.; Andrisano, V.; Recanatini, M.; Rampa, A. Extensive SAR and Computational Studies of 3-{4-[(Benzylmethylamino)methyl]phenyl}-6,7-dimethoxy-2H-2-chromenone (AP2238) Derivatives. *J. Med. Chem.* **2007**, *50* (17), 4250-4254.

(139) Mancini, F.; De Simone, A.; Andrisano, V. Beta-secretase as a target for Alzheimer's disease drug discovery: an overview of in vitro methods for characterization of inhibitors. *Anal. Bioanal. Chem.* **2011**, *400* (7), 1979-1996.

(140) Fernández-Bachiller, M. I.; Pérez, C.; Monjas, L.; Rademann, J.; Rodríguez-Franco, M. I. New Tacrine–4-Oxo-4H-chromene Hybrids as Multifunctional Agents for the Treatment of Alzheimer's Disease, with Cholinergic, Antioxidant, and β-Amyloid-Reducing Properties. *J. Med. Chem.* **2012**, *55* (3), 1303-1317.

(141) Zampieri, D.; Laurini, E.; Vio, L.; Fermeglia, M.; Pricl, S.; Wunsch, B.; Schepmann, D.; Mamolo, M. G. Improving selectivity preserving affinity: new piperidine-4-carboxamide derivatives as effective sigma-1-ligands. *Eur. J. Med. Chem.* **2015**, *90*, 797-808.

(142) Zeng, C.; Rothfuss, J. M.; Zhang, J.; Vangveravong, S.; Chu, W.; Li, S.; Tu, Z.; Xu, J.; Mach, R. H. Functional assays to define agonists and antagonists of the sigma-2 receptor. *Anal. Biochem.* **2014**, *448*, 68-74.

(143) López-Iglesias, B.; Pérez, C.; Morales-García, J. A.; Alonso-Gil, S.; Pérez-Castillo, A.; Romero, A.; López, M. G.; Villarroya, M.; Conde, S.; Rodríguez-Franco, M. I. New Melatonin–N,N-Dibenzyl(N-methyl)amine Hybrids: Potent Neurogenic Agents with Antioxidant, Cholinergic, and Neuroprotective Properties as Innovative Drugs for Alzheimer's Disease. *J. Med. Chem.* **2014**, *57* (9), 3773-3785.

(144) Morales-Garcia, J. A.; Alonso-Gil, S.; Gil, C.; Martinez, A.; Santos, A.; Perez-Castillo, A. Phosphodiesterase 7 inhibition induces dopaminergic neurogenesis in hemiparkinsonian rats. *Stem Cells Transl. Med.* **2015**, *4* (6), 564-575.

(145) Di, L.; Kerns, E. H.; Fan, K.; McConnell, O. J.; Carter, G. T. High throughput artificial membrane permeability assay for blood-brain barrier. *Eur. J. Med. Chem.* **2003**, *38* (3), 223-232.

(146) Cosconati, S.; Marinelli, L.; Di Leva, F. S.; La Pietra, V.; De Simone, A.; Mancini, F.; Andrisano, V.; Novellino, E.; Goodsell, D. S.; Olson, A. J. Protein flexibility in virtual screening: the BACE-1 case study. *J. Chem. Inf. Model.* **2012**, *52* (10), 2697-2704.

(147) Limongelli, V.; Marinelli, L.; Cosconati, S.; Braun, H. A.; Schmidt, B.; Novellino, E. Ensemble-docking approach on BACE-1: pharmacophore perception and guidelines for drug design. *ChemMedChem* **2007**, *2* (5), 667-678.

(148) Massova, I.; Kollman, P. A. Combined molecular mechanical and continuum solvent approach (MM-PBSA/GBSA) to predict ligand binding. *Perspect. Drug Discov. Design* **2000**, *18*, 113-135.

(149) Brodney, M. A.; Barreiro, G.; Ogilvie, K.; Hajos-Korcsok, E.; Murray, J.; Vajdos, F.; Ambroise, C.; Christoffersen, C.; Fisher, K.; Lanyon, L.; Liu, J.; Nolan, C. E.; Withka, J. M.; Borzilleri, K. A.; Efremov, I.; Oborski, C. E.; Varghese, A.; O'Neill, B. T. Spirocyclic sulfamides as beta-secretase 1 (BACE-1) inhibitors for the treatment of Alzheimer's disease: utilization of structure based drug design, WaterMap, and CNS penetration studies to identify centrally efficacious inhibitors. *J. Med. Chem.* **2012**, *55* (21), 9224-9239.

(150) Stachel, S. J.; Coburn, C. A.; Rush, D.; Jones, K. L.; Zhu, H.; Rajapakse, H.; Graham, S. L.; Simon, A.; Holloway, M.; Allison, T. J.; Munshi, S. K.; Espeseth, A. S.; Zuck, P.; Colussi, D.; Wolfe, A.; Pietrak, B. L.; Lai, M. T.; Vacca, J. P. Discovery of aminoheterocycles as a novel beta-secretase inhibitor class: pH dependence on binding activity part 1. *Bioorganic & medicinal chemistry letters* **2009**, *19* (11), 2977-2980.

(151) Tresadern, G.; Delgado, F.; Delgado, O.; Gijsen, H.; Macdonald, G. J.; Moechars, D.; Rombouts, F.; Alexander, R.; Spurlino, J.; Van Gool, M.; Vega, J. A.; Trabanco, A. A. Rational design and synthesis of aminopiperazinones as beta-secretase (BACE) inhibitors. *Bioorg. Med. Chem. Lett.* **2011**, *21* (24), 7255-7260.

(152) Congreve, M.; Aharony, D.; Albert, J.; Callaghan, O.; Campbell, J.; Carr, R. A. E.; Chessari, G.; Cowan, S.; Edwards, P. D.; Frederickson, M.; McMenamin, R.; Murray, C. W.; Patel, S.; Wallis, N. Application of Fragment Screening by X-ray Crystallography to the Discovery of Aminopyridines as Inhibitors of β-Secretase. *Journal of medicinal chemistry* **2007**, *50* (6), 1124-1132.

(153) Back, M.; Nyhlen, J.; Kvarnstrom, I.; Appelgren, S.; Borkakoti, N.; Jansson, K.; Lindberg, J.; Nystrom, S.; Hallberg, A.; Rosenquist, S.; Samuelsson, B. Design, synthesis and SAR of potent statine-based BACE-1 inhibitors: exploration of P1 phenoxy and benzyloxy residues. *Bioorg. Med. Chem.* **2008**, *16* (21), 9471-9486.

(154) Maillard, M. C.; Hom, R. K.; Benson, T. E.; Moon, J. B.; Mamo, S.; Bienkowski, M.; Tomasselli, A. G.; Woods, D. D.; Prince, D. B.; Paddock,

D. J.; Emmons, T. L.; Tucker, J. A.; Dappen, M. S.; Brogley, L.; Thorsett, E. D.; Jewett, N.; Sinha, S.; John, V. Design, Synthesis, and Crystal Structure of Hydroxyethyl Secondary Amine-Based Peptidomimetic Inhibitors of Human β-Secretase. *Journal of medicinal chemistry* **2007**, *50* (4), 776-781.

(155) Weiss, M. M.; Williamson, T.; Babu-Khan, S.; Bartberger, M. D.; Brown, J.; Chen, K.; Cheng, Y.; Citron, M.; Croghan, M. D.; Dineen, T. A.; Esmay, J.; Graceffa, R. F.; Harried, S. S.; Hickman, D.; Hitchcock, S. A.; Horne, D. B.; Huang, H.; Imbeah-Ampiah, R.; Judd, T.; Kaller, M. R.; Kreiman, C. R.; La, D. S.; Li, V.; Lopez, P.; Louie, S.; Monenschein, H.; Nguyen, T. T.; Pennington, L. D.; Rattan, C.; San Miguel, T.; Sickmier, E. A.; Wahl, R. C.; Wen, P. H.; Wood, S.; Xue, Q.; Yang, B. H.; Patel, V. F.; Zhong, W. Design and preparation of a potent series of hydroxyethylamine containing beta-secretase inhibitors that demonstrate robust reduction of central beta-amyloid. *Journal of medicinal chemistry* **2012**, *55* (21), 9009-9024.

(156) Yuan, J.; Venkatraman, S.; Zheng, Y.; McKeever, B. M.; Dillard, L. W.; Singh, S. B. Structure-based design of beta-site APP cleaving enzyme 1 (BACE1) inhibitors for the treatment of Alzheimer's disease. *J. Med. Chem.* **2013**, *56* (11), 4156-4180.

(157) Patel, S.; Vuillard, L.; Cleasby, A.; Murray, C. W.; Yon, J. Apo and inhibitor complex structures of BACE (beta-secretase). *J. Mol. Biol.* **2004**, *343* (2), 407-416.

(158) McGaughey, G. B.; Colussi, D.; Graham, S. L.; Lai, M. T.; Munshi, S. K.; Nantermet, P. G.; Pietrak, B.; Rajapakse, H. A.; Selnick, H. G.; Stauffer, S. R.; Holloway, M. K. Beta-secretase (BACE-1) inhibitors: accounting for 10s loop flexibility using rigid active sites. *Bioorg. Med. Chem. Lett.* **2007**, *17* (4), 1117-1121.

(159) Rahuel, J.; Rasetti, V.; Maibaum, J.; Rüeger, H.; Göschke, R.; Cohen, N. C.; Stutz, S.; Cumin, F.; Fuhrer, W.; Wood, J. M.; Grütter, M. G. Structure-based drug design: the discovery of novel nonpeptide orally active inhibitors of human renin. *Chem. Biol.* **2000**, *7* (7), 493-504.

(160) Wood, J. M.; Maibaum, J.; Rahuel, J.; Grütter, M. G.; Cohen, N.-C.; Rasetti, V.; Rüger, H.; Göschke, R.; Stutz, S.; Fuhrer, W.; Schilling, W.; Rigollier, P.; Yamaguchi, Y.; Cumin, F.; Baum, H.-P.; Schnell, C. R.; Herold, P.; Mah, R.; Jensen, C.; O'Brien, E.; Stanton, A.; Bedigian, M. P. Structure-based design of aliskiren, a novel orally effective renin inhibitor. *Biochem. Biophys. Res. Commun.* **2003**, *308* (4), 698-705.

(161) Charrier, N.; Clarke, B.; Demont, E.; Dingwall, C.; Dunsdon, R.; Hawkins, J.; Hubbard, J.; Hussain, I.; Maile, G.; Matico, R.; Mosley, J.; Naylor, A.; O'Brien, A.; Redshaw, S.; Rowland, P.; Soleil, V.; Smith, K. J.; Sweitzer, S.; Theobald, P.; Vesey, D.; Walter, D. S.; Wayne, G. Second generation of BACE-1 inhibitors part 2: Optimisation of the non-prime side substituent. *Bioorg. Med. Chem. Lett.* **2009**, *19* (13), 3669-3673.

(162) Malamas, M. S.; Erdei, J.; Gunawan, I.; Barnes, K.; Johnson, M.; Hui, Y.; Turner, J.; Hu, Y.; Wagner, E.; Fan, K.; Olland, A.; Bard, J.; Robichaud, A. J. Aminoimidazoles as potent and selective human beta-secretase (BACE1) inhibitors. *J. Med. Chem.* **2009**, *52* (20), 6314-6323.

(163) Glennon, R. A.; Ablordeppey, S. Y.; Ismaiel, A. M.; El-Ashmawy, M. B.; Fischer, J. B.; Howie, K. B. Structural Features Important for .sigma.1 Receptor Binding. *J. Med. Chem.* **1994**, *37* (8), 1214-1219.

(164) Gund, T. M.; Floyd, J.; Jung, D. Molecular modeling of sigma 1 receptor ligands: a model of binding conformational and electrostatic considerations. *J. Mol. Graph Model.* **2004**, *22* (3), 221-230.

(165) Zampieri, D.; Mamolo, M. G.; Laurini, E.; Florio, C.; Zanette, C.; Fermeglia, M.; Posocco, P.; Paneni, M. S.; Pricl, S.; Vio, L. Synthesis, biological evaluation, and three-dimensional in silico pharmacophore model for sigma(1) receptor ligands based on a series of substituted benzo[d]oxazol-2(3H)-one derivatives. *J. Med. Chem.* **2009**, *52* (17), 5380-5393.

(166) Meyer, C.; Schepmann, D.; Yanagisawa, S.; Yamaguchi, J.; Dal Col, V.; Laurini, E.; Itami, K.; Pricl, S.; Wunsch, B. Pd-catalyzed direct C-H bond functionalization of spirocyclic sigma1 ligands: generation of a pharmacophore model and analysis of the reverse binding mode by

docking into a 3D homology model of the sigma1 receptor. *Journal of medicinal chemistry* **2012**, *55* (18), 8047-8065.

(167) Laggner, C.; Schieferer, C.; Fiechtner, B.; Poles, G.; Hoffmann, R. D.; Glossmann, H.; Langer, T.; Moebius, F. F. Discovery of high-affinity ligands of sigma1 receptor, ERG2, and emopamil binding protein by pharmacophore modeling and virtual screening. *Journal of medicinal chemistry* **2005**, *48* (15), 4754-4764.

(168) Laurini, E.; Marson, D.; Dal Col, V.; Fermeglia, M.; Mamolo, M. G.; Zampieri, D.; Vio, L.; Pricl, S. Another brick in the wall. Validation of the sigma1 receptor 3D model by computer-assisted design, synthesis, and activity of new sigma1 ligands. *Mol. Pharm.* **2012**, *9* (11), 3107-3126.

(169) Laurini, E.; Col, V. D.; Mamolo, M. G.; Zampieri, D.; Posocco, P.; Fermeglia, M.; Vio, L.; Pricl, S. Homology model and docking-based virtual screening for ligands of the sigma1 receptor. *ACS medicinal chemistry letters* **2011**, *2* (11), 834-839.

(170) Brune, S.; Schepmann, D.; Klempnauer, K. H.; Marson, D.; Dal Col, V.; Laurini, E.; Fermeglia, M.; Wunsch, B.; Pricl, S. The sigma enigma: in vitro/in silico site-directed mutagenesis studies unveil sigma1 receptor ligand binding. *Biochemistry* **2014**, *53* (18), 2993-3003.

(171) Rossi, D.; Marra, A.; Picconi, P.; Serra, M.; Catenacci, L.; Sorrenti, M.; Laurini, E.; Fermeglia, M.; Pricl, S.; Brambilla, S.; Almirante, N.; Peviani, M.; Curti, D.; Collina, S. Identification of RC-33 as a potent and selective sigma1 receptor agonist potentiating NGF-induced neurite outgrowth in PC12 cells. Part 2: g-scale synthesis, physicochemical characterization and in vitro metabolic stability. *Bioorganic & medicinal chemistry* **2013**, *21* (9), 2577-2586.

(172) Rossi, D.; Pedrali, A.; Gaggeri, R.; Marra, A.; Pignataro, L.; Laurini, E.; Dal Col, V.; Fermeglia, M.; Pricl, S.; Schepmann, D.; Wunsch, B.; Peviani, M.; Curti, D.; Collina, S. Chemical, pharmacological, and in vitro metabolic stability studies on enantiomerically pure RC-33 compounds: promising neuroprotective agents acting as sigma(1) receptor agonists. *ChemMedChem* **2013**, *8* (9), 1514-1527.

(173) Cobos, E. J.; Entrena, J. M.; Nieto, F. R.; Cendán, C. M.; Del Pozo, E. Pharmacology and Therapeutic Potential of Sigma(1) Receptor Ligands. *Curr. Neuropharmacol.* **2008**, *6* (4), 344-366.

(174) Bergeron, R.; Debonnel, G. Effects of low and high doses of selective sigma ligands: further evidence suggesting the existence of different subtypes of sigma receptors. *Psychopharmacology* **1997**, *129* (3), 215-224.

(175) Bermack, J. E.; Debonnel, G. The role of sigma receptors in depression. *J. Pharmacol. Sci.* **2005**, *97* (3), 317-336.

(176) Calabrese, E. J. Hormesis: a revolution in toxicology, risk assessment and medicine. *EMBO Reports* **2004**, *5* (Suppl 1), S37-S40.

(177) Jonsson, T.; Atwal, J. K.; Steinberg, S.; Snaedal, J.; Jonsson, P. V.; Bjornsson, S.; Stefansson, H.; Sulem, P.; Gudbjartsson, D.; Maloney, J.; Hoyte, K.; Gustafson, A.; Liu, Y.; Lu, Y.; Bhangale, T.; Graham, R. R.; Huttenlocher, J.; Bjornsdottir, G.; Andreassen, O. A.; Jonsson, E. G.; Palotie, A.; Behrens, T. W.; Magnusson, O. T.; Kong, A.; Thorsteinsdottir, U.; Watts, R. J.; Stefansson, K. A mutation in APP protects against Alzheimer/'s disease and age-related cognitive decline. *Nature* **2012**, *488* (7409), 96-99.

(178) Macfarlane, S. C., M. Moore. D. Zografidis, A. Missling M. New Exploratory Alzheimer's Drug Anavex 2-73 Changes in Electrophysiological Markers in Alzheimer's Disease - First Patient Data from an Ongoing Phase 2a Study in Mild-to-Moderate Alzheimer's Patients. *Alzheimer's Association International Conference 2015* **2015**.

(179) Rodríguez-Franco, M. I.; Fernández-Bachiller, M. I.; Pérez, C.; Hernández-Ledesma, B.; Bartolomé, B. Novel tacrine-melatonin hybrids as dual-acting drugs for Alzheimer disease, with improved acetylcholinesterase inhibitory and antioxidant properties. *J. Med. Chem.* **2006**, *49* (2), 459-462.

(180) Fernández-Bachiller, M. I.; Pérez, C.; Monjas, L.; Rademann, J.; Rodríguez-Franco, M. I. New tacrine--4-oxo-4*H*-chromene hybrids as multifunctional agents for the treatment of Alzheimer's disease, with

cholinergic, antioxidant, and beta-amyloid-reducing properties. *J. Med. Chem.* **2012**, *55* (3), 1303-1317.

(181) Rodríguez-Franco, M. I.; Fernández-Bachiller, M. I.; Pérez, C.; Hernández-Ledesma, B.; Bartolomé, B. Novel Tacrine−Melatonin Hybrids as Dual-Acting Drugs for Alzheimer Disease, with Improved Acetylcholinesterase Inhibitory and Antioxidant Properties. *J. Med. Chem.* **2006**, *49* (2), 459-462.

(182) Ou, B.; Hampsch-Woodill, M.; Prior, R. L. Development and Validation of an Improved Oxygen Radical Absorbance Capacity Assay Using Fluorescein as the Fluorescent Probe. *J. Agric. Food Chem.* **2001**, *49* (10), 4619-4626.

(183) Zampieri, D.; Laurini, E.; Vio, L.; Fermeglia, M.; Pricl, S.; Wünsch, B.; Schepmann, D.; Mamolo, M. G. Improving selectivity preserving affinity: new piperidine-4-carboxamide derivatives as effective sigma-1-ligands. *Eur. J. Med. Chem.* **2015**, *90*, 797-808.

(184) Meyer, C.; Schepmann, D.; Yanagisawa, S.; Yamaguchi, J.; Dal Col, V.; Laurini, E.; Itami, K.; Pricl, S.; Wünsch, B. Pd-catalyzed direct C-H bond functionalization of spirocyclic sigma1 ligands: generation of a pharmacophore model and analysis of the reverse binding mode by docking into a 3D homology model of the sigma1 receptor. *Journal of medicinal chemistry* **2012**, *55* (18), 8047-8065.

(185) Rossi, D.; Pedrali, A.; Gaggeri, R.; Marra, A.; Pignataro, L.; Laurini, E.; Dal Col, V.; Fermeglia, M.; Pricl, S.; Schepmann, D.; Wünsch, B.; Peviani, M.; Curti, D.; Collina, S. Chemical, pharmacological, and in vitro metabolic stability studies on enantiomerically pure RC-33 compounds: promising neuroprotective agents acting as sigma(1) receptor agonists. *ChemMedChem* **2013**, *8* (9), 1514-1527.

(186) Morales-García, J. A.; Luna-Medina, R.; Alfaro-Cervello, C.; Cortés-Canteli, M.; Santos, A.; García-Verdugo, J. M.; Pérez-Castillo, A. Peroxisome proliferator-activated receptor gamma ligands regulate neural stem cell proliferation and differentiation *in vitro* and *in vivo*. *Glia* **2011**, *59* (2), 293-307.

(187) Bayly, C. I.; Cieplak, P.; Cornell, W.; Kollman, P. A. A well-behaved electrostatic potential based method using charge restraints for deriving atomic charges: the RESP model. *J. Phys. Chem.* **1993**, *97* (40), 10269-10280.

(188) Stachel, S. J.; Coburn, C. A.; Steele, T. G.; Crouthamel, M. C.; Pietrak, B. L.; Lai, M. T.; Holloway, M. K.; Munshi, S. K.; Graham, S. L.; Vacca, J. P. Conformationally biased P3 amide replacements of beta-secretase inhibitors. *Bioorganic & medicinal chemistry letters* **2006**, *16* (3), 641-644.

(189) Morris, G. M.; Huey, R.; Lindstrom, W.; Sanner, M. F.; Belew, R. K.; Goodsell, D. S.; Olson, A. J. AutoDock4 and AutoDockTools4: Automated docking with selective receptor flexibility. *J. Comput. Chem.* **2009**, *30* (16), 2785-2791.

(190) Brune, S.; Schepmann, D.; Klempnauer, K. H.; Marson, D.; Dal Col, V.; Laurini, E.; Fermeglia, M.; Wünsch, B.; Pricl, S. The sigma enigma: in vitro/in silico site-directed mutagenesis studies unveil sigma1 receptor ligand binding. *Biochemistry* **2014**, *53* (18), 2993-3003.

(191) Case, D. A.; Darden, T. A.; Cheatham, T. E.; Simmerling, C. L.; Wang, J.; Duke, R. E.; Luo, R.; Walker, R. C.; Zhang, W.; Merz, K. M.; Roberts, B.; Hayik, S.; Roitberg, A.; Seabra, G.; Swails, J.; Goetz, A. W.; Kolossváry, I.; Wong, K. F.; Paesani, F.; Vanicek, J.; Wolf, R. M.; Liu, J.; Wu, X.; Brozell, S. R.; Steinbrecher, T.; Gohlke, H.; Cai, Q.; Ye, X.; Hsieh, M. J.; Cui, G.; Roe, D. R.; Mathews, D. H.; Seetin, M. G.; Salomon-Ferrer, R.; Sagui, C.; Babin, V.; Luchko, T.; Gusarov, S.; Kovalenko, A.; Kollman, P. A. AMBER 12 (2012) University of California, San Francisco.

(192) Case, D. A.; J.T., B.; Betz, R. M.; Cerutti, D. S.; Cheatham, I. T. E.; Darden, T. A.; Duke, R. E.; Giese, T. J.; Gohlke, H.; Goetz, A. W.; Homeyer, N.; Izadi, S.; Janowski, P.; Kaus, J.; Kovalenko, A.; Lee, T. S.; LeGrand, S.; Li, P.; Luchko, T.; Luo, R.; Madej, B.; Merz, K. M.; Monard, G.; Needham, P.; Nguyen, H.; Nguyen, H. T.; Omelyan, I.; Onufriev, A.; Roe, D. R.; Roitberg, A.; Salomon-Ferrer, R.; Simmerling, C. L.; Smith,

W.; Swails, J.; Walker, R. C.; Wang, J.; Wolf, R. M.; Wu, X.; D.M., Y.; P.A., K. AMBER 14 (2015) University of California, San Francisco.

(193) Jorgensen, W. L.; Chandrasekhar, J.; Madura, J. D.; Impey, R. W.; Klein, M. L. Comparison of simple potential functions for simulating liquid water. *J. Chem. Phys.* **1983**, *79* (2), 926-935.

(194) Tsui, V.; Case, D. A. Theory and applications of the generalized Born solvation model in macromolecular simulations. *Biopolymers* **2000**, *56* (4), 275-291.

(195) Onufriev, A.; Bashford, D.; Case, D. A. Modification of the generalized Born model suitable for macromolecules. *J. Phys. Chem. B* **2000**, *104* (15), 3712-3720.

(196) http://www.esteco.com/home/mode_frontier/mode_frontier.html.

(197) Denizot, F.; Lang, R. Rapid colorimetric assay for cell growth and survival. Modifications to the tetrazolium dye procedure giving improved sensitivity and reliability. *Journal of immunological methods* **1986**, *89* (2), 271-277.

(198) Youdim, M. B.; Edmondson, D.; Tipton, K. F. The therapeutic potential of monoamine oxidase inhibitors. *Nat. Rev. Neurosci.* **2006**, *7* (4), 295-309.

(199) Kalaria, R. N.; Harik, S. I. Blood-brain barrier monoamine oxidase: enzyme characterization in cerebral microvessels and other tissues from six mammalian species, including human. *J. Neurochem.* **1987**, *49* (3), 856-864.

(200) Kennedy, B. P.; Ziegler, M. G.; Alford, M.; Hansen, L. A.; Thal, L. J.; Masliah, E. Early and persistent alterations in prefrontal cortex MAO A and B in Alzheimer's disease. *J. Neural Transm.* **2003**, *110* (7), 789-801.

(201) Saura, J.; Luque, J. M.; Cesura, A. M.; Prada, M. D.; Chan-Palay, V.; Huber, G.; Löffler, J.; Richards, J. G. Increased monoamine oxidase b activity in plaque-associated astrocytes of Alzheimer brains revealed by quantitative enzyme radioautography. *Neuroscience* **1994**, *62* (1), 15-30.

(202) Sherif, F.; Gottfries, C. G.; Alafuzoff, I.; Oreland, L. Brain gamma-aminobutyrate aminotransferase (GABA-T) and monoamine oxidase (MAO) in patients with Alzheimer's disease. *J. Neural. Transm. Park. Dis. Dement. Sect.* **1992**, *4* (3), 227-240.

(203) Chan-Palay, V.; Hochli, M.; Savaskan, E.; Hungerecker, G. Calbindin D-28k and monoamine oxidase A immunoreactive neurons in the nucleus basalis of Meynert in senile dementia of the Alzheimer type and Parkinson's disease. *Dementia* **1993**, *4* (1), 1-15.

(204) Burke, W. J.; Li, S. W.; Chung, H. D.; Ruggiero, D. A.; Kristal, B. S.; Johnson, E. M.; Lampe, P.; Kumar, V. B.; Franko, M.; Williams, E. A.; Zahm, D. S. Neurotoxicity of MAO Metabolites of Catecholamine Neurotransmitters: Role in Neurodegenerative Diseases. *Neurotoxicology* **2004**, *25* (1–2), 101-115.

(205) Caraci, F.; Copani, A.; Nicoletti, F.; Drago, F. Depression and Alzheimer's disease: Neurobiological links and common pharmacological targets. *Eur. J. Pharmacol.* **2010**, *626* (1), 64-71.

(206) Gilley, D. W.; Wilson, R. S.; Beckett, L. A.; Evans, D. A. Psychotic Symptoms and Physically Aggressive Behavior in Alzheimer's Disease. *J. Am. Geriatr. Soc.* **1997**, *45* (9), 1074-1079.

(207) Lee, G. J.; Lu, P. H.; Hua, X.; Lee, S.; Wu, S.; Nguyen, K.; Teng, E.; Leow, A. D.; Jack Jr, C. R.; Toga, A. W.; Weiner, M. W.; Bartzokis, G.; Thompson, P. M. Depressive Symptoms in Mild Cognitive Impairment Predict Greater Atrophy in Alzheimer's Disease-Related Regions. *Biol. Psychiatry* **2012**, *71* (9), 814-821.

(208) Matthews, K. L.; Chen, C. P. L. H.; Esiri, M. M.; Keene, J.; Minger, S. L.; Francis, P. T. Noradrenergic changes, aggressive behavior, and cognition in patients with dementia. *Biol. Psychiatry* **2002**, *51* (5), 407-416.

(209) Gabilondo, A. M.; Hostalot, C.; Garibi, J. M.; Meana, J. J.; Callado, L. F. Monoamine oxidase B activity is increased in human gliomas. *Neurochem. Int.* **2008**, *52* (1–2), 230-234.

(210) Verkhratsky, A.; Olabarria, M.; Noristani, H. N.; Yeh, C.-Y.; Rodriguez, J. J. Astrocytes in Alzheimer's Disease. *Neurotherapeutics : the journal of the American Society for Experimental NeuroTherapeutics* **2010**, *7* (4), 399-412.

(211) O'Carroll, A.-M.; Fowler, C.; Phillips, J.; Tobbia, I.; Tipton, K. The deamination of dopamine by human brain monoamine oxidase. *Naunyn-Schmiedeberg's Arch. Pharmacol.* **1983**, *322* (3), 198-202.

(212) Nowakowska, E.; Kus, K.; Chodera, A.; Rybakowski, J. Investigating potential anxiolytic, antidepressant and memory enhancing activity of deprenyl. *J. Physiol. Pharmacol.* **2001**, *52* (4 Pt 2), 863-873.

(213) Birks, J.; Flicker, L. Selegiline for Alzheimer's disease. *Cochrane Database Syst. Rev.* **2003**, *1*.

(214) Youdim, M. B. Multi target neuroprotective and neurorestorative anti-Parkinson and anti-Alzheimer drugs ladostigil and m30 derived from rasagiline. *Exp. Neurobiol.* **2013**, *22* (1), 1-10.

(215) Nijveldt, R. J.; van Nood, E.; van Hoorn, D. E.; Boelens, P. G.; van Norren, K.; van Leeuwen, P. A. Flavonoids: a review of probable mechanisms of action and potential applications. *Am. J. Clin. Nutr.* **2001**, *74* (4), 418-425.

(216) Gaspar, A.; Matos, M. J.; Garrido, J.; Uriarte, E.; Borges, F. Chromone: A Valid Scaffold in Medicinal Chemistry. *Chem. Rev.* **2014**, *114* (9), 4960-4992.

(217) Keri, R. S.; Budagumpi, S.; Pai, R. K.; Balakrishna, R. G. Chromones as a privileged scaffold in drug discovery: A review. *Eur. J. Med. Chem.* **2014**, *78* (0), 340-374.

(218) Cagide, F.; Silva, T.; Reis, J.; Gaspar, A.; Borges, F.; Gomes, L. R.; Low, J. N. Discovery of two new classes of potent monoamine oxidase-B inhibitors by tricky chemistry. *Chem. Commun.* **2015**, *51* (14), 2832-2835.

(219) Fernandez-Bachiller, M. I.; Perez, C.; Monjas, L.; Rademann, J.; Rodriguez-Franco, M. I. New tacrine-4-oxo-4H-chromene hybrids as multifunctional agents for the treatment of Alzheimer's disease, with

cholinergic, antioxidant, and beta-amyloid-reducing properties. *J. Med. Chem.* **2012**, *55* (3), 1303-1317.

(220) Lee, H.; Lee, K.; Jung, J. K.; Cho, J.; Theodorakis, E. A. Synthesis and evaluation of 6-hydroxy-7-methoxy-4-chromanone- and chroman-2-carboxamides as antioxidants. *Bioorg. Med. Chem. Lett.* **2005**, *15* (11), 2745-2748.

(221) Stoermer, M.; Fairlie, D. A Selective and Versatile Synthesis of Substituted Chromones via Addition of Phenols to Dimethyl Acetylenedicarboxylate. *Aust. J. Chem.* **1995**, *48* (3), 677-686.

(222) Taudou, A.; Delmas, F.; Timon-David, P.; Ecalle, R.; de Saqui-Sannes, G.; Payard, M. Recherche d'activité anti-parasitaire de carboxamido-2 benzopyrones-4. *Eur. J. Med. Chem.* **1987**, *22* (6), 583-585.

(223) McOmie, J. F. W.; Watts, M. L.; West, D. E. Demethylation of aryl methyl ethers by boron tribromide. *Tetrahedron* **1968**, *24* (5), 2289-2292.

(224) Porcelli, S.; Drago, A.; Fabbri, C.; Serretti, A. Mechanisms of antidepressant action: An integrated dopaminergic perspective. *Prog. Neuropsychopharmacol. Biol. Psychiatry* **2011**, *35* (7), 1532-1543.

(225) Kong, P.; Zhang, B.; Lei, P.; Kong, X.; Zhang, S.; Li, D.; Zhang, Y. Neuroprotection of MAO-B inhibitor and dopamine agonist in Parkinson disease. *Int. J. Clin. Exp. Med.* **2015**, *8* (1), 431-439.

(226) Unzeta, M.; Sanz, E., Novel MAO-B inhibitors: potential therapeutic use of the selective MAO-B inhibitor PF9601N in Parkinson's disease. In *Int. Rev. Neurobiol.*, Moussa, B. H. Y.; Peter, D., Eds. Academic Press: 2011; Vol. 100, pp 217-236.

(227) Goldstein, J. M.; Barnett, A.; Malick, J. B. The evaluation of anti-parkinson drugs on reserpine-induced rigidity in rats. *Eur. J. Pharmacol.* **1975**, *33* (1), 183-188.

(228) Skalisz, L. L.; Beijamini, V.; Joca, S. L.; Vital, M. A. B. F.; Da Cunha, C.; Andreatini, R. Evaluation of the face validity of reserpine administration as an animal model of depression–Parkinson's disease

association. *Prog. Neuropsychopharmacol. Biol. Psychiatry* **2002**, *26* (5), 879-883.

(229) Tadaiesky, M. T.; Andreatini, R.; Vital, M. A. B. F. Different effects of 7-nitroindazole in reserpine-induced hypolocomotion in two strains of mice. *Eur. J. Pharmacol.* **2006**, *535* (1-3), 199-207.

(230) Ganapathy, M. E.; Prasad, P. D.; Huang, W.; Seth, P.; Leibach, F. H.; Ganapathy, V. Molecular and Ligand-Binding Characterization of the ς-Receptor in the Jurkat Human T Lymphocyte Cell Line. *J. Pharm. Exp. Ther.* **1999**, *289* (1), 251-260.

(231) Matos, M. J.; Rodríguez-Enríquez, F.; Borges, F.; Santana, L.; Uriarte, E.; Estrada, M.; Rodríguez-Franco, M. I.; Laguna, R.; Viña, D. 3-Amidocoumarins as Potential Multifunctional Agents against Neurodegenerative Diseases. *ChemMedChem* **2015**, *10* (12), 2071-2079.

(232) Mota, S. I.; Ferreira, I. L.; Rego, A. C. Dysfunctional synapse in Alzheimer's disease – A focus on NMDA receptors. *Neuropharmacology* **2014**, *76, Part A*, 16-26.

(233) Danysz, W.; Parsons, C. G. Alzheimer's disease, beta-amyloid, glutamate, NMDA receptors and memantine--searching for the connections. *Br. J. Pharmacol.* **2012**, *167* (2), 324-352.

(234) Meldrum, B. S. Glutamate as a neurotransmitter in the brain: review of physiology and pathology. *J. Nutr.* **2000**, *130* (4S Suppl), 1007S-1015S.

(235) Wenk, G. L. Neuropathologic changes in Alzheimer's disease: potential targets for treatment. *J. Clin. Psychiatry* **2006**, *3*, 3-7.

(236) Doraiswamy, P. M. Alzheimer's disease and the glutamate NMDA receptor. *Psychopharmacol. Bull.* **2003**, *37* (2), 41-49.

(237) Arias, C.; Arrieta, I.; Tapia, R. beta-Amyloid peptide fragment 25-35 potentiates the calcium-dependent release of excitatory amino acids from depolarized hippocampal slices. *J. Neurosci. Res.* **1995**, *41* (4), 561-566.

(238) Harris, M. E.; Wang, Y.; Pedigo, N. W., Jr.; Hensley, K.; Butterfield, D. A.; Carney, J. M. Amyloid beta peptide (25-35) inhibits Na+-dependent

glutamate uptake in rat hippocampal astrocyte cultures. *J. Neurochem.* **1996**, *67* (1), 277-286.

(239) Scott, H. A.; Gebhardt, F. M.; Mitrovic, A. D.; Vandenberg, R. J.; Dodd, P. R. Glutamate transporter variants reduce glutamate uptake in Alzheimer's disease. *Neurobiol. Aging.* **2011**, *32* (3), 553.e551-553.e511.

(240) Fernández-Tomé, P.; Brera, B.; Arévalo, M. a.-A.; de Ceballos, M. a. L. β-Amyloid25-35 inhibits glutamate uptake in cultured neurons and astrocytes: modulation of uptake as a survival mechanism. *Neurobiol. Dis.* **2004**, *15* (3), 580-589.

(241) Lauderback, C. M.; Hackett, J. M.; Huang, F. F.; Keller, J. N.; Szweda, L. I.; Markesbery, W. R.; Butterfield, D. A. The glial glutamate transporter, GLT-1, is oxidatively modified by 4-hydroxy-2-nonenal in the Alzheimer's disease brain: the role of Abeta1-42. *J. Neurochem.* **2001**, *78* (2), 413-416.

(242) Ferreira, I. L.; Bajouco, L. M.; Mota, S. I.; Auberson, Y. P.; Oliveira, C. R.; Rego, A. C. Amyloid beta peptide 1–42 disturbs intracellular calcium homeostasis through activation of GluN2B-containing N-methyl-d-aspartate receptors in cortical cultures. *Cell Calcium* **2012**, *51* (2), 95-106.

(243) Decker, H.; Jurgensen, S.; Adrover, M. F.; Brito-Moreira, J.; Bomfim, T. R.; Klein, W. L.; Epstein, A. L.; De Felice, F. G.; Jerusalinsky, D.; Ferreira, S. T. N-methyl-D-aspartate receptors are required for synaptic targeting of Alzheimer's toxic amyloid-beta peptide oligomers. *J. Neurochem.* **2010**, *115* (6), 1520-1529.

(244) Texidó, L.; Martín-Satué, M.; Alberdi, E.; Solsona, C.; Matute, C. Amyloid β peptide oligomers directly activate NMDA receptors. *Cell Calcium* **2011**, *49* (3), 184-190.

(245) Parameshwaran, K.; Dhanasekaran, M.; Suppiramaniam, V. Amyloid beta peptides and glutamatergic synaptic dysregulation. *Exp. Neurobiol.* **2008**, *210* (1), 7-13.

(246) Hu, M.; Schurdak, M. E.; Puttfarcken, P. S.; El Kouhen, R.; Gopalakrishnan, M.; Li, J. High content screen microscopy analysis of

Aβ1–42-induced neurite outgrowth reduction in rat primary cortical neurons: Neuroprotective effects of α7 neuronal nicotinic acetylcholine receptor ligands. *Brain Res.* **2007**, *1151*, 227-235.

(247) Floden, A. M.; Li, S.; Combs, C. K. Beta-amyloid-stimulated microglia induce neuron death via synergistic stimulation of tumor necrosis factor alpha and NMDA receptors. *J. Neurochem.* **2005**, *25* (10), 2566-2575.

(248) Shelat, P. B.; Chalimoniuk, M.; Wang, J. H.; Strosznajder, J. B.; Lee, J. C.; Sun, A. Y.; Simonyi, A.; Sun, G. Y. Amyloid beta peptide and NMDA induce ROS from NADPH oxidase and AA release from cytosolic phospholipase A2 in cortical neurons. *J. Neurochem.* **2008**, *106* (1), 45-55.

(249) Atri, A.; Molinuevo, J. L.; Lemming, O.; Wirth, Y.; Pulte, I.; Wilkinson, D. Memantine in patients with Alzheimer's disease receiving donepezil: new analyses of efficacy and safety for combination therapy. *Alzheimers Res. Ther.* **2013**, *5* (1).

(250) Wilkinson, D.; Andersen, H. F. Analysis of the effect of memantine in reducing the worsening of clinical symptoms in patients with moderate to severe Alzheimer's disease. *Dement. Geriatr. Cogn. Disord.* **2007**, *24* (2), 138-145.

(251) Leeson, P. D.; Baker, R.; Carling, R. W.; Curtis, N. R.; Moore, K. W.; Williams, B. J.; Foster, A. C.; Donald, A. E.; Kemp, J. A.; Marshall, G. R. Kynurenic acid derivatives. Structure-activity relationships for excitatory amino acid antagonism and identification of potent and selective antagonists at the glycine site on the N-methyl-D-aspartate receptor. *J. Med. Chem.* **1991**, *34* (4), 1243-1252.

(252) Birch, P. J.; Grossman, C. J.; Hayes, A. G. Kynurenic acid antagonises responses to NMDA via an action at the strychnine-insensitive glycine receptor. *Eur. J. Pharmacol.* **1988**, *154* (1), 85-87.

(253) Borza, I.; Kolok, S.; Galgóczy, K.; Gere, A.; Horváth, C.; Farkas, S.; Greiner, I.; Domány, G. Kynurenic acid amides as novel NR2B selective

NMDA receptor antagonists. *Bioorg. Med. Chem. Lett.* **2007**, *17* (2), 406-409.

(254) Sills, M. A.; Fagg, G.; Pozza, M.; Angst, C.; Brundish, D. E.; Hurt, S. D.; Wilusz, E. J.; Williams, M. [3H]CGP 39653: a new N-methyl-D-aspartate antagonist radioligand with low nanomolar affinity in rat brain. *Eur. J. Pharmacol.* **1991**, *192* (1), 19-24.

(255) Moroni, F.; Alesiani, M.; Galli, A.; Mori, F.; Pecorari, R.; Carlá, V.; Cherici, G.; Pellicciari, R. Thiokynurenates: a new group of antagonists of the glycine moduiatory site of the NMBA receptor. *Eur. J. Pharmacol.* **1991**, *199* (2), 227-232.

(256) Zhuravlev, A.; Zakharov, G.; Shchegolev, B.; Savvateeva-Popova, E. Stacking interaction and its role in kynurenic acid binding to glutamate ionotropic receptors. *J. Mol. Model.* **2012**, *18* (5), 1755-1766.

(257) Furukawa, H.; Gouaux, E. Mechanisms of activation, inhibition and specificity: crystal structures of the NMDA receptor NR1 ligand-binding core. *EMBO J.* **2003**, *22* (12), 2873-2885.

(258) Sills, M. A.; Fagg, G.; Pozza, M.; Angst, C.; Brundish, D. E.; Hurt, S. D.; Jay Wilusz, E.; Williams, M. [3H]CGP 39653: a new N-methyl-D-aspartate antagonist radioligand with low nanomolar affinity in rat brain. *Eur. J. Pharmacol.* **1991**, *192* (1), 19-24.

(259) Markesbery, W. R. Oxidative stress hypothesis in Alzheimer's disease. *Free Radic. Biol. Med.* **1997**, *23* (1), 134-147.

(260) Mendes Arent; Souza, L. F. d.; Walz, R.; Dafre, A. L. Perspectives on Molecular Biomarkers of Oxidative Stress and Antioxidant Strategies in Traumatic Brain Injury. *Biomed. Res. Int.* **2014**, *2014*, 18.

(261) Lovell, M. A.; Xie, C.; Markesbery, W. R. Acrolein is increased in Alzheimer's disease brain and is toxic to primary hippocampal cultures. *Neurobiol. Aging.* **2001**, *22* (2), 187-194.

(262) Uchida, K.; Kanematsu, M.; Morimitsu, Y.; Osawa, T.; Noguchi, N.; Niki, E. Acrolein is a product of lipid peroxidation reaction. Formation of free acrolein and its conjugate with lysine residues in oxidized low density lipoproteins. *J. Biol. Chem.* **1998**, *273* (26), 16058-16066.

(263) Choi, B. H. Oxygen, antioxidants and brain dysfunction. *Yonsei Med J* **1993**, *34* (1), 1-10.

(264) Huang, X.; Atwood, C. S.; Hartshorn, M. A.; Multhaup, G.; Goldstein, L. E.; Scarpa, R. C.; Cuajungco, M. P.; Gray, D. N.; Lim, J.; Moir, R. D.; Tanzi, R. E.; Bush, A. I. The A beta peptide of Alzheimer's disease directly produces hydrogen peroxide through metal ion reduction. *Biochemistry* **1999**, *38* (24), 7609-7616.

(265) Wojtunik-Kulesza, K. A.; Oniszczuk, A.; Oniszczuk, T.; Waksmundzka-Hajnos, M. The influence of common free radicals and antioxidants on development of Alzheimer's Disease. *Biomed. Pharmacother.* **2016**, *78*, 39-49.

(266) Mamelak, M. Alzheimer' s disease, oxidative stress and gammahydroxybutyrate. *Neurobiol. Aging.* **2007**, *28* (9), 1340-1360.

(267) Sashidhara, K. V.; Modukuri, R. K.; Jadiya, P.; Dodda, R. P.; Kumar, M.; Sridhar, B.; Kumar, V.; Haque, R.; Siddiqi, M. I.; Nazir, A. Benzofuran-chalcone hybrids as potential multifunctional agents against Alzheimer's disease: synthesis and in vivo studies with transgenic Caenorhabditis elegans. *ChemMedChem* **2014**, *9* (12), 2671-2684.

(268) Sezgin, Z.; Dincer, Y. Alzheimer's disease and epigenetic diet. *Neurochem. Int.* **2014**, *78*, 105-116.

(269) Mancuso, C.; Santangelo, R. Ferulic acid: pharmacological and toxicological aspects. *Food Chem. Toxicol.* **2014**, *65*, 185-195.

(270) Chojnacki, J. E.; Liu, K.; Yan, X.; Toldo, S.; Selden, T.; Estrada, M.; Rodríguez-Franco, M. I.; Halquist, M. S.; Ye, D.; Zhang, S. Discovery of 5-(4-Hydroxyphenyl)-3-oxo-pentanoic Acid [2-(5-Methoxy-1H-indol-3-yl)-ethyl]-amide as a Neuroprotectant for Alzheimer's Disease by Hybridization of Curcumin and Melatonin. *ACS Chem. Neurosci.* **2014**, *5* (8), 690-699.

(271) Minders, C.; Petzer, J. P.; Petzer, A.; Lourens, A. C. U. Monoamine oxidase inhibitory activities of heterocyclic chalcones. *Bioorg. Med. Chem. Lett.* **2015**, *25* (22), 5270-5276.

(272) Morales-Camilo, N.; Salas, C. O.; Sanhueza, C.; Espinosa-Bustos, C.; Sepulveda-Boza, S.; Reyes-Parada, M.; Gonzalez-Nilo, F.; Caroli-Rezende, M.; Fierro, A. Synthesis, Biological Evaluation, and Molecular Simulation of Chalcones and Aurones as Selective MAO-B Inhibitors. *Chem. Biol. Drug Des.* **2015**, *85* (6), 685-695.

(273) Mecocci, P.; Polidori, M. C. Antioxidant clinical trials in mild cognitive impairment and Alzheimer's disease. *BBA-Mol. Basis Dis.* **2012**, *1822* (5), 631-638.

(274) Goto G., N. A. Piperidinoalkyl derivatlves of carboxylic acld amides. *Eur. Pat. Appl. (1989), 19 pp. CODEN:EPXXDW; EP330026* **1989**.

(275) Hindmarch, I.; Hashimoto, K. Cognition and depression: the effects of fluvoxamine, a sigma-1 receptor agonist, reconsidered. *Hum. Psychopharmacol.* **2010**, *25* (3), 193-200.